

DISSERTATION ZUR ERLANGUNG DES DOKTORGRADES
DER FAKULTÄT FÜR CHEMIE UND PHARMAZIE
DER LUDWIG-MAXIMILIANS-UNIVERSITÄT MÜNCHEN

**NEW OXYGEN-RICH MATERIALS AS
HIGH-ENERGY DENSE OXIDISERS
BASED ON POLYNITRO COMPOUNDS**

MARCOS ADRIAN KETTNER

AUS

MÜNCHEN, DEUTSCHLAND

2015

ERKLÄRUNG

Diese Dissertation wurde im Sinne von §7 der Promotionsordnung vom 28. November 2011 von HERRN PROF. DR. THOMAS M. KLAPÖTKE betreut.

EIDESSTATTLICHE VERSICHERUNG

Diese Dissertation wurde eigenständig und ohne unerlaubte Hilfe erarbeitet.

München, den 21. Mai 2015

Marcos A. Kettner

Marcos A. Kettner

Dissertation eingereicht am:

1. Gutachter:

2. Gutachter:

Mündliche Prüfung am:

27. März 2015

Prof. Dr. T. M. Klapötke

Prof. Dr. K. Karaghiosoff

11. Mai 2015

For my family.



"Mankind will not forever remain on Earth, but in the pursuit of light and space will first timidly emerge from the bounds of the atmosphere, and then advance until he has conquered the whole of circumsolar space" (1911)

- KONSTANTIN EDUARDOVICH TSIOLKOVSKY -
(1857–1935)

Picture source: International Space Hall of Fame at the New Mexico Museum of Space History
(http://www.nmspacemuseum.org/halloffame/images.php?image_id=27; accessed: March 20, 2015)

ACKNOWLEDGEMENTS

First and foremost I want to thank my doctoral father **PROF. DR. THOMAS M. KLAPÖTKE** for the acceptance of my person at his professorship for energetic materials research at the Ludwig-Maximilian University of Munich and the interesting and challenging topic of my doctoral thesis. He gave me the chance of totally free and independent research on energetic oxidisers for solid rocket propellants and, moreover, to visit not only three times the *Seminar on New Trends in the Research of Energetic Materials*, but also to visit the *European Workshop on Phosphorus Chemistry*. Moreover, I want to thank him for the chance and his confidence in me to represent him and his chair on at least two invited lectures on international conferences about the topic of this thesis in Toulouse and Milano between famous and outstanding scientists around the world. Last but not least I want to thank him for his unrestricted love for dogs, which he rescues from their surely death after accident or mistreatment in Eastern Europe. Thank you very much!

Secondly I am indebted to and want to thank **PROF. DR. KONSTANTIN KARAGHIOSOFF** for innumerable pleasurable evenings working, discussing results, measuring NMR spectra as well as solving X-ray structures, and of course also for having fun in the university. He involved me in his chair over the last five years, inspired me on phosphorus chemistry during the master thesis and additionally took me on conference journeys to Budapest, Münster, Rennes and Regensburg. Thank you very much for your friendship and collegueship, and your endless enthusiasm even in hopeless situations. Finally, I thank him for the acceptance to be my second expertise at my doctoral thesis and second examinant of my thesis defense.

In this last context I also want to thank **PROF. DR. PAUL KNOCHEL**, **PROF. DR. HANS-CHRISTIAN BÖTTCHER** and **PROF. DR. EM. WOLFGANG BECK** for their acceptance and attendance to my thesis defense.

DR. JÖRG STIERSTORFER is thanked for many inspiring discussions about my topic, informations about competing research groups, organising group trips and other events, and finally for having a lot of fun during those. **DR. BURKHARD KRUMM** is thanked for safety advices, for multinuclear NMR measurements, and his delicious garden fruits.

MRS. IRENE SCHECKENBACH is thanked gratefully for solutions of nummerous bureaucratic barriers. She often made things less complicated and easier to handle. She is indispensable for the whole group. I also want to thank her for her unlimited love for all kinds of animals.

MR. STEFAN HUBER is thanked a lot for introducing me in most of the research group facilities, measuring all the sensitivities and the amusing chats every time I met him. Thank you! **MR. PETER MAYER** is thanked for continuos and fast measurements of all standard NMR spectra over the years.

My former mentor and teacher during the Master thesis **DR. ANIAN NIEDER** and my mother **ANA KETTNER** are thanked gratefully for fast and careful proofreading and for correction of the English language. You facilitated the accomplishment of my annoying perfectionism, thus your recommendations led to a thesis of higher quality in form and content. Thank you!

My laboratory mates over the past years **DR. FRANZ MARTIN, DR. ANIAN NIEDER, DR. MAGDALENA RUSAN, THOMAS G. MÜLLER, VERA HARTDEGEN, MARTIN HÄRTEL, BENEDIKT STIASNY, JOHANN GLÜCK** and **MICHAEL WILLMANN** are thanked for the great working atmosphere and for tolerating the continuous music irradiation. Thanks a lot!

For collaboration within the topic of oxidisers I want to thank my colleagues and so-called oxidiser-team comprised of **QUIRIN J. AXTHAMMER, REGINA SCHARF, DR. RICHARD MOLL** and **SEBASTIAN F. REST**. For introducing me into the world of theoretic and computational chemistry and for her friendship from my first day on within the working group I thank **CAMILLA EVANGELISTI**. In the context of good collaboration within the whole group I would also like to thank gratefully **CAROLIN PFLÜGER, DR. ALEXANDER PENGINEER, DR. ALEXANDER DIPPOLD, DENNIS** and **DR. NIKO FISCHER, PHILIPP SCHMID, THOMAS REICH, CHRISTINA HETTSTEDT, DR. ANDREAS ECKART, TOMASZ G. WITKOWSKI, ANDREAS PREIMESSER, PHILIPP SCHOPF, MAURUS VÖLKL, JÖRN MARTENS, DÁNIEL IZSÁK** and **TOBIAS HERRMANN**. You made research and teamwork more interesting, easier and sometimes even rather amusing. Thanks to all of you!

Regarding research and teamwork I also want to thank my Bachelor, Master and research students over the years, which are **LEONHARD KADE, DR. MANUEL JOAS, JORGE DUHAUTPAS, CHRISTOPH ZOLLER, BIANCA AAS, THOMAS G. MÜLLER, JOHANNES FEIERFEIL, SWETLANA WUNDER** and **MICHAEL WILLMANN**.

My colleagues, fellow students and friends who accompanied me during at least the last five years are thanked for their tolerance, patience and friendship. Thanks to **CAMILLA EVANGELISTI, DR. ANIAN NIEDER, MARTIN HÄRTEL, MICHAEL FELLER, MANUEL SCHICKINGER, KATHY BEYER, FELIX MEYNER, MICHAEL WILLMANN, SWETLANA WUNDER, DR. ANDREAS ECKART, DR. SEBASTIAN KÖCK, DR. STEFAN CRETNIK, DR. IMMANUEL STAHL, ANDREW WHITNEY-STEEL, STEFFEN ROHBATSCHER, SARAH BURGHARDT, DR. OLIVER SCHEICKL, ERIC MASCALL, MIRIAM KRAUSE, SCARLET RICHTER, STEPHAN SLIWENSKI, DR. ALWIN REITER, DR. FLORIAN HINTERHOLZINGER, DR. THOMAS J. KIMBROUGH, TIMO KERN, RALPH HERING, ANNA FRANZ**, and all the others... Thank you!

I am deeply indebted to and thank my parents and whole family **ANA, ERWIN, LILIAN** and **LUNA KETTNER**, who made this thesis possible, who beared my moods, and always are there when I need them. I love you!

For her love, friendship, helpfulness and not finally her patience with me I thank my beloved girl **ANGELA ALKOFER**, the only person on this planet that may (sometimes) calm me down.

TABLE OF CONTENTS

SCOPE.....	10
I GENERAL INTRODUCTION	11
1 Milestones and Strategies in the Development of Energetic Materials	11
2 Brief History of the Development of Space Rockets	15
3 Classification of Energetic Materials	16
4 Definitions all around Solid Rocket Composite Propellants.....	20
5 Motivation: Ammonium Perchlorate's Uses and resulting Problems	22
6 Requirements for and Challenges in the Development of new Oxidisers	25
7 Objective Target.....	26
9 References	27
II SUMMARY	29
III RESULTS AND DISCUSSION	32
Chapter 1: The Chemistry of <i>N</i>-Methylnitramine	33
1.1 Introduction	34
1.2 Syntheses.....	35
1.3 NMR Spectroscopy	39
1.4 Vibrational Spectroscopy	41
1.5 X-ray Diffraction.....	42
1.6 Physical, Chemical and Energetic Properties	57
1.7 Summary, Conclusions and Outlook	62
1.8 Experimental Section	64
1.9 References	74
Chapter 2: Asymmetric Carbamate Derivatives	77
2.1 Introduction	78
2.2 Syntheses.....	81
2.3 NMR Spectroscopy	83
2.4 Vibrational Spectroscopy	84
2.5 X-ray Diffraction.....	85
2.6 Physical, Chemical and Energetic Properties	96
2.7 Preliminary Qualitative Burning Test of TNE-NAP-Nitrocarbamate	99
2.8 Theoretical Evaluation of the Energetic Properties of DNDA-4 as Plasticiser	100
2.9 Summary, Conclusions and Outlook	102
2.10 Experimental Section	103
2.11 References	107

Chapter 3: Polynitrotetrazoles	111
3.1 Introduction	112
3.2 Syntheses	113
3.3 Multinuclear NMR Spectroscopy.....	115
3.4 Vibrational Spectroscopy	117
3.5 X-ray Crystal Structures	118
3.6 Physical, Chemical and Energetic Properties.....	133
3.7 Summary, Conclusions and Outlook.....	136
3.8 Experimental	138
3.9 References	143
 Chapter 4: Energetic Bi-Oxadiazoles.....	 147
4.1 Introduction	148
4.2 Syntheses	149
4.3 Multinuclear NMR Spectroscopy.....	151
4.4 Vibrational Spectroscopy	154
4.5 X-ray Crystal Structures	155
4.6 Physical, Chemical and Energetic Properties.....	165
4.7 Computational Evaluation of the Energetic Performance of 5,5'-Bi-(2-Polynitromethyl-1,3,4-Oxadiazoles)	168
4.8 Summary, Conclusions and Outlook.....	171
4.9 Experimental Section	173
4.10 References	176
 IV GENERAL PROCEDURES.....	 181
1 General Synthetical Methods	181
2 Chemicals	181
3 Analytical Methods and Facilities	181
4 X-ray Diffraction Measurements.....	183
5 Computational Details and Thermodynamic Background	183
6 References	185
 V APPENDIX	 188
1 Abbreviations	188
2 List of Compounds Prepared in the Present Thesis.....	189
3 List of Publications.....	191

SCOPE

Part I of this thesis represents the general introduction. It starts with an historical overview about energetic materials and strategies in their improvement followed by the historical beginnings of space rocket development. The general classification of energetic materials is described then, leading into the topic of solid rocket composite propellants with important definitions. Furthermore, it covers the conceptual formulation and objectives of this thesis.

Part II is a brief summary of the highlights worked out in the present thesis.

Part III contains the results obtained during this dissertation together with their discussion. It comprises four chapters according to the chemistry applied and the publications that arised from each topic:

Chapter 1 consists of two parts: the salts of *N*-methylnitramine and energetic building blocks derived from *N*-methylnitramine, which will be used in the following chapters.

Chapter 2 describes addition reactions of an isocyanate derivative with polynitro alcohols furnishing carbamates that were further nitrated to the corresponding nitrocarbamates.

Chapter 3 connects similar polynitro of the previous chapter with the building block tetrazole yielding powerful, oxygen- and nitrogen-rich compounds.

Chapter 4 uses bi-oxadiazoles as connecting functionalities for polynitromethyl groups furnishing compounds with outstanding densities and good propulsive performance.

Part IV includes the general procedures applied in the present work including the standard synthetic procedures, analytical methods and computational details.

Part V constitutes the appendix to this thesis with abbreviations and a list of newly prepared compounds.

I GENERAL INTRODUCTION

1 Milestones and Strategies in the Development of Energetic Materials

The literature references agree that the beginning of the development of energetic materials starts with the accidental discovery of *black powder* in China at about 220 BC. In Europe it was established at least in the 13th century, when the English monk ROGER BACON in 1249 and the German monk BERTHOLD SCHWARZ in 1320 respectively started to investigate the properties and behaviour of black powder. Its composition was permanently changed and the best ratio of oxidiser and fuels was found to be 75% potassium nitrate, 10% sulfur and 15% charcoal.^[1] Then it was finally introduced into the military world, where it was introduced as propellant charge for smaller and later also for large calibre guns.^[2] As the time bar shows (Figure 1), until the 19th century this explosive mixture remained the only propellant for all kinds of firearms.

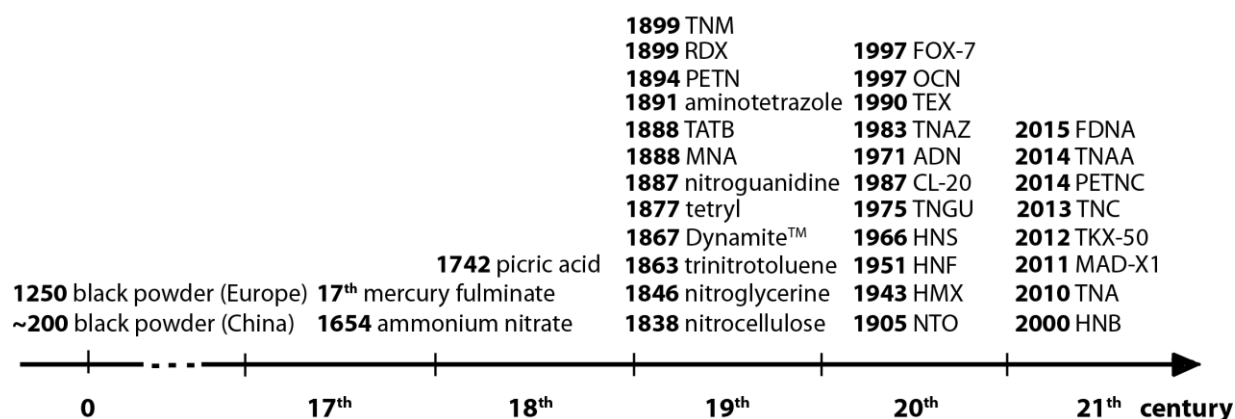


Figure 1: Time bar of energetic material inventions.^[3] Abbreviations: TNM trinitromethane, RDX hexogen, PETN pentaerythritol tetranitrate or nitropenta, TATB triaminotrinitrobenzene, MNA methylnitramine, tetryl trinitrophenylmethylnitramine, FOX-7 2,2-dinitroethene-1,1-diamine, OCN octanitrocubane, TEX 4,10-dinitro-2,6,8,12-tetraoxa-4,10-diazaisowurtzitane, TNAZ 1,3,3-trinitroazetidine, ADN ammonium dinitramide, CL-20 hexanitroisowurtzitan, TNGU or SORGUYL tetranitroglycoluril, HNS hexanitrostilbene, HNF hydroxylammonium nitroformate, HMX octogen, NTO 3-nitro-1,2,4-triazol-5-one, FDNA fluorodinitroamine, TNAA tetranitroacetimidic acid, PETNC pentaerythritol tetranitrocarbamate, TNC 2,2,2-trinitroethyl nitrocarbamate, TKX-50 dihydroxylammonium 5,5'-bitetrazole-1,1'-diolate, MAD-X1 dihydroxylammonium 3,3'-dinitro-5,5'-bis-1,2,4-triazole-1,1'-diol, TNA trinitramine, HNB hexanitrobutane dianion.

The technical progress of energetic materials began with the discovery of polynitro compounds. The first was *nitroglycerine* (NG) by the Italian chemist ASCANIO SOBRERO in 1846. Later, in 1863 IMMANUEL NOBEL together with his son ALFRED commercialised the NG production in a small factory near Stockholm, where it was synthesised by nitration of highly purified glycerine. NG was complicated to handle owing to its high impact sensitivity and unreliable initiation by black powder. In order to reduce the sensitivity NOBEL mixed 75%

NG with 25% kieselguhr and patented the mixture as "GUHR DYNAMITE" in 1867.^[4] Another invention of ALFRED NOBEL was the metal blasting cap detonator, in which he replaced the black powder with *mercury fulminate* $\text{Hg}(\text{CNO})_2$,^[5] which was already known since the 17th century.^[2] In 1867 it was shown that mixtures of NG or dynamite with *ammonium nitrate* (AN) showed enhanced performance. After WW II manufacturers started to develop explosives which were waterproof and solely contained the less hazardous AN. The most prominent formulation was *Ammonium Nitrate Fuel Oil* (ANFO), which found extensive use in civil applications such as mining.^[1, 2]

Simultaneously with the investigation of NG several research groups worked on the nitration of cellulose to produce *nitrocellulose* (NC). In 1875 again ALFRED NOBEL discovered formulations of NC with NG that formed blasting gelatines upon further refinement.^[1, 2, 6]

In the following time many explosives on the basis of nitro-aromatic compounds were developed or re-investigated, such as *picric acid* (PA), first reported by GLAUBER in 1742, *trinitrotoluene* (TNT), *triaminotrinitrobenzene* (TATB) and *tetryl*. PA replaced black powder in nearly all military operations world-wide. Although pure PA can be handled safely, a drawback of PA is its tendency to form impact sensitive metal salts when in direct contact with shell walls. These *picrates* are primary explosives. This disadvantage was prevailed by the introduction of cast-able and press-able TNT. In the early 20th century TNT replaced PA almost completely and it became the standard explosive used in WW I. It still remains the most important explosive for blasting charges. A further famous explosive discovered at the end of the 19th century is *nitroguanidine* (NQ) that was first prepared by JOUSSELIN in 1887. Nowadays 50% of NQ is used with NG and NC in so-called triple-base propellants to reduce the muzzle flash (compare the propellants section of this general introduction).^[2]

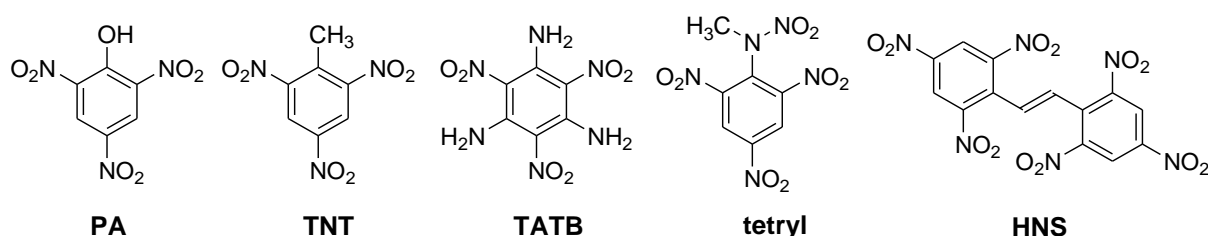


Figure 2: Molecular structures of explosives based on nitro-aromatic compounds.

The most widely used explosives in WW II beside TNT were *hexogen* (RDX) and *pentaerythritol tetranitrate* (nitropenta, PETN).^[7] RDX was first prepared in 1899 by HENNING, and PETN in 1894 by the Rheinisch-Westfälische SPRENGSTOFF AG in Cologne,^[8] both initially for medical use against angina pectoris owing to their widening effect of the blood vessels caused by nitric oxide formed within the human body by metabolism. Since PETN is more sensitive and chemically less stable than RDX, RDX was and still is the most used high explosive. PETN is used in grenades, blasting caps, detonation cords and boosters due to its great shattering effect.^[2, 7] In 2014 in the group of KLAPÖTKE the analogue *pentaerythritol tetranitrocarbamate* (PETNC) and salts thereof have been synthesised for the first time, which are considerably more thermally stable and less sensitive than PETN.^[9]

After WW II also *octogen* (HMX) became available, which can accrue as by-product from the synthesis of RDX by nitration of urotropine under certain conditions. Continuing to today, most high explosive compositions for military use are based on TNT, RDX and HMX.^[2]

Known and used until today as heat- and radiation-resistant secondary explosives are *hexanitrostilbene* (HNS) and *triaminotrinitrobenzene* (TATB). Both materials show excellent thermal stabilities above 300 °C and are therefore of great interest for applications in the oil industry (hot deep oil drilling) and for the US NAVY (fuel fires). They are produced commercially since 1966 (HNS) and 1978 (TATB), respectively.^[2, 10]

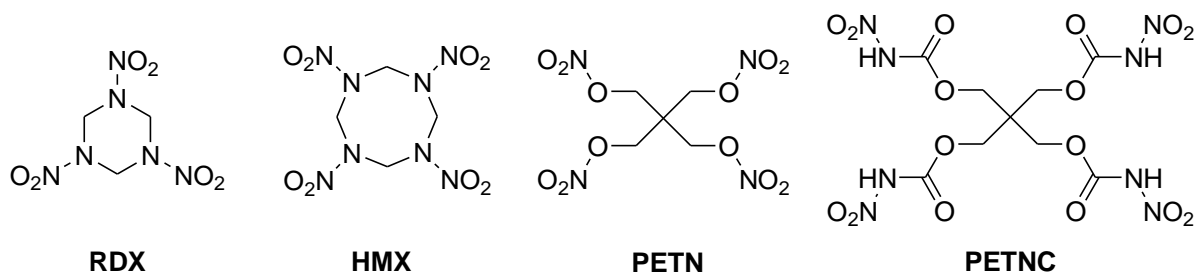


Figure 3: Molecular structures of cyclic nitramine based explosives RDX and HMX, and nitrate ester and nitrocarbamate based explosives PETN and PETNC.

A modern trend in energetic materials research became molecules with geometrically caused strain owing to their enhanced energy output not least due to their higher densities. The most prominent explosives based on strained ring or cage structures are *1,3,3-trinitroazetidine* (TNAZ), *hexanitroisowurtzitan* (CL-20) and *octanitrocubane* (ONC). TNAZ was first synthesised by ARCHIBALD in 1983 and consists of a strained four-membered ring backbone with both C-nitro and nitramine functionalities.^[11] CL-20 was first synthesised in 1987 by NIELSEN at the NAVAL AIR WARFARE CENTER (NAWF) in China Lake.^[12] It exhibits a density of about 2.00 g·cm⁻³, which explains the better performance compared with RDX and HMX. ONC has first been reported by EATON in 1997.^[13] While CL-20 is now already produced in 100 kg quantities (*e.g.* by SNPE, France or Thiokol, USA) on industrial pilot scale plants, ONC is only available on a milligram to gram scale because of its challenging synthesis.^[2]

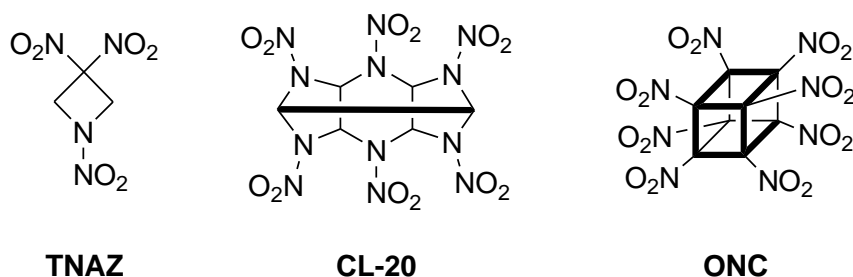


Figure 4: Molecular structures of TNAZ, CL-20, and ONC.

Two excellent explosives recently developed in the group of KLAPÖTKE are the dihydroxylammonium salts of 5,5'-bitetrazole-1,1'-diolate (TKX-50)^[14] and 3,3'-dinitro-5,5'-bis-1,2,4-triazole-1,1'-diol (MAD-X1)^[15] with superior insensitivity and higher performance than RDX. Both combine the strategies of using nitrogen-rich and non-fused five-membered ring systems with *N*-oxides for achieving enhanced densities. Their molecular structures are depicted in Chapter 4 of the present thesis.

Diaminodinitroethene (FOX-7)^[16] and *guanylurea dinitramide* (FOX-12)^[17] were synthesised and developed by LATYPOV at the SWEDISH DEFENCE RESEARCH AGENCY (FOI). Although neither FOX-7 nor FOX-12 meet RDX in terms of performance, both compounds are so more

insensitive than RDX that they might be of interest with respect to their insensitive munitions properties.^[2] These days they are produced by EURENCO BOFORS in Sweden.^[18]

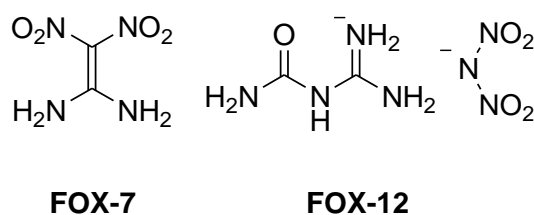


Figure 5: Molecular structures of FOX-7 and FOX-12.

For sure the simplest salt of dinitramine is *ammonium dinitramide* (ADN), which was first synthesised in 1971 at ZELINSKY INSTITUTE in Moscow, but was treated strictly confidential by the Russians. It was claimed in the Western hemisphere that ADN was used in the TOPOL M intercontinental ballistic missiles^[19] and that it was produced in ton-size quantities in the former USSR.^[20] In 1988 ADN was 're-invented' by BOTTARO and co-workers at the STANFORD RESEARCH INSTITUTE (SRI) in the US,^[21] and reported as an interesting new oxidiser that may have potential uses as environmentally benign rocket propellant ingredient and as a cationic phase transfer agent. In the early 90s the FOI started research on ADN for minimum smoke propellants for tactical missile applications. ADN is now produced by EURENCO BOFORS in Sweden.^[18] Please find more information about ADN in the propellant section of this general introduction.

The significance of the oxygen balance for energetic materials had been recognised long time before, but is even more important for the development of oxygen-carriers for solid rocket composite propellants. One step ahead from dinitramine stands *trinitramine* (TNA). Just by introducing one more nitro group the excellent oxygen balance of ADN becomes brilliant. It was experimentally detected for the first time in 2010 by RAHM and BRINCK.^[22] However, the compound is not stable even at low temperatures and could not be isolated. In contrast, the introduction of one fluorine atom instead of the nitro group into the dinitramide anion forming isolatable *fluorodinitroamine* (FDNA) accomplished by CHRISTE and co-workers for sure represents one of the latest milestones in the chemistry of dinitramine.^[23] However again, this compound may stay an academically interesting molecule owing to its relatively low stability. The carbon analogue molecule of the trinitramine is the *trinitromethanide* anion (TNM) derived from neutral nitroform and known for over a century.^[24] The most prominent representative salts of TNM may be *hydrazinium trinitromethanide* (HNF). Since its discovery in the early 1950s and patenting in 1965,^[25] a multitude of publications have appeared, showing that HNF is of continued interest particularly as ingredient for propellant formulations.^[26] Please find more information about HNF in the propellant section.

A higher carbon homologue of the trinitromethanide anion is *hexanitroisobutene* dianion (HNB), which was first presented by GAKH from the OAK RIDGE NATIONAL LABORATORY in 2000.^[27] Current investigations try to find cations capable to stabilise this unstable anion.

In the group of KLAPÖTKE mostly neutral oxygen-rich compounds were prepared in order to form an alternative for the environmental harmful ammonium perchlorate. An example is 2,2,2-trinitroethyl nitrocarbamate (TNC),^[28] and many more will be presented in the present thesis. Recently also SHREEVE and co-workers from the UNIVERSITY OF IDAHO presented a neutral oxidiser containing the trinitromethyl functionality, which is formally TNC minus

formaldehyde. *Tetranitroacetimidic acid* (TNAA) was prepared by nitration of the insensitive explosive FOX-7 described above.^[29]

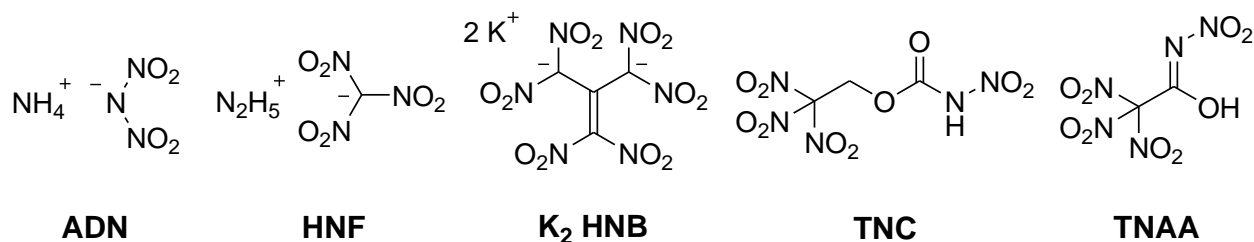


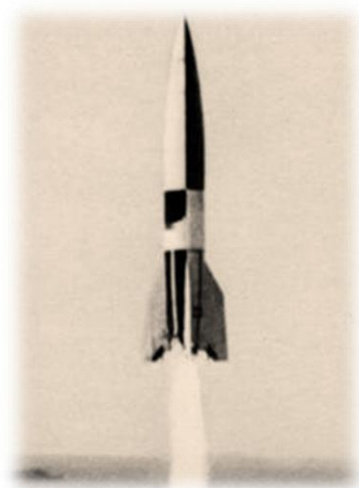
Figure 6: Molecular structures of ADN, HNF, K₂ HNB, TNC and TNAA.

2 Brief History of the Development of Space Rockets

The Father of Astronautics and Rocket Dynamics, KONSTANTIN EDUARDOVICH TSIOLKOVSKY (1857–1935), once said: *"The Earth is the cradle of humanity, but mankind cannot stay in the cradle forever. The solar system will be our play school."*^[30] Since his derivation of the "Formula of Aviation" in 1903 that establishes the relationship between the change in the rocket's speed, the specific impulse of the engine, and the mass loss of the rocket during its flight, the understanding of the physical fundamentals has improved enormously. The near future could see TSIOLKOVSKY's prophecy be proven correct after all, as humanity strives to develop new propellants and engines at an increasingly rate.

The American physicist ROBERT H. GODDARD (1882–1945) was the first to successfully start a liquid fuel rocket on March 16, 1926 – just 10 years before the German rocket pioneers started their research on rocket propulsion. The development of liquid rocket propellants was the basic requirement for modern astronautics. Unfortunately for GODDARD and his home country, at the time, his research did not attract the attention it deserved and so scientific breakthroughs were discovered especially in Germany, which got ahead rather fast in the development of military missiles.^[30]

The physicist HERMANN OBERTH (1894–1989), who was originally from Siebenbürgen, was inspired by the futuristic novel *"From the Earth to the Moon"* (*De la Terre à la Lune*, 1865) from JULES VERNE. He recognised that for the impetus of a rocket there would be no alternative of using the principle of repulsion engines. Independently from TSIOLKOVSKY he re-discovered the "Formula of Aviation" and developed the principle of the multistage missile.^[30] To prevent OBERTH from collaborating with the enemy the Germans nationalised him and forced him to develop missiles with his former student WERNHER VON BRAUN on the island of Usedom in 1938. VON BRAUN (1912–1977), a young engineering prodigy, was recruited to join the secret army program on research and development of long-range cannons in 1932. VON BRAUN still believed in exploring outer space with rockets, and did not initially see the military value of missile technology. However, his person is still discussed controversially as he was a member of the National Socialist German Workers' Party (NSDAP).^[31] The A4 rocket (*"Aggregat 4"*) developed by his team was the first rocket capable of reaching space.^[32] It was equipped with a warhead, re-named into V2 (*"Vergeltungswaffe 2"*), and repeatedly fired against enemy soldiers and civilians alike, starting with an attack against London on September 8, 1944. In addition to the British



The A4 rocket was the first rocket capable to reach space (84 km). It was misapplied by the Germans in WW II as the so-called V2 missile.

capital, Antwerp bore the brunt of the approximately 2500 V2 rocket attacks. All the same, the weapon was a tactical as well as strategic failure, used mainly in desperation to bluff and force the Allies into giving more favourable peace terms. During their occupation of Germany in 1944, US forces seized any remaining missiles, as well as detained scientists such as VON BRAUN, and used them as the cornerstone of their own rocket program. In 1959 his team became part of the NASA and developed the SATURN rockets in the scope of the APOLLO program.^[31, 33]

The Space Race between the Cold War rivals, the United States and the Soviet Union, the latter which also captured advanced German rocket technology and scientists had started. So even while having its roots in WW II terror weapons and a Cold War mutual-assured destruction mentality, rocketry has also lead the way into peaceful applications, providing humanity with previously unheard advances in science, communication and much more.^[33]

The first human-made object to reach the surface of the Moon was the Soviet Union's LUNA 2 mission, on September 13, 1959.^[34] Many more objects came after in the following years. The Space Race peaked with the lunar landing of the manned spacecraft APOLLO 11 on July 20, 1969 and the first human being NEIL ARMSTRONG stepping on the Moon's surface speaking the phrase that would become legend: *"That's one small step for [a] man, one giant leap for mankind."*^[35]

Since then outer space missions have become progressively multifaceted, and the requirements on chemical rocket propulsion for such undertakings grow with the rising distances and complexities of the missions. Therefore, military as well as civilian institutions make great efforts in research of new energetic materials in order to meet the future's demands even today.

3 Classification of Energetic Materials

The American Society for Testing and Materials defines an energetic material as *"...a compound or mixture of substances which contains both the fuel and the oxidiser and reacts readily with the release of energy and gas..."*^[36]

Today energetic materials are classified on the basis of their properties and the resulting uses into three major classes: *explosives*, *pyrotechnics* and *propellants*.^[37] Each of them can be divided into further subclasses.^[2] Explosives can be defined as chemical substances which are capable of propagating a chemical reaction within the material that releases gas, pressure and high temperature at certain speeds, capable of causing damage to the surroundings.^[2, 38] The class of explosives is further divided into primary and secondary explosives (Figure 7).

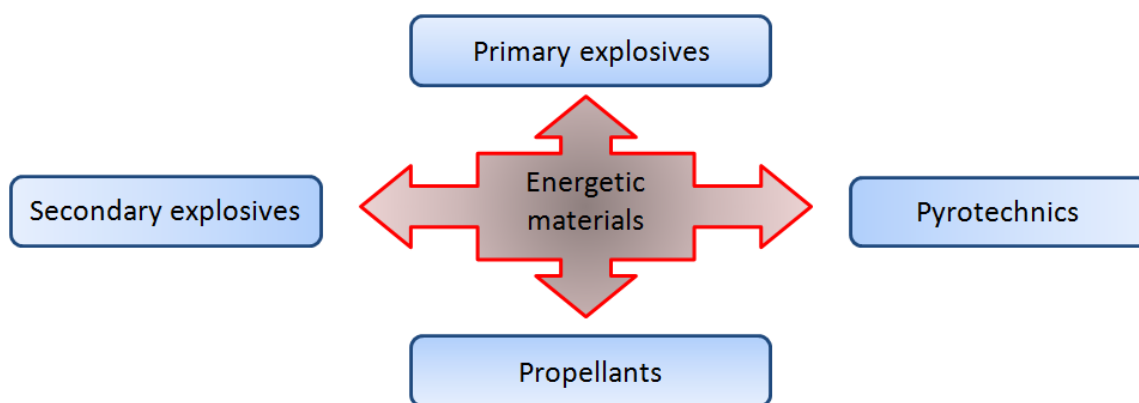


Figure 7: Classification of energetic materials.

Explosives

The sensitive class of *primary explosives* such as lead(II) azide $\text{Pb}(\text{N}_3)_2$, lead(II) styphnate $\text{Pb}(\text{C}_6\text{H}_3\text{N}_3\text{O}_6)_2$ or mercury(II) fulminate $\text{Hg}(\text{CNO})_2$ (Figure 8) can easily be set off by electric sparks, heat, friction and impact. They usually do not exhibit very high performance values (energy release per time), but their initiation leads to a very fast deflagration to detonation transition (DDT) with a shock wave that is capable to initiate a less sensitive charge (secondary explosive) of an explosive device. Therefore they are used in all sorts of igniters. Often their compositions include toxic heavy metal cations. Therefore investigations are driven towards less toxic, metal free as well as organic compounds with similar sensitivities for an easy ignition. Also the replacement of the toxic cations with less toxic metals like silver, copper, iron or even potassium is of current interest.^[2, 37]

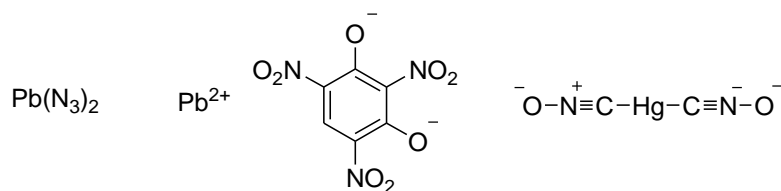


Figure 8: Commonly used primary explosives: lead azide, lead styphnate and mercury fulminate.

Secondary explosives such as TNT, RDX, HMX or CL-20 (Figures 2–4) cannot be ignited by the same external stimuli as primary explosives, since they are not only much more stable in terms of heat, friction, impact and electric spark, but also kinetically stable (meta-stable) compounds. Therefore they have to be ignited by much larger stimuli, such as the detonation shockwave of a primary explosive. Although their initiation requires much higher energies, secondary explosives reveal much higher detonation performances than primary explosives. Therefore their application field is widely spread through all kinds of military as well as civilian uses. Investigations on the development of new secondary explosives depend strongly on the application, but mainly focus on higher performance, less sensitivities and generally less toxicity.^[2, 10]

Pyrotechnics

Pyrotechnic compositions are supposed to emit light, generate smoke or produce heat during combustion. In general every pyrotechnic formulation contains a reducing and an oxidising agent. Moreover, they might contain colourants, smoke generators, primary charges and propellants. They are used in both civilian and military fields such as fireworks, signalling or tactical decoy flares. A rather long burning time, low toxicity, bright colours or dense smokes are the major requirements depending on purpose for new investigations.^[39]

Propellants

Also propellants are energetic materials consisting of one compound carrying both, oxidiser and fuel, or a mixture of these. They differ from primary and secondary explosives in that their prime objective is to deflagrate and not to detonate. For obtaining a large specific impulse I_{sp} , a high combustion temperature T_C and a small averaged mole weight of the gaseous combustion products is required. Propellants can be initiated by flames or sparks. By deflagrating, propellants build up relatively high pressures without the presence of a higher velocity shock wave. By conduction of the combustion products through a nozzle a mass flow is produced, which finally provides a propulsive force in order to move objects or vehicles. This might be gun bullets, firework rockets with a pyrotechnical load, tactical missiles sending secondary explosives in their warheads, or rockets carrying satellites or testing probes into space. The most famous and oldest propellant is black powder.^[2, 40]

The category of *propellants* can principally be divided according their state of mater into liquid and solid propellants (Figure 9). In this context also hybrid (solid fuel and liquid oxidiser) and gelled propellants (solids that become liquid under pressure or heat) should be mentioned here, but they will not be treated in the present thesis.

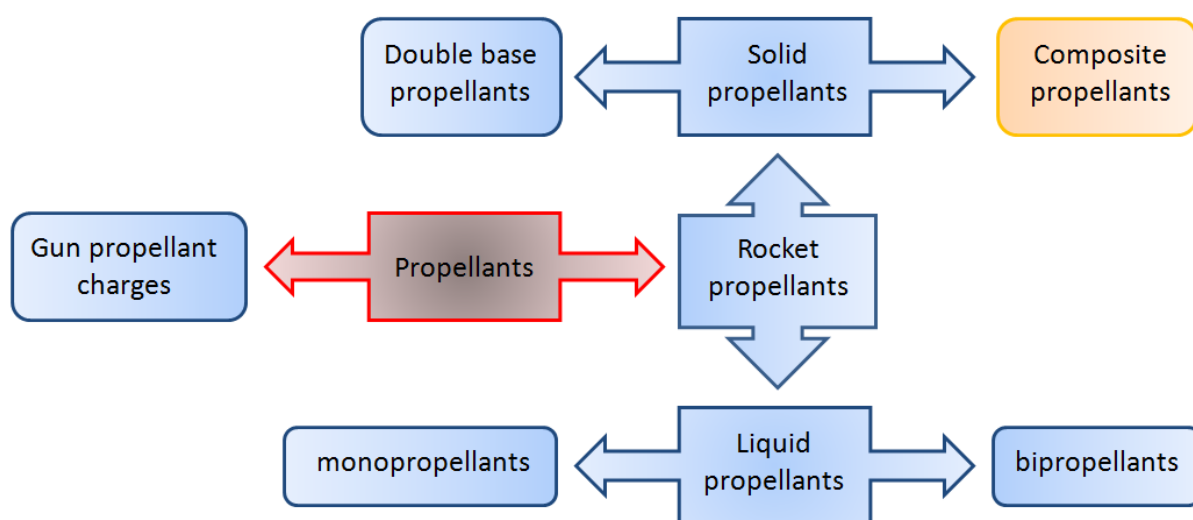


Figure 9: Classification of propellants into gun propellant charges and rocket propellants. The later can further classified according their state of matter into liquid and solid propellants.^[2] The present work deals essentially with ingredients for composite propellants.

Liquid propellants are mainly used in space exploration and technology.^[30] They can be distinguished into monopropellants and bipropellants. *Monopropellants* are endothermic liquids such as hydrazine (N_2H_4) and monomethylhydrazine (MMH), hydrogen peroxide (H_2O_2) or nitromethane (CH_3NO_2). They decompose exothermically in the absence of oxygen. As they possess a relatively small energy content and specific impulse they are only used in small missiles and satellites for correcting orbits, where no large thrusts but long storage times are necessary.^[40]

Hydrazines used as liquid fuels build hypergolic systems when mixed with various oxidisers such as N_2O_4 , HNO_3 or F_2 . These so-called *bipropellants* need to be transported in separated tanks and are further divided into cryogenic and storable bipropellants, or in accordance with their ignition behaviour in hypergolic and non-hypergolic mixtures. Cryogenic bipropellants such as compressed hydrogen (LH_2) and oxygen (LOX) can be used for throttleable propulsion engines. Hypergolic propellants are comprised mostly of oxidisers and reducing agents, which on contact react spontaneously in less than 20 ms, and ignite partly explosively.^[2]

Solid propellants can be distinguished according their homogeneity into two major classes: *Double- or triple-based propellants* and *composite propellants*. *Double base propellants* are used in smaller propellant charges, predominantly in hand firearms and mortars. They are usually comprised of nitrocellulose and nitroglycerine. To prevent the increased erosion and to reduce the muzzle flash caused by this mixture, in large calibre tank weapons nitroguanidine is added as a third ingredient for the reduction of the combustion temperature giving *triple-base propellants*.^[2, 40] *Composite propellants* will be emblazed in the next section since the main goal of the present work cares in particular about those.

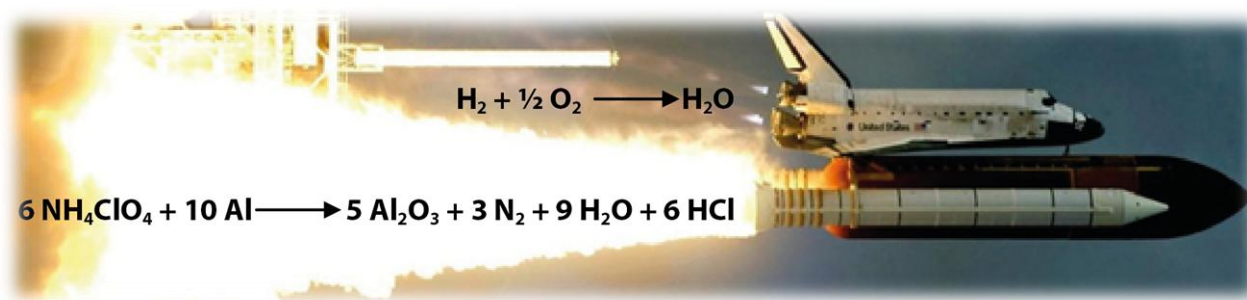


Figure 10: The SPACE SHUTTLE mission setup used a combination of solid and liquid propellants. For the initial lift-off the solid boosters (white tanks) are necessary in combination with a cryogenic liquid propellant mixture (huge dark tank). The solid boosters are comprised of an ammonium perchlorate composite propellant (APCP), and the cryogenic propellant tank carries liquid oxygen (LOX) and liquid hydrogen (LH_2). The orbital maneuvering subsystem (top) uses a hypergolic mixture of monomethyl hydrazine (MMH) and nitrogen tetroxide (N_2O_4).

4 Definitions all around Solid Rocket Composite Propellants

Composite propellants are based on a physical mixture of a metal powder as the reductive fuel and a solid oxygen-carrier or oxidiser for its combustion. These mixtures usually are embedded in a polymeric matrix, which also can contain burning rate catalysts in very small ratios and other energetic ingredients. Essentially all large solid rocket boosters that are meant to overcome Earth gravitation in order to reach outer space use this type of propellant.

Fuel and Oxidiser

Light metals like aluminium in high-power rocketry or magnesium in pyrotechnics, but also alloys with zinc and nickel are principally used as fuels. Aluminium (Al) for high-power rocketry brings along several advantages such as low costs, high burning temperatures and high energy of formation of the combustion product aluminium oxide (Al_2O_3), as well as a high availability. However, aluminium is tried to be substituted by even higher energy components such as metal hydrides, for instance alane (AlH_3). These are currently under investigation since they are qualified to increase the performance considerably.^[2]

The oxidiser in general is a compound with high oxygen content (see oxygen balance), which is capable to provide oxygen for the appropriate combustion of the fuel in an oxygen deficient environment. As solid oxidiser mainly ammonium perchlorate (AP) is used. Solid propellants comprised of Al and AP are known as ammonium perchlorate composite propellants (APCP) and are essentially used for all large solid rocket boosters.^[7, 40] AP deserves special attention and will be focused on in the motivation section.

Polymeric Matrices

These two above mentioned ingredients are embedded in a rubber-like binder such as polybutadiene derivatives that determines the propellants burning properties, protects the ingredients from all kinds of stimuli and additionally acts as secondary fuel. In the past mainly carboxy-terminated polybutadiene (CTPB) or polybutadiene acrylonitrile (PBAN) were used, which nowadays are gradually replaced by hydroxy-terminated polybutadiene (HTPB).^[41] Even energetic polymers like glycidyl azide polymer (GAP) are considered particularly for missiles to increase the performance once again.^[2] The advantages of HTPB versus formerly used PBAN lies in the curing process: while PBAN requires curing with epoxides or aziridines at increased temperatures for some days, HTPB can be cured within some hours at room temperature with diisocyanates, which also makes it more attractive for smaller rocket or missile types. Also the solid loading of HTPB is slightly higher than for PBAN increasing again the energy load and therefore the performance (Table 1).^[41, 42]

Table 1: Selected properties of HTPB versus PBAN ^[42]

	PBAN	HTPB
Specific Impulse I_{sp} [s]	262	264
Flame temperature [K]	3370	3560
Solids loading [%]	84–86	88–90
Aluminium content [%]	16–17	18–20
Cross linking agent	epoxides or aziridines	diisocyanates
Operating temperatures [K]	278–305	228–339
Hazard Classification	1.3	1.3

Oxygen Balance Ω

In general an oxidiser is a material with a positive value for its oxygen balance Ω . The positive value describes the ability of a CHNOX material (X = halogen) to form additional O_2 beside H_2O , N_2 , HX , CO/CO_2 during its combustion, which is then available for the oxidation of another material, the fuel. The absolute oxygen balances Ω , assuming the formation of CO_2 or CO at higher combustion temperatures according to the BOUDOIR Equilibrium can easily be calculated from the sum formula $C_aH_bN_cO_dX_e$ (X = Cl, F) according to the following equations:^[2]

$$\Omega_{CO_2} = dO - 2aC - \frac{1}{2}(b - eX) H \left(\frac{1600}{M} \right)$$

$$\Omega_{CO} = dO - aC - \frac{1}{2}(b - eX) H \left(\frac{1600}{M} \right)$$

It is mentionable that the combustion temperature T_C is considerably increased when aluminium is used as fuel [$\Delta H_f^0 (Al_2O_3) = 1676 \text{ kJ mol}^{-1}$],^[43] therefore Ω_{CO} assuming the formation CO may be of higher importance. In the present thesis also the Ω_{CO_2} assuming the formation CO_2 will be specified for compounds containing carbon atoms. Since the real oxygen balance Ω depends on the composition of the combustion products its value will range between these theoretical Ω_{CO} and Ω_{CO_2} according to an ideal combustion. For compounds without carbon atoms Ω_{CO} and Ω_{CO_2} show the same value Ω .

Specific Impulse

The performance of a propellant mixture depends on its specific impulse I_{sp} . It can be described according to the following equation as a function of the thrust F during the burning time t_b divided by the propellant mass m and the Earth gravitation factor g_0 for standardisation and setting the unit to seconds [s]:^[2]

$$I_{sp} = \frac{1}{m \cdot g_0} \int_0^{t_b} F(t) dt_b$$

For the chemistry it is more important that I_{sp} is proportional to the square root of the combustion temperature T_C divided by the average molecular mass of the gaseous combustion products M according:^[2]

$$I_{sp} \propto \sqrt{\frac{T_C}{M}}$$

Formula of Aviation

The ideal rocket equation was first deployed by TSIOLKOVSKY in 1903, and later independently also by OBERTH and GODDARD. It considers the simplest case of a self-accelerating vehicle with a starting mass m_0 by expelling parts of its mass with high speed and move due to the conservation of momentum while neglecting gravity and friction. By

doing so it describes the fundamental motion of a vehicle accelerated through a continuous expulsion of a working mass (propellant). The engine ejects the working mass with a constant velocity v starting from Earth with a velocity of zero. The Earth gravitation factor g_0 , which is dependent on the changing altitude, has to be subtracted. Therefore, after time t the velocity u of the rocket corresponds to:

$$\Delta u(t) = v \cdot \ln \frac{m_0}{m_t} - \int_0^t g_0(t') dt'$$

This means, although the ejection of the propellant has a constant velocity v , with decreasing mass Δm and Earth gravitation g_0 the rocket is accelerated with increasing altitude.^[2]

5 Motivation: Ammonium Perchlorate's Uses and resulting Problems

As mentioned above ammonium perchlorate composite propellants (APCPs) are common in all high-power rocketry. AP has an excellent oxygen balance Ω of 34 %, and the common used mixtures with about 15–20 % aluminium embedded in about 10–15 % inert polybutadiene binders are capable to provide specific impulses I_{sp} of up to 264 s. Therefore AP continues being the solely used oxidiser for solid rocket boosters and missiles. Beside high-power and amateur rocketry, and due to its simplicity, reliability and high I_{sp} APCPs are also used for pyrotechnic devices like warning flares and fireworks, find application in air bag inflators and aircraft injection seats (Figure 11). Moreover, AP appears as a contaminant in agricultural fertilisers. Owing to its high stability and solubility in water it has been widely distributed in surface and groundwater systems world-wide and particularly in the south-western US due to its multiple applications.^[2, 44]



Figure 11: Applications of AP. Top left to right: US warning flares, injection seat test, DELTA II boosters (picture taken with courtesy of the NASA). Bottom left to right: fireworks, air bag inflator, High-Power Rocketry launch meeting at the Black Rock Desert in Nevada.

Only very few incidents are known that can be ascribed to the use of AP, which again reflect the reliability of this material on the one hand, but also represent its explosive hazard on the other hand (Figure 12):

- The CHALLENGER Tragedy in 1986 is only indirectly connected with the deficient use of AP, because the actual reason was a fracture in the sealing ring of one of the SPACE SHUTTLE solid rocket boosters. However, the rocket exploded violently leading to the death of its seven crew members.^[45]
- The PEPCON Disaster in 1988 can directly be connected to the explosive hazard and oxidising properties of AP, which was stored in amounts of about 4000 t at the production site and led to the devastating explosion of the whole production plant.^[46]
- The explosion of an unmanned DELTA II rocket with nine solid rocket boosters in 1997, which again can be attributed to a defective rocket assembling.^[47]



Figure 12: Prominent accidents during the use of AP. Left to right: Crack in the sealing ring of SPACE SHUTTLE solid rocket booster and following CHALLENGER explosion*, PEPCON Disaster, DELTA II explosion*. *) Pictures taken with courtesy of the NASA.

Unluckily this very cheap salt AP has been detected as toxic, not least due to its solubility. In vertebrates the perchlorate anion competes with iodide for the iodide binding sides of the thyroid gland due to a similar diameter (iodide 2.11 Å, perchlorate 2.25 Å).^[48] This leads to dysfunction and affects both growth and development. Also amphibians' normal pigmentation and growth is disturbed by exposure to AP. Furthermore, AP might be toxic to a large number of maritime life forms of unknown degree (Figure 13).^[49]

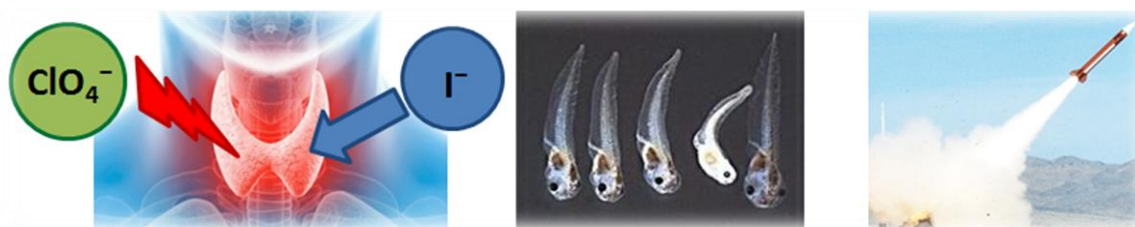


Figure 13: Problems of AP. Left to right: Competition of perchlorate and iodide on the thyroid gland binding sides. *Xenopus* embryos exposed to different concentrations of AP with the control sample on the right side. Visible expulsion of the MIM-104A PATRIOT launch.

Additional problems are caused by APCPs combustion products, most likely hydrogen chloride, which is formed in large quantities during combustion and may cause acid rain formation. Chlorine containing compounds are potentially hazardous for ozone depletion.^[50] A further disadvantageously aspect of APCPs is the visible and detectable expulsion (Al_2O_3) particularly for tactical missiles.^[51] For instance, the first MIM rockets of the PATRIOT system and several other missiles used APCPs based motors until being replaced by smoke-reduced motors (Figure 13).^[52]

Perchlorate free compounds, which are considered as alternatives for AP, are capable to overcome some these harms, but new inconveniences arise from them:

- Ammonium nitrate (AN) has a high Ω of 20.0 %, and is easily available and very cheap. However, this salt shows slight hygroscopicity, and its various polymorphs can result in burning rate problems due to cracks in the resulting propellant formulations. Phase-stabilised ammonium nitrate (PSAN) is capable to overcome the later.^[53] However, in general any AN-based propellant cannot provide the high energy output produced by APCPs.
- Ammonium dinitramide (ADN) shows a very high Ω of 25.8 %, but its low thermal stability of $T_{\text{dec}} = 127\text{ }^\circ\text{C}$ is a critical subject for application. Currently 1 kg of ADN costs about 4000 Euro.^[18]
- Another rather expensive research chemical is hydrazinium nitroformate (HNF). It contains one carbon atom and shows a high Ω_{CO} of 21.8 % and a moderate Ω_{CO_2} of 13.1 %. In formulations it burns very rapidly and with a very high combustion efficiency. But also this material suffers from a low thermal stability of $T_{\text{dec}} = 129\text{ }^\circ\text{C}$, and additionally from a high friction sensitivity.^[25, 26] Furthermore, the use of the hydrazinium cation may be problematic due to the potential release of highly hazardous hydrazine caused by thermal stress or alkaline conditions.
- Generally hydroxylammonium salts such as the research compounds hydroxylammonium nitrate (HAN) or hydroxylammonium dinitramide (HADN) can increase the oxygen content of various ammonium salts. Often such salts show hygroscopicity, and also hydroxylamine has a mutagenic impact if released from the salt. It can convert the nucleic acid cytosine into uracil within the DNA. However, since uracil does not appear in the DNA, such errors are easily recognised in healthful organisms and repaired by DNA-repair mechanisms.

As described above, currently there is no fielded substitute for AP as oxidiser in solid rocket composite propellants. Consequentially scientific research world-wide is further driven towards environmentally more acceptable options as replacement or partially replacement of AP. At the same time these problems associated with the use of AP and the growing requirements for space missions are the motivation of the present thesis.

6 Requirements for and Challenges in the Development of new Oxidisers

The use of halogen-free CHNO materials that contain high amounts of oxygen and nitrogen achieved by highly nitrated compounds gain more and more interest since they mainly decompose into environmentally benign gaseous products. Many factors influence the development of suitable oxidisers. The primary factors include facility of synthesis procedure, high performance, low costs and hazards. In the group of PROF. KLAPÖTKE at the Ludwig-Maximilian University of Munich (LMU) also some general requirements as internal benchmark were defined, which novel oxidisers should fulfil. These are the following:^[2]

- High oxygen balance of $\Omega_{\text{CO}} \geq 25 \%$
- Density ρ as high as possible, best close to $2 \text{ g}\cdot\text{cm}^{-3}$
- High thermal stability, at least $T_{\text{dec}} \geq 150 \text{ }^{\circ}\text{C}$
- Low sensitivities towards impact (4 J), friction (80 N), and electrostatic discharge (0.1 J)
- Compatibility with fuel and binder systems
- Environmental acceptance
- Minimum number of synthesis steps
- Low vapour pressure

The challenge in the development of new oxidisers is – as for all energetic materials research – to find a good balance between performance and physical properties. In the case of oxygen-carriers for composite propellants this is the compromise between a high specific impulse and high oxygen balance on the one hand, and good thermal stabilities and low mechanical sensitivities on the other hand (Figure 14).^[54]

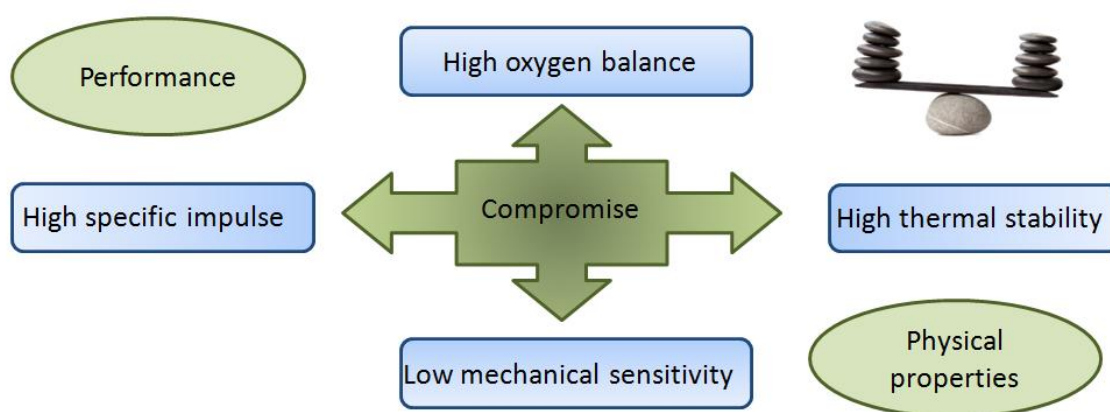


Figure 14: The challenge in the development of new oxidisers for composite propellants is the finding of a compromise between performance and physical properties depending on the application requirements.

7 Objective Target

The main objective of this thesis is the synthesis and investigation of new molecules, which contain a high amount of oxygen and therefore qualify themselves as oxidisers. These compounds should meet the challenge of finding the compromise between convincing performance and good physical and chemical properties, and thereby fulfil as much requirements as possible for new advanced oxidisers.

The general concept for the achievement of the main objective is the connection of various polynitro moieties with suitable building blocks as linkers to accomplish a high oxygen content of the resulting compounds. Promising and employed polynitro building blocks are the trinitromethyl functionality, the fluorodinitromethyl moiety, as well as the *N*-methylnitramine group. The search for chemical classes as appropriate linkers for these polynitro moieties shall be an essential topic.

Beside the development of strategies for easy syntheses also the chemical characterisation of the resulting compounds must be performed. This includes investigations of intra- and intermolecular interactions in the molecules, which are often present in polynitro compounds and have a general influence on the properties. In addition to the chemical characterisation, the physical properties of the materials should be determined. Finally, their energetic performance shall be examined to evaluate their suitability for energetic material applications, particularly as oxygen-carriers for solid rocket composite propellants.

9 References

- [1] a) J. R. Partington, *A History of Greek Fire and Gunpowder*, The Johns Hopkins University Press, **1999**. b) J. Gartz, *Vom griechischen Feuer zum Dynamit. Eine Kulturgeschichte der Explosivstoffe*, 1. Aufl., Mittler & Sohn, **2007**.
- [2] a) T. M. Klapötke, *Chemie der hochenergetischen Materialien*, de Gruyter, Berlin (Germany), New York (USA), **2009**; b) T. M. Klapötke, *Chemistry of High-Energy Materials*, 2nd Eng. ed., de Gruyter, Berlin (Germany), New York (USA), **2011**.
- [3] Freely adapted, corrected and expanded from: J. Stierstorfer, *Dissertation*, LMU München (Germany), **2009**.
- [4] A. Nobel, *US 78317 A*, **1868**.
- [5] A. Nobel, *US 141455 A*, **1873**.
- [6] a) A. Nobel, *US 141455 A*, **1873**; b) A. Nobel, *US 175735 A*, **1876**.
- [7] N. Kubota, *Propellants and Explosives*, Wiley, VCH, Weinheim, **2002**.
- [8] J. A. Zukas, W. P. Walters: *Explosive effects and application*, Springer, New York, **1998**.
- [9] Q. J. Axthammer, B. Krumm, T. M. Klapötke, *Eur. J. Org. Chem.* **2015**, 723–729.
- [10] P. W. Cooper, *Explosives Engineering*, 1st ed., Wiley-VCH, Weinheim, Germany, **1996**.
- [11] T. G. Archibald, R. Gilardi, K. Baum, C. George, *J. Org. Chem.* **1990**, 55, 2920–2924.
- [12] A. T. Nielsen, R. A. Nissan. D. J. Vanderah. C. L. Coon, R. D. Gilardi, C. F. George, J. Flippen-Anderson, *J. Org. Chem.* **1990**, 55, 1459–1466.
- [13] M.-X. Zhang, P. E. Eaton, R. Gilardi, *Angew. Chem.* **2000**, 112, 422–426.
- [14] a) D. Fischer, N. Fischer, T. M. Klapötke, D. G. Piercey, J. Stierstorfer, *J. Mater. Chem.* **2012**, 22, 20418–20422; b) T. M. Klapötke, N. Fischer, D. Fischer, D. Piercey, J. Stierstorfer, M. Reymann, *WO 2013026768 A1*, **2013**.
- [15] A. Dippold, T. M. Klapötke, F. A. Martin, *Z. Anorg. Allg. Chem.* **2011**, 637, 1181–1193.
- [16] N. Latypov, A. Langlet, U. Wellmar, *WO 9903818 A1*, **1999**.
- [17] N. Latypov, A. Langlet, *WO 9946202 A1*, **1999**.
- [18] EURENCO BOFORS AB, Karlskoga, Sweden, **2008**
- [19] M. B. Talawar, R. Sivabalan, M. Anniyappan, G. M. Gore, S. N. Asthana, B. R. Gandhe, *Combust. Explo. Shock* **2007**, 43(1), 62–72.
- [20] U. Teipel, *Energetic Materials: Particle Processing and Characterisation*, st ed., Wiley-VCH, Weinheim, **2004**.
- [21] J. C. Bottaro, P. E. Penwell, R. J. Schmitt, *J. Am. Chem. Soc.* **1997**, 119, 9405–9310.
- [22] M. Rahm, S. V. Dvinskikh, I. Furó and T. Brinck, *Angew. Chem. Int. Ed.* **2011**, 50, 1145–1148.
- [23] K. O. Christe, W. W. Wilson, G. Bélanger-Chabot, R. Haiges, J. A. Boatz, M. Rahm, G. K. S. Prakash, T. Saal, M. Hopfinger, *Angew. Chem.Int. Ed.* **2015**, 54(4), 1316–1320.
- [24] A. Hantzsch, A. Rinckenberger, *Chem. Ber.* **1899**, 32, 628–641.
- [25] J. N. Godfrey, *US 3196059*, **1965**.
- [26] G. Von Elbe, R. Friedman, J. Levy, B. Joseph, S. J. Adams, NASA, *AD-352186*, **1964**, pp. 26.
- [27] V. M. Khutoretsky, N. B. Matveeva, A. A. Gakh, *Angew. Chem. Int. Ed.* **2000**, 39(14), 2545–2547.
- [28] Q. J. Axthammer, T. M. Klapötke, B. Krumm, R. Moll, S. F. Rest, *Z. Anorg. Allg. Chem.* **2014**, 640(1), 76–83.
- [29] T. T. Vo, D. A. Parrish, J. M. Shreeve, *J. Am. Chem. Soc.* **2014**, 136(34), 11934–11937.
- [30] J. D. Clark, *Ignition! An Informal History of Liquid Rocket Propellants*, Rutgers University Press, New Brunswick, New Jersey, **1972**.

- [31] S. Brauburger, *Wernher von Braun – Ein deutsches Genie zwischen Untergangswahn und Raketenträumen*, Pendo, München, **2009**.
- [32] R. Blank, *Militär-geschichtliche Zeitschrift* **2007**, 66, 101–118.
- [33] R. Eisfeld, *Mondsüchtig. Wernher von Braun und die Geburt der Raumfahrt aus dem Geist der Barbarei*, Rowohlt, Reinbek bei Hamburg, **2000**.
- [34] E. Clark, *Soviets hit moon, data flow improves*, *Space Technol.*, 2(4), 4–6 Oct., **1959**.
- [35] http://www.nasa.gov/mission_pages/apollo/apollo11_40th.html (accessed: March 20, 2015)
- [36] www.astm.org.
- [37] J. Akhavan, *The Chemistry of Explosives*, 2nd ed., The Royal Society of Chemistry, Cambridge, **2004**.
- [38] J. F. Köhler, R. Meyer, A. Homburg, *Explosivstoffe*, 10. Aufl., Wiley-VCH Verlag GmbH & Co. KGaA, Weinheim, **2008**.
- [39] J. A. Conkling, *Chemistry of Pyrotechnics: Basic Principles and Theory*, Taylor & Francis Group, New York, **1985**.
- [40] G. P. Sutton, *Rocket Propulsion Elements*, 7th ed., John Wiley & Sons, **2001**.
- [41] H. G. Ang, S. Pisharath, *Energetic Polymers*, 1st ed., Wiley-VCH, Weinheim, **2012**.
- [42] T. L. Moore, *Assessment of HTPB and PBAN propellant usage in the US*, American Institute of Aeronautics and Astronautics, Inc., **1997**.
- [43] NIST Chemistry WebBook, <http://webbook.nist.gov/cgi/cbook.cgi?ID=C1344281&Mask=2#Thermo-Condensed> (accessed 26. Nov. 2014)
- [44] a) B. Gu, J. D. Coates, *Perchlorate: Environmental Occurrence, Interactions and Treatment*, Springer Verlag, New York, **2006**; b) W. E. Motzer, *Environ. Forensics* **2001**, 4(2), 301–311.
- [45] W. P. Rogers, *Report of the Presidential Commission on the Space Shuttle Challenger Accident*, Commission report, **1986**.
- [46] J. G. Routley, *Fire and Explosions at Rocket Fuel Plant in Henderson, Nevada*, Report 021 of the Major Fires Investigation Project conducted by TriData Corporation under contract EMW-8-4321 to the United States Fire Administration, Federal Emergency Management Agency, **1988**.
- [47] CNN interactive, *Unmanned rocket explodes after liftoff*, Jan 17, **1997**, <http://edition.cnn.com/TECH/9701/17/rocket.explosion> (accessed 26. Nov. 2014)
- [48] A. F. Holleman, *Lehrbuch der Anorganischen Chemie*, 101st ed., de Gruyter, Berlin, New York, **1995**.
- [49] a) E. D. McLanahan *et al.*, *Toxicol. Sci.* **2007**, 97(2), 308; b) R. E. Tarone, L. Lipworth, J. K. McLaughlin, *J. Occup. Environ. Med.* **2010**, 52(6), 653; c) J. Dumont, *The Effects of Ammonium Perchlorate on Reproduction and Development of Amphibians*, SERDP Project ER-1236, **2008**.
- [50] A. Makhijani, K. R. Gurney, *Mending the Ozone Hole: Science, Technology, and Policy*, Institute for Energy and Environmental Research, **1995**.
- [51] A. M. Mebel, M. C. Lin, K. Morokuma, C. F. Melius, *The Journal of Physical Chemistry* **1995**, 99, 6842–6848
- [52] J. W. R. Taylor, K. Munson, *Jane's All the World's Aircraft 1981-82*, Jane's Publishing Company Limited, London, **1981**.
- [53] A. E. Oberth, *US 5071630 A*, **1991**.
- [54] M. A. Kettner, T. M. Klapötke, *Electronic Proceedings of the Workshop on New Energetic Materials and Propulsion Techniques for Space Exploration*, Milano (Italy), 9–10 June, **2014**.

II SUMMARY

In the course of the present thesis, various new energetic materials based on polynitro compounds were synthesised and examined. Most of the compounds have a positive oxygen balance and therefore belong to the general class of oxidisers or oxygen-carriers. The applied concept of connecting polynitro functionalities with appropriate linkers led to the creation of promising compounds for further investigations, which may also be useful for energetic applications other than propellants. All novel materials have been characterised thoroughly by multiple analytical methods, including in most cases their X-ray molecular structures. In addition their physical properties such as thermal stability and sensitivities towards external stimuli were determined experimentally, and their energetic performances were computed based on quantum chemical calculations.

The results and discussion section consists of four chapters that are built up one on another presenting the development of the strategy for realisation of the drawn concept.

Chapter 1: The Chemistry of *N*-Methylnitramine

This chapter starts with the crystallisation of *N*-methylnitramine 126 years after its discovery. Several known alkaline, alkaline earth and transition metal salts as well as unknown nitrogen-rich salts resultant therefrom have been synthesised. For many of them their crystal structures were elucidated for the very first time. Particularly some of the nitrogen-rich salts derived from *N*-methylnitramine exhibit promising energetic properties that make these salts attractive for application as ingredients for propellants or for low vulnerability munitions. Moreover, 2-nitro-2-azapropyl compounds derived from *N*-methylnitramine have been synthesised and characterised chemically including the low temperature crystal structures of these mostly liquid compounds. Interesting insights have been obtained about the chemical behaviour from the structures of those compounds. These mostly rather reactive molecules represent the precursors for compounds synthesised in the following Chapters 2 and 3.

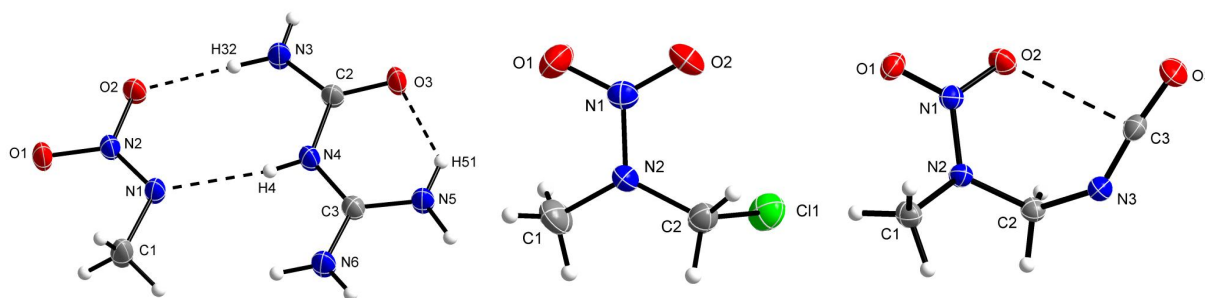


Figure 1: Low temperature X-ray structures of *N*-guanylnitramine with promising insensitive munition properties, and 2-nitro-2-azapropyl chloride and isocyanate as reactive building blocks for the following two chapters.

Chapter 2: Asymmetric Carbamate Derivatives

This chapter mainly is about addition reactions of several polynitroalcohols with 2-nitro-2-azapropyl isocyanate (Figure 1, right) synthesised in the previous chapter furnishing a series

of carbamate derivatives. These can be further nitrated at the nitrogen atom of the carbamate unit other than carbamate compounds, in which an electron with-drawing substituent prevents the electropositive substitution by the nitronium cation as shown during investigations prior to the present one. The resulting nitrocarbamates exhibit positive oxygen balances qualifying them as oxygen carriers for the appropriate combustion of an additional fuel in propellant formulations. Moreover, the interesting compound 1,3-dinitro-1,3-diazabutane derived from the precursors was formed during this study (Figure 2).

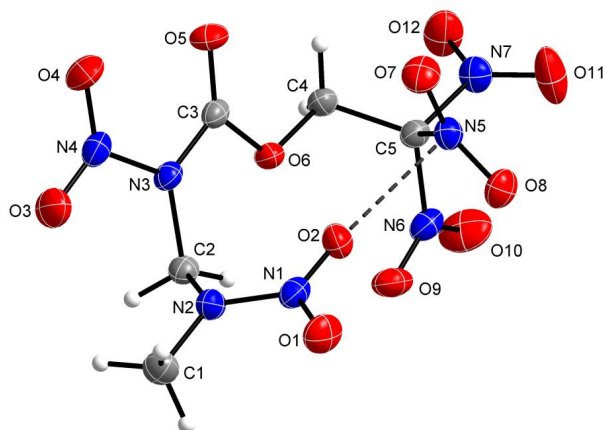


Figure 2: Low temperature X-ray structures of 2,2,2-trinitroethyl-(2-nitro-2-azapropyl)-nitrocarbamate with promising oxidiser properties.

Chapter 3: Polynitrotetrazoles

In this chapter a new linker for the previous polynitro functionalities is introduced. Here the trinitromethyl and 2-nitro-2-azapropyl moieties are linked through the nitrogen-rich five-membered tetrazole ring. This combination leads to oxygen-rich and very high performing materials with sensitivities in the range of primary explosives. However, the alkylation of the parent 5-polynitro-tetrazoles with 2-nitro-2-azapropyl chloride (Figure 1) overcomes the problematic acidities associated with polynitro-azoles. Moreover, the treatment of 5-(trinitromethyl)-tetrazole with strong nucleophiles like hydroxylamine promotes the separation of one nitro group and furnished the dihydroxylammonium 5-(dinitromethide)-tetrazolate showing an outstanding calculated specific impulse. Also the hitherto unknown crystal structure of the dipotassium salt of the latter dianion was determined. The compound shows energetic properties in the range of detonator materials with enhanced performance.

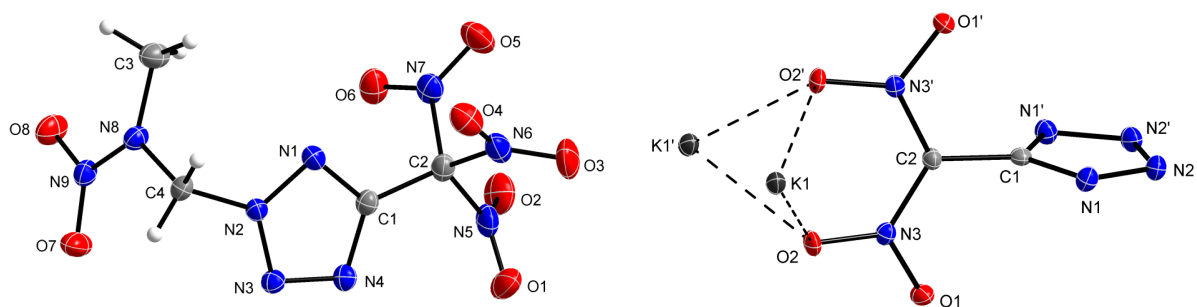


Figure 3: Low temperature X-ray structures of 2-(2-nitro-2-azapropyl)-5-(trinitromethyl)-tetrazole and dipotassium 5-(dinitromethide)-tetrazolate.

Chapter 4: Energetic Bi-Oxadiazoles

Chapter 4 combines two polynitromethyl functionalities with a five-membered ring system other than nitrogen-rich tetrazole or triazole. Generally, the introduction of oxadiazoles increases the oxygen content of the latter. In addition the use of a non-fused bicyclic ringsystem increases the density of the materials and therefore the energy output. The 3,3'-bi-(5-polynitromethyl-1,2,4-oxadiazoles) presented in this chapter exhibit densities in the range of the most dense energetic materials, and formulations with aluminium reveal calculated specific impulse values in the range of ammonium perchlorate composite propellants (Figure 3).

Moreover, this chapter shows how to transfer the applied concept into analogue bi-1,3,4-oxadiazoles by the synthesis of polyfluoromethyl compounds. Theoretical calculations on corresponding polynitromethyl analogues indicate that such materials may exhibit even higher performance than the synthesised bi-1,2,4-oxadiazoles.

Publications

Within the framework of the present thesis of new energetic oxidisers, several manuscripts have been published in European Journal of Inorganic Chemistry, Chemistry – A European Journal, and Chemical Communications. One of them was elected as frontispiece free of charge for Chemistry – A European Journal (Figure 4). The collected results of the whole team on energetic oxidisers have been presented by the author of this thesis on international conferences in Czech Republik, France and Italy. Please find the complete publication list at the end of this thesis.

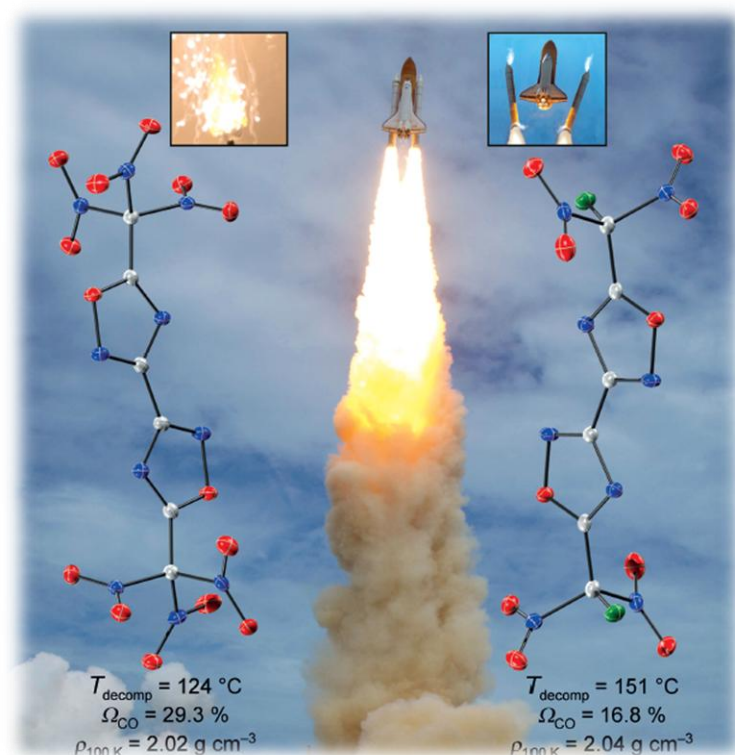


Figure 4: Frontcover of a publication in Chemistry – A European Journal: "3,3'-Bi-(1,2,4-oxadiazoles) Featuring the Fluorodinitromethyl and Trinitromethyl Groups", **2014**, 20, 7622–7631.

III RESULTS AND DISCUSSION

This section is divided into four chapters depending on the chemistry of the linker for connecting one or two polynitro functionalities and on the publications that arose from each topic. Each following chapter is comprised of a brief introduction and the sections syntheses, discussion of the NMR and vibrational spectroscopy as well as the X-ray crystal structures, energetic properties, conclusions with recommendations for future work, and the experimental section. Furthermore, some of the chapters include special sections such as theoretical calculations or burning tests.

Chapter 1: The Chemistry of *N*-Methylnitramine

CHRISTOPH ZOLLER and THOMAS G. MÜLLER are gratefully acknowledged for participation in this project associated with this chapter within the scopes of their Bachelor and Master degree's theses, respectively.

Chapter 2: Asymmetric Carbamate Derivatives

BIANCA AAS and CHRISTOPH ZOLLER are acknowledged for participation in this project associated with this chapter within the scope of their practical course of their Master degree studies and Bachelor thesis, respectively.

Chapter 3: Polynitrotetrazoles

SWETLANA WUNDER and JOHANNES FEIERFEIL are acknowledged for participation in this project associated with this chapter within the scopes of their practical courses of their Master degree studies.

Chapter 4: Energetic Bi-Oxadiazoles

SWETLANA WUNDER and TOMASZ G. WITKOWSKI are gratefully acknowledged for participation and collaboration in this project associated with this chapter within the scope of their practical course of the Master degree studies and doctoral thesis, respectively.

CHAPTER 1

THE CHEMISTRY OF *N*-METHYLNITRAMINE

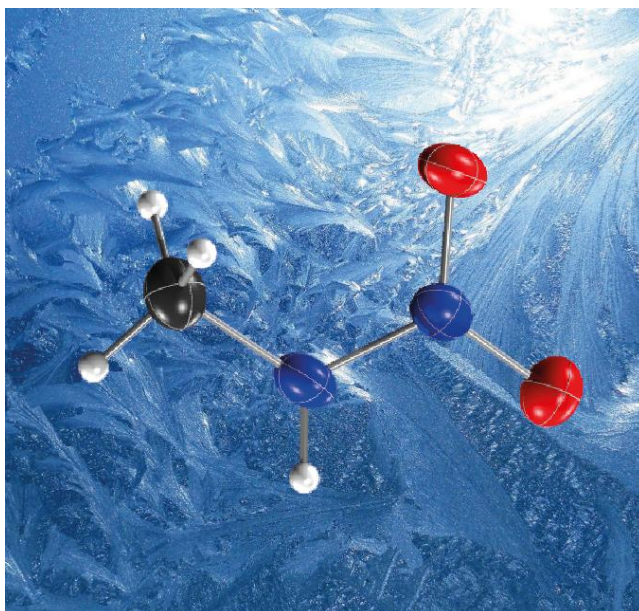
This chapter reports the hitherto unknown crystal structure of N-methylnitramine, its alkaline, earth alkaline and some transition metal salts as well as nitrogen-rich salts. Moreover, it describes the chemistry of N-methylnitramine towards 2-nitro-2-azapropyl derivatives. Within this scope the hitherto unknown crystal structures of important building blocks for the insertion of the 2-nitro-2-azapropyl moiety into energetic molecules as described in the following chapters were determined and are compared to their gas phase structures. The main part of this chapter is reproduced with permission from:

M. A. Kettner, T. M. Klapötke,* T. G. Müller, M. Sućeska

“Contributions to the Chemistry of *N*-Methylnitramine: Crystal Structure, Synthesis of Nitrogen-Rich Salts, and Reactions towards 2-Nitro-2-azapropyl Derivatives”^[1]

DOI: 10.1002/ejic.201402441

Copyright 2014 Wiley European Journal of Inorganic Chemistry



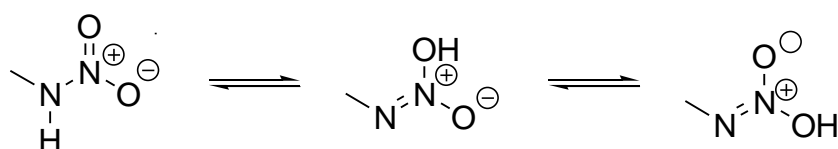
1.1 Introduction

In 1888 the Dutch organic chemist A. P. N. FRANCHIMONT reported for the first time the synthesis and isolation of *N*-methylnitramine, which represents the most simple aliphatic primary nitramine.^[2] He prepared *N*-methylnitramine by nitration of methylurethane with absolute nitric acid yielding methylnitrourethane and subsequent aminolysis.^[3] In the following years, FRANCHIMONT investigated the *N*-methylnitramine and described three tautomeric formulas, which are responsible for the acidity of *N*-methylnitramine (Scheme 1).^[4] *N*-Methylnitramine can also be prepared from the hydrolysis of an appropriate secondary nitramide such as *N,N'*-dinitro-*N,N'*-dimethylsulfamide, *N,N'*-dinitro-*N,N'*-dimethyloxamide or *N,N'*-dinitro-*N,N'*-dimethylurea.^[5]



Antoine Paul Nicolas
Franchimont (1844–1919)

Neat nitramide ($\text{H}_2\text{N}-\text{NO}_2$) is also known since 1894.^[6] Its crystal structure was investigated within the group of T. M. Klapötke in 2002.^[7] Further methylation of *N*-methylnitramine and the products *N,N*-dimethylnitramine and *N,O*-dimethylnitramine were also reported by FRANCHIMONT.^[8] In 1977 a Russian research group determined the gaseous phase structure of *N*-methylnitramine.^[9] The self-condensation reaction of *N*-methylnitramine by using formaldehyde in acidic media is also known. The reaction product 2,4-dinitro-2,4-diazapentane (DNDA-5) and mixtures of *N*-methylnitramine with DNDA-5 were investigated as energetic plasticizers.^[10] In the meanwhile this condensation can also be carried out in a continuous-flow microreactor for optimisation of the reaction rate.^[11] Investigations in the 1980s by the US NAVY tried to use *N*-methylnitramine as a possible RDX replacement, but the results revealed a lower performance than RDX and problematic for applications owing to the acidity of the primary nitramine.^[5, 12]



Scheme 1: Tautomerisation of *N*-methylnitramine.^[4]

N-Methylnitramine is a weak acid with a pK_A of 6.0.^[5, 13] Hence some alkaline and alkaline earth salts of *N*-methylnitramine are known. These salts were used to study the structural situation of primary nitramines, but were only characterised by IR, Raman and NMR spectroscopy.^[8b, 14] According to the literature the heavy metal salts of *N*-methylnitramine should be primary explosives.^[4b] But no detailed information on the performance or sensitivities of these salts are denoted. In addition to the metal salts the ammonium salt and alkylated ammonium derivatives are the only non-metal *N*-methylnitramine salts mentioned in the literature.^[8a, 15]

The MANNICH type reaction product of *N*-methylnitramine with formaldehyde is the secondary nitramine 2-nitro-2-azapropanol.^[16] This compound and halogenated derivatives like 2-nitro-2-azapropyl chloride^[17] represent important building blocks for the introduction of the secondary nitramine, for instance the alkylation of cyclic polyazoles (see Chapter 3).^[18]

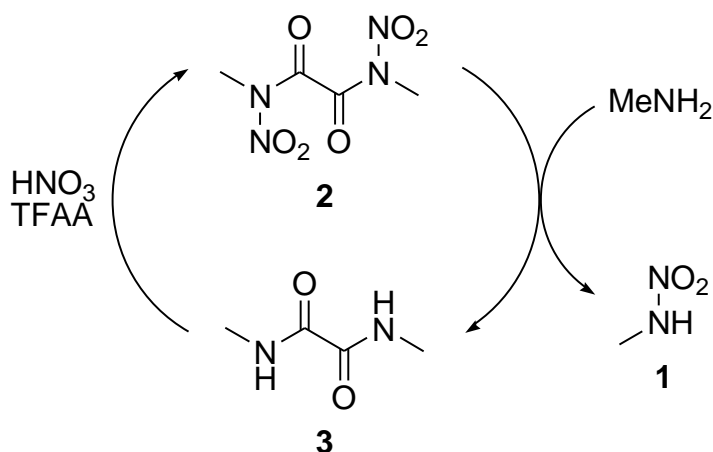
The reaction products show – not as a rule, but in most cases – clearly separated melting points from the decomposition points. This might be due to additional hydrogen bonds and attractive intermolecular interactions build up by the 2-nitro-2-azapropyl moiety in the crystal structures. Depending on which region the melting range is, such materials can be used for melt-castable applications or as energetic plasticisers. For example, a mixture of the above mentioned DNDA-5 with 2,4-dinitro-2,4-diazaheptane and 3,5-dinitro-3,5-diazaheptane (called DNDA-57) is used as plasticiser in propellant charges.^[10]

Further interesting energetic derivatives are 2-nitro-2-azapropyl azide (ANAP)^[18a, 19] and 1,1,1,3-tetranitro-3-azabutane,^[20] however, both show too high sensitivities towards external stimuli for any applications. Nevertheless ANAP represents a useful building block for the cycloaddition with alkynes towards 1,2,3-triazoles.^[19] Analogue 2-nitro-2-azapropyl amine is only mentioned once in the literature as its nitrate salt, furnished by the nitrolysis of tris-(2-nitro-2-azapropyl)amine.^[21] By reacting 2-nitro-2-azapropyl chloride with silver cyanate the corresponding isocyanate is formed,^[22] which represents a further building block for the syntheses of carbamates and urea derivatives. These reactions will be subject of Chapter 2.

This chapter summarises the syntheses of some alkali (Li, Na, K, Cs), alkali earth (Ca, Sr, Ba) and three transition metal salts (Ag, Zn, Cu) of general interest in energetic materials research. Moreover a series of nitrogen-based and -rich salts were synthesised and investigated. Nitrogen-rich molecules are of great interest in energetics research, as the formation of the nitrogen-nitrogen triple bond of elemental N₂ produces a very high energy output during the combustion of such materials.^[23] Furthermore the hitherto unknown crystal structures of the above mentioned 2-nitro-2-azapropyl derivatives were investigated and two of them compared to their gas phase structures.

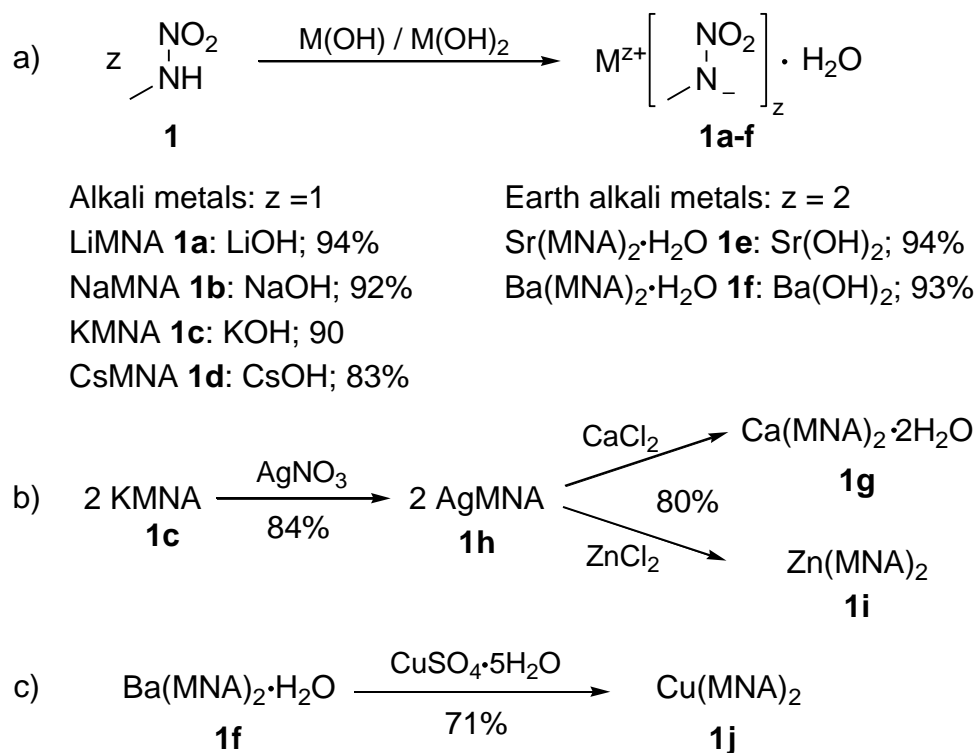
1.2 Syntheses

The title compound *N*-methylnitramine (MNA, **1**) was synthesised according to the literature known procedures from *N,N'*-dinitro-*N,N'*-dimethyloxamide **2** with aqueous ammonia^[24] or methylamine furnishing high yields and very high purities.^[10] In the reaction route that uses ammonia, oxamide is recovered by filtration but has to be methylated and nitrated in two steps to re-obtain the starting material *N,N'*-dimethyloxamide **3**. By using methylamine instead of ammonia, the methylation step can be skipped and therefore a faster reaction cycle is established as depicted in Scheme 2.^[10] However, by using this method, the yield of MNA (**1**) is slightly decreased from 92% (NH₃) to 88% (MeNH₂). During each reaction cycle, the loss of *N,N'*-dimethyloxamide **3** is about 20%. The nitration of **3** was performed in a mixture of trifluoroacetic acid and fuming nitric acid giving high yields (93%).^[10]



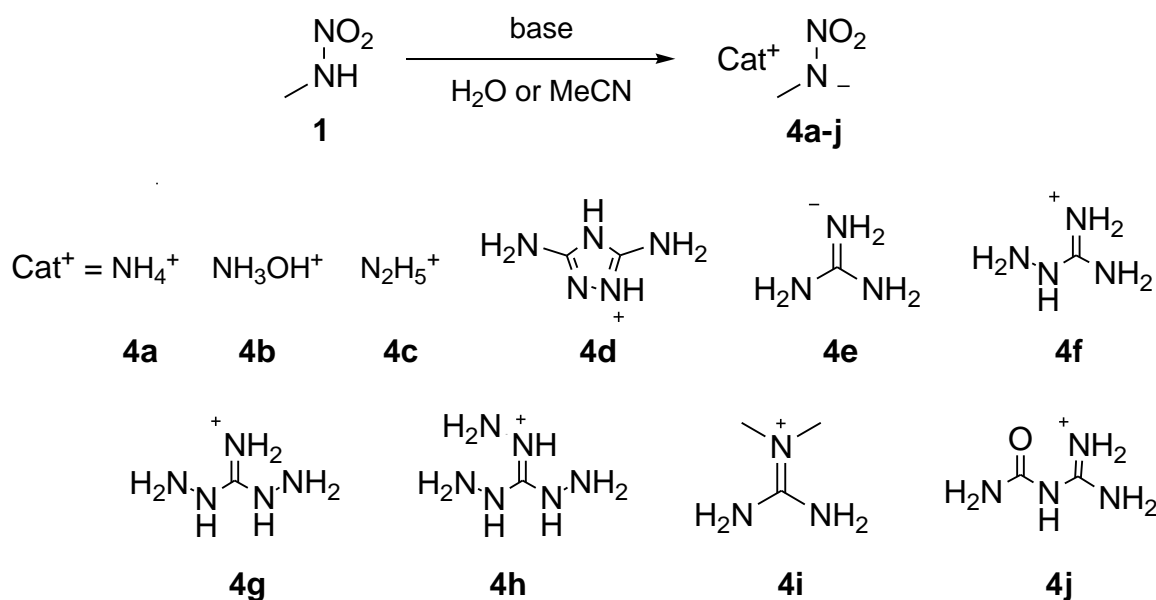
Scheme 2: Synthesis cycle for *N*-methylnitramine (**1**).^[10]

The alkaline salts LiMNA (**1a**), NaMNA (**1b**), KMNA (**1c**), CsMNA (**1d**) as well as the alkaline earth salts Sr(MNA)₂·H₂O (**1e**·H₂O) and Ba(MNA)₂·H₂O (**1f**·H₂O) were synthesised directly from MNA (**1**) using stoichiometric amounts of the corresponding metal hydroxides.^[16] They were obtained in high yields after recrystallisation from ethanol (Scheme 3a). The silver salt (**1h**) was formed by treatment of KMNA (**1c**) with an equimolar amount of silver nitrate under exclusion of light. Ca(MNA)₂·2H₂O (**1g**·2H₂O) and also Zn(MNA)₂ (**1i**) were prepared from this silver intermediate **1h** by ion metathesis reactions with CaCl₂ and ZnCl₂, respectively (Scheme 3b). Cu(MNA)₂ (**1j**) was synthesised from the barium salt **1f** (Scheme 3c). All salts were synthesised in aqueous solution. The molar contents of hydration water of the alkaline earth *N*-methylnitramides **1e–g** were determined by elemental analysis.



Scheme 3: Syntheses of a) alkali and alkali earth salts **1a–f**, b) Ag^I (**1h**), Ca^{II} (**1g**) and Zn^{II} (**1i**) salts, and c) Cu^{II} salt (**1j**).

The nitrogen-rich ammonium (NH_4MNA , **4a**),^[8a] hydroxylammonium (HxMNA , **4b**), hydrazinium (HyMNA , **4c**) and 3,5-diamino-1,2,4-triazolium (DATMNA , **4d**) salts were synthesised from the free acid MNA (**1**) by addition of the corresponding aqueous bases or in the case of 3,5-diamino-1,2,4-triazolium in acetonitrile (Scheme 4). These salts **4a–d** are all hygroscopic. Compounds **4a** and **4b** in particular were deliquescent and could not be isolated in pure form. They were only obtained in aqueous solutions. Nevertheless, compound **4c** and **4d** were isolated in high yields of 80 and 85% after recrystallisation from hot ethanol.

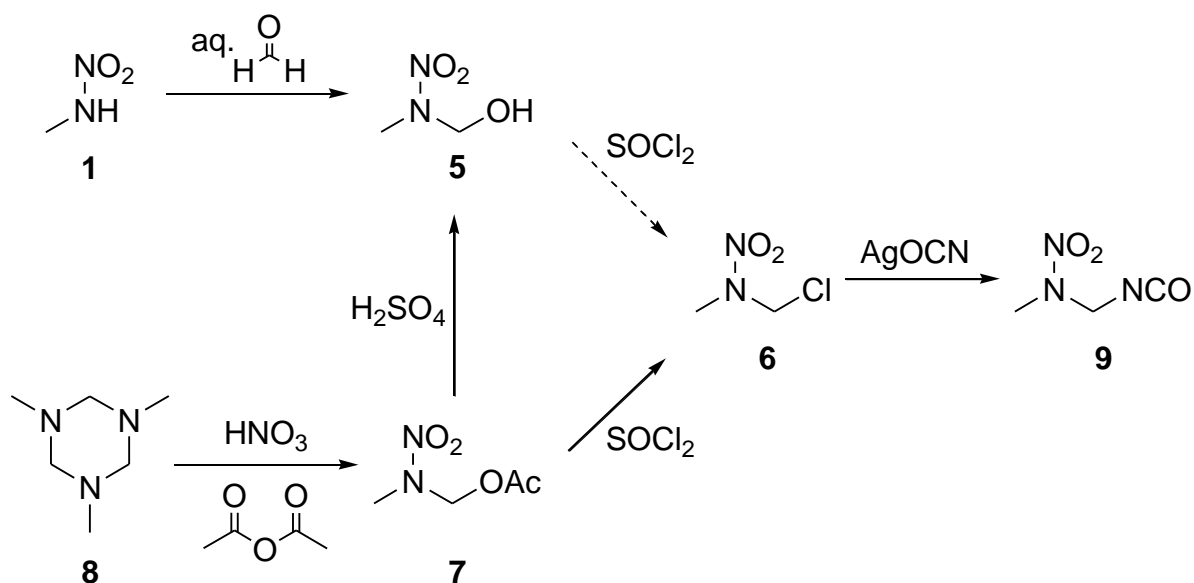


Scheme 4: Synthetic pathway towards the formation of nitrogen-rich salts **4a–j** by treatment of compound **1** with the corresponding bases.

Furthermore, nitrogen-rich salts from the guanidinium family were synthesised. Guanidinium (GMNA , **4e**) and aminoguanidinium *N*-methylnitramide (AGMNA , **4f**) were furnished from the reaction of the free acid MNA (**1**) with guanidinium carbonate and aminoguanidiniumhydrogen carbonate, respectively, just by moderate warming of the solutions with CO_2 evolution [the formation of CO_2 was confirmed by precipitation of BaCO_3 from a $\text{Ba}(\text{OH})_2$ solution]. Compounds **4e** and **4f** were obtained in high yields (90 and 85%) and purity after recrystallisation from hot ethanol. Diaminoguanidinium (DAGMNA , **4g**) and triaminoguanidinium *N*-methylnitramide (TAGMNA , **4h**) were synthesised from AgMNA (**1h**) with diaminoguanidinium and triaminoguanidinium chloride under exclusion of light by using the low solubility of the generated silver halides. After recrystallisation from hot ethanol both compounds were obtained in good yields of 70 (**4g**) and 77% (**4h**). Compounds **4g** and **4h** also show slight hygroscopic properties and were stored under argon atmosphere. The *N,N*-dimethylguanidinium salt (DMGMNA , **4i**, 90%) and the *N*-guanylurea salt (GuMNA , **4j**, 85%) were prepared from $\text{Ba}(\text{MNA})_2$ (**1f**· H_2O) by addition of *N,N*-dimethylguanidinium sulfate and *N*-guanylurea sulphate in water. Precipitated BaSO_4 was removed from the aqueous solution by filtration (Scheme 4).

The MANNICH type reaction of MNA (**1**) with formaldehyde yields 2-nitro-2-azapropanol (NAP-OH , **5**).^[16] The compound is unstable at ambient temperature in terms of its back-reaction to compound **1** and formaldehyde and should be kept in a freezer. Analogue 2-nitro-

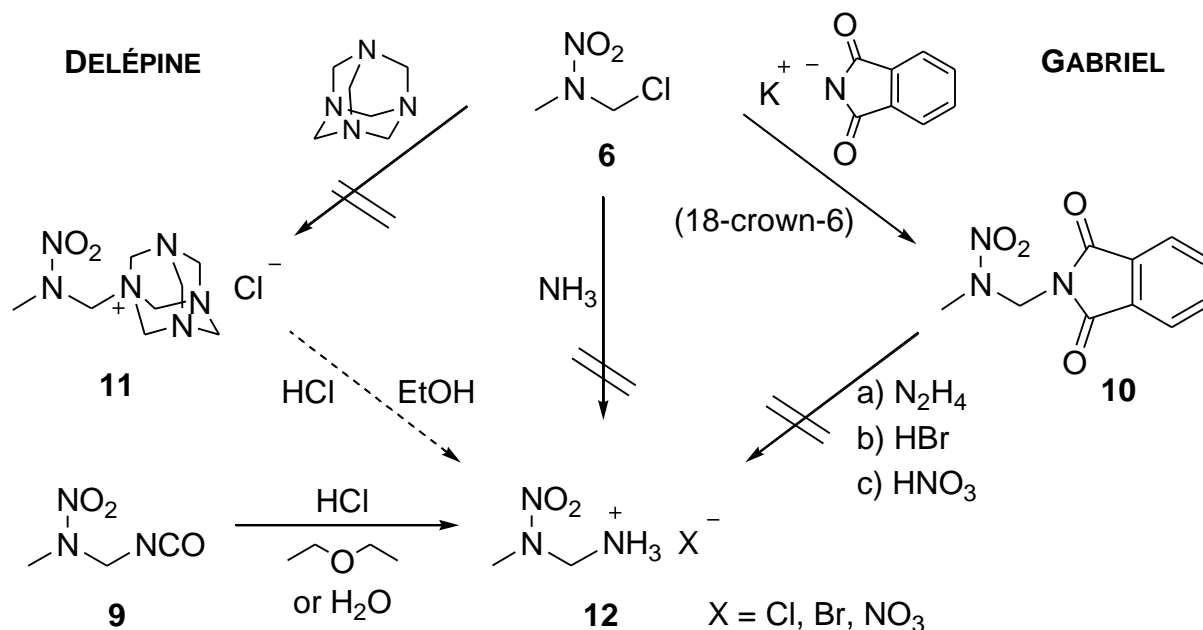
2-azapropyl chloride (NAP-Cl, **6**) is synthesised from corresponding 2-nitro-2-azapropyl acetate (NAP-OAc, **7**), which is furnished by nitrolysis of commercially available 1,3,5-trimethyl-1,3,5-triazahehexane (**8**).^[17] The conversion of compound **5** from **6** should also be possible, and is known in a similar way in the literature not affecting the secondary nitramine moiety.^[25] The treatment of NAP-Cl (**6**) with an excess of silver cyanate in an argon atmosphere and under exclusion of light furnishes 2-nitro-2-azapropyl isocyanate (NAP-NCO, **9**) that can be isolated by distillation (Scheme 5).^[22] Compound **9** is the key building block for the compounds synthesised in Chapter 2.



Scheme 5: Synthetic approach towards the NAP derivatives **5**, **6**, **7** and **9**: starting from MNA (**1**) or commercially available 1,3,5-trimethyl-1,3,5-triazahehexane (**8**), NAP-Cl (**6**) and NAP-NCO (**9**) are easily accessible (dashed arrow: not carried out in the present work).

Synthetic efforts towards NAP-amine **12** from **6** included – after the unsuccessful amination using ammonia – the DELÉPINE and the GABRIEL reaction.^[26, 27] The DELÉPINE reaction describes a convenient route to primary amines. In a first step the alkyl halide (**6**) reacts with urotropine via a S_N2 mechanism and should yield the quaternary amine **11**. The protection group can be cleaved by reaction with hydrochloric acid in ethanol.^[26] Unfortunately the nitro group of compound **6** was cleaved during refluxing with urotropine as proved by a ^{14}N NMR measurement. Hence, this reaction condition in combination with the basicity of urotropine promoted the decomposition of the nitramine group. Another convenient and mild route for the synthesis of primary amines is the GABRIEL reaction, which includes as first step the reaction of an alkyl halide with potassium phthalimide.^[27] Refluxing compound **6** with potassium phthalimide in acetonitrile furnished 2-nitro-2-azapropyl phthalimide **10** in good yield, which was further increased by using 18-crown-6. The hitherto unknown crystal structure of compound **10** was determined. Attempted cleavage reactions included treatment of compound **10** with a) hydrazine,^[27c] b) hydrobromic acid, or c) nitric acid (65 and 100%). However, the desired amine **12** could not be synthesised by these routes. Instead compound **12** was obtained by refluxing the isocyanate **9** with aqueous hydrochloric acid with 30% yield or with hydrochloric acid in anhydrous diethyl ether yielding 80% or highly pure

product (Scheme 6). Please find further information about derivatives of compound **12** respectively **9** in Chapter 2.



Scheme 6: Attempted syntheses of NAP-NH₂ (**12**) or salts thereof from NAP-Cl (**6**) including amination with ammonia, the DELÉPINE^[26] and GABRIEL reaction,^[27] and successful treatment of NAP-NCO **9** with anhydrous or aqueous hydrochloric acid with subsequent decarboxylation to yield the desired amine **12** as hydrochloride salt.

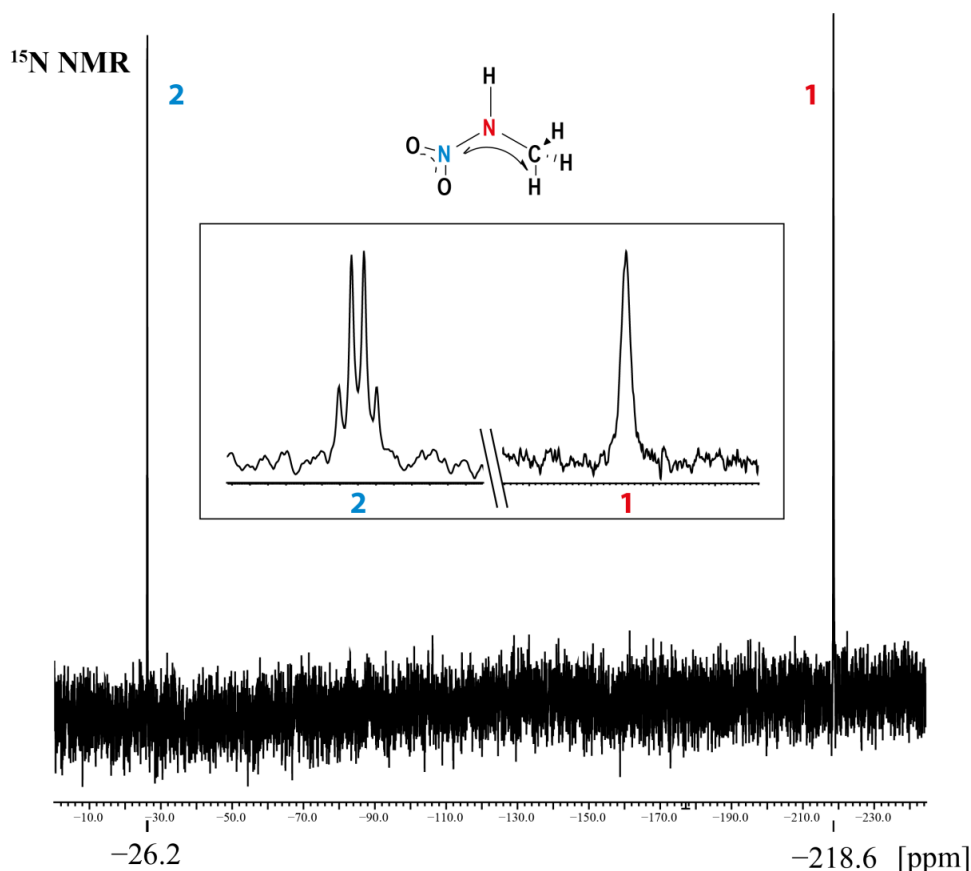
1.3 NMR Spectroscopy

All compounds were characterised by ¹H, ¹³C{¹H} and ¹⁴N{¹H} NMR spectroscopy. In the ¹H NMR spectra of MNA (**1**) and all its salts **1a–j** and **4a–j**, the singlet for the terminal methyl group can be observed in the range of $\delta = 3.13\text{--}2.93$ ppm in D₂O. The NAP derivatives **5**, **6**, **7**, **9**, **10** and **12** show this group slightly shifted to lower field in the range of $\delta = 3.54\text{--}3.16$ ppm in CDCl₃ (and D₂O for **12**), while the methylene group in these compounds is observed in the range of $\delta = 5.63\text{--}5.10$ ppm (and at $\delta = 4.85$ ppm in D₂O for **12**). The signal of the amino group in compound **12** is observed at $\delta = 8.32$ ppm in D₂O as broad singlet. The ¹³C{¹H} NMR spectra shows the methyl group of **1** at $\delta = 32.8$ ppm and in all other compounds described in this chapter in the range of $\delta = 39.1\text{--}31.8$ ppm in D₂O or CDCl₃. The methylene groups of compounds **5**, **6**, **7**, **9** and **10** are observed in the expected range of $\delta = 74.9(\mathbf{5})\text{--}53.4(\mathbf{10})$ ppm depending on the substituents attached (Table 1). The signals of the carbonyl groups of compounds **7** and **10** are observed at 170.4 and 167.1 ppm, respectively, in the ¹³C NMR spectra. Additionally the chemical shift of the methyl group of the acetate group in compound **7** is observed at 20.3 ppm, and the signals of the aromatic carbon atoms in NAP-phthalimide (**10**) at 134.8, 131.6 and 124.0 ppm.^[28]

Table 1: NMR chemical shifts of analogue moieties in compounds **1**, **5**, **6**, **7**, **9**, **10** and **12**.

Nucleus	Assignment	1	5	6	7	9	10	12
^1H	CH_3	3.13	3.35	3.33	3.39	3.36	3.54	3.16
	CH_2	—	5.10	5.56	5.53	5.20	5.63	4.85 (br)
	random	8.72 (br, NH)	4.39 (br, OH)	—	1.97 (CH_3)	—	7.91–7.25 (arom.CH)	8.32 (br, NH_3)
^{13}C	CH_3	32.8	37.7	37.6	38.4	37.8	39.1	31.8
	CH_2	—	74.9	60.4	72.8	60.1	53.4	81.8
^{14}N	NO_2	−27	−28	−32	−30	−28	−31	−26
	NNO_2	−219 (br)	−201 (br)	−204 (br)	−211 (br)	−201 (br)	−234 (br)	
(br) broad								

In the $^{14}\text{N}\{^1\text{H}\}$ NMR spectra the signals of the nitro groups of all compounds can be observed in the expected range between $\delta = -24$ and -32 ppm. The the chemical shifts of the deprotonated amine group of all MNA salts **1a–j** and **4a–j** is observed between $\delta = -107$ and -118 ppm, while the signals of the ternary coordinated NNO_2 of all discussed NAP derivatives are in the range of $\delta = -201$ (**5**) and -234 (**10**) ppm, all as broad singlets. The signal of the isocyanate nitrogen atom in NAP-NCO (**9**) can be observed at $\delta = -351$ ppm, and the signal of the amino group in compound **12** is shifted to $\delta = -362$ ppm.^[29] The ^{15}N NMR spectrum of MNA (**1**) shows a quartet for the nitrogen atom of the nitro group (N2) owing to the coupling to the methyl group at $\delta = -26.2$ ppm ($^3J_{15\text{N-H}} = 2.8$ Hz). The signal of the NH (N1) group is observed at $\delta = -218.6$ ppm as slightly broadened singlet (Figure 1).

**Figure 1:** ^{15}N NMR spectrum of MNA **1** showing the quartet of the NO_2 group due to $^3J_{15\text{N-H}}$ coupling with a coupling constant of 2.8 Hz.

1.4 Vibrational Spectroscopy

The vibrational analysis of solid compound **1** shows the stretching modes of the methyl group [$\nu(\text{C-H})$, $\nu_s(\text{CH}_3)$ and $\nu_{as}(\text{CH}_3)$] at frequencies between $\tilde{\nu} = 3031$ and 2924 cm^{-1} . A very broad band is observed for $\nu(\text{N-H})$ at $\tilde{\nu} = 3220\text{ cm}^{-1}$ in the IR spectrum. The vibration mode δ of N-H can be observed at $\tilde{\nu} = 720\text{ cm}^{-1}$ in the IR spectrum, the characteristic asymmetric NO_2 stretching vibration ν_{as} at $\tilde{\nu} = 1575\text{ cm}^{-1}$ and the symmetric NO_2 stretching vibration ν_s at $\tilde{\nu} = 1380\text{ cm}^{-1}$. The C-N stretching vibration ν_s is observed at $\tilde{\nu} = 1112\text{ cm}^{-1}$.^[30] An IR spectrum recorded from the gas phase of MNA **1** showed no significant differences, except for the asymmetric stretching mode ν_{as} of the NO_2 group. Owing to the ability of rotation of the NO_2 group and the lower π character of the elongated N-N bond in the gaseous phase, this frequency is shifted to higher energy by ca. 45 cm^{-1} from $\tilde{\nu} = 1575$ to 1621 cm^{-1} . A comparable rotation of the NO_2 group is observed for NAP-Cl **6** (see below). All MNA salts **1a-j** and **4a-j** show similar vibrational modes (except the $\nu(\text{N-H})$ band observed for **1**), which can be assigned according to the literature.^[14c]

The NAP derivatives **6**, **9** and **10** show the stretching modes of the methyl and methylene groups [$\nu(\text{C-H})$, $\nu_s(\text{CH})$ and $\nu_{as}(\text{CH})$] in the expected range of $\tilde{\nu} = 3110\text{--}2838\text{ cm}^{-1}$. The characteristic asymmetric NO_2 stretching vibrations ν_{as} are observed in the range of $\tilde{\nu} = 1557\text{--}1528\text{ cm}^{-1}$, and the symmetric NO_2 stretching vibrations ν_s in the range of $\tilde{\nu} = 1308\text{--}1287\text{ cm}^{-1}$. In addition to the liquid phase IR spectrum of NAP-Cl **6**, also its gas phase spectrum was measured. Whereas the asymmetric NO_2 stretching vibration ν_{as} is observed at $\tilde{\nu} = 1557\text{ cm}^{-1}$ in the spectrum of liquid compound **6**, the gas phase spectrum shows it shifted to higher energy by ca. 40 cm^{-1} to $\tilde{\nu} = 1596\text{ cm}^{-1}$. This again agrees with the rotation of the NO_2 group out of the CNC plane and a lower π character of the elongated N-N bond in the gas phase structure (please see X-ray diffraction section for further comparison). The isocyanate group in compound **9** shows the characteristic very strong band for the stretching vibration ν at $\tilde{\nu} = 2230\text{ cm}^{-1}$.^[30]

1.5 X-ray Diffraction

Single crystals suitable for low temperature X-ray diffraction measurements were obtained from compounds **1**, **1a**, **1c**, **4e**, **4f**, **4j**, **5**, **6**, **9** and **10**. Compounds **1**, **5**, **6** and **9** crystallised as neat compounds in a $-30\text{ }^{\circ}\text{C}$ (**1**, **5**, **6**) or respectively a $-80\text{ }^{\circ}\text{C}$ (**9**) freezer. Compounds **1a** and **1c** were re-crystallised from water, compounds **4e**, **4f** and **4j** were re-crystallised from ethanol, and compound **10** from a 1:1 mixture of chloroform and isohexane. Tables 2+3 include all relevant crystallographic and structural refinement data of these compounds. Refined atom positions and anisotropic thermal displacement parameters are listed in the Appendix.

Table 2: Crystal structure parameters of compounds MNA (**1**), LiMNA (**1a**), KMNA (**1c**), GMNA (**4e**) and AGMNA (**4f**). Standard deviations are given in parentheses.

	1	1a	1c	4e	4f
Refined formula	$\text{CH}_4\text{N}_2\text{O}_2$	$\text{CH}_3\text{N}_2\text{O}_2\text{Li}$	$\text{CH}_3\text{N}_2\text{O}_2\text{K}$	$\text{C}_2\text{H}_9\text{N}_5\text{O}_2$	$\text{C}_2\text{H}_{10}\text{N}_6\text{O}_2$
Formula weight [$\text{g}\cdot\text{mol}^{-1}$]	76.06	81.99	114.14	135.13	150.14
Crystal dimensions [mm]	$0.45\times 0.20\times 0.05$	$0.40\times 0.05\times 0.05$	$0.20\times 0.15\times 0.06$	$0.40\times 0.20\times 0.15$	$0.33\times 0.28\times 0.06$
Crystal description	colourless rod	colourless needle	colourless block	colourless block	colourless block
Crystal system	orthorhombic	monoclinic	triclinic	monoclinic	triclinic
Space group	<i>Pbca</i>	<i>P21/c</i>	<i>P-1</i>	<i>C2/c</i>	<i>P-1</i>
<i>a</i> [Å]	8.865(4)	9.976(2)	6.847(2)	10.041(5)	4.883(4)
<i>b</i> [Å]	6.673(3)	5.264(1)	7.325(1)	10.502(5)	7.392(5)
<i>c</i> [Å]	11.324(6)	6.555(2)	8.749(1)	12.986(5)	9.966(5)
α [°]	90	90	77.87(1)	90	77.66(2)
β [°]	90	100.26(2)	79.07(1)	104.96(5)	81.36(2)
γ [°]	90	90	85.821(7)	90	78.68(1)
<i>V</i> [Å ³]	669.9(6)	338.7(1)	421.0(1)	1323.0(1)	342.4(5)
<i>Z</i>	8	4	4	8	2
ρ_{calcd} [$\text{g}\cdot\text{cm}^{-3}$]	1.508	1.280	1.801	1.357	1.456
μ [mm^{-1}]	0.141	0.114	1.109	0.116	0.124
Temperature [K]	173(2)	173(2)	173(2)	173(2)	173(2)
θ range [°]	4.27–27.00	4.39–24.99	4.21–25.00	4.20–25.50	4.28–26.00
F(000)	320	135	232	576	160
Dataset <i>h</i>	$-11 \leq h \leq 9$	$-11 \leq h \leq 8$	$-8 \leq h \leq 8$	$-12 \leq h \leq 10$	$-6 \leq h \leq 6$
Dataset <i>k</i>	$-8 \leq k \leq 6$	$-6 \leq k \leq 5$	$-8 \leq k \leq 8$	$-12 \leq k \leq 6$	$-9 \leq k \leq 9$
Dataset <i>l</i>	$-6 \leq l \leq 14$	$-5 \leq l \leq 7$	$-10 \leq l \leq 10$	$-15 \leq l \leq 15$	$-9 \leq l \leq 12$
Reflections measured	1735	1150	2575	2520	1757
Reflections independent	732	588	1473	1231	1318
Reflections unique	479	524	1254	1029	951
<i>R</i>_{int}	0.0357	0.0202	0.0392	0.0208	0.0922
<i>R</i>1, <i>wR</i>2 (2σ data)	0.0453, 0.0992	0.1929, 0.4463	0.0344, 0.0787	0.0352, 0.0872	0.0533, 0.1282
<i>R</i>1, <i>wR</i>2 (all data)	0.0754, 0.1203	0.1974, 0.4539	0.0425, 0.0872	0.0437, 0.0932	0.0764, 0.1425
Data/restraint/parameter	732/0/62	588/0/55	1473/0/133	1231/0/118	1318/0/131
GOOF on <i>F</i>²	1.029	2.205	1.078	1.112	0.981
Residual electron density	−0.244/0.220	−0.567/2.855	−0.342/0.338	−0.239/0.185	−0.289/0.256
CCDC number	956913	not deposited	956916	957100	957101

Table 3: Crystal structure parameters of compounds GUMNA (**4j**), NAP-OH (**5**), NAP-Cl (**6**), NAP-NCO (**9**) and NAP-phthalimide (**10**). Standard deviations are given in parentheses.

	4j	5	6	9	10
Refined formula	C ₃ H ₁₀ N ₆ O ₃	C ₂ H ₆ N ₂ O ₃	C ₂ H ₅ N ₂ O ₂ Cl	C ₃ H ₅ N ₃ O ₃	C ₁₀ H ₉ N ₃ O ₄
Formula weight [g·mol ⁻¹]	178.15	106.08	124.53	131.09	235.196
Crystal dimensions [mm]	0.35×0.05×0.04	0.40×0.20×0.03	0.21×0.15×0.10	0.20×0.20×0.04	0.25×0.15×0.12
Crystal description	colourless block	colourless rod	colourless block	colourless block	colourless block
Crystal system	orthorhombic	monoclinic	monoclinic	monoclinic	triclinic
Space group	<i>Pnma</i>	<i>P2₁/c</i>	<i>P2₁/n</i>	<i>P2₁/c</i>	<i>P</i> -1
<i>a</i> [Å]	14.044(1)	6.025(1)	6.242(1)	6.010(2)	7.684(1)
<i>b</i> [Å]	6.296(1)	19.405(2)	8.174(1)	8.912(1)	7.715(1)
<i>c</i> [Å]	8.500(1)	11.956(1)	10.215(1)	10.564(1)	9.526(1)
α [°]	90	90	90	90	82.81(2)
β [°]	90	99.10(1)	93.42(1)	99.25(1)	78.57(1)
γ [°]	90	90	90	90	75.61(1)
<i>V</i> [Å ³]	751.6(1)	1380.3(1)	520.2(1)	558.4(1)	534.4(1)
<i>Z</i>	4	12	4	4	2
ρ_{calcd} [g·cm ⁻³]	1.574	1.531	1.590	1.559	1.462
μ [mm ⁻¹]	0.136	0.142	0.622	0.139	0.166
temperature [K]	173(2)	293(2)	173(2)	100(2)	298(2)
θ range [°]	4.28–28.24	4.21–26.00	4.49–24.99	4.32–25.99	4.33–25.50
<i>F</i> (000)	376	672	256	272	244
dataset <i>h</i>	−18 ≤ <i>h</i> ≤ 7	−7 ≤ <i>h</i> ≤ 7	−7 ≤ <i>h</i> ≤ 4	−7 ≤ <i>h</i> ≤ 7	−5 ≤ <i>h</i> ≤ 9
dataset <i>k</i>	−3 ≤ <i>k</i> ≤ 8	−23 ≤ <i>k</i> ≤ 12	−9 ≤ <i>k</i> ≤ 8	−10 ≤ <i>k</i> ≤ 10	−8 ≤ <i>k</i> ≤ 9
dataset <i>l</i>	−5 ≤ <i>l</i> ≤ 11	−12 ≤ <i>l</i> ≤ 14	−11 ≤ <i>l</i> ≤ 12	−13 ≤ <i>l</i> ≤ 13	−11 ≤ <i>l</i> ≤ 11
reflections measured	2149	5208	1930	5381	2653
reflections independent	1009	2685	913	1082	1966
reflections unique	811	2097	826	958	1557
<i>R</i> _{int}	0.0215	0.0228	0.0150	0.0269	0.0118
<i>R</i> 1, <i>wR</i> 2 (2 σ data)	0.0573, 0.1464	0.0334, 0.0699	0.0259, 0.0648	0.0262, 0.0566	0.0399, 0.0943
<i>R</i> 1, <i>wR</i> 2 (all data)	0.0697, 0.1586	0.0507, 0.7730	0.0299, 0.0680	0.0309, 0.0681	0.0528, 0.1050
Data/restraints/parameter	1009/0/95	2685/0/262	913/0/84	1082/0/102	1966/0/190
GOOF on <i>F</i> ²	1.080	1.028	1.114	1.050	1.044
Residual electron density	−0.294/0.782	−0.166/0.195	−0.295/0.250	−0.176/0.145	−0.185/0.210
CCDC number	990339	957102	940502	940468	1043154

Crystal Structure of *N*-Methylnitramine (**1**)

N-Methylnitramine (**1**) crystallises as colourless needles in the orthorhombic space group *Pbca* with eight molecules per unit cell and a calculated maximum density of 1.508 g·cm⁻³ at 173(2) K. The molecule is almost planar and shows an intramolecular electrostatic interaction between C1 and O2 with 2.63(1) Å, which is clearly under the sum of van der Waals radii [$\Sigma\text{vdW}(\text{N},\text{O}) = 3.22 \text{ Å}$].^[31] Hydrogen bonds fix the molecules within layers (Table 4), which assemble a wave-like arrangement (Figure 2).

Table 4: Structural parameters for the hydrogen bonds in the crystal structure of MNA (**1**) presented in Figure 2 (top).

D–H···A	<i>d</i> (D–H) [Å]	<i>d</i> (H···A) [Å]	<i>d</i> (D–H···A) [Å]	\angle (D–H···A) [°]
N1–H1···O2(i)	0.831(25)	2.073(25)	2.902(3)	175.4(2)
C1–H3···O1(i)	0.931(26)	2.959(25)	3.629(3)	130.1(1)
Symmetry operator (i): $\frac{1}{2}+x, y, \frac{1}{2}-z$.				

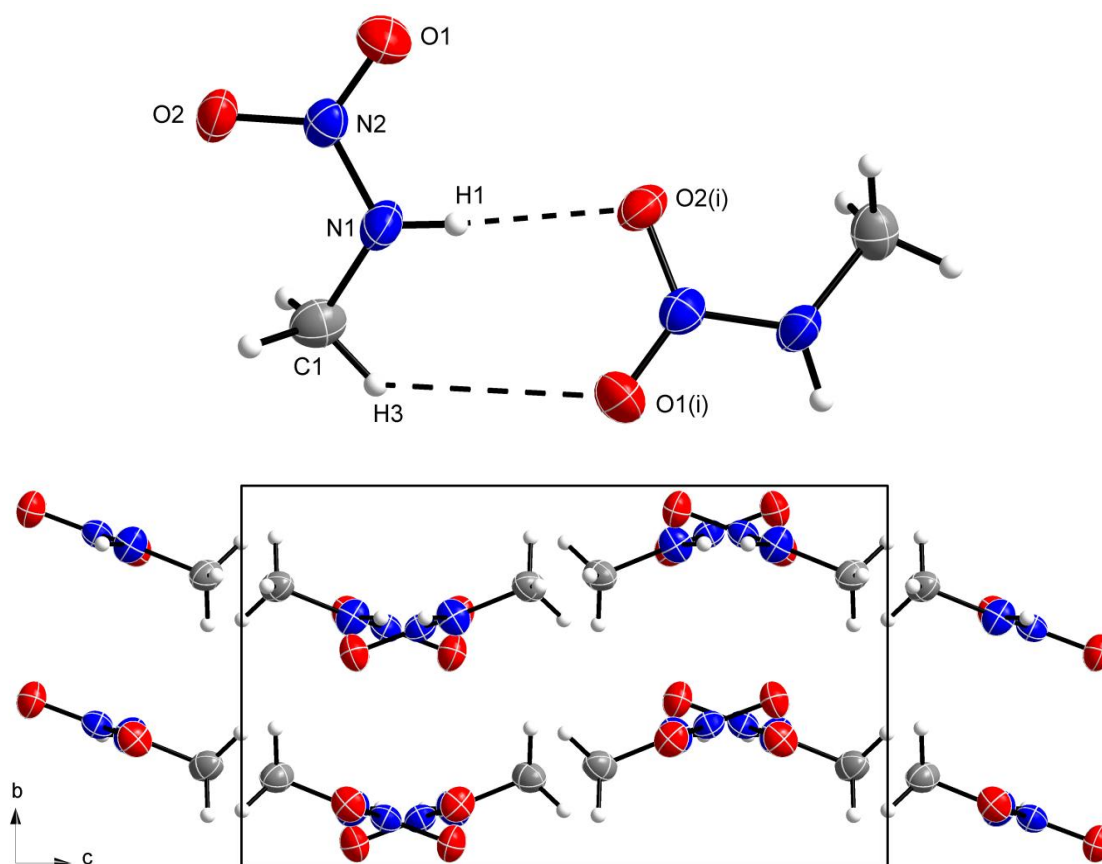


Figure 2: Top: Crystal structure of MNA (**1**) with hydrogen bonding scheme between two molecules (listed in Table 4). Symmetry operator (i): $\frac{1}{2}+x, y, \frac{1}{2}-z$. Selected bond lengths and angles are listed in Table 5. Bottom: View along the a axis displaying the wave-like arrangement.

Table 5 shows the main parameters for compound **1** in comparison to its gas phase structure determined by SADOVA *et al.* in 1977.^[9] As mentioned in the vibrational analysis part, the N1–N2 bond in the crystal structure is shortened [from 1.381(6) to 1.318(2) Å], which indicates the higher π character of the bond in the solid state. Thus, the rotation of the NO₂ group out of the CNC plane in the gas phase structure stands in agreement with the higher energetic asymmetrical stretching vibration ν_{as} found in the gas phase IR spectrum of the compound. This again shortens the C1–N1 bond [from 1.452(6) to 1.436(3) Å] and slightly elongates the average N2–O bonds [from 1.228(3) to 1.236(2) Å].

Table 5: Selected bond lengths [Å] and angles [°] in the crystal structure of compound **1** depicted in Figure 2 (top) in comparison to the gas phase structure.^[9]

Bond lengths [Å]	Crystal structure	Gas phase structure ^[9]
N2–O	1.236(2)	1.228(3)
N1–N2	1.318(2)	1.381(6)
C1–N1	1.436(3)	1.452(6)
Angles [°]		
O1–N2–O2	123.5(1)	125.3(1)
C1–N1–N2	120.6(1)	109.0(1)
Standard bond lengths [Å]: N–N 1.46, C–N 1.47, N–O 1.45, N=N 1.20, C=N 1.22, N=O 1.17. ^[32]		

Crystal Structure of Lithium N-Methylnitramide (1a)

Due to the high hygroscopicity of lithium *N*-methylnitramide (**1a**) only crystals of bad constitution were obtained. Therefore the refinement of this structure resulted in a high structure factor of $wR_2 = 37.4\%$ (all data). Compound **1a** crystallises in the monoclinic space group $P2_1/c$ with four molecules per unit cell and a calculated maximum density of $1.608\text{ g}\cdot\text{cm}^{-3}$ at $173(2)\text{ K}$. Its asymmetric unit in the crystal structure is depicted in Figure 3.

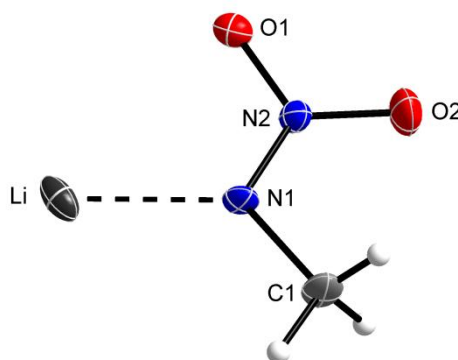


Figure 3: Asymmetric unit in the crystal structure of LiMNA (**1a**). Selected bond lengths [\AA] and angles [$^\circ$]: $\text{Li}\cdots\text{N1}$ 2.073(2), N1-N2 1.292(6), N2-O1 1.306(6), N2-O2 1.272(6), N1-C1 1.462(6), N2-N1-C1 111.3(4), O2-N2-O1 116.4(4), C1-N1-N2-O2 $-0.6(8)$.

Each lithium cation is coordinated by four methylnitramide anions (Figure 4), thereby lying in layers horizontal to the *b* axis with the anions [N2 , O1(ii) and O2(iii)] and connecting each layer to two neighbouring layers above [O1(ii)] and below [O1(i)].

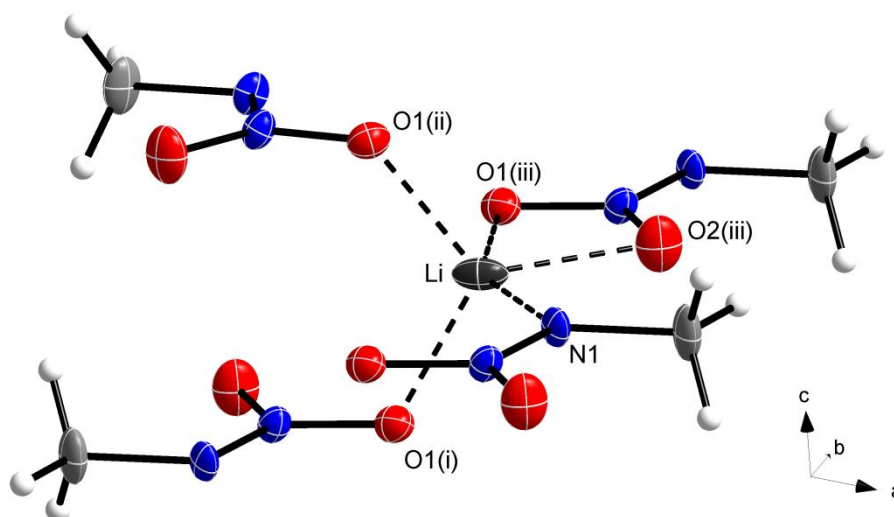


Figure 4: Coordination sphere of the lithium cation in the layer like structure of LiMNA (**1a**). Selected atom distances [\AA]: $\text{Li}\cdots\text{N1}$ 2.073(2), $\text{Li}\cdots\text{O1(i)}$ 1.956(1), $\text{Li}\cdots\text{O1(ii)}$ 1.958(2), $\text{Li}\cdots\text{O1(iii)}$ 2.289(1), $\text{Li}\cdots\text{O2(iii)}$ 2.129(1). Symmetry operators: (i) $-x, 1-y, -z$; (ii) $-x, \frac{1}{2}+y, \frac{1}{2}-z$; (iii) $x, 1+y, z$.

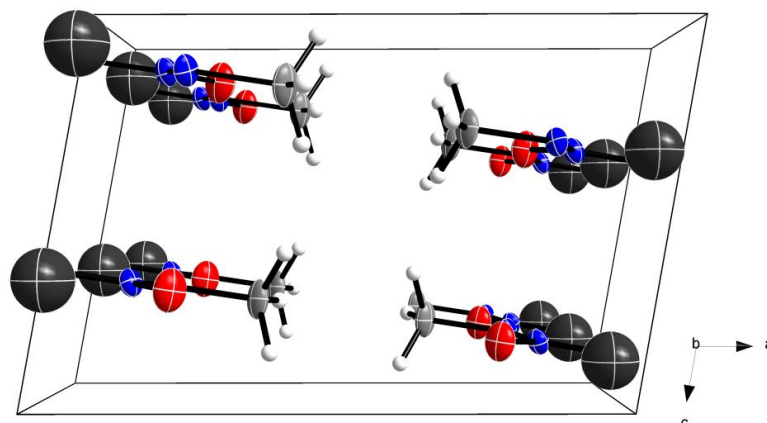


Figure 5: View along the *b* axis of the unit cell in the structure of compound **1a** displaying its layers.

Crystal Structure of Potassium N-Methylnitramide (1c)

The potassium salt **1c** crystallises as colourless blocks in the triclinic space group *P*–1 with four molecules per unit cell and a calculated maximum density of 1.801 g·cm^{–3} at 173(2) K. Its asymmetric unit in the crystal structure consists of two crystallographically independent pairs of cations and anions that strain non-planar layers as it is depicted in Figure 6. The bond lengths in the two anions clearly vary by comparison, indicating the different coordination of the potassium cations to the oxygen atoms of the nitro groups. It is remarkable that N3 coordinates to K1(i) [2.849(2) Å], while in the surroundings of N1 no cation is found.

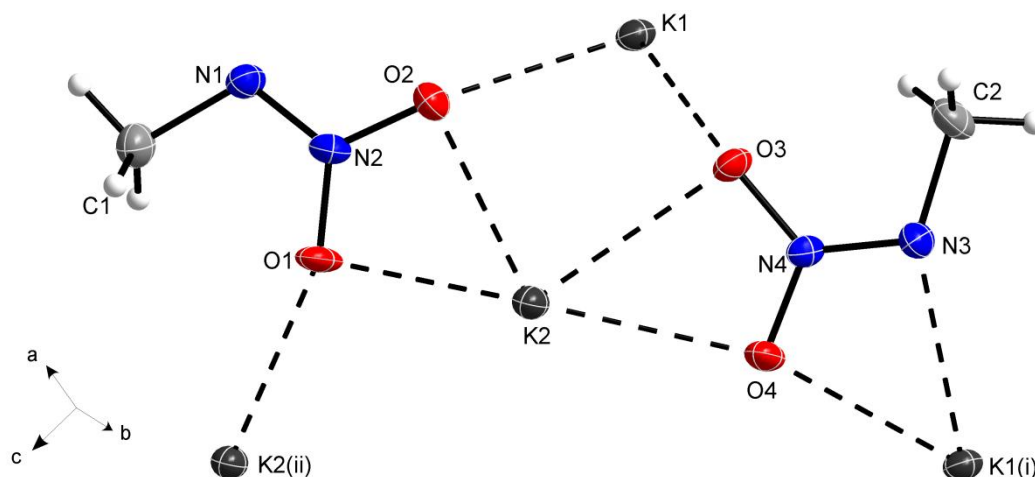


Figure 6: Asymmetric unit in the crystal structure of KMNA (**1c**). Selected bond lengths [Å] and angles [°]: K1···O2 2.742(2), K1···O3 2.744(2), K2···O4 2.747(2), K2···O1 2.801(2), K2···O3 2.824(2), K2···O2 2.863(1), K1(i)···O4 2.958(2), K1(i)···N3 2.849(2), K2(ii)···O1 2.764(1), O2–N2 1.291(3), O1–N2 1.275(3), O4–N4 1.288(3), O3–N4 1.284(3), N1–N2 1.282(3), N4–N3 1.277(3), N3–C2 1.458(4), N1–C1 1.457(4); O2–K1–O3 81.51(6), O3–K2–O2 78.07(5), O1–K2–O2 45.73(5), O4–K2–O3 46.73(5), O1–N2–O2 118.1(2), O3–N4–O4 118.5(2), C1–N1–N2–O2 –178.6(2), O4–N4–N3–C2 –178.6(2). Symmetry operators: (i) $-1+x, 1+y, z$; (ii) $-x, 1-y, 2-z$.

Comparison of the Crystal Structures of MNA (1), LiMNA (1a) and KMNA (1c)

By comparison of the crystal structures of MNA (**1**), KMNA (**1a**) and LiMNA (**1c**) some differences in the bond length and angles are observed (Table 6). The bond lengths between the two nitrogen atoms N1–N2 vary from 1.277(3) Å in KMNA (**1c**) to 1.318(2) Å in MNA (**1**). As expected this bond lengths are shortened in the salts due to stabilisation of the negative charge by delocalisation to the nitro group. This also influences the average N2–O (and N4–O in **1c**) bond lengths, which are slightly elongated compared to neutral compound **1**. The C1–N1 (and C2–N3 in **1c**) bond lengths of all three compounds have values which are close to an average C–N single bond (1.47 Å).^[32] In the alkali methylnitramides (**1a+c**) the C1–N1–N2 angles are found to be sharper than in neutral MNA (**1**) as expected. In the case of the lithium salt **1a** the cation lies in plane with the molecule (C1–N1–N2–O₂). As expected the lithium cation is strictly orientated to the free electron pairs at the nitrogen (N1) and oxygen atoms, while the potassium cations in compound **1c** are located above and below the molecule layers.

Table 6: Comparison of selected bond lengths [Å] and angles [°] in *N*-methylnitramine (**1**) with the lithium (**1a**) and potassium (**1c**) methylnitramide anions.

Bond length[Å]	1	1a	1c
N1–N2, N3–N4	1.318(2)	1.292(6)	1.282(2), 1.277(3)
N2–O1, N4–O3	1.234(2)	1.306(6)	1.275(3), 1.284(3)
N2–O2, N4–O4	1.239(2)	1.272(6)	1.291(3), 1.288(3)
N1–C1, N3–C2	1.436(3)	1.462(6)	1.457(4), 1.458(4)
N1–H	0.83(3)	–	–
Angles [°]			
C1–N1–N2, C2–N3–N4	120.6(2)	111.1(5)	112.3(2), 113.1(2)
O1–N2–O2, O3–N4–O4	123.5(2)	114.5(6)	118.1(2), 118.5(2)
C1–N1–H, N2–N1–H	120.8(1), 116.4(2)	–	–

Crystal Structure of Guanidinium N-Methylnitramide (4e)

The guanidinium salt **4e** crystallises as colourless blocks in the monoclinic space group *C2/c* with eight formula units in the unit cell and a calculated maximum density of 1.357 g·cm^{−3} at 173(2) K. All hydrogen atoms of the guanidinium cation participate in hydrogen bonds; two of them are illustrated within the asymmetric unit of compound **4e** in Figure 7 and are listed in Table 7.

Table 7: Structural parameters for the hydrogen bonds in the structure of GMNA (**4e**) presented in Figures 7 and 8.

D–H···A	d (D–H) [Å]	d (H···A) [Å]	d (D–H···A) [Å]	∠ (D–H···A) [°]
N3–H31···O2	0.87(2)	2.10(1)	2.962(2)	170.8(2)
N5–H52···N1	0.85(2)	2.12(2)	2.954(2)	165.3(2)
N5–H51···O1(i)	0.84(2)	2.12(2)	2.952(1)	168.3(1)
N4–H42···O2(i)	0.85(2)	2.06(2)	2.094(2)	132.1(1)
N4–H41···O1(ii)	0.90(1)	2.20(2)	3.041(2)	154.4(2)
N3–H32···O2(iii)	0.83(1)	2.40(2)	2.880(2)	117.6(1)
Symmetry operators: (i) ½+x, ½+y, z; (ii) ½+x, ½−y, ½+z; (iii) −x, y, ½−z.				

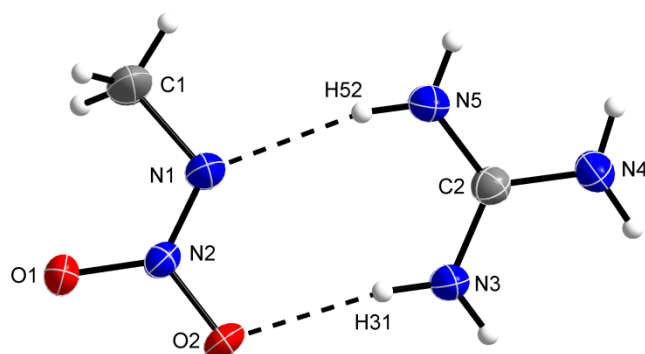


Figure 7: Crystal structure of GMNA (**4e**) with hydrogen bonding between the ions (listed in Table 7). Selected bond lengths [Å] and angles [°]: N2–N1 1.267(1), O2–N2 1.292(1), O1–N2 1.281(1), N1–C1 1.455(2), N3–C2 1.323(1), N4–C2 1.329(1), C2–N5 1.322(2); O1–N2–O2 118.12(10), N2–N1–C1 113.72(12), O2–N2–N1–C1 –179.8(1).

All hydrogen atoms of the guanidinium cation participate in hydrogen bonding to N1, O1 and O2, respectively (Table 7). These form two intercalating layers within the structure as seen by view along the *c* axis (Figure 8).

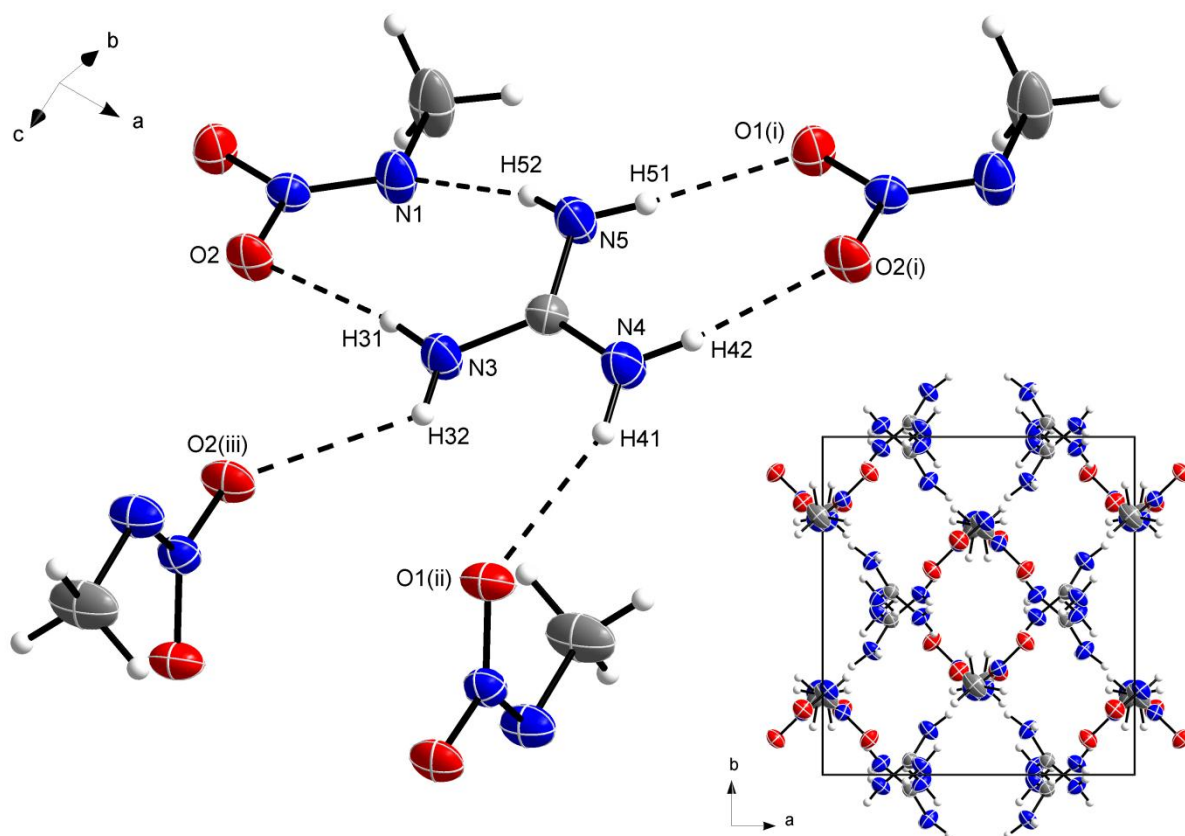


Figure 8: Cutout from the structure of GMNA (**4e**) showing all its hydrogen bonds (Table 7), and view along the *c* axis of the unit cell displaying the two intercalating layers. Symmetry operators: (i) $\frac{1}{2}+x, \frac{1}{2}+y, z$; (ii) $\frac{1}{2}+x, \frac{1}{2}-y, \frac{1}{2}+z$; (iii) $-x, y, \frac{1}{2}-z$.

Crystal Structure of Aminoguanidinium N-Methylnitramide (4f)

The aminoguanidinium salt **4f** crystallises as colourless blocks in the triclinic space group *P*−1 with two molecules per unit cell and a calculated maximum density of 1.456 g·cm^{−3} at 173(2) K. Its asymmetric unit in the crystal structure is depicted in Figure 9 and the hydrogen bonds between the ions listed in Table 8.

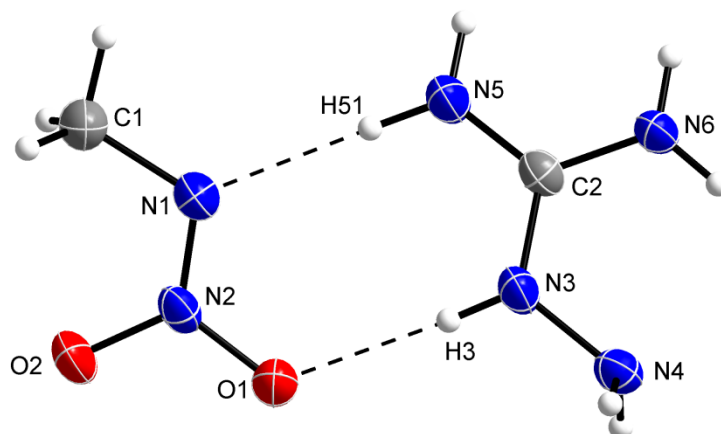


Figure 9: Crystal structure of AGMNA (**4f**) with hydrogen bonding between the ions (Table 8). Selected bond lengths [Å] and angles [°]: O1–N2 1.305(2), O2–N2 1.277(2), N2–N1 1.267(3), N1–C1 1.455(3), N3–C2 1.343(3), N3–N4 1.406(3), N6–C2 1.326(3), N5–C2 1.318(3), N2–N1–C1 113.1(2), O1–N2–O2 117.2(2), N5–C2–N3 119.2(2), C1–N1–N2–O1 178.1(2), N4–N3–C2–N5 174.5(2).

Table 8: Structural parameters for the hydrogen bonds in the structure of AGMNA (**4f**) presented in Figures 9 and 10 (red highlights the layer connecting hydrogen bond in Figure 10).

D–H···A	d (D–H) [Å]	d (H···A) [Å]	d (D–H···A) [Å]	∠ (D–H···A) [°]
N5–H51···N1	0.91(1)	2.03(1)	2.934(3)	178.6(1)
N3–H3···O1	0.83(1)	2.07(1)	2.892(2)	170.9(1)
N5–H52···O2(i)	0.90(2)	2.02(2)	2.891(3)	163.6(2)
N6–H62···O1(i)	0.87(3)	2.11(2)	2.945(3)	163.1(3)
N6–H61···N4(ii)	0.89(2)	2.32(2)	3.054(3)	139.9(2)
N2(ii)–H21(ii)···N4				
N4–H41···O1(iii)	0.86(2)	2.48(1)	3.263(1)	151.7(2)
N4(v)–H41(v)···O1(iv)				
Symmetry operators: (i) <i>x</i> , −1+ <i>y</i> , <i>z</i> ; (ii) − <i>x</i> , − <i>y</i> , 1− <i>z</i> ; (iii) 1− <i>x</i> , 1− <i>y</i> , 1− <i>z</i> ; (iv) −1+ <i>x</i> , <i>y</i> , <i>z</i> ; (v) − <i>x</i> , 1− <i>y</i> , 1− <i>z</i> .				

As common for aminoguanidinium salts all hydrogen atoms of the aminoguanidinium cation participate in hydrogen bonds (Table 8). This fact combined with the almost perfect planarity of the cation and anion results in a layer-like structure. In Figure 10 the black dashed lines build up the layers, while the red dashed lines connect the layers through the nitrogen atom N4 with each other.

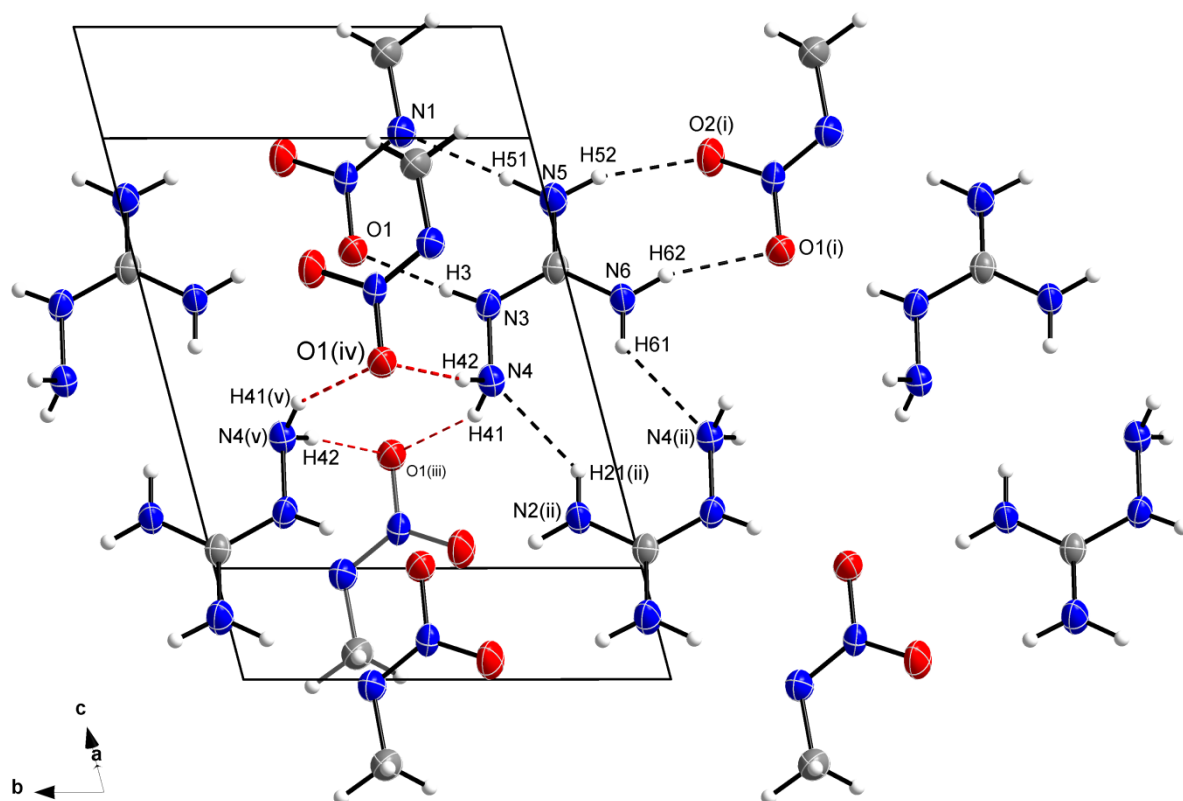


Figure 10: Cutout from the structure of AGMNA (**4f**) showing one layer build up by the hydrogen bonds of the aminoguanidinium cation (black), and the layer connecting hydrogen bonds (red, listed in Table 8). Symmetry operators: (i) $x, -1+y, z$; (ii) $-x, -y, 1-z$; (iii) $1-x, 1-y, 1-z$; (iv) $-1+x, y, z$; (v) $-x, 1-y, 1-z$.

Crystal Structure of Guanylurea *N*-Methylnitramide (**4j**)

The guanylurea salt **4j** crystallises as colourless blocks in the orthorhombic space group $Pmna$ with four molecules per unit cell and a calculated maximum density of $1.574 \text{ g}\cdot\text{cm}^{-3}$ at 173(2) K. Its asymmetric unit in the crystal structure is depicted in Figure 11 (top) and the hydrogen bonds between the ions are listed in Table 9. The methyl group C1 shows disorder, thus no interactions are discussed here. Within the structure the molecules are arranged in parallel planes perpendicular to the b axis with a distance of $3.13(2) \text{ \AA}$ (Figure 11, bottom). The planarity of the guanylurea cation is reflected in the sum of the angles around C2 and C3, which are 360° each.

Table 9: Structural parameters for the hydrogen bonds in the structure of GUMNA (**4j**) presented in Figure 11.

D–H \cdots A	d (D–H) [\AA]	d (H \cdots A) [\AA]	d (D–H \cdots A) [\AA]	\angle (D–H \cdots A) [$^\circ$]
N3–H32 \cdots O2	0.87(2)	1.92(2)	2.797(2)	178.7(4)
N4–H4 \cdots N1	0.79(2)	2.18(1)	2.960(3)	171.2(2)
N5–H51 \cdots O3	0.90(1)	1.94(3)	2.638(1)	132.2(5)

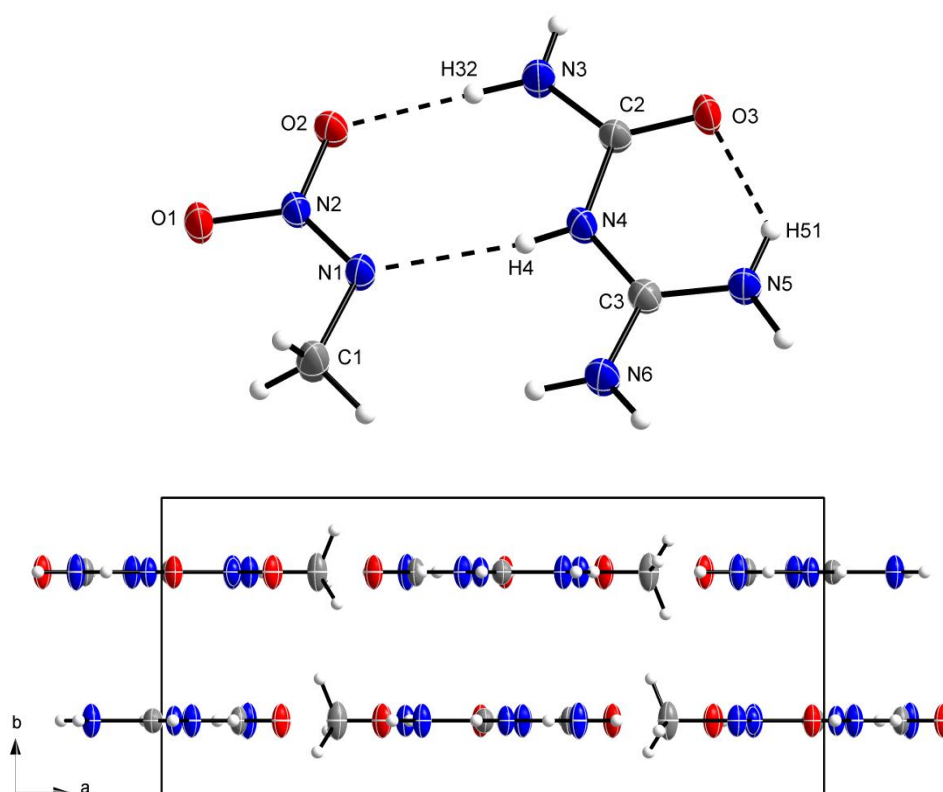


Figure 11: Top: asymmetric unit in the crystal structure of GUMNA (**4j**) with hydrogen bonding between the ions (listed in Table 9). Selected bond length [Å] and angles [°]: O2–N2 1.287(3), O1–N2 1.279(3), N4–C3 1.358(4), N4–C2 1.402(3), O3–C2 1.234(3), N2–N1 1.272(3), N1–C1 1.469(3); N2 N1 C1 113.7(2); O2–N2–N1–C1 180.0(1); C2–N4–C3–N6 180.0(1). Bottom: parallel plane arrangement with a distance of 3.13(2) Å by view along the *c* axis.

Crystal Structure of 2-Nitro-2-Azapropanol (5)

NAP-OH (**5**) crystallises as colourless needles in the monoclinic space group $P2_1/c$ with 12 molecules per unit cell and a calculated maximum density of $1.531 \text{ g}\cdot\text{cm}^{-3}$ at ambient temperature [293(2) K]. Its asymmetric unit in the crystal structure consists of three molecules with different orientated hydroxy groups and is depicted in Figure 12. Within the asymmetric unit no intermolecular interactions are observed, but the hydroxy groups form hydrogen bonds in a chain-like manner through the structure in direction of the *a* axis, (Figure 13, Table 10) while the hydrophobe methyl groups are directed to each other.

Table 10: Structural parameters for the hydrogen bonds in the structure of NAP-OH (**5**) presented in Figure 13.

D–H⋯A	d (D–H) [Å]	d (H⋯A) [Å]	d (D–H⋯A) [Å]	∠ (D–H⋯A) [°]
O6(i)–H2(i)⋯O3	0.81(2)	1.92(2)	2.718(1)	173.7(2)
O6(iv)–H2(iv)⋯O3(iii)				
O3–H1⋯O9(ii)	0.83(1)	1.87(2)	2.694(2)	173.8(3)
O3(iii)–H1(iii)⋯O9				
O9–H3⋯O6(i)	0.82(2)	1.85(2)	2.661(2)	170.9(2)
Symmetry operators: (i) $1-x, \frac{1}{2}+y, \frac{1}{2}-z$; (ii) $1+x, y, z$; (iii) $-1+x, y, z$; (iv) $-x, \frac{1}{2}+y, \frac{1}{2}-z$.				

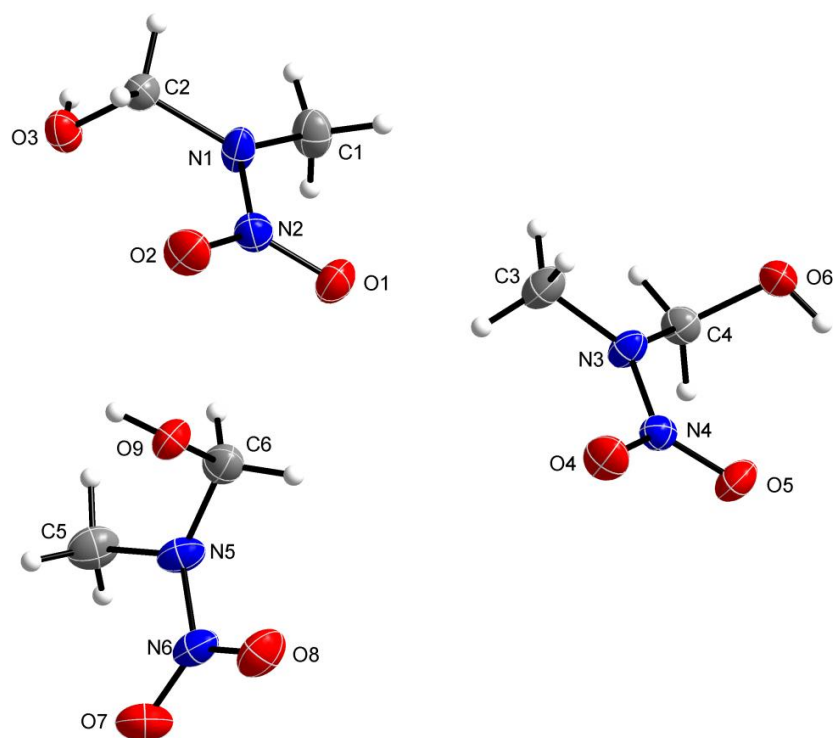


Figure 12: Asymmetric unit in the crystal structure of NAP-OH (**5**) consisting of three crystallographically independent molecules with different orientation of the hydroxy groups. Selected bond length [Å] and angles [°]: O1–N2 1.230(2), O5–N4 1.235(2), O8–N6 1.230(2), O3–C2 1.401(2), O6–C4 1.398(2), O9–C6 1.400(2), N1–N2 1.350(1), N3–N4 1.340(2), N5–N6 1.356(2), N1–C2 1.448(2), N3–C4 1.446(2), N5–C6 1.447(2), N1–C1 1.454(2), O4–N4 1.234(2), O9–H3 0.82(2), O3–H1 0.83(2), O6–H2 0.81(2), C2–O3–H1 105.8(1), C4–O6–H2 108.5(1), C6–O9–H3 108.5(1), average O–N–O 124.2(2), C1–N1–N2–O1 8.1(2), C3–N3–N4–O4 6.8(2), C5–N5–N6–O7 10.9(2).

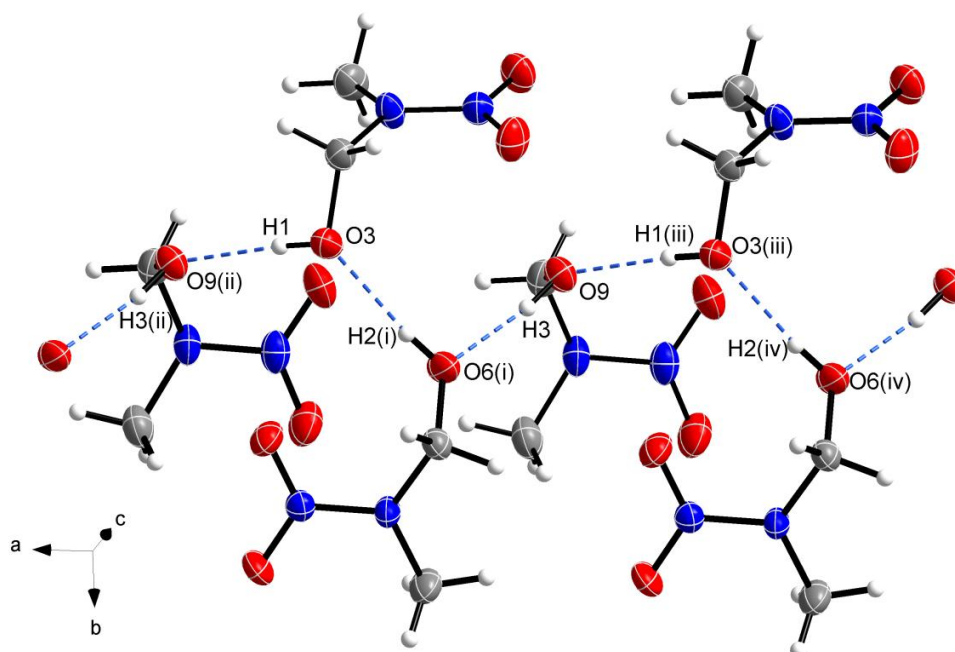


Figure 13: Hydrogen bonds present in the structure of NAP-OH (**5**) forming chains along the *a* axis (listed in Table 10). Symmetry operators: (i) $1-x, \frac{1}{2}+y, \frac{1}{2}-z$; (ii) $1+x, y, z$; (iii) $-1+x, y, z$; (iv) $-x, \frac{1}{2}+y, \frac{1}{2}-z$.

Crystal Structure of 2-Nitro-2-Azapropyl Chloride (6)

NAP-Cl (**6**) crystallises as colourless blocks in the monoclinic space group $P 2_1/n$ with four molecules in the unit cell and a calculated maximum density of $1.590 \text{ g}\cdot\text{cm}^{-3}$ at 173(2) K. The molecular structure is shown in Figure 14. N2 is in plane with C1–C2–N1. The nitro group is almost planar in the C1–C2–N1 plane bended out with $1.7(1)^\circ$. The chlorine atom turns out of this plane with $67.2(1)^\circ$ and the C2–Cl1 bond length [$1.81(1) \text{ \AA}$] is clearly elongated compared to a standard C–Cl bond (1.76 \AA),^[32] thus giving one explanation for the high reactivity towards nucleophilic attack at C2.

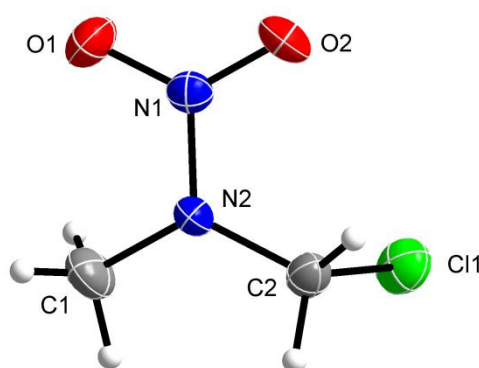


Figure 14: Crystal structure of NAP-Cl (**6**). Selected bond lengths and angles are listed in Table 11.

Table 11 shows selected bond lengths and angles of the crystal structure in comparison to the gas phase structure determined by IVSHIN *et al.* in 1982.^[33] Similar to the solid state of MNA (**1**) the N1–N2 bond in the crystal structure of compound **6** is shortened [from $1.424(5)$ to $1.358(2) \text{ \AA}$], which indicates a higher π character of the bond in the solid state. Thus the rotation of the nitro group out of the CNC-plane with about 30° in the gas phase structure stands in agreement with the higher energetic asymmetrical stretching vibration ν_{as} found in the gas phase IR spectrum of the compound (see vibrational spectroscopy section). This also affects the C2–N2 bond, which is shortened from $1.476(9)$ to $1.419(2) \text{ \AA}$.

Table 11: Selected bond length [\AA] and angles [$^\circ$] in the crystal structure of compound **6** depicted in Figure 14 in comparison to the gas phase structure.^[33]

Bond lengths [\AA]	Crystal structure	Gas phase structure ^[33]
N1–N2	1.358(2)	1.424(5)
N1–O1	1.231(2)	1.212(2)
C2–N2	1.419(2)	1.476(9)
N2–C1	1.459(2)	1.476(9)
C2–Cl1	1.811(2)	1.809(4)
Angles [$^\circ$]		
N1–N2–C1	117.0(1)	116.6(0)
C2–N2–N1	118.0(1)	116.6(6)
C1–N2–C2	122.8(1)	127.0(9)
N2–C2–Cl1	112.8(1)	107.7(9)
O1–N1–N2–C2	178.3(1)	–
Standard bond lengths [\AA]: N–N 1.46, C–N 1.47, N–O 1.45, C–Cl 1.76, N=N 1.20, C=N 1.22, N=O 1.17. ^[32]		

The structure of NAP-Cl (**6**) is constructed by several intermolecular interactions. The hydrogen bonds build up layers, which are connected through electrostatic interactions between the nitro groups well below the sum of van der Waals radii, and the typical chlorine electrostatic interaction [C2–H4···Cl1(ii)] resulting in a wave-like arrangement (Table 12, Figure 15).

Table 12: Interactions in the structure of NAP-Cl (**6**) presented in Figure 15.

D–H···A	d (D–H) [Å]	d (H···A) [Å]	d (D–H···A) [Å]	∠ (D–H···A) [°]
C2–H4···Cl1	0.96(2)	3.01(2)	3.630(2)	124.1(3)
C1–H3···O1(iii)	0.95(3)	2.54(2)	3.461(1)	162.2(2)
Electrostatic interaction			d (X···Y) [Å]	ΣvdWals radii ^[31]
O2···N2(i), O2(i)···N2			2.924(2)	3.07 Å
Symmetry operators: (i) $-x, 1-y, -z$; (ii) $\frac{1}{2}-x, \frac{1}{2}+y, \frac{1}{2}-z$; (iii) $\frac{1}{2}+x, \frac{1}{2}-y, \frac{1}{2}+z$.				

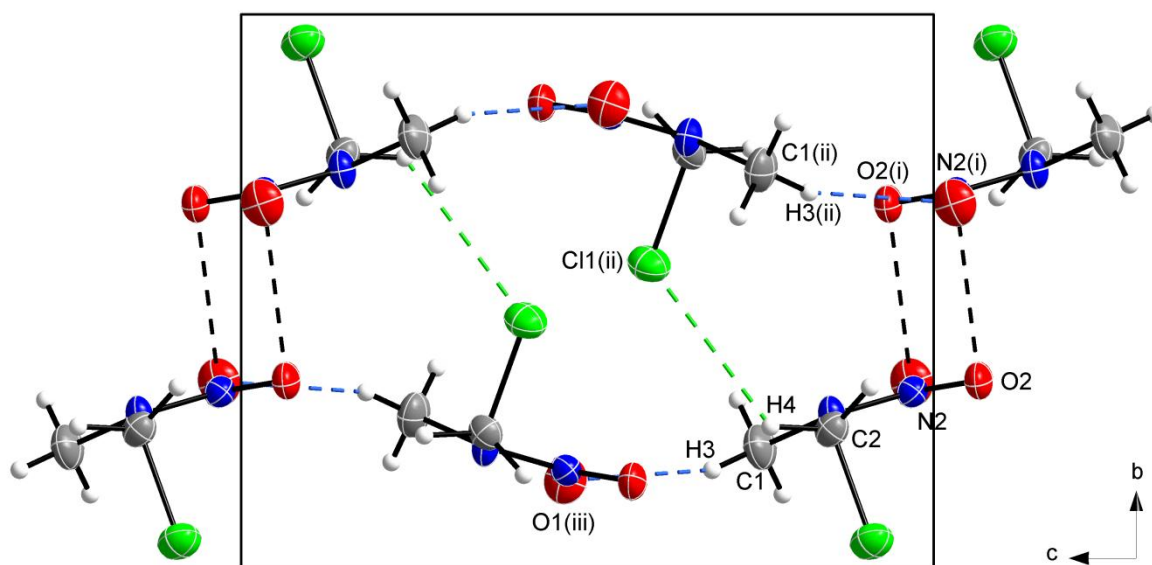


Figure 15: Unit cell of compound **6** with view along the a axis: one hydrogen bond (blue) and two electrostatic interactions (black and green), listed in Table 12. Symmetry operators: (i) $-x, 1-y, -z$; (ii) $\frac{1}{2}-x, \frac{1}{2}+y, \frac{1}{2}-z$; (iii) $\frac{1}{2}+x, \frac{1}{2}-y, \frac{1}{2}+z$.

Crystal Structure of 2-Nitro-2-Azapropyl Isocyanate (9)

NAP-NCO (**9**) crystallises as colourless blocks in the monoclinic space group $P 2_1/c$ with four molecules in the unit cell and a calculated maximum density of $1.559 \text{ g}\cdot\text{cm}^{-3}$ at 100(2) K. The molecular structure is shown in Figure 16 (right). It shows a weak electrostatic intramolecular interaction between O2 of the secondary nitramine group and C3 of the isocyanate moiety, with $2.83(1) \text{ \AA}$ clearly under the sum of the van der Waals radii [$\Sigma\text{vdW}(\text{C},\text{O}) = 3.22 \text{ \AA}$]^[31] forming a six-membered ring. Interestingly a previous calculation on the gas phase structure of compound **9** at the MP2 level of theory predicts such interaction between $\text{C3}\cdots\text{O2}$, however with 3.12 \AA considerably elongated (Figure 16, left).

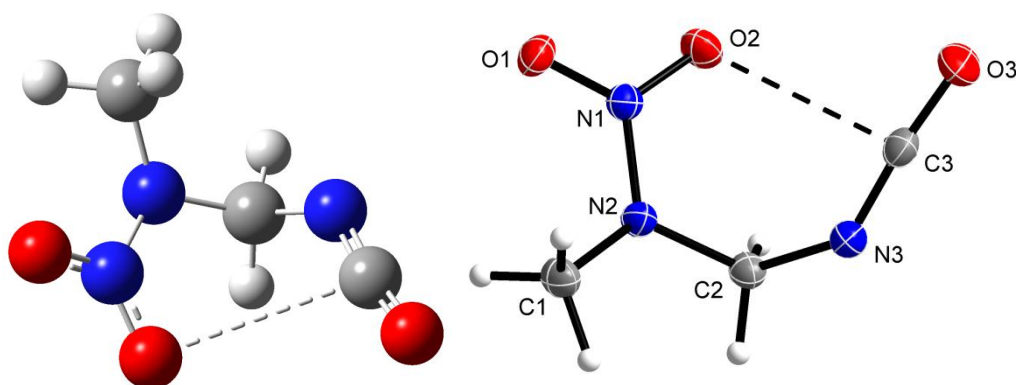


Figure 16: Molecular structure of compound **9**. Left: gas phase structure calculated at the MP2 level of theory: $\text{O2}\cdots\text{C3}$ 3.12 \AA . Right: crystal structure with intramolecular interaction: $\text{O2}\cdots\text{C3}$ $2.83(1) \text{ \AA}$; $\Sigma\text{vdW}(\text{C},\text{O}) = 3.22 \text{ \AA}$.^[31] Selected bond lengths [\AA] and angles [$^\circ$]: O2-N1 $1.244(1)$, O1-N1 $1.229(1)$, O3-C3 $1.173(1)$, N3-C3 $1.200(1)$, N3-C2 $1.459(2)$, N2-N1 $1.350(2)$, N2-C2 $1.445(1)$, N2-C1 $1.459(2)$, C3-N3-C2 $131.3(1)$, O1-N1-O2 $124.6(1)$, O3-C3-N3 $171.9(1)$, C2-N2-N1-O2 $5.8(1)$.

Figure 17 shows the view along the a axis with a weak intermolecular interaction between C3 and O3(i) of the isocyanate moiety. With $3.21(1) \text{ \AA}$ it is just in the range of the sum of van der Waals radii [$\Sigma\text{vdW}(\text{C},\text{O}) = 3.22 \text{ \AA}$], thus indicating the general possible dimerisation of isocyanates.

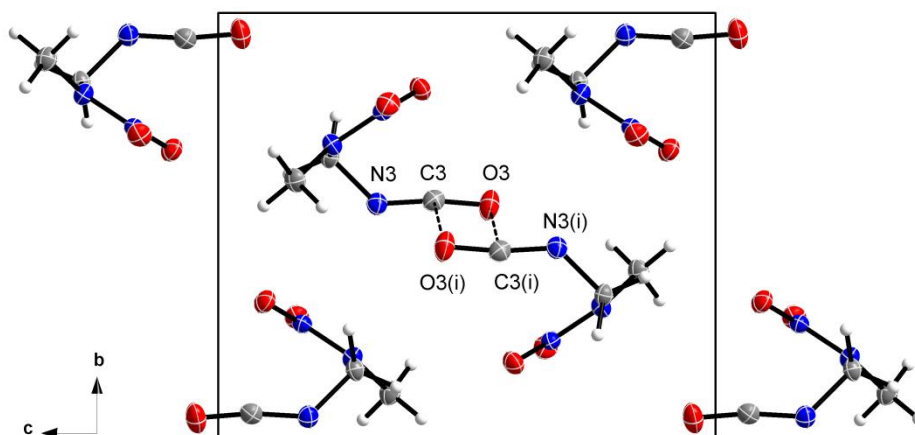


Figure 17: View along the a axis in the crystal structure of compound **9**. Very weak intermolecular interaction: C3-O3(i) $3.21(1) \text{ \AA}$; $\Sigma\text{vdW}(\text{C},\text{O}) = 3.22 \text{ \AA}$.^[31] Symmetry operator (i): $x, \frac{1}{2}-y, -\frac{1}{2}+z$.

Crystal Structure of 2-Nitro-2-Azapropyl Phthalimide (10)

2-Nitro-2-azapropyl phthalimide (**10**) crystallises as colourless blocks in the triclinic space group $P\bar{1}$ with two molecules in the unit cell and a calculated maximum density of $1.462\text{ g}\cdot\text{cm}^{-3}$ at ambient temperature [298(2) K] (Figure 18).

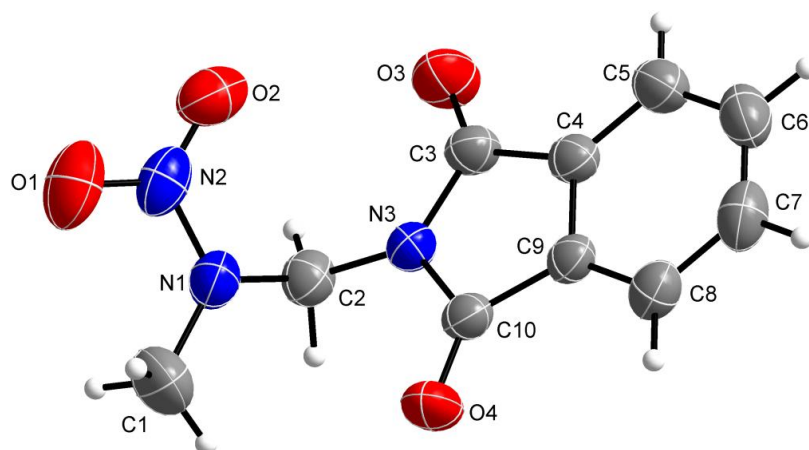


Figure 18: Crystal structure of NAP-phthalimide (**10**). Selected bond lengths [\AA] and angles [$^\circ$]: O4–C10 1.209(2), O3–C3 1.208(2), N3–C2 1.443(2), N1–N2 1.358(2), N1–C2 1.450(2), average N2–O 1.229(2), N1–C2–N3 114.0(2).

As expected the phthalimide unit is planar and the nitramine unit is bent out of this plane by $114.0(2)^\circ$ (N1–C2–N3), thus forming a wave-like arrangement observed by view along the b axis (Figure 19).

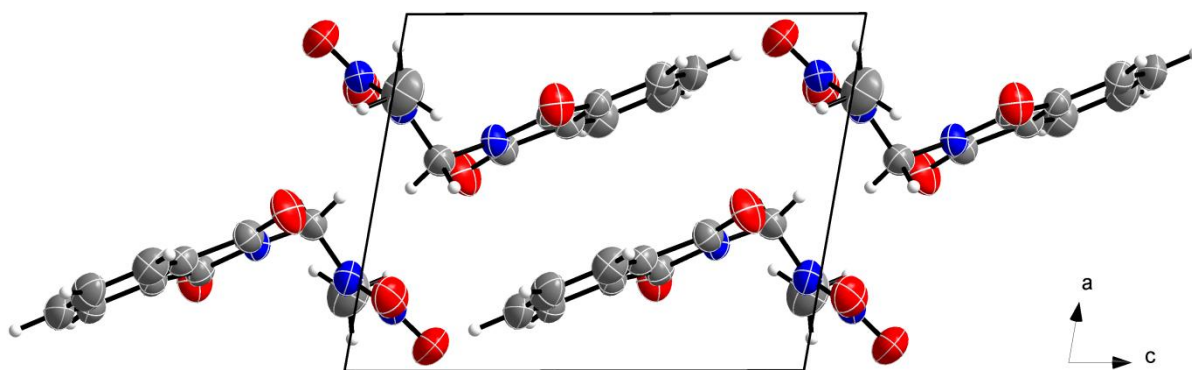


Figure 19: Unit cell with view along the b axis in the crystal structure of compound **10** illustrating the wave-like arrangement in consequence of the intramolecular angle N1–C2–N3.

1.6 Physical, Chemical and Energetic Properties

The physical and chemical properties of compounds **1**, **1a–j**, **4c–j** are listed in Table 13; the predicted detonation and combustion parameters calculated with the EXPLO5 program package (Version 6.02)^[34] of compounds **1**, **1a–c**, **1g**, **1j**, **4c–j** are summarized in Table 14. Compounds which are not listed could either not be measured due to instability or high hygroscopicity (**4a–c**), or could not be calculated due to not implemented elements either within GAUSSIAN^[35] or EXPLO5^[34] (**1d–f**, **1h–i**, **4a–c**). The NAP derivatives **5**, **6**, **7**, **9** and **10** are excluded from this section as these are either known compounds with properties published elsewhere or not stable at ambient conditions.

No decomposition point for MNA (**1**) could be determined in a range up to 400 °C even when using a closed vessel in the DSC owing to its boiling point at 85 °C. In addition, a longterm stability test of **1** was performed with a RADEX V5 oven.^[36] The test was performed in a glass test vessel at atmospheric pressure with 312 mg of **1**. It was previously shown that tempering a substance for 48 h at 40 °C below its decomposition temperature results in storage periods over approximately 50 years at room temperature.^[37] A temperature below the boiling point of **1** was chosen and elemental analysis before the test and after 48 h was carried out. According to elemental analysis MNA (**1**) showed no decomposition after tempering for 48 h at 75 °C.

All compounds except compound **1** show melting points higher than 100 °C. For compounds **1a**, **1h–1j**, **4c**, **4g** and **4h** no melting was observed. Compounds **1g**, **4e**, **4f** and **4i** have melting ranges of approximately 90 to 125 °C. The decomposition temperatures of the alkali and alkaline earth salts were found between 208 °C for KMNA (**1c**) and 269 °C for LiMNA (**1a**). The transition metal salts **1h**, **1i** and **1j** show onset decomposition temperatures of 230 (AgMNA), 238 [Zn(MNA)₂] and 168 °C [Cu(MNA)₂], respectively (Figure 20). For the nitrogen rich salts **4c–4j** decomposition temperatures between 179 °C for the diaminoguanidinium (**4g**), and an outstanding high temperature of 259 °C for the 3,5-diamino-1,2,4-triazolium salt (**4d**) were observed.

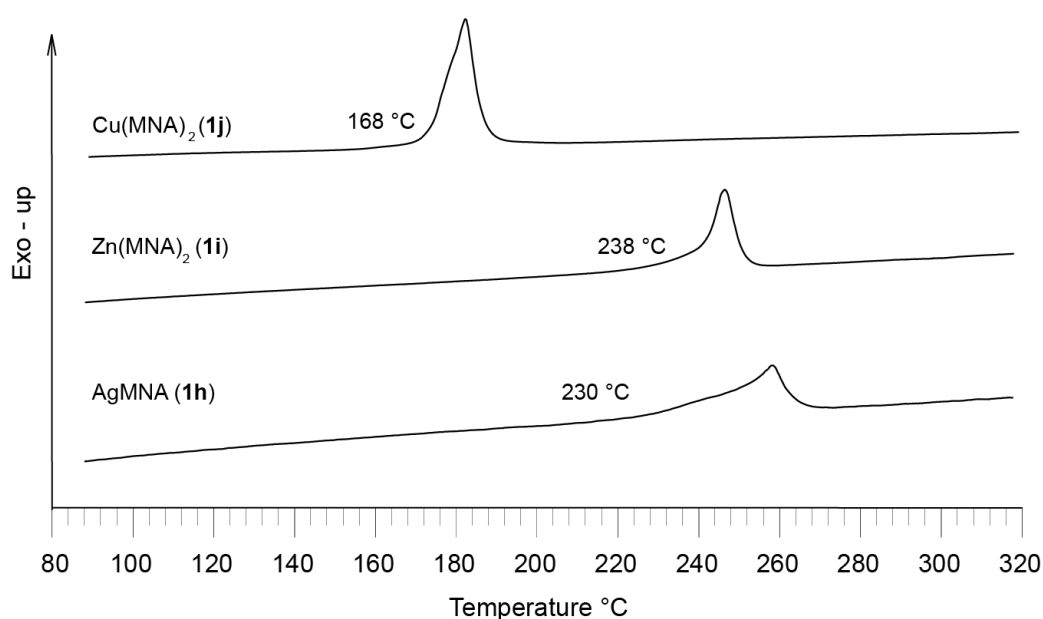


Figure 20: DSC plots of AgMNA (**1h**), Zn(MNA)₂ (**1i**) and Cu(MNA)₂ (**1j**) recorded with a heating rate of 5 °C·min⁻¹.

Table 13: Physical and thermodynamic properties determined for compounds **1**, **1a–j** and **4c–j**.

	1	1a	1b	1c	1d	1e·H₂O	
Formula	CH ₄ N ₂ O ₂	CH ₃ N ₂ O ₂ Li	CH ₃ N ₂ O ₂ Na	CH ₃ N ₂ O ₂ K	CH ₃ N ₂ O ₂ Cs	C ₂ H ₈ N ₄ O ₅ Sr	
FW [g·mol^{−1}]	76.05	82.04	98.04	114.15	207.95	255.96	
IS [J]^a	20	40	40	30	40	40	
FS [N]^b	240	360	360	324	360	360	
ESD [J]^c	0.15	1.5	1.5	1.25	1.5	1.5	
N [%]^d	36.83	34.17	28.57	24.54	13.47	21.91	
T_{melt} [°C]^e	35	–	169	145	199	229	
T_{dec} [°C]^f	–	269	232	208	228	240	
ρ_{RT} [g·cm^{−3}]^g	1.48	1.59	1.92	1.77	–	1.98	
Δ_fH° [kJ·mol^{−1}]^h	−58	−59	−118	−221	–	–	
ΔU° [kJ·kg^{−1}]ⁱ	−630	−614	−1116	−1860	–	–	
	1f·H₂O	1g·2H₂O	1h	1i	1j	4c	
Formula	C ₂ H ₈ N ₄ O ₅ Ba	C ₂ H ₁₀ N ₄ O ₆ Ca	CH ₃ N ₂ O ₂ Ag	C ₂ H ₆ N ₄ O ₄ Zn	C ₂ H ₆ N ₄ O ₄ Cu	CH ₈ N ₄ O ₂	
FW [g·mol^{−1}]	305.44	226.20	305.44	215.47	213.64	108.06	
IS [J]^a	40	40	5	40	1	30	
FS [N]^b	360	360	48	360	28	216	
ESD [J]^c	1.0	1.5	0.06	1.5	0.75	1.25	
N [%]^d	18.34	24.77	15.31	26.00	20.21	51.83	
T_{melt} [°C]^e	145	123	–	–	–	–	
T_{dec} [°C]^f	208	234	230	238	168	185	
ρ_{RT} [g·cm^{−3}]^g	2.42	1.87	–	–	2.05	1.60	
Δ_fH° [kJ·mol^{−1}]^h	–	−96*	–	–	860	88	
ΔU° [kJ·kg^{−1}]ⁱ	–	−414*	–	–	4107	975	
	4d	4e	4f	4g	4h	4i	4j
Formula	C ₃ H ₉ N ₇ O ₂	C ₂ H ₉ N ₅ O ₂	C ₂ H ₁₀ N ₆ O ₂	C ₂ H ₁₁ N ₇ O ₂	C ₂ H ₁₂ N ₈ O ₂	C ₄ H ₁₃ N ₅ O ₂	C ₃ H ₁₀ N ₆ O ₃
FW [g·mol^{−1}]	175.08	135.13	150.14	165.15	180.17	163.18	178.15
IS [J]^a	40	40	40	40	40	40	40
FS [N]^b	360	360	360	360	360	360	360
ESD [J]^c	1.5	1.5	1.5	1.5	1.5	1.5	1.5
N [%]^d	55.98	51.83	55.97	59.37	62.19	42.92	47.17
T_{melt} [°C]^e	191	128	120	–	–	128	160
T_{dec} [°C]^f	259	218	207	179	223	230	185
ρ_{RT} [g·cm^{−3}]^g	1.55	1.34	1.44	1.45	1.43	1.58	1.54
Δ_fH° [kJ·mol^{−1}]^h	153	−72	33	147	264	−72	−248
ΔU° [kJ·kg^{−1}]ⁱ	1001	−386	368	1040	1617	−289	−1257

a) Impact sensitivity (BAM drophammer, method 1 out of 6);^[38–40] b) friction sensitivity (BAM friction tester, method 1 out of 6);^[40–42] c) electrostatic discharge sensitivity (OZM);^[43, 44] a–c) grain size <100 μm; d) nitrogen content; e) melting temperature from DSC at a heating rate of 5 °C min^{−1}; f) decomposition temperature from DSC at a heating rate of 5 °C min^{−1}; g) density measured with pycnometer at ambient temperature; h) calculated heat of formation at the CBS-4M level of theory; i) energy of formation; *calculated for the anhydrous compound.

According to the UN recommendations on the transport of dangerous goods,^[45] *N*-methylnitramine (**1**) shall be classified as sensitive towards both impact (20 J) and friction (240 N). The prepared alkaline and alkaline earth salts are insensitive, except the potassium salt **1c**, which shows slightly increased sensitivities towards impact (30 J), friction (324 N) and electrostatic discharge (1.25 J). The alkaline earth salts **1e–g** were measured as mono- or dihydrates, respectively. The silver (**1h**) and copper (**1j**) salt are very sensitive and have to be handled with care, whereas Zn(MNA)₂ (**1i**) is insensitive. The nitrogen rich salts shall be classified as insensitive, except the hydrazinium salt (**2c**), which shows slightly increased sensitivities towards impact (30 J), friction (216 N) and electrostatic discharge (1.25 J). The electrostatic discharge test was carried out to determine whether the compounds are ignitable

by the human body, which can generate up to 0.025 J of static energy.^[43, 44] All measured compounds are insensitive towards this energy.

The calculation of the detonation and combustion parameters was performed using the calculated heats of formation and densities obtained by pycnometer measurements at ambient temperature (Table 13). In the EXPLO5 computer code a temperature dependent covolume of the detonation products H₂O and NH₃ has been introduced, which should improve the accuracy of results for compounds with high nitrogen and hydrogen contents. Therefore the calculations of the detonation parameters for all MNA salts have been performed using the 'BKW EOS' equation of state with the 'BKWG-CC1' set of constants, which include those covolume corrections.^[34] These results as well as calculations of the specific impulse I_{sp} of aluminised mixtures with and without 12% HTPB are listed in Table 14 and are discussed in the following.

Table 14: Detonation and combustion parameters of compounds **1**, **1a–c**, **1g**, **1j** and **4c–j** calculated with the EXPLO5 computer code (Version 6.02).^[34]

	1	1a	1b	1c	1g*	1j	4c
$-\Delta_{\text{Ex}}U^\circ$ [kJ·kg ⁻¹] ^a	5549	8309	6141	4468	6209	8155	5951
T_{det} [K] ^b	3346	3904	3249	2756	4065	5300	2976
p_{CJ} [kbar] ^c	235	276	316	214	293	350	370
D_V [m·s ⁻¹] ^d	7804	8961	9049	8015	8013	7987	9632
V_0 [L·kg ⁻¹] ^e	967	573	473	415	644	639	1087
I_{sp} (neat) [s] ^f	247 (2360)	255 (2633)	215 (2106)	185 (1992)	259 (3318)	285 (3758)	258 (2154)
I_{sp} (+20% Al) [s] ^g	278 (3180)	256 (2679)	238 (2728)	212 (2726)	246 (2998)	270 (3857)	289 (2841)
I_{sp} (+25% Al) [s] ^g	272 (2967)	253 (2805)	236 (2841)	213 (2842)	234 (3022)	257 (3639)	285 (2893)
I_{sp} (+30% Al) [s] ^g	265 (2977)	251 (2878)	233 (2903)	211 (2905)	233 (3035)	246 (3368)	281 (2933)
I_{sp} (+18% Al, 12% HTPB) [s] ^h	260 (2391)	245 (2409)	228 (2297)	206 (2296)	270 (2787)	260 (3092)	271 (2282)
	4d	4e	4f	4g	4h	4i	4j
$-\Delta_{\text{Ex}}U^\circ$ [kJ·kg ⁻¹] ^a	4169	3737	4184	4589	4938	3575	3131
T_{det} [K] ^b	2569	2346	2468	2617	2757	1981	2117
p_{CJ} [kbar] ^c	253	184	236	254	255	288	223
D_V [m·s ⁻¹] ^d	8249	7436	8180	8409	8441	9062	7882
V_0 [L·kg ⁻¹] ^e	919	1027	1033	1041	1048	992	949
I_{sp} (neat) [s] ^f	210 (1530)	204 (1297)	214 (1393)	224 (1512)	233 (1650)	198 (1247)	188 (1223)
I_{sp} (+20 % Al) [s] ^g	243 (2448)	252 (2229)	256 (2241)	260 (2401)	264 (2549)	245 (2149)	240 (2251)
I_{sp} (+25 % Al) [s] ^g	241 (2684)	248 (2306)	252 (2478)	257 (2632)	262 (2734)	243 (2220)	237 (2305)
I_{sp} (+30 % Al) [s] ^g	240 (2887)	245 (2563)	250 (2703)	255 (2802)	260 (2885)	239 (2303)	233 (2480)
I_{sp} (+18% Al, 12% HTPB) [s] ^h	237 (2208)	244 (2156)	248 (2170)	251 (2184)	254 (2196)	236 (2063)	233 (2175)

*Calculated as anhydrous compound; a–e) Detonation parameters calculated with EXPLO5 (V6.02) using the 'BKW EOS' equation of state with the 'BKWG-CC1' set of constants;^[34] a) heat of detonation; b) detonation temperature; c) detonation pressure; d) detonation velocity; e) volume of gaseous detonation products (assuming only gaseous products); f–h) Isobaric combustion parameters calculated with EXPLO5 (V6.02) using isobaric combustion conditions,^[34] chamber pressure of 70.0 bar versus ambient pressure with equilibrium expansion conditions at the nozzle throat; isobaric combustion temperature in the combustion chamber in parentheses [K]; f) specific impulse of the neat compound; g) specific impulse of mixtures with 20–30% aluminium; h) specific impulse of mixtures with 18% aluminium, 10% hydroxyterminated poly-butadiene (HTPB) and 2% hexamethylene diisocyanate as curing agent; the analogue mixture with AP reveals $I_{sp} = 264$ s and $T_C = 3564$ K.

The detonation parameters of neutral MNA (**1**) reveal a performance in the range between those calculated for trinitrotoluene (TNT; 1.65 g·cm⁻³; $D_V = 7241$ m·s⁻¹, $p_{\text{CJ}} = 207$ kbar) and 1,3,5-trinitroperhydro-1,3,5-triazine (RDX; 1.80 g·cm⁻³; $D_V = 8838$ m·s⁻¹, $p_{\text{CJ}} = 343$ kbar). For testing the ignitability and explosiveness of *N*-methylnitramine (**1**), a small scale

reactivity test (SSRT) with a standard igniter was performed.^[46] Therefore compound **1** (406 mg) was pressed into a perforated steel block and topped with a commercially available detonator (Orica, DYNADET-C2-0ms).^[47] Initiation resulted in a dented aluminium block below the steel block (Figure 21). The depth of the dent caused by **1** was measured by filling it with sand. Despite the fact that *N*-methylnitramine (**1**) was successfully ignited, the depth of the dent was in the range of TNT and RDX, which stands in agreement with its (**1**) calculated detonation velocity D_V of $7804 \text{ m}\cdot\text{s}^{-1}$ and the detonation pressure p_{CJ} of 235 kbar. The calculated specific impulse I_{sp} of the aluminised MNA (**1**) mixture embedded in 12% HTPB reveals 260 s, which is in the range of commonly used aluminised mixtures of AP in HTPB (264 s), although MNA (**1**) shows a rather negative oxygen balance Ω_{CO_2} of -42.1% ($\Omega_{CO} = -21.0\%$). However, in comparison to the AP mixture the calculated temperature in the combustion chamber T_C is significantly decreased from 3564 to 2391 K (Table 14).

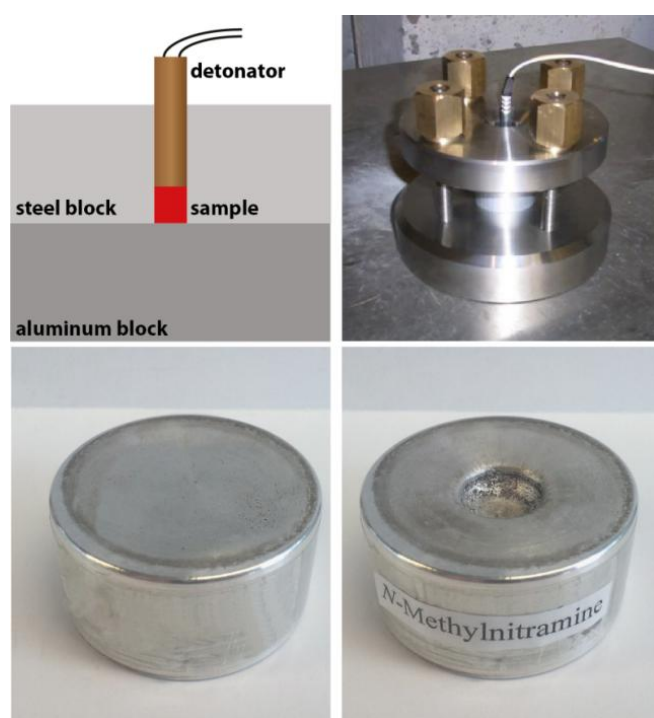


Figure 21: Top: test setup for the SSRT. Bottom: aluminium block before and after initiation of compound **1**.

The detonation velocities D_V of the lithium (**1a**) and sodium (**1b**) salts were calculated to be significantly higher than that of *N*-methylnitramine (**1**), while the D_V of the potassium (**1c**), anhydrous calcium (**1g**) and copper (**1j**) salts are found to be in the range of *N*-methylnitramine (**1**). Additionally the flame colours of the alkaline and alkaline earth salts **1a–f** were tested in a Bunsen burner flame, as these were initially synthesised in consideration for pyrotechnical applications. Unfortunately, all these salts show flame colours that are too pale for visible pyrotechnical applications (Figure 22).^[48]

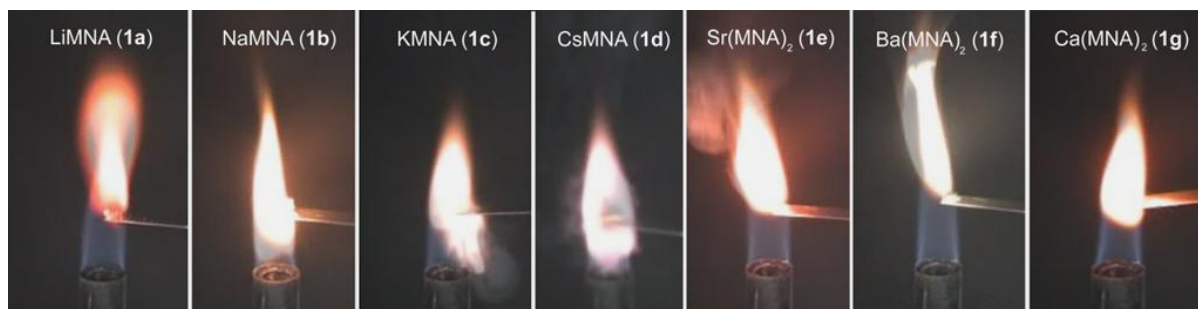


Figure 22: Flame colour test of alkaline and alkaline earth MNA salts **1a–g**.

In addition the copper(II) salt **1j** was tested on its ignitibility by laser irradiation. Therefore a confined sample of compound **1j** [220 mg + 5% polytetrafluoroethylene (PTFE)] on an aluminium plate was irradiated by a laser pulse with a wavelength of 940 nm and a pulse length of 100 μ s. The test showed that $\text{Cu}(\text{MNA})_2$ (**1j**) is ignitable by laser irradiation, and the aluminium plate was deformed by the shock wave (Figure 23). However, compound **1j** shows very high sensitivities and therefore it is not suitable for safe handling or any applications.^[49]



Figure 23: Left: Confined sample of $\text{Cu}(\text{MNA})_2$ (**1j**) with PTFE connected to optical fibre cable. Right: aluminium plate after laser initiation of $\text{Cu}(\text{MNA})_2$ (**1j**).

When comparing the nitrogen rich salts **4c–j**, the hydrazinium salt **4c** clearly shows the highest detonation velocity D_V of $9623 \text{ m}\cdot\text{s}^{-1}$ ($p_{\text{CJ}} = 370 \text{ kbar}$) and volume of gaseous detonation products V_0 of $1087 \text{ L}\cdot\text{kg}^{-1}$. The specific impulse I_{sp} of compound **4c** in the 18% aluminised mixture embedded in HTPB as used in solid rocket motors was calculated to be 271 s (Table 14), which is about 7 s higher than that of commonly used ammonium perchlorate composite propellants of about 264 s.^[50] As a rule of thumb, an increase in the value for I_{sp} by 20 s leads empirically to a doubling of the usual carried payload (satellite or warhead).^[23] However, as mentioned above, the compound is slightly hygroscopic and contains the toxic and pollutant hydrazinium cation, which might limit the possible applications of this compound.

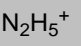
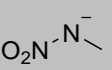
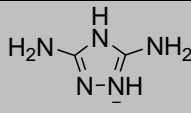
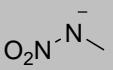
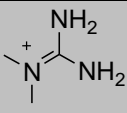
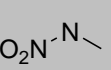
The detonation velocity D_V of DATMNA (**4d**) was calculated to be $8249 \text{ m}\cdot\text{s}^{-1}$, thus clearly higher than that calculated for MNA (**1**). Taking into account its very low mechanical sensitivities ($\text{IS} = 40 \text{ J}$, $\text{FS} = 360 \text{ N}$, $\text{ESD} = 1.5 \text{ J}$) and high decomposition temperature of 259°C (higher than FOX-12/GUDN: $T_{\text{dec}} = 215^\circ\text{C}$),^[51] this salt might be interesting for application in low vulnerability (LOVA) munitions.

When comparing the insensitive salts derived from the guanidinium cation **4e–i** the expected trend is easy to observe: with increasing nitrogen content ($G < AG < DAG < TAG < DMG$) the detonation velocity D_V increases from 7436 (**4e**) to 9062 $\text{m}\cdot\text{s}^{-1}$ (**4i**), as also does the detonation pressure and temperature. The volume of gaseous detonation products is rather high in this nitrogen-rich series **4e–i** in the range of $1000 \text{ L}\cdot\text{kg}^{-1}$. The 18% aluminised mixture of TAGMNA (**4h**) embedded in HTPB achieves the highest specific impulse I_{sp} of 254 s in this series, which is almost that of commonly used ammonium perchlorate composite propellants.^[50] The detonation velocity D_V of the *N*-guanylurea salt (**4j**) was calculated to be $7882 \text{ m}\cdot\text{s}^{-1}$, thus between the guanidinium (**4e**) and the aminoguanidinium salt (**4f**).

1.7 Summary, Conclusions and Outlook

N-Methylnitramine (**1**) can easily be prepared in high purity from *N,N'*-dinitro-*N,N'*-dimethyloxamide. The acidity of the primary nitramine **1** was utilised to synthesise several metal and hitherto unknown nitrogen-rich salts. The crystal structures of **1**, its potassium (**1c**), guanidinium (**4e**), aminoguanidinium (**4f**), guanylurea (**4j**) salts, as well as the NAP derivatives **5**, **6**, **9**, **10** and **12** derived from MNA (**1**), which are important building blocks for the introduction of this moiety into other molecules, were determined by low temperature single crystal X-ray diffraction. All compounds were characterised by multinuclear (^1H , ^{13}C and ^{14}N) NMR spectroscopy, elemental analysis, vibrational spectroscopy and differential scanning calorimetry.

Table 15: Molecular structures of the promising compounds **4c**, **4d** and **4i** with their characteristic properties and possible applications.

	4c	4d	4i
Molecular structure	 	 	 
IS [J]	30	40	40
FS [N]	216	360	360
T_{dec} [$^{\circ}\text{C}$]	185	259	236
D_V [$\text{m}\cdot\text{s}^{-1}$]	9632	8249	9062
p_{CJ} [kbar]	370	253	288
V_0 [$\text{L}\cdot\text{kg}^{-1}$]	1087	919	922
I_{sp} (Al+HTPB) [s]	271	237	236
Possible applications	propellant / gas generator	LOVA munition	LOVA munition

The sensitivities of the MNA salts towards impact, friction and electrostatic discharge were determined according to BAM standard methods and characterised according the UN recommendations. As expected, the silver (**1h**) and copper (**1j**) salts of MNA are the most sensitive ones with impact sensitivities of less than 5 J (**1h**) and 1 J (**1j**), and friction sensitivities of 48 (**1h**) and 28 N (**1j**), respectively. In contrast, the nitrogen-rich salts are insensitive towards these stimuli. Especially the hydrazinium (**4c**), diamino-1,2,4-

triazolium (**4h**) and *N,N*-dimethylguanidinium *N*-methylnitramide (**4h**) show promising performances in combination with insensitivities, whereby these compounds could be considered as nitrogen-rich and perchlorate-free composite propellants (**4c**) or as ingredients in double- and triple-based LOVA munition (**4d+i**, Table 15).

1.8 Experimental Section

N-Methylnitramine (1): *Method 1:* 500 mg *N,N'*-dimethyl-*N,N'*-dinitrooxamide (**2**, 2.4 mmol) was added with stirring at 0 °C to a solution of ammonia (25%, 10 mL). After 1 h the colourless dimethyloxamide (**3**) was removed by filtration and washed with small amounts of water. The aqueous phase was acidified with sulfuric acid (2 M) until reaching pH = 3 and extracted with diethyl ether (3 × 50 mL). After drying over magnesium sulfate the solvent was removed under reduced pressure yielding 335 mg of compound **1** (4.4 mmol, 92%).

Method 2: 500 mg *N,N'*-dimethyl-*N,N'*-dinitrooxamide (**2**, 2.4 mmol) was added with stirring to a solution of methylamine (40%, 0.9 mL, 11.8 mmol). After 1 h the colourless dimethyloxamide (**3**) was removed by filtration and washed with small amounts of water. The aqueous phase was acidified with sulfuric acid (2 M) until reaching pH = 3 and extracted with diethyl ether (3 × 50 mL). After drying over magnesium sulfate the solvent was removed under reduced pressure yielding 320 mg of compound **1** (4.2 mmol, 88%).

DSC (T_{onset}): $T_{\text{melt}} = 35\text{ °C}$, $T_{\text{dec}} = 86\text{ °C}$; **^1H NMR** (CD_2Cl_2): $\delta = 8.72$ (s, 1 H, NH), 3.13 (s, 3 H, CH_3) ppm; **$^{13}\text{C}\{^1\text{H}\}$ NMR** (CD_2Cl_2): $\delta = 32.8$ (CH_3) ppm; **$^{14}\text{N}\{^1\text{H}\}$ NMR** (CD_2Cl_2): $\delta = -27$ (NO_2), -219 (NH) ppm; **^{15}N NMR** (CD_2Cl_2): $\delta = -26.2$ (q, $^3J_{15\text{N-H}} = 2.8\text{ Hz}$, NO_2), -218.6 (s, NH) ppm; **EA**: $\text{CH}_4\text{N}_2\text{O}_2$ ($76.03\text{ g}\cdot\text{mol}^{-1}$): calcd. C 15.79, H 5.30, N 36.83; found C 16.05, H 5.06, N 36.42 %; **IR** (solid phase): $\tilde{\nu}$ (rel. int.) = 3220 (s), 3092 (m), 2924 (m), 2496 (w), 2360 (w), 2332 (w), 1700 (w), 1684 (w), 1652 (w), 1635 (w), 1575 (s), 1468 (s), 1433 (s), 1380 (s), 1332 (vs), 1173 (s), 1112 (s), 945 (m), 773 (m), 720 (m), 667 (m) cm^{-1} ; **IR** (gaseous phase): $\tilde{\nu}$ (rel. int.) = 3204 (m), 2970 (w), 1621 (s), 1572 (m), 1470 (m), 1440 (m), 1390 (s), 1323 (vs), 1171 (m), 1121 (m), 924 (w), 910 (w), 772 (w), 594 (w) cm^{-1} ; **Raman** (500 mW): $\tilde{\nu}$ (rel. int.) = 3628 (15), 3233 (18), 3031 (36), 3001 (38), 2957 (100), 1440 (26), 1387 (16), 1175 (24), 1117 (88), 950 (66), 598 (27), 105 (93), 86 (99) cm^{-1} ; **MS** (DEI^+): $m/z = 29.08$ [CH_3N^+], 30.06 [CH_4N^+], 46.08 [NO_2^+], 76.07 [M^+], (DCI^+): $m/z = 77.05$ [$\text{M}+\text{H}^+$]; **drophammer**: 20 J; **friction tester**: 240 N; **ESD**: 0.15 J; **grain size**: <100 μm ; **RADEX** (75 °C, 48 h): no decomposition.

General procedure for lithium, sodium, potassium, caesium, strontium and barium N-methylnitramide (1a–f): A solution of 230 mg MNA (**1**, 3.0 mmol) in water (10 mL) was combined with a stirred solution of equimolar lithium, potassium, caesium (3.0 mmol), strontium or barium hydroxide (1.5 mmol), respectively. After stirring for 30 min the solvent was removed under reduced pressure and the colourless residues were re-crystallised from hot ethanol or water yielding compounds **1a–f**.

Lithium N-Methylnitramide (1a): Yield 233 mg (2.84 mmol, 94%).

DSC (T_{onset}): $T_{\text{melt}} = 145\text{ °C}$, $T_{\text{dec}} = 208\text{ °C}$; **^1H NMR** (D_2O): $\delta = 2.96$ (s, 3 H, CH_3) ppm; **$^{13}\text{C}\{^1\text{H}\}$ NMR** (D_2O): $\delta = 38.4$ (CH_3) ppm; **$^{14}\text{N}\{^1\text{H}\}$ NMR** (D_2O): $\delta = -24$ (NO_2), -109 (NNO_2) ppm; **EA**: $\text{CH}_3\text{LiN}_2\text{O}_2$ ($82.04\text{ g}\cdot\text{mol}^{-1}$): calcd. C 14.65, H 3.69, N 34.17; found C 14.87, H 3.55, N 34.14 %; **IR**: $\tilde{\nu}$ (rel. int.) = 3022 (w), 2955 (w), 2921 (m), 2851 (w), 2438 (w), 2163 (w), 1567 (w), 1506 (s), 1490 (vs), 1427 (m), 1387 (m), 1370 (s), 1309 (m), 1288 (vs), 1170 (m), 1084 (m), 945 (m), 755 (s), 728 (m) cm^{-1} ; **Raman** (500 mW): $\tilde{\nu}$ (rel. int.) = 3028 (40), 2957 (25), 2922 (100), 2851 (11), 1491 (18), 1441 (16), 1386 (31), 1175 (12),

1089 (5), 954 (26), 726 (8), 624 (17) cm^{-1} ; **MS** (FAB^+): $m/z = 7.0$ [Li^+], (FAB^-): $m/z = 75.0$ [MNA^-]; **drophammer**: 40 J; **friction tester**: 360 N; **ESD**: 1.5 J; **grain size**: <100 μm .

Sodium *N*-Methylnitramide (1b): Yield 270 mg (2.76 mmol, 92%).

DSC (T_{onset}): $T_{\text{dec}} = 269$ $^{\circ}\text{C}$; ^1H **NMR** (D_2O): $\delta = 2.96$ (s, 3 H, CH_3) ppm; $^{13}\text{C}\{^1\text{H}\}$ **NMR** (D_2O): $\delta = 38.4$ (CH_3) ppm; $^{14}\text{N}\{^1\text{H}\}$ **NMR** (D_2O): $\delta = -24$ (NO_2), -113 (NNO_2) ppm; $\text{CH}_3\text{N}_2\text{NaO}_2$ (98.04 $\text{g}\cdot\text{mol}^{-1}$): calcd. C 12.25, H 3.08, N 28.57; found C 12.35, H 3.37, N 26.43; **IR**: $\tilde{\nu}$ (rel. int.) = 3004 (w), 2941 (w), 2908 (w), 2410 (w), 2362 (w), 2339 (w), 2074 (w), 1917 (w), 1789 (w), 1636 (m), 1560 (m), 1470 (s), 1427 (s), 1380 (m), 1336 (w), 1263 (vs), 1141 (s), 1084 (s), 927 (m), 880 (m), 746 (s), 684 (m) cm^{-1} ; **Raman** (500 mW): $\tilde{\nu}$ (rel. int.) = 3008 (66), 2908 (100), 1519 (31), 1429 (17), 1385 (37), 1145 (23), 1102 (21), 933 (61), 706 (16), 634 (28) cm^{-1} ; **MS** (FAB^+): $m/z = 23.0$ [Na^+], (FAB^-): $m/z = 75.0$ [MNA^-]; **drophammer**: 40 J; **friction tester**: 360 N; **ESD**: 1.5 J; **grain size**: <100 μm .

Potassium *N*-Methylnitramide (1c): Yield 318 mg (2.79 mmol, 93%).

DSC (T_{onset}): $T_{\text{melt}} = 169$ $^{\circ}\text{C}$, $T_{\text{dec}} = 297$ $^{\circ}\text{C}$; ^1H **NMR** (D_2O): $\delta = 3.01$ (s, 3 H, CH_3) ppm; $^{13}\text{C}\{^1\text{H}\}$ **NMR** (D_2O): $\delta = 38.2$ (CH_3) ppm; $^{14}\text{N}\{^1\text{H}\}$ **NMR** (D_2O): $\delta = -24$ (NO_2), -114 (NNO_2) ppm; **EA**: $\text{CH}_3\text{KN}_2\text{O}_2$ (114.15 $\text{g}\cdot\text{mol}^{-1}$): calcd. C 10.52, H 2.65, N 24.54; found C 10.09, H 2.49, N 22.50 %; **IR**: $\tilde{\nu}$ (rel. int.) = 2989 (w), 2911 (w), 2853 (w), 2363 (w), 2340 (w), 1637 (w), 1589 (m), 1459 (s), 1433 (m), 1372 (s), 1347 (m), 1292 (vs), 1150 (s), 1080 (s), 929 (m), 860 (w), 764 (s), 752 (m), 699 (s) cm^{-1} ; **Raman** (500 mW): $\tilde{\nu}$ (rel. int.) = 2993 (74), 2932 (100), 2915 (97), 2851 (27), 1447 (25), 1435 (28), 1388 (16), 1367 (38), 1165 (14), 1147 (21), 930 (65), 707 (12), 641 (20), 629 (16), 608 (12) cm^{-1} ; **MS** (FAB^+): $m/z = 38.9$ [K^+], (FAB^-): $m/z = 75.0$ [MNA^-]; **drophammer**: 30 J; **friction tester**: 324 N; **ESD**: 1.25 J; **grain size**: <100 μm .

Caesium *N*-Methylnitramide (1d): Yield 518 mg (2.49 mmol, 83%).

DSC (T_{onset}): $T_{\text{melt}} = 199$ $^{\circ}\text{C}$, $T_{\text{dec}} = 228$ $^{\circ}\text{C}$; ^1H **NMR** (D_2O): $\delta = 3.00$ (s, 3 H, CH_3) ppm; $^{13}\text{C}\{^1\text{H}\}$ **NMR** (D_2O): $\delta = 38.5$ (CH_3) ppm; $^{14}\text{N}\{^1\text{H}\}$ **NMR** (D_2O): $\delta = -24$ (NO_2), -113 (NNO_2) ppm; **EA**: $\text{CH}_3\text{CsN}_2\text{O}_2$ (207.95 $\text{g}\cdot\text{mol}^{-1}$): calcd. C 5.78, H 1.45, N 13.47; found C 5.77, H 1.71, N 12.70 %; **IR**: $\tilde{\nu}$ (rel. int.) = 2979 (w), 2936 (w), 2194 (w), 1788 (w), 1651 (m), 1574 (m), 1456 (s), 1431 (s), 1398 (w), 1367 (s), 1286 (vs), 1146 (s), 1091 (s), 925 (m), 764 (m), 696 (m) cm^{-1} ; **Raman** (500 mW): $\tilde{\nu}$ (rel. int.) = 2980 (56), 2916 (100), 2839 (20), 1463 (16), 1429 (24), 1378 (31), 1300 (8), 1151 (37), 1095 (11), 927 (67), 698 (20), 631 (26) cm^{-1} ; **MS** (FAB^+): $m/z = 133.0$ [Cs^+], (FAB^-): $m/z = 75.0$ [MNA^-]; **drophammer**: 40 J; **friction tester**: 360 N; **ESD**: 1.5 J; **grain size**: <100 μm .

Strontium *N*-Methylnitramide Monohydrate (1e): Yield 721 mg (2.82 mmol, 94%).

DSC (T_{onset}): $T_{-\text{H}_2\text{O}} = 125$ $^{\circ}\text{C}$, $T_{\text{melt}} = 229$ $^{\circ}\text{C}$, $T_{\text{dec}} = 240$ $^{\circ}\text{C}$; ^1H **NMR** (D_2O): $\delta = 2.94$ (s, 3 H, CH_3) ppm; $^{13}\text{C}\{^1\text{H}\}$ **NMR** (D_2O): $\delta = 38.2$ (CH_3) ppm; $^{14}\text{N}\{^1\text{H}\}$ **NMR** (D_2O): $\delta = -24$ (NO_2), -113 (NNO_2) ppm; **EA**: $\text{C}_2\text{H}_8\text{N}_4\text{O}_5\text{Sr}$ (255.96 $\text{g}\cdot\text{mol}^{-1}$): calcd. C 9.39, H 3.15, N 21.91; found C 9.46, H 3.04, N 21.86 %; **IR**: $\tilde{\nu}$ (rel. int.) = 3022 (w), 2948 (w), 2914 (m), 2437 (w), 2361 (m), 2337 (w), 1695 (w), 1505 (s), 1491 (vs), 1428 (w), 1383 (s), 1376 (m), 1302 (vs), 1278 (s), 1172 (m), 1164 (m), 1090 (s), 943 (m), 767 (m), 751 (s), 720 (m), 706 (m), 668 (w) cm^{-1} ;

Raman (500 mW): $\tilde{\nu}$ (rel. int.) = 3024 (32), 3003 (13), 2949 (28), 2916 (100), 2846 (13), 2740 (13), 1492 (23), 1441 (12), 1383 (26), 1309 (8), 1171 (12), 1093 (5), 948 (37), 724 (10), 637 (5) cm^{-1} ; **MS** (FAB⁻): m/z = 75.0 [MNA⁻]; **drophammer**: 40 J; **friction tester**: 360 N; **ESD**: 1.5 J; **grain size**: <100 μm .

Barium N-Methylnitramide Monohydrate (1f): Yield 852 mg (2.79 mmol, 93%).

DSC (T_{onset}): T_{melt} = 167 °C, T_{dec} = 242 °C; **¹H NMR** (D₂O): δ = 2.83 (s, 3 H, CH₃) ppm; **¹³C{¹H} NMR** (D₂O): δ = 38.1 (CH₃) ppm; **¹⁴N{¹H} NMR** (D₂O): δ = -24 (NO₂), -107 (NNO₂) ppm; **EA**: C₂H₈BaN₄O₅ (305.44 g·mol⁻¹): calcd. C 7.86, H 2.64, N 18.34; found C 7.99, H 2.53, N 18.19 %; **IR**: $\tilde{\nu}$ (rel. int.) = 3016 (w), 2998 (w), 2944 (w), 2910 (m), 2842 (w), 2425 (w), 2362 (m), 2334 (w), 2163 (w), 1982 (w), 1796 (w), 1684 (m), 1654 (m), 1560 (w), 1484 (vs), 1425 (m), 1376 (s), 1293 (vs), 1272 (s), 1164 (m), 1090 (s), 940 (m), 754 (m), 731 (m), 714 (m), 699 (m) cm^{-1} ; **Raman** (500 mW): $\tilde{\nu}$ (rel. int.) = 3017 (35), 3004 (19), 2945 (26), 2913 (100), 2840 (18), 1485 (30), 1438 (12), 1382 (30), 1295 (5), 1170 (13), 1093 (6), 945 (45), 716 (11), 616 (6) cm^{-1} ; **MS** (FAB⁻): m/z = 75.0 [MNA⁻]; **drophammer**: 40 J; **friction tester**: 360 N; **ESD**: 1.0 J; **grain size**: <100 μm .

Silver N-Methylnitramide (1h): 228 mg KMNA (**1c**, 2.0 mmol) was dissolved in water (10 mL). Under constant stirring and exclusion of light, a solution of 340 mg silver nitrate (2.0 mmol) in water (5 mL) was added. Instantly the product **1h** started to precipitate and was then filtered and washed with small amounts of water. The colourless residue was dried at high vacuum yielding 366 mg of compound **1h** (1.7 mmol, 85%).

DSC (T_{onset}): T_{dec} = 230 °C; **¹H NMR** (D₂O): δ = 3.10 (s, 3 H, CH₃) ppm; **¹³C{¹H} NMR** (D₂O): δ = 32.0 (CH₃) ppm; **¹⁴N{¹H} NMR** (D₂O): δ = -20 (NO₂), -109 (NNO₂) ppm; **EA**: CH₃AgN₂O₂ (181.92 g·mol⁻¹): calcd. C 6.57, H 1.65, N 15.31; found C 6.65, H 1.58, N 15.19 %; **IR**: $\tilde{\nu}$ (rel. int.) = 3044 (w), 2964 (w), 2925 (w), 2242 (w), 1790 (w), 1675 (m), 1576 (m), 1482 (vs), 1425 (s), 1370 (s), 1284 (s), 1260 (s), 1177 (m), 1074 (m), 1064 (s), 949 (s), 734 (m), 722 (m) cm^{-1} ; **MS** (FAB⁺): m/z = 106.9 [Na⁺], (FAB⁻): m/z = 75.0 [MNA⁻]; **drophammer**: 5 J; **friction tester**: 48 N; **ESD**: 0.06 J; **grain size**: <100 μm .

Calcium and Zinc N-Methylnitramide (1g and 1i): 228 mg KMNA (**1c**, 2.0 mmol) was dissolved in water (10 mL). Under constant stirring and exclusion of light, a solution of 340 mg silver nitrate (2.0 mmol) in water (5 mL) was added. AgMNA (**1h**) was filtered and washed with small amounts of water, and transferred without drying into a reaction vessel, which contained an aqueous solution of 111 mg CaCl₂ (1.0 mmol) or 136 mg ZnCl₂ (1.0 mmol). Instantly silver chloride started to precipitate and was removed by filtration. The solvent was removed under reduced pressure and the colourless residues were re-crystallised from hot ethanol.

Calcium N-Methylnitramide Dihydrate (1g): Yield 143 mg (0.8 mmol, 80%).

DSC (T_{onset}): T_{melt} = 123 °C, T_{dec} = 234 °C; **¹H NMR** (D₂O): δ = 2.94 (s, 3 H, CH₃) ppm; **¹³C{¹H} NMR** (D₂O): δ = 38.2 (CH₃) ppm; **¹⁴N{¹H} NMR** (D₂O): δ = -24 (NO₂), -115 (NNO₂) ppm; **EA**: C₂H₁₀CaN₄O₆ (226.20 g·mol⁻¹): calcd. C 10.62, H 4.46, N 24.77; found C 9.70, H 4.07, N 21.61 %; **IR**: $\tilde{\nu}$ (rel. int.) = 2953 (w), 2922 (m), 1624 (m), 1488 (s), 1444 (m),

1379 (s), 1292 (vs), 1168 (w), 1155 (m), 1088 (s), 820 (m), 751 (m), 742 (m), 728 (m), 712 (m), 698 (w) cm^{-1} ; **Raman** (500 mW): $\tilde{\nu}$ (rel. int.) = 3023 (14), 2999 (23), 2960 (31), 2924 (100), 2855 (15), 2757 (7), 1492 (20), 1444 (13), 1388 (30), 1297 (5), 1169 (9), 1155 (12), 1095 (5), 939 (38), 715 (10), 633 (5) cm^{-1} ; **MS**: (FAB⁻): m/z = 75.0 [MNA⁻]; **drophammer**: 40 J; **friction tester**: 360 N; **ESD**: 1.5 J; **grain size**: <100 μm .

Zinc *N*-Methylnitramide Dihydrate (1i): Yield 143 mg (0.8 mmol, 80%).

DSC (T_{onset}): T_{dec} = 238 °C; **^1H NMR** (D_2O): δ = 2.99 (s, 3 H, CH_3) ppm; **$^{13}\text{C}\{^1\text{H}\}$ NMR** (D_2O): δ = 36.5 (CH_3) ppm; **$^{14}\text{N}\{^1\text{H}\}$ NMR** (D_2O): δ = -23 (NO_2), -109 (NNO_2) ppm; **EA**: $\text{C}_2\text{H}_6\text{N}_4\text{O}_4\text{Zn}$ (215.47 $\text{g}\cdot\text{mol}^{-1}$): calcd. C 11.15, H 2.81, N 26.00; found C 7.18, H 2.33, N 17.98 %; **IR**: $\tilde{\nu}$ (rel. int.) = 3012 (w), 2956 (w), 2931 (w), 2456 (w), 2360 (m), 2341 (w), 1625 (m), 1581 (m), 1486 (s), 1441 (m), 1381 (s), 1813 (vs), 1204 (w), 1176 (m), 1120 (m), 1102 (m), 974 (m), 957 (m), 825 (m), 757 (m), 732 (w), 715 (m), 672 (w) cm^{-1} ; **Raman** (500 mW): $\tilde{\nu}$ (rel. int.) = 3026 (45), 2967 (36), 2939 (100), 2922 (86), 2855 (23), 1500 (11), 1446 (21), 1387 (23), 1318 (27), 1191 (20), 1127 (8), 1067 (49), 971 (42), 725 (10), 672 (8) cm^{-1} ; **MS**: (FAB⁻): m/z = 75.0 [MNA⁻]; **drophammer**: 40 J; **friction tester**: 360 N; **ESD**: 1.0 J; **grain size**: <100 μm .

Copper *N*-Methylnitramide (1j): 306 mg $\text{Ba}(\text{MNA})_2\cdot\text{H}_2\text{O}$ (**1f**, 1.0 mmol) was dissolved in water (10 mL). Under constant stirring a solution of 250 mg copper sulfate pentahydrate (1.0 mmol) in water (5 mL) was added. Instantly barium sulfate started to precipitate and was removed by filtration. The solvent of the filtrate was removed under reduced pressure and the dark blue residue was re-crystallised from hot ethanol yielding 152 mg of compound **1j** (0.7 mmol, 71%).

DSC (T_{onset}): T_{dec} = 168 °C; **EA**: $\text{C}_2\text{H}_6\text{CuN}_4\text{O}_4$ (213.64 $\text{g}\cdot\text{mol}^{-1}$): calcd. C 11.24, H 2.83, N 26.22; found C 11.12, H 2.74, N 25.63 %; **IR**: $\tilde{\nu}$ (rel. int.) = 3021 (m), 2929 (m), 2360 (m), 2341 (m), 1674 (m), 1653 (m), 1479 (s), 1434 (s), 1378 (s), 1296 (vs), 1253 (s), 1170 (m), 1123 (m), 1098 (s), 1022 (m), 964 (s), 910 (w), 770 (m), 754 (m), 734 (m), 723 (m), 669 (m) cm^{-1} ; **MS**: (FAB⁻): m/z = 75.0 [MNA⁻]; **drophammer**: 1 J; **friction tester**: 28 N; **ESD**: 0.75 J; **grain size**: <100 μm .

General procedure for ammonium, hydroxylammonium and hydrazinium *N*-methylnitramide (4a–c): 0.19 mL of an aqueous ammonia solution (25%, 2.5 mmol), 0.15 mL of an aqueous hydroxylamine solution (50%, 2.5 mmol) or 0.12 mL of an aqueous hydrazinium solution (50%, 2.5 mmol) was added to a stirring and ice-cooled solution of 190 mg MNA (**1**, 2.5 mmol) in water (10 mL). After 1 h stirring the solvent was removed under reduced pressure and compound **4a** or **4b** were obtained in aqueous solution but could not be isolated owing to their very high hygroscopicity. In contrast compound **4c** was obtained as a colourless hygroscopic solid after recrystallisation from hot ethanol.

Ammonium *N*-Methylnitramide (4a):

^1H NMR (D_2O): δ = 3.04 (s, 3 H, CH_3) ppm; **$^{13}\text{C}\{^1\text{H}\}$ NMR** (D_2O): δ = 35.1 (CH_3) ppm; **$^{14}\text{N}\{^1\text{H}\}$ NMR** (D_2O): δ = -22 (NO_2), -117 (NNO_2), -357 (NH_4^+) ppm; **MS** (FAB⁺): m/z = 18.0 [NH_4^+], (FAB⁻): m/z = 75.0 [MNA⁻].

Hydroxylammonium *N*-Methylnitramide (4b):

¹H NMR (D₂O): δ = 3.02 (s, 3 H, CH₃) ppm; **¹³C{¹H} NMR** (D₂O): δ = 36.8 (CH₃) ppm; **¹⁴N{¹H} NMR** (D₂O): δ = -23 (NO₂), -111 (NNO₂), -302 (HONH₃⁺) ppm; **MS** (FAB⁺): m/z = 34.0 [HONH₃⁺], (FAB⁻): m/z = 75.0 [MNA⁻].

Hydrazinium *N*-Methylnitramide (4c): Yield 216 mg (2.00 mmol, 80%).

DSC (T_{onset}): T_{dec} = 185 °C; **¹H NMR** (D₂O): δ = 2.96 (s, 3 H, CH₃) ppm; **¹³C{¹H} NMR** (D₂O): δ = 38.0 (CH₃) ppm; **¹⁴N{¹H} NMR** (D₂O): δ = -24 (NO₂), -118 (NNO₂), -331 (H₂NNH₃⁺) ppm; **EA**: CH₈N₄O₂ (108.10 g·mol⁻¹): calcd. C 11.11, H 7.46, N 51.83; found C 10.58, H 7.63, N 47.61 %; **IR**: $\tilde{\nu}$ (rel. int.) = 3312 (m), 3143 (w), 2950 (m), 1601 (m), 1562 (w), 1512 (w), 1459 (s), 1420 (s), 1363 (s), 1252 (s), 1140 (m), 1107 (s), 1082 (vs), 975 (m), 933 (m), 766 (m), 706 (m) cm⁻¹; **Raman** (500 mW): $\tilde{\nu}$ (rel. int.) = 3323 (27), 3162 (36), 3062 (30), 3006 (84), 2950 (74), 2911 (100), 1604 (11), 1468 (26), 1431 (28), 1366 (33), 1160 (23), 1084 (11), 978 (23), 938 (98), 711 (20), 629 (21) cm⁻¹; **MS** (FAB⁺): m/z = 33.1 [H₂NNH₃⁺], (FAB⁻): m/z = 75.0 [MNA⁻]; **drophammer**: 30 J; **friction tester**: 216 N; **ESD**: 1.25 J; **grain size**: <100 μm .

3,5-Diamino-1,2,4-triazolium *N*-methylnitramide (4d): 198 mg 3,5-Diamino-1,2,4-triazole (2.0 mmol) was added to a stirring solution of 152 mg MNA (**1**, 2.0 mmol) in acetonitrile (10 mL). After 1 h stirring the solvent was removed under reduced pressure and the colourless hygroscopic residue was re-crystallised from hot ethanol yielding 298 mg of compound **4d** (1.7 mmol, 85%).

DSC (T_{onset}): T_{melt} = 191 °C, T_{dec} = 259 °C; **¹H NMR** (D₂O): δ = 2.97 (s, 3 H, CH₃) ppm; **¹³C{¹H} NMR** (D₂O): δ = 156.8 (3,5-DAT), 37.1 (CH₃) ppm; **¹⁴N{¹H} NMR** (D₂O): δ = -21 (NO₂), -110 (NNO₂) ppm; **EA**: C₃H₉N₇O₂ (175.08 g·mol⁻¹): calcd. C 20.57, H 5.18, N 55.98; found C 20.43, H 4.95, N 57.35 %; **IR**: $\tilde{\nu}$ (rel. int.) = 3108 (m), 2361 (m), 2342 (m), 1692 (m), 1651 (s), 1622 (s), 1559 (s), 1470 (s), 1443 (m), 1390 (s), 1361 (vs), 1173 (m), 1118 (m), 1057 (m), 1007 (w), 932 (w), 741 (w), 668 (w) cm⁻¹; **Raman** (500 mW): $\tilde{\nu}$ (rel. int.) = 3399 (18), 3304 (36), 3202 (41), 3101 (65), 1648 (26), 1632 (34), 1593 (35), 1541 (14), 1496 (24), 1402 (57), 1350 (14), 1152 (10), 1058 (61), 1028 (100), 796 (15), 666 (70), 468 (22) cm⁻¹; **MS** (FAB⁺): m/z = 100.1 (3,5-DAT⁺), (FAB⁻): m/z = 75.0 [MNA⁻]; **drophammer**: 40 J; **friction tester**: >360 N; **ESD**: 1.5 J; **grain size**: <100 μm .

General procedure for guanidinium and aminoguanidinium *N*-methylnitramide (4e and 4f): A solution of 270 mg guanidinium carbonate (1.5 mmol) or a solution of 408 mg aminoguanidinium bicarbonate (3.0 mmol) in water (10 mL) was added to a stirred solution of 228 mg MNA (**1**, 3.0 mmol) in water (10 mL). The resulting solution was heated to 60 °C and for 1 h. After cooling to room temperature, the solvent was removed under reduced pressure and the colourless residue was re-crystallised from hot ethanol yielding compounds **2e** or **2f**.

Guanidinium *N*-Methylnitramide (4e): Yield 365 mg (2.7 mmol, 90%).

DSC (T_{onset}): T_{melt} = 128 °C, T_{dec} = 218 °C; **¹H NMR** (D₂O): δ = 2.93 (s, 3 H, CH₃) ppm. **¹³C{¹H} NMR** (D₂O): δ = 158.0 [(H₂N)₃C], 38.3 (CH₃) ppm; **¹⁴N{¹H} NMR** (D₂O): δ = -24 (NO₂), -109 (NNO₂), -305 ((H₂N)₃C) ppm; **EA**: C₂H₉N₅O₂ (135.13 g·mol⁻¹): calcd. C 17.78,

H 6.71, N 51.83; found C 18.57, H 6.26, N 50.96 %; **IR**: $\tilde{\nu}$ (rel. int.) = 3150 (m), 2977 (w), 2362 (m), 2339 (m), 1652 (vs), 1570 (m), 1467 (s), 1431 (s), 1378 (s), 1282 (s), 1157 (s), 1103 (s), 935 (m), 752 (m), 706 (m), 668 (w) cm^{-1} ; **Raman** (500 mW): $\tilde{\nu}$ (rel. int.) = 3408 (8), 3390 (9), 3197 (19), 2978 (43), 2956 (24), 2913 (45), 1654 (10), 1572 (13), 1470 (16), 1436 (24), 1379 (36), 1157 (17), 1059 (9), 1015 (100), 936 (71), 724 (10), 708 (10), 637 (15), 542 (17), 519 (18) cm^{-1} ; **MS** (FAB⁺): m/z = 60.1 [G⁺]; (FAB⁻): m/z = 75.0 [MNA⁻]; **drophammer**: 40 J; **friction tester**: >360 N; **ESD**: 1.5 J; **grain size**: <100 μm .

Aminoguanidinium *N*-Methylnitramide (4f): Yield 390 mg (2.6 mmol, 87%).

DSC (T_{onset}): T_{melt} = 120 °C, T_{dec} = 207 °C; **¹H NMR** (D₂O): δ = 2.98 (s, 3 H, CH₃) ppm; **¹³C{¹H} NMR** (D₂O): δ = 159.0 (CAG), 37.0 (CH₃) ppm; **¹⁴N{¹H} NMR** (D₂O): δ = -23 (NO₂), -115 (NNO₂), -310 (NH₂) ppm; **EA**: C₂H₁₀N₆O₂ (150.14 g·mol⁻¹): calcd. C 16.00, H 6.71, N 55.97; found C 16.27, H 6.53, N 55.49 %; **IR**: $\tilde{\nu}$ (rel. int.) = 3399 (m), 3307 (m), 3072 (w), 2994 (w), 2900 (w), 2194 (w), 1674 (s), 1619 (m), 1465 (s), 1419 (m), 1371 (s), 1292 (vs), 1163 (m), 1092 (m), 1077 (s), 982 (m), 954 (w), 938 (s), 758 (s), 704 (m) cm^{-1} ; **Raman** (500 mW): $\tilde{\nu}$ (rel. int.) = 3304 (31), 3259 (41), 3234 (37), 3000 (67), 2954 (52), 2908 (100), 2731 (12), 1656 (24), 1594 (8), 1586 (12), 1573 (15), 1476 (18), 1437 (25), 1378 (36), 1159 (20), 1124 (16), 1006 (10), 967 (47), 938 (58), 707 (10), 624 (21), 601 (9), 515 (11) cm^{-1} ; **MS** (FAB⁺): m/z = 75.1 [AG⁺], (FAB⁻): m/z = 75.0 [MNA⁻]; **drophammer**: 40 J; **friction tester**: 360 N; **ESD**: 1.5 J; **grain size**: <100 μm .

General procedure for diaminoguanidinium and triaminoguanidinium *N*-methylnitramide (4g and 4h): 342 mg KMNA (**1c**, 3.0 mmol) was dissolved in water (10 mL). Under constant stirring a solution of 510 mg silver nitrate (3.0 mmol) in water was added. AGMNA (**1h**) instantly started to precipitate, was filtered off and washed with small amounts of water. Without drying it was transferred into a reaction vessel, which contained a solution of 377 mg diaminoguanidinium chloride (3.0 mmol) or 422 mg triaminoguanidinium chloride (3.0 mmol). Instantly silver chloride started to precipitate and was removed by filtration. The solvent was removed under reduced pressure and the colourless solid was recrystallised from hot ethanol yielding compound **4g** or **4h**.

Diaminoguanidinium *N*-methylnitramide (4g): Yield 347 mg (2.1 mmol, 70%)

DSC (T_{onset}): T_{dec} = 179 °C; **¹H NMR** (D₂O): δ = 2.99 (s, 3 H, CH₃) ppm; **¹³C{¹H} NMR** (D₂O): δ = 160.2 (CDAG), 38.4 (CH₃) ppm; **¹⁴N{¹H} NMR** (D₂O): δ = -24 (NO₂), -113 (NNO₂), -287 [(H₂NNH)₂CNH₂], -312 [(H₂NNH)₂CNH₂] ppm; **EA**: C₂H₁₁N₇O₂ (165.10 g·mol⁻¹): calcd. C 14.54, H 6.71, N 59.37; found C 11.71, H 5.52, N 47.84 %; **IR**: $\tilde{\nu}$ (rel. int.) = 3062 (w), 2992 (w), 2840 (m), 2360 (w), 2342 (w), 1666 (vs), 1621 (s), 1580 (m), 1465 (s), 1434 (m), 1370 (s), 1342 (s), 1271 (s), 1151 (m), 1087 (m), 958 (s), 944 (m), 762 (w), 668 (w) cm^{-1} ; **Raman** (500 mW): $\tilde{\nu}$ (rel. int.) = 3267 (98), 3238 (97), 2994 (21), 2912 (42), 1677 (18), 1628 (11), 1541 (20), 1467 (15), 1431 (28), 1383 (38), 1187 (20), 1161 (26), 1054 (19), 972 (21), 936 (100), 701 (11), 656 (10), 620 (21), 551 (12) cm^{-1} ; **MS** (FAB⁺): m/z = 90.1 [DAG⁺], (FAB⁻): m/z = 75.0 [MNA⁻]; **drophammer**: 40 J; **friction tester**: <360 N; **ESD**: 1.5 J; **grain size**: <100 μm .

Triaminoguanidinium *N*-methylnitramide (4h): Yield 414 mg (2.3 mmol, 77%).

DSC (T_{onset}): $T_{\text{melt}} = 113\text{ }^{\circ}\text{C}$, $T_{\text{dec}} = 212\text{ }^{\circ}\text{C}$; **^1H NMR** (D_2O): $\delta = 2.98$ (s, 3 H, CH_3) ppm; **$^{13}\text{C}\{^1\text{H}\}$ NMR** (D_2O): $\delta = 159.6$ (TAG^+), 37.8 (CH_3) ppm; **$^{14}\text{N}\{^1\text{H}\}$ NMR** (D_2O): $\delta = -24$ (NO_2), -117 (NNO_2), -291 [$(\text{H}_2\text{NNH})_3\text{C}$] ppm; **EA**: $\text{C}_2\text{H}_{12}\text{N}_8\text{O}_2$ ($180.17\text{ g}\cdot\text{mol}^{-1}$): calcd. C 13.33, H 6.71, N 62.19; found C 11.09, H 6.64, N 55.03 %; **IR**: $\tilde{\nu}$ (rel. int.) = 3017 (w), 2975 (w), 2835 (m), 2361 (w), 2341 (w), 1680 (s), 1463 (s), 1433 (m), 1370 (s), 1275 (vs), 1132 (s), 1087 (m), 1050 (w), 957 (m), 929 (s), 823 (m), 762 (m), 668 (w) cm^{-1} ; **Raman** (500 mW): $\tilde{\nu}$ (rel. int.) = 3422 (57), 3302 (68), 3231 (70), 3000 (86), 2953 (58), 2908 (100), 1690 (16), 1664 (21), 1575 (13), 1468 (32), 1434 (38), 1378 (64), 1160 (38), 1082 (12), 967 (87), 938 (99), 707 (25), 624 (40), 515 (26) cm^{-1} ; **MS** (FAB^+): $m/z = 105.1$ [TAG^+], (FAB^-): $m/z = 75.0$ [MNA^-]; **drophammer**: 40 J; **friction tester**: $>360\text{ N}$; **ESD**: 1.5 J; **grain size**: $<100\text{ }\mu\text{m}$.

General procedure for *N,N*-dimethylguanidinium and *N*-guanylurea *N*-methylnitramide (4i and 4j): 305 mg $\text{Ba}(\text{MNA})_2\cdot\text{H}_2\text{O}$ (**1f**, 1.0 mmol) was dissolved in water (20 mL). Under stirring a solution of 272 mg *N,N*-dimethylguanidinium sulfate (1.0 mmol) or a solution of 302 mg *N*-guanylurea sulfate (1.0 mmol) in water was added. Instantly barium sulphate started to precipitate and was removed by filtration. The solvent of the filtrate was removed under reduced pressure and the colourless residue was re-crystallised from hot ethanol yielding compound **4i** or **4j**.

***N,N*-Dimethylguanidinium *N*-methylnitramide (4i):** Yield 294 mg (1.8 mmol, 90%).

DSC (T_{onset}): $T_{\text{melt}} = 128\text{ }^{\circ}\text{C}$, $T_{\text{dec}} = 230\text{ }^{\circ}\text{C}$; **^1H NMR** (D_2O): $\delta = 2.99$ (s, 6 H, CH_3), 2.94 (s, 3 H, O_2NNCH_3) ppm; **$^{13}\text{C}\{^1\text{H}\}$ NMR** (D_2O): $\delta = 156.8$ (CDMG), 38.3 (CH_3), 38.2 [$\text{CH}_3(\text{DMG})$] ppm; **$^{14}\text{N}\{^1\text{H}\}$ NMR** (D_2O): $\delta = -24$ (NO_2), -114 (NNO_2), -293 (DMG), -321 (DMG) ppm; **EA**: $\text{C}_4\text{H}_{13}\text{N}_5\text{O}_2$ ($163.11\text{ g}\cdot\text{mol}^{-1}$): calcd. C 29.44, H 8.03, N 42.92; found C 29.16, H 7.71, N 41.64 %; **IR**: $\tilde{\nu}$ (rel. int.) = 3071 (m), 2938 (w), 2904 (m), 2773 (w), 1668 (m), 1641 (s), 1546 (m), 1460 (s), 1433 (s), 1375 (s), 1336 (vs), 1148 (m), 1117 (m), 1097 (s), 1082 (s), 1067 (s), 1025 (m), 934 (m), 928 (m), 764 (m), 737 (m), 705 (w) cm^{-1} ; **Raman** (500 mW): $\tilde{\nu}$ (rel. int.) = 3004 (58), 2948 (100), 2921 (88), 2832 (24), 2782 (47), 1677 (9), 1528 (7), 1442 (25), 1366 (29), 1303 (31), 1148 (17), 1028 (18), 930 (45), 789 (51), 707 (9), 626 (21), 562 (5) cm^{-1} ; **MS** (FAB^+): $m/z = 88.1$ [DMG^+], (FAB^-): $m/z = 75.0$ [MNA^-]; **drophammer**: 40 J; **friction tester**: 360 N; **ESD**: 1.5 J; **grain size**: $<100\text{ }\mu\text{m}$.

***N*-Guanylurea *N*-methylnitramide (4j):** Yield 303 mg (1.7 mmol, 85%).

DSC (T_{onset}): $T_{\text{melt}} = 160\text{ }^{\circ}\text{C}$, $T_{\text{dec}} = 185\text{ }^{\circ}\text{C}$; **^1H NMR** (D_2O): $\delta = 3.03$ (s, 3 H, CH_3) ppm; **$^{13}\text{C}\{^1\text{H}\}$ NMR** (D_2O): $\delta = 157.1$ (Gu), 156.2 (Gu), 38.0 (CH_3) ppm; **$^{14}\text{N}\{^1\text{H}\}$ NMR** (D_2O): $\delta = -23$ (NO_2), -114 (NNO_2), -226 (Gu), -294 (Gu) ppm; **EA**: $\text{C}_3\text{H}_{10}\text{N}_6\text{O}_3$ ($178.15\text{ g}\cdot\text{mol}^{-1}$): calcd. C 20.23, H 5.66, N 47.17; found C 20.16, H 5.38, N 46.10 %; **IR**: $\tilde{\nu}$ (rel. int.) = 3492 (m), 3319 (m), 3115 (m), 2991 (w), 2896 (w), 2303 (w), 1728 (s), 1696 (s), 1626 (s), 1469 (s), 1432 (m), 1368 (s), 1276 (vs), 1150 (s), 1099 (s), 1063 (m), 930 (m), 805 (w), 752 (m), 705 (m) cm^{-1} ; **Raman** (500 mW): $\tilde{\nu}$ (rel. int.) = 3332 (10), 3132 (24), 2995 (42), 2953 (32), 2904 (50), 1701 (29), 1628 (10), 1599 (10), 1472 (11), 1434 (31), 1377 (38), 1167 (21), 1134 (11), 1065 (23), 948 (100), 712 (20), 643 (21), 579 (9), 456 (28) cm^{-1} ; **MS** (FAB^+): $m/z = 103.0$

[Gu⁺], (FAB⁻): m/z = 75.0 [MNA⁻]; **drophammer**: 40 J; **friction tester**: >360 N; **ESD**: 1.5 J; **grain size**: <100 μm .

2-Nitro-2-azapropanol (5):^[16] 400 mg (5.70 mmol) MNA (**1**) was added to 0.5 mL (5.70 mmol) of an aqueous formaldehyde solution (35%) and stirred at room temperature for 1 h. The reaction mixture was extracted with dichloromethane (3 \times 30 mL) and the combined organic layers were dried over sodium sulfate. The solvent was removed under reduced pressure yielding 500 mg of compound **5** (4.5 mmol, 80%) as colourless oil with traces of MNA (**1**) according to NMR measurements. It crystallised after storage for 3 days in a -30 °C freezer.

¹H NMR (CDCl₃): δ = 5.10 (s, 2 H, CH₂), 4.39 (s, 1 H, OH), 3.35 (s, 3 H, CH₃) ppm; ¹³C{¹H} NMR (CDCl₃): δ = 74.9 (s, CH₂), 37.7 (s, CH₃) ppm; ¹⁴N{¹H} NMR (CDCl₃): δ = -28 (s, NO₂), -201 (s, NNO₂) ppm; **MS** (FAB⁻) m/z = 89 [M-OH⁻], 75 [H₃CNNO₂⁻], 59 [M-NO₂⁻].

2-Nitro-2-azapropyl acetate (7):^[17, 18b] 25.0 g (193.5 mmol) 1,3,5-trimethyl-1,3,5-triazahexane (**8**) was dissolved dropwise and under ice-cooling in acetic acid anhydride (25 mL). This mixture was then added dropwise over the course of 1 h and under vigorous stirring into a precooled (-10 °C) nitration mixture of 30.0 mL nitric acid (100%, 719.9 mmol) in acetic acid anhydride (90 mL), while keeping the temperature below -5 °C. After addition the mixture was heated to 70 °C for 1 h (under formation of nitrous fumes). After cooling to room temperature water (100 mL) was added and the mixture was adjusted to pH \approx 6 by addition of ammonium carbonate. The resulting mixture was extracted with dichloromethane (4 \times 50 mL) and the combined organic phases were dried over magnesium sulfate. The solvent was removed under reduced pressure yielding yellow oil. Purification by distillation (14 mbar, 100 °C) furnished 63.9 g of compound **7** (43.2 mmol, 67%) as yellowish oil.

¹H NMR (CDCl₃): δ = 5.53 (s, 2 H, CH₂), 3.39 (s, 3 H, NCH₃), 1.97 (s, 3 H, COCH₃) ppm; ¹³C{¹H} NMR (CDCl₃): δ = 170.4 (s, CO₂), 72.8 (s, CH₂), 38.4 (s, NCH₃), 20.3 (s, OCH₃) ppm; ¹⁴N{¹H} NMR (CDCl₃): δ = -30 (s, NO₂), -211 (s, NNO₂) ppm.

2-Nitro-2-azapropyl chloride (6):^[17, 18b] 21.3 g NAP-OAc (**7**, 144.0 mmol), 0.8 mL acetic acid and two drops of sulfuric acid (96%) were dissolved in dichloromethane (35 mL). 34.3 mL Thionylchloride (288.0 mmol) was added dropwise under vigorous stirring. The yellow solution was refluxed for 1 h. After cooling to room temperature the solvent was removed under reduced pressure furnishing yellowish oil. Purification by distillation (14 mbar, 97 °C) yielded 12.9 g of compound **6** (103.7 mmol, 72%) as colourless oil, which crystallised anhydrously after 4 days storage in a -30 °C freezer.

DSC (T_{onset}): T_{dec} = 185 °C; ¹H NMR (CDCl₃): δ = 5.56 (s, 2 H, CH₂), 3.33 (s, 3 H, CH₃) ppm; ¹³C{¹H} NMR (CDCl₃): δ = 60.4 (s, CH₂), 37.6 (CH₃) ppm; ¹⁴N{¹H} NMR (CDCl₃) δ = -32 (NNO₂), -204 (NNO₂) ppm; **IR** (liquid phase): $\tilde{\nu}$ (rel. int.) = 3077 (w), 3005 (vw), 2945 (vw), 2838 (vw), 2240 (vw), 1760 (vw), 1557 (vs), 1443 (s), 1413 (s), 1308 (vs), 1283 (vs), 1257 (vs), 1188 (s), 1110 (w), 1088 (w), 996 (s), 916 (m), 860 (w), 852 (w), 820 (vw), 764 (m), 667 (m), 631 (m), 597 (m), 516 (w); **IR** (gaseous phase): $\tilde{\nu}$ (rel. int.) = 3061 (vw), 2963 (w), 2821 (vw), 2238 (vw), 1795 (vw), 1596 (vs), 1550 (s), 1444 (m), 1414 (w), 1309 (vs),

1283 (s), 1257 (vs), 1189 (w), 1120 (w), 990 (m), 915 (w), 852 (vw), 765 (vw), 679 (w), 628 (w), 596 (vw), 513 (vw); **drophammer**: >40 J; **friction tester**: 252 N.

2-Nitro-2-azapropyl isocyanate (9):^[19] 1.5 g silver cyanate (10.0 mmol) was suspended in absolute diethyl ether (50 mL) under argon atmosphere and 1.0 g 2-nitro-2-azapropyl chloride (**6**, 8.0 mmol) was added. The reaction mixture was stirred under argon atmosphere and exclusion of light for 24 h at room temperature. The colourless precipitation was filtered by means of a *Schlenk* frit (Pore 3). The resulting solution was first distilled under argon atmosphere to remove diethyl ether and further purification was carried out by fractional distillation under reduced pressure yielding 1.1 g of compound **9** (8.36 mmol, 96%) as a colourless oil, which crystallised after 1 week storage in a -80 °C freezer.

¹H NMR (Et₂O): δ = 5.21 (s, 2 H, CH₂), 3.34 (s, 3 H, CH₃) ppm; **¹³C{¹H} NMR** (Et₂O): δ = 127.9 (NCO), 60.1 (CH₂), 37.8 (CH₃) ppm; **¹⁴N{¹H} NMR** (Et₂O): δ = -28 (NNO₂), -201 (NNO₂), -351 (NCO) ppm; **IR**: $\tilde{\nu}$ (rel. int.) = 2949 (vw), 2230 (vs), 1528 (vs), 1469 (m), 1421 (m), 1373 (m), 1329 (w), 1287 (vs), 1250 (vs), 1174 (w), 1118 (w), 1011 (s), 959 (m), 867 (s), 768 (s), 657 (s) cm⁻¹.

2-Nitro-2-azapropyl phthalimide (10): 357 mg potassium phthalimide (1.93 mmol) was added to a solution of 200 mg 2-nitro-2-azapropyl chloride (**6**, 1.61 mmol) in acetonitrile (5 mL). The suspension was refluxed for 12 h. After cooling to room temperature precipitated potassium chloride was filtered and washed with acetonitrile. The clear solution was evaporated under reduced pressure and the resulting colourless solid was re-crystallised from chloroform/isohehexane (1:1) yielding 290 mg of compound **10** (1.23 mmol, 63%) as colourless crystals.

¹H NMR (CDCl₃) δ = 7.91–7.89 (m, 2 H, CH_{arom}), 7.78–7.25 (m, 2 H, CH_{arom}), 5.63 (s, 2 H, CH₂), 3.54 (s, 3 H, CH₃) ppm; **¹³C{¹H} NMR** (CDCl₃) δ = 167.1 (CO₂), 134.8 (C_{arom}), 131.6 (C_{arom}), 124.0 (C_{arom}), 53.4 (CH₂), 39.1 (CH₃) ppm; **¹⁴N{¹H} NMR** (CDCl₃) δ = -31 (NO₂), -234 (NNO₂) ppm; **EA**: C₁₀H₉N₃O₄ (235.20 g·mol⁻¹): calcd. C 51.07, H 3.86, N 17.87 %; found C 51.10, H 3.98, N 17.84 %; **IR**: $\tilde{\nu}$ (rel. int.) = 3021 (vw), 1772 (w), 1718 (s), 1609 (vw), 1529 (m), 1463 (m), 1417 (m), 1398 (s), 1370 (m), 1349 (m), 1288 (s), 1256 (s), 1222 (m), 1185 (m), 1106 (w), 1086 (w), 1015 (m), 949 (s), 867 (m), 760 (m), 727 (vs), 708 (vs) cm⁻¹; **Raman** (200 mW): $\tilde{\nu}$ (rel. int.) = 3110 (25), 3088 (68), 3060 (42), 3034 (38), 2978 (45), 2946 (28), 2887 (10), 1773 (100), 1721 (15), 1616 (20), 1467 (7), 1420 (8), 1349 (11), 1290 (7), 1259 (6), 1189 (40), 1157 (8), 1017 (22), 975 (7), 870 (16), 836 (7), 719 (27) cm⁻¹; **MS** (DEI⁺): m/z = 236.1 [M+H⁺], 189.1 [M+H-NO₂⁺], 160.1 [M+H-N₂O₂CH₃⁺].

2-Nitro-2-azapropyl amine hydrochloride (12): 750 mg silver cyanate (5.0 mmol) was suspended in absolute diethyl ether (40 mL) under argon atmosphere and 500 mg 2-nitro-2-azapropyl chloride (**6**, 4.0 mmol) was added. The reaction mixture was stirred under argon atmosphere and exclusion of light for 20 h at room temperature, before the colourless precipitation was filtered by means of a *Schlenk* frit (Pore 3). From here two different methods were performed.

Method 1: The solvent was removed under reduced pressure and to the remaining isocyanate **9** aqueous hydrochloric acid (6M, 40 mL) was added. The solution was refluxed for 4 h, the solvent removed under reduced pressure and the resulting colourless solid was

re-crystallised from water yielding 170 mg of compound **12** (1.2 mmol, 30%) as colourless solid.

Method 2: Hydrochloric acid gas was bubbled into the etheric solution of isocyanate **9** and the solution was stirred at room temperature. Compound **12** precipitated continuously over the following three days and was collected by filtration. Re-crystallisation from water yielded 450 mg of compound **12** (3.2 mmol, 80%) as colourless solid.

DSC (T_{onset}): $T_{\text{melt}} = 103\text{ }^{\circ}\text{C}$, $T_{\text{dec}} = 109\text{ }^{\circ}\text{C}$; **^1H NMR** (D_2O) $\delta = 4.85$ (br, 2 H, CH_2), 3.16 (s, 3 H, CH_3) ppm; **$^{13}\text{C}\{^1\text{H}\}$ NMR** (D_2O) $\delta = 81.8$ (CH_2), 31.8 (CH_3) ppm; **$^{14}\text{N}\{^1\text{H}\}$ NMR** (D_2O) $\delta = -26$ (NO_2), -362 (NH_3^+) ppm; **EA**: $\text{C}_2\text{H}_8\text{N}_3\text{O}_2\text{Cl}$ ($141.56\text{ g}\cdot\text{mol}^{-1}$): calcd. C 29.68, H 5.70, N 29.68 %; found C 16.87, H 5.73, N 29.05%; **IR**: $\tilde{\nu}$ (rel. int.) = 3038 (w), 2784 (m), 2613 (w), 1528 (s), 1502 (vs), 1429 (s), 1300 (s), 1285 (vs), 1252 (s), 1130 (m), 1089 (m), 1013 (m), 972 (m), 887 (m), 833 (vw), 760 (s), 637 (w), 610 (m) cm^{-1} ; **MS** (FAB^+): $m/z = 106.1$ [$\text{M}+\text{H}^+$], 89.0 [$\text{M}+\text{H}-\text{NH}_2^+$]; **MS** (FAB^-): $m/z = 35.0$ [Cl^-].

1.9 References

- [1] M. A. Kettner, T. M. Klapötke, T. G. Müller, M. Sućeska, *Eur. J. Inorg. Chem.* **2014**, 4756–4771.
- [2] http://de.wikipedia.org/wiki/Antoine_Paul_Nicolas_Franchimont, status: 25.08.2014.
- [3] A. P. N. Franchimont, E. A. Klobbie, *Recl. Trav. Chim. Pays-Bas* **1888**, 7, 343–357.
- [4] T. L. Davis, *The Chemistry of Powder and Explosives*, Vol. 1&2, Massachusetts Institute of Technology, **1943**.
- [5] J. P. Agrawal, R. D. Hodgson, *Organic Chemistry of Explosives*, Wiley, 1st ed., **2007**, 230.
- [6] J. Thiele, A. Lachman, *Ber. Dtsch. Chem. Ges.* **1894**, 27, 1909–1910.
- [7] A. Häußler, T. M. Klapötke, H. Piotrowski, *Z. Naturforsch.* **2002**, 57b, 151–156.
- [8] a) A. P. N. Franchimont, *Recl. Trav. Chim.* **1894**, 13, 308–330; b) N. Jonathan, *J. Mol. Spectrosc.* **1960**, 5, 101–109.
- [9] N. I. Sadova, G. E. Slepnev, N. A. Tarasenko, A. A. Zenkin, L. V. Vilkov, I. F. Shishkov, Yu. A. Pankrushev, *Zh. Strukt. Khim.* **1977**, 18, 865–872.
- [10] T. Knott, *WO 2001/64627 A1*, **2001**.
- [11] a) B. V. Farahani, F. H. Rajabi, B. Hosseindoust, N. Zenooz, *J. Phase Equilib. Diffus.* **2010**, 31, 536–541; b) J. Antes, M. Schwarzer, W. Janitschek, S. Löbbecke, H. Krause, *A Novel Approach to DNDA-57 Synthesis by Microreaction Technology*, 41st Int. Annu. Conf. ICT: Energetic Materials – Structure and Properties, June 29–July 2, **2010**, Karlsruhe, Germany.
- [12] G. W. Naufflett, *US 4513148*, **1985**.
- [13] A. L. Fridman, V. P. Ivshin, S. S. Novikov, *Russ. Chem. Rev.* **1969**, 38, 640–654.
- [14] a) M. Ya. Myagi, E. T. Lippmaa, S. A. Shevelev, V. I. Erashko, A. A. Fainzilberg, *Izv. Akad. Nauk SSSR Ser. Khim.* **1970**, 6, 1450; b) V. G. Avakyan, V. A. Chekrygin, V. A. Shlyapochnikov, A. N. Kisilinskii, *Izv. Akad. Nauk SSSR Ser. Khim.* **1969**, 11, 2606–2608; c) V. A. Shlyapochnikov, N. O. Cherskaya, N. S. Morozova, V. P. Ivshin, T. N. Ivshina, K. I. Bakhtin, *Zh. Obshch. Khim.* **1983**, 53, 2334–2339.
- [15] R. G. Gafurov, B. S. Fedorov, L. T. Eremenko, *Izv. Akad. Nauk SSSR Ser. Khim.* **1978**, 10, 2289–2292.
- [16] G. A. Gareev, N. A. Cherkashina, V. A. Matveev, T. A. Danilova, *Zh. Org. Khim.* **1971**, 7, 623–624.
- [17] J. Denkstein, V. Kaderabek, *Collect. Czech. Commun.* **1960**, 25, 2334–2340.
- [18] a) R. Böse, T. M. Klapötke, P. Mayer, V. Verma, *Propellants Explos. Pyrotech.* **2006**, 31(4), 263–268; b) N. Fischer, K. Karaghiosoff, T. M. Klapötke, J. Stierstorfer, *Z. Anorg. Allg. Chem.* **2010**, 636(5), 735–749; c) T. M. Klapötke, A. Penger, C. Pflüger, *New Trends in Research of Energetic Materials* (NTREM), Proceedings of the Seminar, 14th, Pardubice, Czech Republic, Apr. 13–15, **2011**, Part 2, 743–751; d) T. M. Klapötke, C. Pflüger, M. Suceska, *New Trends in Research of Energetic Materials* (NTREM), Proceedings of the Seminar, 17th, Pardubice, Czech Republic, Apr. 9–11, **2014**, Part 2, 754–768.
- [19] B. Unterhalt, F. Leiblein, *Arch. Pharm.* **1979**, 312(2), 159–164.
- [20] a) I. S. Shvartz, M. M. Krayushkin, V. V. Sevost'yanova, V. N. Yarovenko, *Russ. Chem. Bull.* **1979**, 28, 1000–1002; b) T. M. Klapötke, B. Krumm, M. Scherr, G. Spieß, F. X. Steemann, *Z. Anorg. Allg. Chem.* **2008**, 634, 1244–1246.
- [21] J. Majer, J. Denkstein, *Collect. Czech. Commun.* **1966**, 31(6), 2547–2557.
- [22] B. Unterhalt, F. Leiblein, *Arch. Pharm.* **1981**, 314, 459–464.
- [23] a) T. M. Klapötke, *Chemie der hochenergetischen Materialien*, de Gruyter, Berlin, New York, **2009**; b) T. M. Klapötke, *Chemistry of High-Energy Materials*, 2nd Eng. ed., de Gruyter, Berlin, New York, **2011**.

- [24] N. M. Baranchik, I. V. Grachev, D. Z. Zavel'skii, *Zh. Obshch. Khim.* **1957**, 27, 117–126.
- [25] V. P. Ivshin, M. S. Komelin, N. P. Belik, *Zh. Obshch. Khim.* **1980**, 16(6), 1166–1170.
- [26] a) M. Delépine, *Bull. Soc. Chim. Fr.* **1895**, 13, 352–361; b) N. Blazevic, D. Kolbah, B. Belin, V. Sunjic, F. Kafjez, *Synthesis* **1979**, 161–176.
- [27] a) S. Gabriel, *Ber. Dtsch. Chem. Ges.* **1887**, 20, 2224–2236; b) M. S. Gibson, R. W. Bradshaw, *Angew. Chem.* **1968**, 80, 986–996; *Angew. Chem. Int. Ed. Engl.* **1968**, 7, 919; c) H. R. Ing, R. H. F. Manske, *J. Chem. Soc.* **1926**, 2348–2351.
- [28] H.-O. Kalinowski, S. Berger, S. Braun, *¹³C NMR-Spektroskopie*, Georg Thieme Verlag, Stuttgart, New York, **1984**.
- [29] M. Witanowski, L. Stefaniak, G. A. Webb, *Annual Reports on NMR Spectroscopy*, Vol. 25, Academic Press Inc., London, **1993**.
- [30] a) M. Hesse, H. Meier, B. Zeeh, *Spektroskopische Methoden in der organischen Chemie*, Georg Thieme Verlag KG, Stuttgart, **2005**; b) G. Socrates, *Infrared and Raman Characteristic Group Frequencies: Tables and Charts*, 3rd ed., Wiley, New York, **2004**.
- [31] A. Bondi, *J. Phys. Chem.* **1964**, 68, 441–451.
- [32] A. F. Holleman, *Lehrbuch der Anorganischen Chemie*, 101st ed., Walter de Gruyter GmbH & Co., Berlin, New York, **1995**.
- [33] I. F. Shishkov, N. I. Sadova, L. V. Vilkov, V. P. Ivshin, *Zh. Strukt. Khim.* **1982**, 23, 73–78.
- [34] a) EXPLO5, Version 6.02, M. Sućeska, Zagreb, Croatia, **2014**; b) M. Sućeska, *Propellants Explos. Pyrotech.* **1991**, 16, 197–202; c) M. Sućeska, *Propellants Explos. Pyrotech.* **1999**, 24, 280–285; d) M. Sucasca, H. G. Ang, H. Y. Chan, *Mater. Sci. Forum* **2011**, 673, 47–52.
- [35] a) GAUSSIAN09W, Version 7.0, M. J. Frisch, G. W. Trucks, H. B. Schlegel, G. E. Scuseria, M. A. Robb, J. R. Cheeseman, G. Scalmani, V. Barone, B. Mennucci, G. A. Petersson, H. Nakatsuji, M. Caricato, X. Li, H. P. Hratchian, A. F. Izmaylov, J. Bloino, G. Zheng, J. L. Sonnenberg, M. Hada, M. Ehara, K. Toyota, R. Fukuda, J. Hasegawa, M. Ishida, T. Nakajima, Y. Honda, O. Kitao, H. Nakai, T. Vreven, J. A. Montgomery Jr., J. E. Peralta, F. Ogliaro, M. Bearpark, J. J. Heyd, E. Brothers, K. N. Kudin, V. N. Staroverov, R. Kobayashi, J. Normand, K. Raghavachari, A. Rendell, J. C. Burant, S. S. Iyengar, J. Tomasi, M. Cossi, N. Rega, J. M. Millam, M. Klene, J. E. Knox, J. B. Cross, V. Bakken, C. Adamo, J. Jaramillo, R. Gomperts, R. E. Stratmann, O. Yazyev, A. J. Austin, R. Cammi, C. Pomelli, J. W. Ochterski, R. L. Martin, K. Morokuma, V. G. Zakrzewski, G. A. Voth, P. Salvador, J. J. Dannenberg, S. Dapprich, A. D. Daniels, Ö. Farkas, J. B. Foresman, J. V. Ortiz, J. Cioslowski, D. J. Fox, Gaussian, Inc., Wallingford CT, **2009**; b) GAUSS-VIEW 5, Version 5.0.8, T. K. R. Dennington, J. Millam, Semichem Inc., Shawnee Mission, **2009**.
- [36] <http://www.systag.ch>.
- [37] T. M. Klapötke, N. K. Minar, J. Stierstorfer, *Polyhedron* **2009**, 28, 13–26.
- [38] *NATO Standardization Agreement (STANAG) on Explosives*, Impact Tests, no. 4489, 1st ed., Sept. 17, **1999**.
- [39] *WIWEB-Standardarbeitsanweisung 4-5.1.02, Ermittlung der Explosionsgefährlichkeit, hier der Schlagempfindlichkeit mit dem Fallhammer*, Nov. 08, **2002**.
- [40] a) Bundesanstalt für Materialforschung (BAM), <http://www.bam.de>, which lays down test methods pursuant to Regulation (EC) No. 1907/2006 of the European Parliament and of the Council on the Evaluation, Authorisation and Restriction of Chemicals (REACH), ABl. L142, **2008**; b) T. M. Klapötke, B. Krumm, N. Mayr, F. X. Steemann, G. Steinhäuser, *Safety Science* **2010**, 48, 28–34.
- [41] *NATO Standardization Agreement (STANAG) on Explosives*, Friction Tests, no. 4487, 1st ed., Aug. 22, **2002**.
- [42] *WIWEB-Standardarbeitsanweisung 4-5.1.03, Ermittlung der Explosionsgefährlichkeit, hier der Reibempfindlichkeit mit dem Reibeapparat*, Nov. 08, **2002**.

- [43] *NATO Standardization Agreement (STANAG) on Explosives, Electrostatic Discharge Sensitivity Tests*, no. 4490, 1st ed., Feb. 19, **2001**.
- [44] <http://www.ozm.cz/en/sensitivity-tests/esd-2008a-small-scaleelectrostatic-spark-sensitivity-test/>.
- [45] a) *Test methods according to the UN Manual of Tests and Criteria, Recommendations on the Transport of Dangerous Goods*, United Nations Publication, New York, Geneva, 4th revised ed., **2003**: Impact: insensitive >40 J, less sensitive ≥ 35 J, sensitive ≥ 4 J, very sensitive ≤ 3 J; friction: insensitive >360 N, less sensitive: 360 N, sensitive <360 N and >80 N, very sensitive ≤ 80 N, extremely sensitive ≤ 10 N; b) www.reichel-partner.de.
- [46] a) J. E. Felts, H. W. Sandusky, R. H. Granholm, *Development of the small-scale shock sensitivity test (SSST)*, *AIP Conf. Proc.* **2009**, 1195, 233; b) H. W. Sandusky, R. H. Granholm, D. G. Bohl, *Small-Scale Shock Reactivity Test (SSRT)*, IHTR 2701, Naval Surface Warfare Center, Indian Head, MD, Aug. 12th, **2005**.
- [47] <http://www.oricaminingservices.com>.
- [48] J. A. Conkling, *Chemistry of Pyrotechnics: Basic Principles and Theory*, Taylor & Francis Group, New York, **1985**.
- [49] M. Joas, *Dissertation*, Ludwig-Maximilian University of Munich, **2014**.
- [50] G. P. Sutton, *Rocket Propulsion Elements*, 7th ed., John Wiley & Sons, New York, **2001**.
- [51] H. Östmark, U. Bemm, H. Bergmann, A. Langlet, *Thermochim. Acta* **2002**, 384, 253–259.

CHAPTER 2**ASYMMETRIC CARBAMATE DERIVATIVES**

This chapter deals with the addition reactions of polynitro alcohols with 2-nitro-2-azapropyl isocyanate yielding symmetrically and asymmetrically substituted carbamate derivatives. While at the oxygen atom of the carbamate unit the 2,2,2-trinitroethyl group is attached, the 2-nitro-2-azapropyl moiety is introduced to the nitrogen atom to allow further nitration towards the corresponding N-nitrocarbamate. The main part of this chapter is reproduced with permissions from:

B. Aas, M. A. Kettner, T. M. Klapötke,* M. Sućeska, C. Zoller

“Asymmetric Carbamate Derivatives Containing Secondary Nitramine, 2,2,2-Trinitroethyl, and 2-Fluoro-2,2-dinitroethyl Moieties”^[1]

DOI: 10.1002/ejic.201301114

Copyright 2014 Wiley European Journal of Inorganic Chemistry

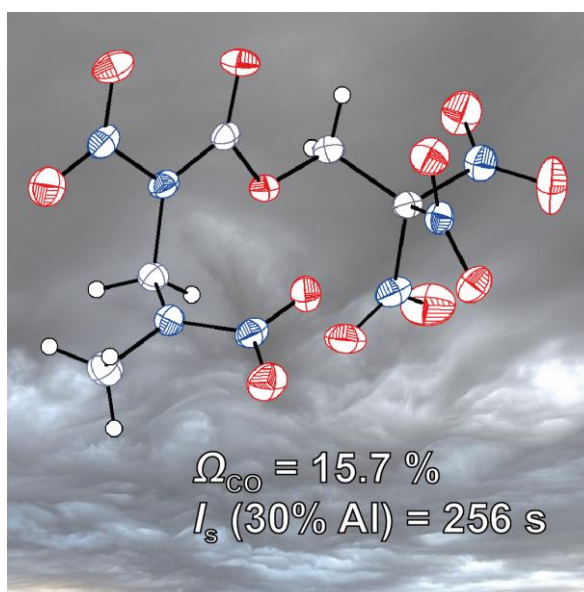
and:

M. A. Kettner, T. M. Klapötke,* T. G. Müller, M. Sućeska

“Contributions to the Chemistry of N-Methylnitramine: Crystal Structure, Synthesis of Nitrogen-Rich Salts, and Reactions towards 2-Nitro-2-azapropyl Derivatives”^[2]

DOI: 10.1002/ejic.201402441

Copyright 2014 Wiley European Journal of Inorganic Chemistry



2.1 Introduction

One approach in the synthesis of new energetic materials and oxidisers are the derivatives of urea and urethane (carbamic acid ester).^[3] As amine derivatives of the carboxylic acid, these amides represent the most inert derivatives regarding nucleophilic attack at the carbonyl carbon atom.^[4] The thermal stabilities of ureas, urethanes and also carbonates are valuable for energetic materials.^[5] Numerous carbamate and carbonate derivatives featuring polynitro groups have been investigated as energetic materials and oxidisers in the 1960s, many of them by FRANKEL and HILL *et al.*^[6] Several different synthetic processes^[7] and strategies for these materials including syntheses in ionic liquids were investigated in the following years.^[8] Some selected compounds with high oxygen contents have been re-investigated in the group of KLAPÖTKE as only little information was given in the literature, for instance derivatives of carbonate featuring two, three or four polynitroethyl groups,^[9] and various carbamate derivatives.^[10] Also various novel asymmetric carbamates and nitrocarbamates with both the trinitroethyl and fluorodinitroethyl groups were synthesised in the last few years (Figure 1).^[11]

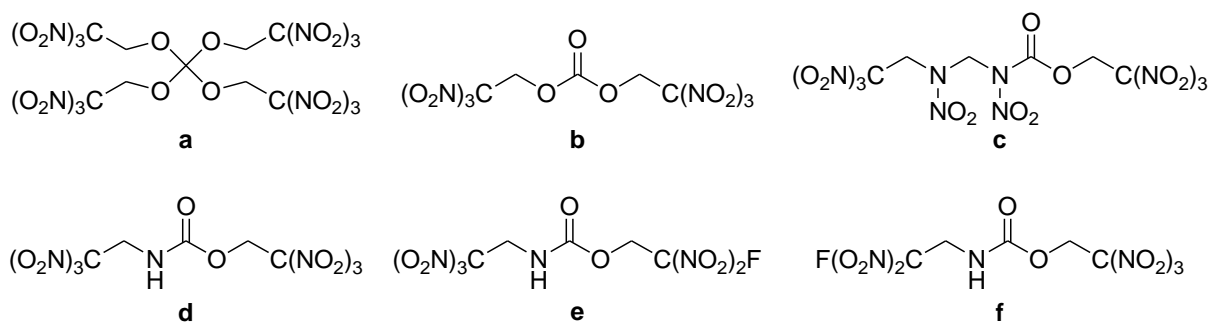
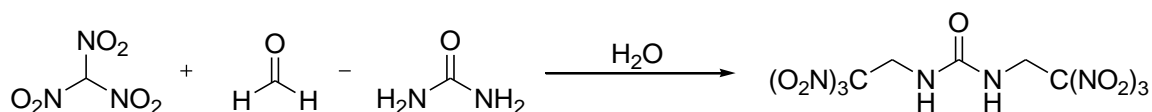


Figure 1: Selected materials re-investigated in the group of Klapötke: a) tetrakis(2,2,2-trinitroethyl) orthocarbonate;^[9b] b) bis(2,2,2-trinitroethyl)carbonate;^[9a] c) 2,2,2-Trinitroethyl (nitro(2,2,2-trinitroethyl)amino)methyl nitrocarbamate;^[10] d) bis(2,2,2-trinitroethyl)-carbamate;^[11] e) 2-fluoro-2,2-dinitroethyl (2,2,2-trinitroethyl)carbamate;^[11] f) 2,2,2-trinitroethyl (2-fluoro-2,2-dinitroethyl)carbamate.^[11]

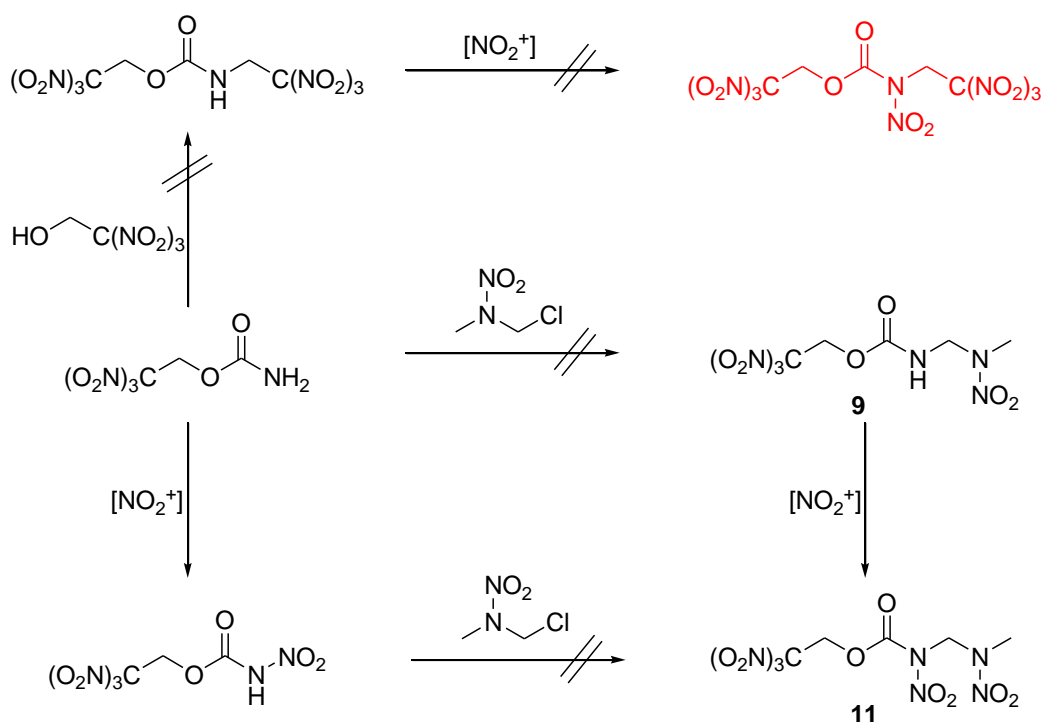
The most simple urea derivative featuring two trinitromethyl groups is the symmetrically substituted *N,N*-bis-(2,2,2-trinitroethyl)-urea (BTNEU), first synthesised by WETTERHOLM in 1954.^[12] It can be formed for instance from an aqueous nitroform solution, which usually contains up to 10% urea as stabilising agent,^[13] by treatment with formaldehyde. BTNEU precipitates instantly from this solution as a colourless solid (Scheme 1), which should be kept in mind when performing MANNICH type reactions with such stabilised nitroform solutions with formaldehyde.



Scheme 1: Formation of *N,N*-bis-(2,2,2-trinitroethyl)urea (BTNEU) from an aqueous solution of nitroform, urea and formaldehyde.

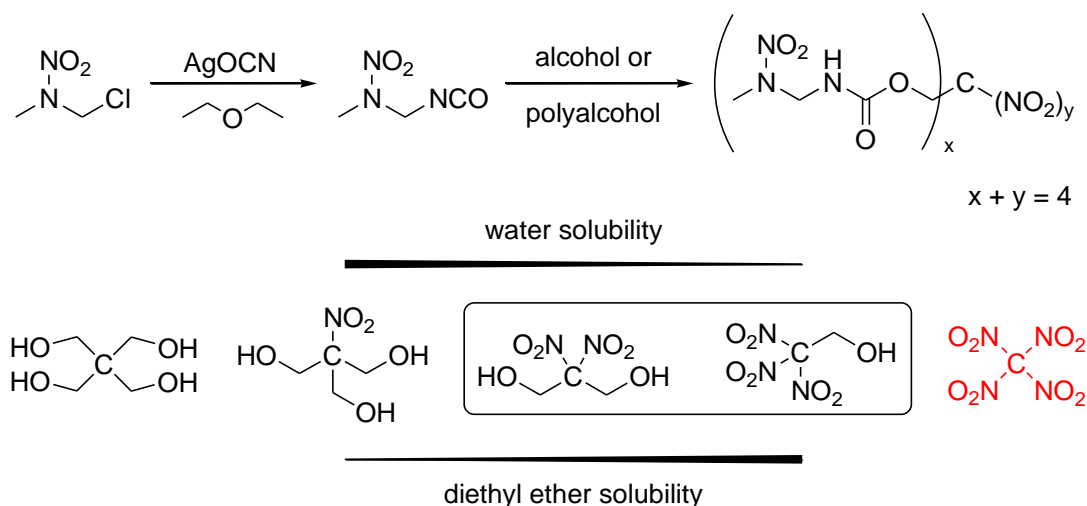
BTNEU shows enhanced thermal stabilities due to the delocalisation of the π electron pair of the nitrogen atom. According to a DSC measurement it decomposes at 185 °C. It reveals a counterbalanced oxygen balance assuming the formation of carbon dioxide Ω_{CO_2} , and 20.7% assuming the formation of carbon monoxide Ω_{CO} . However, the sensitivities towards mechanical stimuli measured in the group of KLAPÖTKE show low values (IS = 3 J, FS = 160 N), thus in the range of primary explosives.

The carbamate moiety as linker for two aliphatic polynitro groups seemed to be the next level to increase the oxygen balances Ω_{CO} and Ω_{CO_2} . The re-investigated *N,O*-bis-(2,2,2-trinitroethyl)-carbamate (BTNEC) has Ω_{CO} = 26.9% and Ω_{CO_2} = 6.2%, melts at 164 °C and decomposes at 186 °C.^[11] Moreover and in contrast to carbonate derivatives the carbamate group shows the possibility of introducing an additional nitro group at the nitrogen atom. Nitrourea derivatives were neglected in this study due to their high sensitivities towards hydrolysis and mechanical stimuli.^[14] The previously known BTNEC^[15] was tried to be nitrated at the nitrogen atom of the carbamate unit in the group of KLAPÖTKE, but several synthetic efforts including also mild and acid-free nitration methods (e.g. NO_2BF_4 , N_2O_5) failed in doing so. The electron withdrawing character of the trinitroethyl group was called to generate a lack of electron density at this position, thus inhibiting further nitration and other substitutions (Scheme 2, top). This could also be confirmed by consideration of the charge distribution calculated at the CBS-4M level of theory.^[16]



Scheme 2: Unfeasible pathways to different promising molecules that were tested during the synthetic efforts for new oxidisers in the group of KLAPÖTKE. Top: failed nitration of *N,O*-bis-(2,2,2-trinitroethyl)carbamate to synthesise according nitrocarbamate (red),^[16] which formation has not been confirmed to date. Middle: attempted condensation of 2,2,2-trinitroethyl carbamate^[17, 18] with 2-nitro-2-azapropyl chloride to yield compound **9**. Bottom: attempted condensation at 2,2,2-trinitroethyl nitrocarbamate^[18] with 2-nitro-2-azapropyl chloride to yield compound **11**. The syntheses of compounds **9** and **11** will be shown and discussed in the next section.

Because of these observations and in order to facilitate further nitration of the nitrogen atom at the carbamate nitrogen atom, the 2-nitro-2-azapropyl moiety was chosen to be attached at this position, while remaining the oxygen rich trinitroethyl group at the opposite side of the carbamate. Several routes might be considered for the synthesis of the desired compounds **9** and **11** (Scheme 2). The literature known 2,2,2-trinitroethyl carbamate^[17] showed very low reactivity concerning substitution at the nitrogen atom, which might be explained on closer examination of its crystal structure determined by KLAPÖTKE *et al.* in 2013 showing full planarity of the carbamate unit. Apparently the only feasible reaction of this molecule leading to an useful material was shown to be the nitration furnishing 2,2,2-trinitroethyl nitrocarbamate with a very high oxygen balance Ω that turned out to be a rather promising oxidiser.^[18] Instead the formation of the carbamate unit with the secondary nitramine attached to the nitrogen atom was achieved by the addition reaction of an alcohol derivative to the parent 2-nitro-2-azapropyl isocyanate (Scheme 3).^[19]

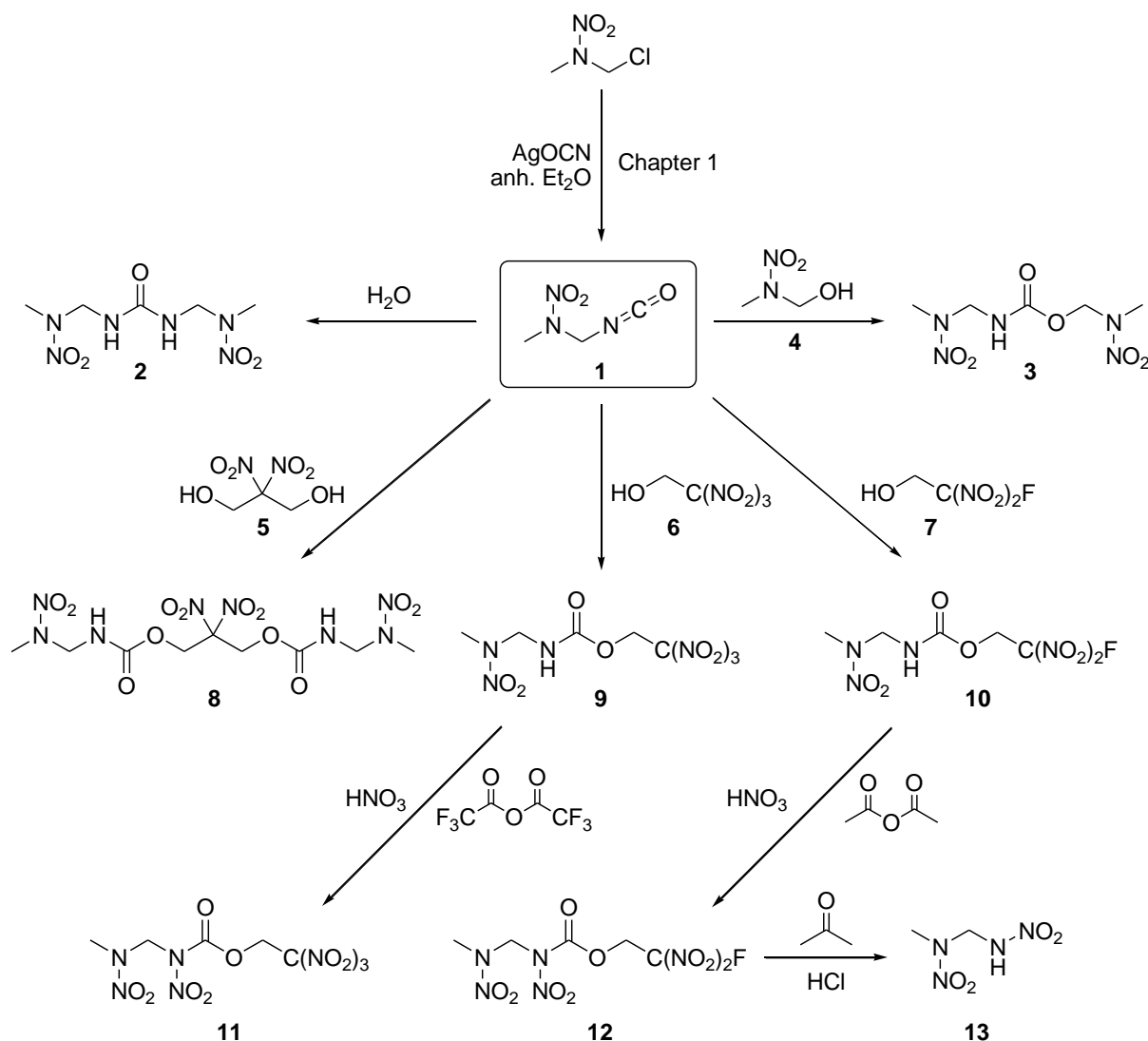


Scheme 3: Top: *in situ* generation of 2-nitro-2-azapropyl isocyanate in diethyl ether and subsequent addition of alcohols or polyalcohols. Bottom: successive row from 2,2-bis(hydroxymethyl)propane-1,3-diol to tetranitromethane (red, not possible) considered for the addition reaction with 2-nitro-2-azapropyl isocyanate and their solubilities in water and diethyl ether. The alcohols in the box were finally chosen for the reaction shown on top.

Finally only a few alcohols were chosen for the addition reactions with 2-nitro-2-azapropyl isocyanate, owing to their oxygen content with intention to synthesise compounds with high oxygen balances. Also their solubilities in diethyl ether were of certain importance, because the *in situ* formation of the isocyanate with subsequent filtration of the remaining solids (AgCl and AgOCN, please find more information about the synthesis in Chapter 1) demands the use of diethyl ether. Several trials of the filtration in other solvents (e.g. MeCN or THF) failed, because these remaining solids got slightly diluted. The other considered polyalcohols such as 2,2-bis(hydroxymethyl)propane-1,3-diol and 2-(hydroxymethyl)-2-nitropropane-1,3-diol (Scheme 4) did not fulfill the requirement of the high oxygen content, as this study was considered to produce oxygen-carriers for composite propellants. In conclusion the chosen alcohols were 2,2,2-trinitroethanol, 2-fluoro-2-dinitroethanol and 2,2-dinitropropan-1,3-diol.

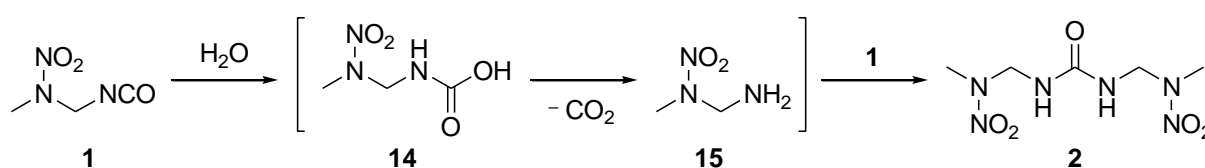
2.2 Syntheses

All syntheses in this chapter started with the *in situ* generation of 2-nitro-2-azapropyl isocyanate (**1**, NAP-NCO) in anhydrous diethyl ether as described in Chapter 1 (Scheme 4).^[19] There is no need to isolate the isocyanate **1**, but the formed silver chloride and traces of remaining silver cyanate need to be filtered off under argon atmosphere before the selected alcohols **4**, **5**, **6** or **7** are added to the solution.



Scheme 4: Syntheses of all compounds described in this chapter started from *in situ* generated 2-nitro-2-azapropyl isocyanate (**1**). Addition reactions of water (½ eq.), 2-nitro-2-azapropyl alcohol (**4**), 2,2-dinitropropane-1,3-diol (**5**, ½ eq.), 2,2,2-trinitroethanol (**6**) and 2-fluoro-2,2-dinitroethanol (**7**) in diethyl ether furnished bisNAPurea (**2**, 47%), bisNAPcarbamate (**3**, 41%), bi-carbamate **8** (45%), TNE-NAP-C (**9**, 40%) and FDNE-NAP-C (**10**, 50%), respectively (2-step yield in parenthesis). Nitration using standard *N*-nitration methods of the polynitro carbamates **9** and **10** yielded corresponding TNE-NAP-NC (**11**, 64%) and FDNE-NAP-NC (**12**, 80%). During the attempted crystallisation of nitrocarbamate **12** in acidified acetone the compounds hydrolysed forming DNDA-4 (**13**).

If water was present or added (half equivalent) to this etheric solution *N,N'*-bis-(2-nitro-2-azapropyl)-urea (bisNAPurea, **2**) was formed. Owing to its symmetry bisNAPurea (**2**) can easily be identified by ^1H NMR measurements, thus representing a very useful indicator for inaccurate use of the SCHLENK technique while preparing the isocyanate **1** or not using anhydrous addition reagents (**4**, **5**, **6** or **7**). The suggested reaction mechanism towards compound **2** is illustrated in Scheme 5: The isocyanate reacts with water to NAP-carbamic acid **14**, which decarboxylates to 2-nitro-2-azapropyl amine (NAP-NH₂, **15**).^[5] The formation of CO₂ was confirmed by precipitation of BaCO₃ from a Ba(OH)₂ solution in an airlock. The amine **15** subsequently reacts with the parent isocyanate **1** to form bisNAPurea (**2**). Attempted isolation of the amine **15** by using stoichiometric amounts of water failed (please compare Chapter 1 containing attempted syntheses of compound **15**).



Scheme 5: Suggested mechanism for the formation of bisNAPurea (**2**) from NAP-NCO (**1**) and water in diethyl ether. Compounds **14** and **15** could not be isolated.

Various alcohols with high oxygen (respectively nitro group) content were selected for addition reactions with the isocyanate **1**. Most successful addition reactions with good yields were accomplished with the monoalcohols 2-nitro-2-azapropanol (NAP-OH, **4**), 2,2,2-trinitroethanol (TNE, **6**) and 2-fluoro-2,2-dinitroethanol (FDNE, **7**). These were previously purified and dried by distillation or sublimation, respectively. The obtained etheric solutions were stirred for 12 hours and after evaporation of the solvent and washing with cold water the crude carbamates *N,O*-bis-(2-nitro-2-azapropyl)-carbamate (bisNAPcarbamate, **3**), 2,2,2-trinitroethyl-(2-nitro-2-azapropyl)-carbamate (TNE-NAP-C, **9**) and 2-fluoro-2,2-dinitroethyl-(2-nitro-2-azapropyl)-carbamate (FDNE-NAP-C, **10**) were obtained as colourless solids. Recrystallisation from dichloromethane furnished carbamates **3**, **9** and **10** as pure crystalline products. The addition reaction of two equivalents of isocyanate **1** to the dialcohol 2,2-dinitropropane-1,3-diol (**5**) also furnished satisfactory yields. However, the formed bi-carbamate **8** had to be purified by silica column chromatography in ethyl acetate. The nitration of the carbamates **9** and **10** were performed in a mixture of trifluoroacetic acid anhydride (**9**) or acetic acid anhydride (**10**) and fuming nitric acid starting at temperatures below 10 °C and were allowed to warm up to ambient temperature within two hours. Trifluoroacetic acid anhydride can be removed with all liquids under reduced pressure into a cooling trap (−90 °C) and the crude nitrocarbamate TNE-NAP-NC (**11**) was obtained as colourless solid with a yield of 64%. The nitration of FDNE-NAP-C (**10**) furnished crude nitrocarbamate FDNE-NAP-NC (**8**) as colourless solid in high yield (80%). Compound **11** was re-crystallised from dichloromethane or acetone. During the crystallisation process of compound **12** in slightly acidified acetone the molecule hydrolysed forming 2,4-dinitro-2,4-diazabutane (DNDA-4, **13**), which represents the nitrated derivative of NAP-amine (**14**), which neither could be isolated from the reaction of NAP-NCO (**1**) with water (Scheme 6),

nor could be synthesised from other synthesis routes as described in Chapter 1. The hitherto unknown material represents a mixed primary and secondary nitramine and might reveal interesting combined properties from the dinitrodiaza family (DNDA-X).^[20]

2.3 NMR Spectroscopy

Compounds **2**, **3**, and **8–12** were characterized by ^1H , $^{13}\text{C}\{^1\text{H}\}$ and $^{14}\text{N}\{^1\text{H}\}$ NMR spectroscopy. Additionally the ^{19}F NMR spectra of fluorine containing compounds **10** and **12** were recorded (Table 1). In the ^1H NMR spectra the singlet for the terminal methyl groups of all compounds (**2**, **3**, **8–12**) can be observed in the range of $\delta = 3.52\text{--}3.39$ ppm in *d6*-acetone. Compounds **2**, **3**, **8**, **9** and **10** show doublets for the methylene groups in the range of $\delta = 5.15\text{--}5.04$ ppm, respectively, due to $^3J_{\text{H-H}}$ coupling to the NH group of the carbamate (and urea for **2**) moiety all with coupling constants in the expected range of 6.3–6.9 Hz. The signals of the NH groups can be observed in the range of $\delta = 8.13\text{--}6.04$ ppm depending on the solvent, either CDCl_3 (ca. 8.00 ppm) or *d6*-acetone (ca. 6.00 ppm). Only in the spectrum of the urea derivative **2** the resolution was high enough to observe the otherwise broad singlet as a triplet due to $^3J_{\text{H-H}}$ coupling with the appropriate coupling constant of 6.5 Hz. The chemical shifts of the methylene groups attached to the oxygen atom in the carbamate derivatives **3**, **8–12** are observed in the range of $\delta = 6.17\text{--}5.09$ ppm and are splitted into doublets for the fluorine containing compounds **10** and **12** due to $^3J_{\text{H-F}}$ coupling with coupling constants of 16.2 and 15.6 Hz, respectively.^[21]

Table 1: Multinuclear NMR chemical shifts [ppm] of compounds **2**, **3**, and **8–12**.

Nucleus	Assignment	2	3	8	9	10	11	12
^1H	CH_3	3.47	3.47, 3.45	3.39	3.41	3.40	3.52	3.52
	OCH_2	–	5.72	5.09	5.79	5.47 (d)	6.17	5.80 (d)
	NCH_2	5.05 (d)	5.04 (d)	5.11 (d)	5.15 (d)	5.12 (d)	6.05	6.04
	NH	6.05 (t)	6.04 (br)	7.92 (br)	8.13 (br)	8.00 (br)	–	–
^{13}C	CH_3	39.1	39.3, 38.6	39.2	38.1	39.0	39.2	39.1
	OCH_2	–	73.9	58.7	57.9	62.1 (d)	63.5	63.5 (d)
	NCH_2	57.2	57.9	62.2	61.5	58.8	64.4	64.2
	C=O	156.8	155.7	155.6	154.3	155.5	148.0	148.3
	$\text{C}(\text{NO}_2)_x$	–	–	115.5	124.6	120.9 (d)	122.9	119.2 (d)
^{14}N	NNO_2	–28	–29, –31	–28	–29	–28	–30	–30
	$\text{C}(\text{NO}_2)_x$	–	–	–17	–33	–23	–34	–25
^{19}F	$\text{C}(\text{NO}_2)_2\text{F}$	–	–	–	–	–112.0(br)	–	–111.4(br)
(d) doublet, (t) triplet, (br) broad								

In the $^{13}\text{C}\{^1\text{H}\}$ spectra the signals of the methyl groups of all discussed compounds are observed in the narrow range of $\delta = 39.3\text{--}38.1$ ppm. All signals of the methylene groups are shifted in the range of $\delta = 73.9\text{--}57.2$ ppm as expected. In the fluorine containing compounds **10** and **12** these signals are splitted into doublets due to $^2J_{\text{C-F}}$ coupling with coupling constants of 20.1 and 19.2 Hz, respectively. The chemical shifts of the carbonyl groups of all carbamate and urea compounds can be observed in the range of $\delta = 156.8\text{--}154.3$ ppm, and are shifted to higher field of $\delta = 148.3$ and 148.0 ppm for the nitrocarbamates **11** and **12**. The signals of the

polynitrocarbon atoms in compounds **8–12** are shifted to the range of $\delta = 124.6\text{--}115.5$ ppm and are splitted into doublets for the fluorine containing compounds **10** and **12** due to $J_{\text{C-F}}$ coupling with a typical average coupling constant of 292.6 Hz.^[21]

The $^{14}\text{N}\{^1\text{H}\}$ NMR spectra show all signals of the nitro groups in the expected range of $\delta = -17$ ppm (compound **8**, $\text{C}(\text{NO}_2)_2$) to -34 ppm (compound **11**, $\text{C}(\text{NO}_2)_2\text{F}$).^[22] In the ^{19}F NMR spectra of compounds **10** and **12** the chemical shifts δ are observed at -112.13 (**10**) and -111.4 (**8**) ppm. They only differ slightly from the chemical shift of the starting material 2-fluoro-2,2-dinitroethanol of $\delta = -111.9$ ppm and show broad signals indicating multiple couplings.^[23]

2.4 Vibrational Spectroscopy

Compounds **2**, **3**, and **8–12** were also investigated by IR and Raman spectroscopy. The characteristic IR vibrational modes were assigned according to the literature and are listed in Table 2.^[24] The weak bands of all compounds observed in the range of $\tilde{\nu} = 3039\text{--}2880\text{ cm}^{-1}$ can be assigned to the stretching modes of the methyl and methylene groups [$\nu(\text{CH})$, $\nu_s(\text{CH})$ and $\nu_{\text{as}}(\text{CH})$]. In the IR spectra of compounds **2**, **3**, and **8–10** the valence vibration $\delta(\text{NH})$ bands are in the range of $\tilde{\nu} = 3040$ (**3**) $\text{--} 3233$ (**8**) cm^{-1} . The characteristic carbonyl stretching vibration $\nu(\text{C=O})$ of all carbamates (**3** and **8–12**) is observed in the narrow range of $\tilde{\nu} = 1758$ (**12**) $\text{--} 1728$ (**3**) cm^{-1} , and for the urea derivative **2** at a slightly higher energy at $\tilde{\nu} = 1651\text{ cm}^{-1}$.

Table 2: Assignment of the characteristic IR vibrations of compounds **2**, **3**, and **8–12** [cm^{-1}].

Nucleus	2	3	8	9	10	11	12
$\nu(\text{CH}_2/\text{CH}_3)$	3039–2949	2954	2971–2880	3034–2960	2981	3020	3051–2963
$\delta(\text{NH})$	3331	3404	3233	3318	3361	–	–
$\nu(\text{C=O})$	1651	1728	1731	1729	1735	1731	1758
$\nu_{\text{as}}(\text{CNO}_2)$	–	–	1568	1580	1523	1508	1525
$\nu_s(\text{CNO}_2)$	–	–	1347	1299	1311	1300	1331
$\nu_{\text{as}}(\text{NNO}_2)$	1502	1503	1587	1599	1599	1599	1600
$\nu_s(\text{NNO}_2)$	1286	1295	1259	1222	1212	1260	1309
$\nu(\text{C-F})$	–	–	–	–	1260	–	1263

In the IR spectra of all compounds the characteristic asymmetric nitramine stretching vibrations $\nu_{\text{as}}(\text{NNO}_2)$ are observed in the range of $\tilde{\nu} = 1600$ (**12**)– 1502 (**2**) cm^{-1} , and the symmetric stretching vibrations $\nu_s(\text{NNO}_2)$ in the range of $\tilde{\nu} = 1295\text{--}1212\text{ cm}^{-1}$. They can rather clearly be distinguished from the bands of the C–NO₂ stretching modes observed in the spectra of compounds **8–12**. These show the characteristic asymmetric nitro stretching vibrations $\nu_{\text{as}}(\text{CNO}_2)$ in the range of $\tilde{\nu} = 1580$ (**9**)– 1508 (**11**) cm^{-1} and the symmetric stretching vibrations $\nu_s(\text{CNO}_2)$ in the range of $\tilde{\nu} = 1309\text{--}1212\text{ cm}^{-1}$. The fluorine containing compounds **10** and **12** show the C–F stretching vibration ν at $\tilde{\nu} = 1260$ and 1263 cm^{-1} , respectively.

2.5 X-ray Diffraction

Crystals of compounds **2**, **3**, **9**, **10**, **11** and **15** suitable for X-ray diffraction were obtained by slow evaporation of the corresponding solvent at 8 °C. The solvents for recrystallisation were dichloromethane (**2**, **9**, **10** and **11**), methane (**3**) and slightly acidified acetone (**10** and **15**), respectively. Tables 3+4 include all relevant crystallographic and structural refinement data of these compounds. Refined atom positions and anisotropic thermal displacement parameters are listed in the Appendix 2.10.

Table 3: Crystal structure parameters of compounds bisNAPurea (**2**), bisNAPurea monohydrate (**2·H₂O**), bisNAPcarbamate (**3**) and TNE-NAP-C (**9**). Standard deviations are given in parentheses.

	2	2·H₂O	3	9
Refined formula	C ₅ H ₁₂ N ₆ O ₅	C ₅ H ₁₄ N ₆ O ₆	C ₅ H ₁₁ N ₅ O ₆	C ₅ H ₈ N ₆ O ₁₀
Formula weight [g·mol⁻¹]	236.19	254.22	237.19	312.15
Crystal dimensions [mm]	0.35×0.10×0.05	0.58×0.30×0.28	0.23×0.18×0.05	0.30×0.15×0.10
Crystal description	colourless needle	colourless block	colourless block	colourless block
Crystal system	orthorhombic	triclinic	triclinic	monoclinic
Space group	<i>Pccn</i>	<i>P</i> -1	<i>P</i> -1	<i>P</i> 2 ₁ / <i>c</i>
<i>a</i> [Å]	12.479(1)	6.629(1)	8.269(1)	9.350(1)
<i>b</i> [Å]	8.597(1)	8.352(2)	11.452(2)	9.357(1)
<i>c</i> [Å]	9.248(1)	10.994(1)	11.660(1)	13.557(1)
α [°]	90	88.09(2)	68.90(2)	90
β [°]	90	76.14(1)	80.79(1)	96.44(1)
γ [°]	90	67.00(2)	75.39(1)	90
<i>V</i> [Å³]	992.2(1)	542.7(2)	993.8(3)	1178.6(1)
<i>Z</i>	4	2	4	4
ρ_{calcd} [g·cm⁻³]	1.581	1.556	1.585	1.759
μ [mm⁻¹]	0.139	0.140	0.144	0.171
temperature [K]	104(2)	173(2)	173(2)	173(2)
θ range [°]	4.41–26.48	4.33–28.28	4.18–28.70	4.15–26.00
<i>F</i>(000)	496	268	496	640
dataset <i>h</i>	−15 ≤ <i>h</i> ≤ 15	−3 ≤ <i>h</i> ≤ 8	−9 ≤ <i>h</i> ≤ 9	−11 ≤ <i>h</i> ≤ 11
dataset <i>k</i>	−10 ≤ <i>k</i> ≤ 10	−10 ≤ <i>k</i> ≤ 11	−13 ≤ <i>k</i> ≤ 13	−11 ≤ <i>k</i> ≤ 11
dataset <i>l</i>	−11 ≤ <i>l</i> ≤ 11	−13 ≤ <i>l</i> ≤ 14	−13 ≤ <i>l</i> ≤ 9	−16 ≤ <i>l</i> ≤ 16
reflections measured	9532	3360	6125	11565
reflections independent	1020	2627	3274	2314
reflections unique	886	2159	2171	1921
<i>R</i>_{int}	0.0397	0.0148	0.0562	0.0520
<i>R</i>1, <i>wR</i>2 (2σ data)	0.0294, 0.0700	0.0354, 0.0840	0.0716, 0.1907	0.0343, 0.0795
<i>R</i>1, <i>wR</i>2 (all data)	0.0360, 0.0740	0.0463, 0.0933	0.1022, 0.2253	0.0447, 0.0859
Data/restraints/parameters	1020/0/92	2627/0/210	3274/0/297	2314/0/84
GOOF on <i>F</i>²	1.043	1.050	1.047	1.039
Residual electron density	−0.257/0.206	−0.269/0.184	−0.483/0.445	−0.235/0.240
CCDC number	957942	1050466	958074	940416

Table 4: Crystal structure parameters of compounds FDNE-NAP-C (**10**), TNE-NAP-NC (**11**) and DNDA-4 (**13**). Standard deviations are given in parentheses.

	10	11	13
Refined formula	C ₅ H ₈ N ₅ O ₈ F	C ₅ H ₇ N ₇ O ₁₂	C ₂ H ₆ N ₄ O ₄
Formula weight [g·mol⁻¹]	285.14	357.15	150.09
Crystal dimensions [mm]	0.40×0.30×0.04	0.25×0.15×0.10	0.40×0.25×0.15
Crystal description	colourless block	colourless block	colourless block
Crystal system	monoclinic	monoclinic	tetragonal
Space group	<i>P</i> 2 ₁ / <i>c</i>	<i>P</i> 2 ₁ / <i>c</i>	<i>I</i> 4 ₁ / <i>acd</i>
<i>a</i> [Å]	9.325(2)	9.363(1)	11.542(2)
<i>b</i> [Å]	9.662(1)	20.257(1)	11.542(2)
<i>c</i> [Å]	12.213(1)	6.807(1)	38.324(3)
α [°]	90	90	90
β [°]	91.25(1)	90.77(1)	90
γ [°]	90	90	90
<i>V</i> [Å³]	1100.1(1)	1290.8(2)	5105.4(4)
<i>Z</i>	4	4	32
ρ_{calcd} [g·cm⁻³]	1.722	1.838	1.562
μ [mm⁻¹]	0.172	0.183	0.147
temperature [K]	173(2)	173(2)	298(2)
θ range [°]	4.22–26.00	4.19–26.99	4.26–25.98
<i>F</i>(000)	584	728	2496
dataset <i>h</i>	−11 ≤ <i>h</i> ≤ 9	−11 ≤ <i>h</i> ≤ 11	−14 ≤ <i>h</i> ≤ 14
dataset <i>k</i>	−11 ≤ <i>k</i> ≤ 5	−25 ≤ <i>k</i> ≤ 25	−14 ≤ <i>k</i> ≤ 14
dataset <i>l</i>	−15 ≤ <i>l</i> ≤ 7	−8 ≤ <i>l</i> ≤ 8	−47 ≤ <i>l</i> ≤ 47
reflections measured	3039	13925	23180
reflections independent	2074	2806	1245
reflections unique	1599	2210	1001
<i>R</i>_{int}	0.0150	0.0437	0.0324
<i>R</i>1, <i>wR</i>2 (2σ data)	0.0360, 0.0827	0.0351, 0.0795	0.0363, 0.0942
<i>R</i>1, <i>wR</i>2 (all data)	0.0531, 0.0939	0.0503, 0.0868	0.0469, 0.1024
Data/restraints/parameters	2074/2/204	2806/0/245	1245/0/115
GOOF on <i>F</i>²	1.026	1.029	1.038
Residual electron density	−0.213/0.203	−0.202/0.257	−0.132/0.206
CCDC number	940375	940373	1043160

Crystal Structure of *N,N'*-Bis-(2-Nitro-2-Azapropyl)-Urea (**2**)

BisNAPurea (**2**) crystallises as colourless needles in the orthorhombic space group *Pccn* with four molecules in the unit cell and a calculated maximum density of 1.581 g·cm⁻³ at 104(2) K. The molecule has a centre of inversion as depicted in Figure 2. Therefore the two 2-nitro-2-azapropyl moieties are bent into opposite directions from the urea unit, which is almost planar owing to the *sp*² hybridisation of the carbon atom. The C3–O3 bond length of 1.239(2) Å clearly shows character of a standard double bond (C=O 1.19 Å).^[25] The N1–N2 bond length does not differ from all the nitramine N–N bond length of the NAP derivatives discussed in Chapter 1 and is in the typical range for nitramines with 1.357(1) Å.

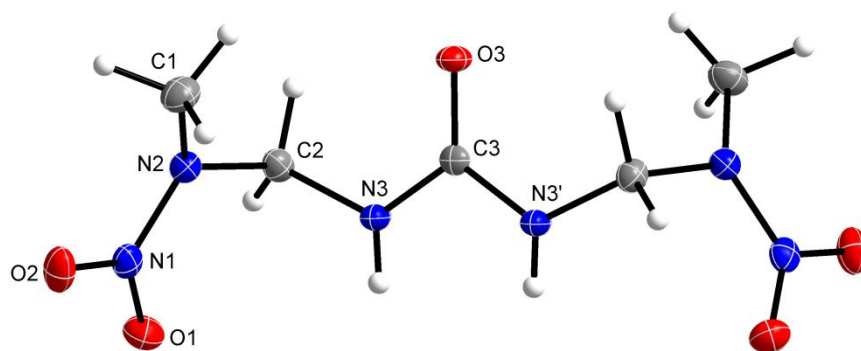


Figure 2: Crystal structure of bisNAPurea (**2**). Selected bond lengths [Å] and angles [°]: N1–N2 1.357(1), N1–O1 1.243(1), N1–O2 1.233(1), N2–C1 1.466(2), N2–C2 1.468(2), C2–N3 1.439(2), N3–C3 1.364(1), C3–O3 1.239(2); O2–N1–O1 124.3(2), C3–N3–C2 121.9(2), N1–N2–C1 116.4(2); C2–N2–N1–O2 169.7(1), C1–N2–N1–O1 –168.2(1). Symmetry operator: ') $\frac{1}{2}-x, \frac{1}{2}-y, z$.

The crystal structure is mainly build up by two hydrogen bonds between N3/N3' and O3(i) presented as blue dashed lines in Figure 3. These hydrogen bonds form chains of alternating mirror molecules along the *c* axis. Two chains with opposite orientation intercalate with each other through an intermolecular electrostatic interaction between N1/N1(ii) and O2/O2(ii) of the nitro groups presented as yellow dashed lines in Figure 3 with a distance under the sum of van der Waals radii [$\Sigma_{\text{vdW}}(\text{N},\text{O}) = 3.07 \text{ Å}$].^[26]

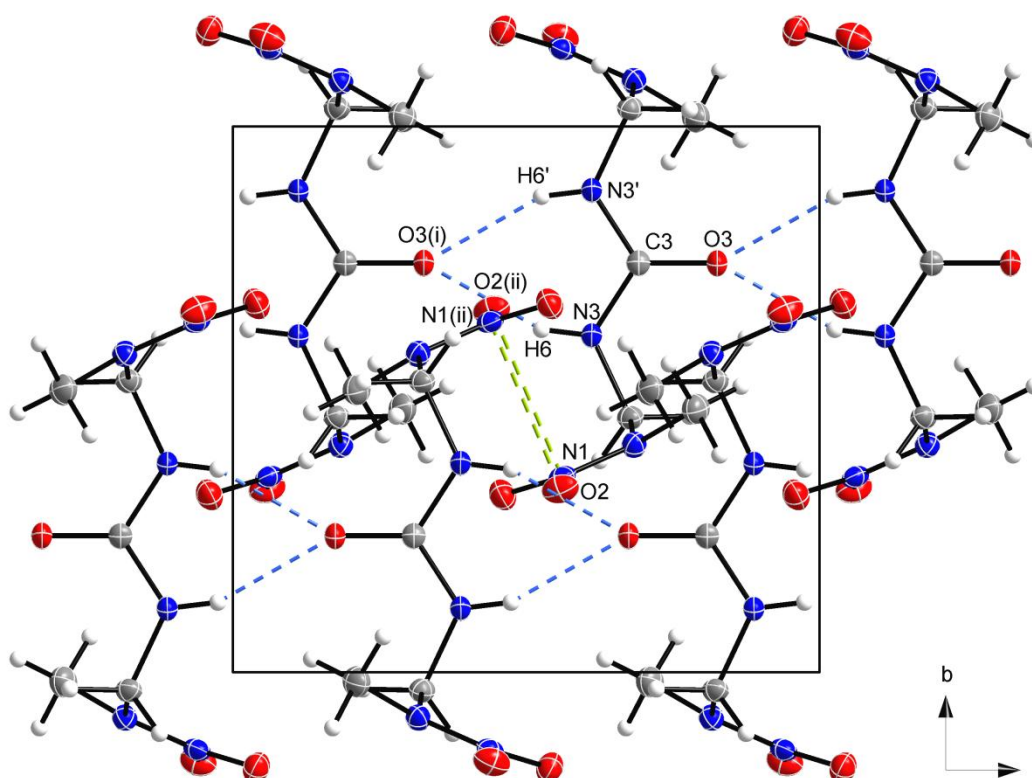


Figure 3: Unit cell of the structure of compound **2** with view along the *a* axis showing two intercalating chains of molecules with different orientation. The hydrogen bonds as blue dashed lines and the electrostatic interaction between the nitro groups as yellow dashed lines (Table 5). Symmetry operators: ') $\frac{1}{2}-x, \frac{1}{2}-y, z$; (i) $x, \frac{1}{2}-y, \frac{1}{2}+z$; (ii) $1-x, 1-y, -z$.

Table 5: Structural parameters for the intermolecular interactions in the crystal structure of compound **2** presented in Figure 3.

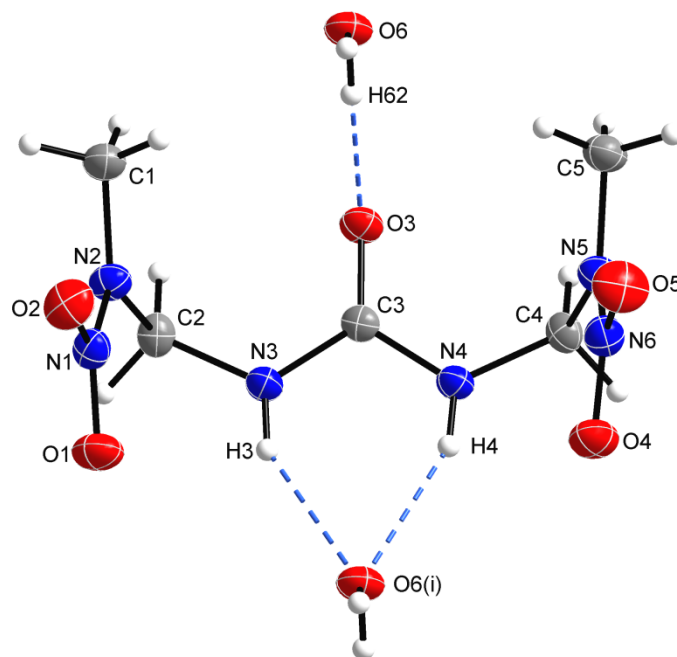
D–H···A	d (D–H) [Å]	d (H···A) [Å]	d (D–H···A) [Å]	∠ (D–H···A) [°]
N3–H6···O3(i)	0.80(2)	2.13(2)	2.884(2)	155.5(2)
N3'–H6'···O3(i)				
Electrostatic interaction			d (X···Y) [Å]	ΣvdWaals radius ^[26]
O2···N1(ii), N1···O2(ii)			2.927(1)	3.07 Å
Symmetry operators: 'i) ½–x, ½–y, z; (i) x, ½–y, ½+z; (ii) 1–x, 1–y, –z.				

Crystal Structure of *N,N'*-Bis-(2-Nitro-2-Azapropyl)-Urea Monohydrate (**2**·H₂O)

BisNAPurea monohydrate (**2**·H₂O) crystallises as colourless blocks in the triclinic space group *P*–1 with two molecules in the unit cell and a calculated maximum density of 1.556 g·cm^{–3} at 173(2) K (Figure 4). The main difference compared to the structure anhydrous compound **2** is that the two 2-nitro-2-azapropyl groups are bent to the same side of the planar urea unit. The water molecules connect layers of bisNAPurea molecules through hydrogen bonds forming chains along the *a* axis.

Table 6: Structural parameters for the intermolecular hydrogen bonds in the crystal structure of compound **2**·H₂O presented in Figure 4.

D–H···A	d (D–H) [Å]	d (H···A) [Å]	d (D–H···A) [Å]	∠ (D–H···A) [°]
N3–H3···O6(i)	0.85(2)	2.16(2)	2.935(2)	150.6(2)
N4–H4···O6(i)	0.85(3)	2.09(2)	2.883(2)	154.9(2)
N6–H62···O3	0.88(3)	1.90(3)	2.774(2)	174.6(2)
Symmetry operator: (i) –1+x, y, z.				

**Figure 4:** Crystal structure of bisNAPurea monohydrate (**2**·H₂O) with hydrogen bonds (listed in Table 6). Selected bond lengths [Å] and angles [°]: N1–N2 1.337(1), N5–N6 1.340(2), average N–H 0.852(2), O3–C3 1.234(1), average N–O 1.238(2), N3–C3 1.364(2), N4–C3 1.361(2), O2–N1–O1 123.8(2), N4–C3–N3 113.8(1), C1–N2–N1–O2 0.8(2), C5–N5–N6–O5 –3.7(2) C4–N4–C3–O3 3.8(2).

Crystal Structure of Bis-O,N-(2-Nitro-2-Azapropyl)-Carbamate (3)

Compound **3** crystallises as colourless blocks in the triclinic space group $P\bar{1}$ with four molecules per unit cell and a calculated maximum density of $1.585 \text{ g}\cdot\text{cm}^{-3}$ at $173(2) \text{ K}$. Its asymmetric unit consists of two crystallographically independent molecules as depicted in Figure 5. The carbamate unit is planar, thus similar to the analogue urea derivative **2**. Differing to compound **2** the 2-nitro-2-azapropyl moieties are bend to the same side of the carbamate, whereat within the asymmetric unit the nitro groups intercalate with each other by the typical electrostatic interactions between the nitrogen and oxygen atoms of the nitro groups in the range of the sum of van der Waals radii [$\Sigma\text{vdW}(\text{O},\text{N}) = 3.07 \text{ \AA}$],^[26] for instance $\text{N5}\cdots\text{O7}\cdots\text{N1}\cdots\text{O11}$ (Figure 5). This results in a staggered molecules chain like structure.

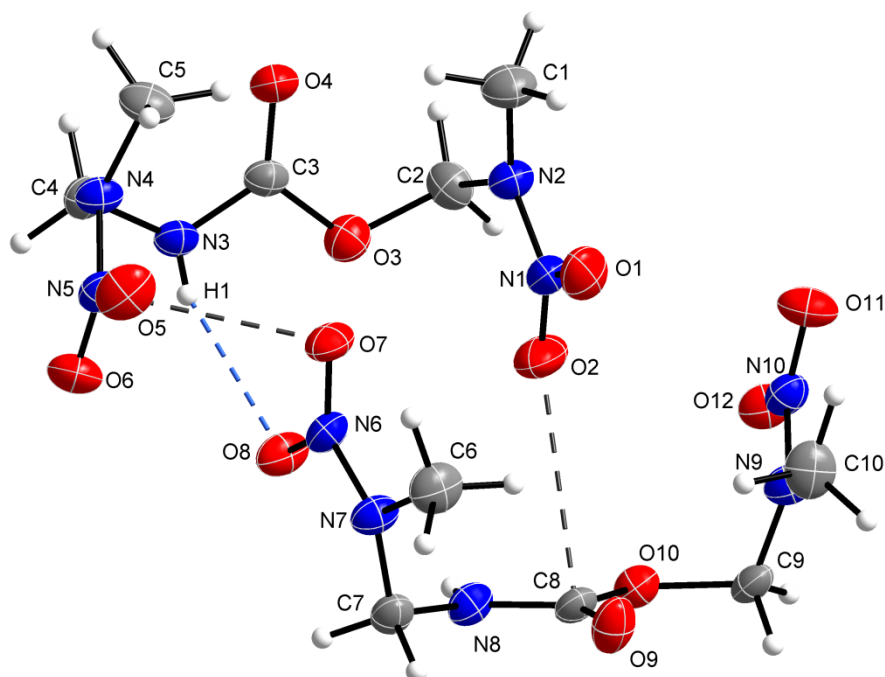


Figure 5: Asymmetric unit in the crystal structure of compound **3** with one hydrogen bond (blue dashed line) and two attractive intermolecular interactions (black dashed lines) between the molecules for the structural parameters listed in Table 7. Selected bond lengths [\AA] and angles [$^\circ$]: N6-N7 1.350(4), N2-N1 1.362(5), N4-N5 1.347(4), N9-N10 1.352(4), O4-C3 1.206(5), O9-C8 1.214(5), O1-N1 1.233(5), O5-N5 1.231(4), O7-N6 1.223(4), O8-N6 1.243(4); O2-N1-O1 124.7(4), O5-N5-O6 124.8(3), O7-N6-O8 124.3(3), N3-C3-O3 110.6(3), N8-C8-O10 111.5(3); C2-O3-C3-N3 $-175.8(3)$, C7-N8-C8-O10 $-175.2(3)$, C9-N9-N10-O11 173.0(3).

Table 7: Structural parameters for the intermolecular interactions in the crystal structure of compound **3** presented in Figure 3.

D-H \cdots A	d (D-H) [\AA]	d (H \cdots A) [\AA]	d (D-H \cdots A) [\AA]	\angle (D-H \cdots A) [$^\circ$]
N3-H1\cdotsO8	0.71(2)	2.39(2)	3.047(5)	155.0(9)
Electrostatic interactions			d (X \cdots Y) [\AA]	ΣvdW radius ^[26]
N5\cdotsO7			2.944(2)	3.07 \AA
C8\cdotsO2			3.183(5)	3.22 \AA

Crystal Structure of 2,2,2-Trinitroethyl-(2-Nitro-2-Azapropyl)-Carbamate (9)

The carbamate **9** crystallises as colourless blocks in the monoclinic space group $P2_1/c$ with four molecules in the unit cell and a calculated maximum density of 1.759 g cm^{-3} at $173(2) \text{ K}$. The molecular structure is shown in Figure 6. The carbamate unit is planar as expected and the N3–C3 bond length is shortened compared to a standard single bond (1.47 \AA).^[25] This indicates the stabilisation of the tautomeric iminol form of the carbamate unit. The two functionalities are bent to the same side of this linker.

Within the trinitroethyl moiety several intramolecular steric and electrostatic interactions between the nitro groups well below the sum of van der Waals radii are observed. However, it is remarkable that the nitro groups do not arrange in the typical propeller-like conformation as observed in many compounds containing this functionality,^[27] which is reflected in the dihedral torsion angles C4–C5–N–O (Figure 7).

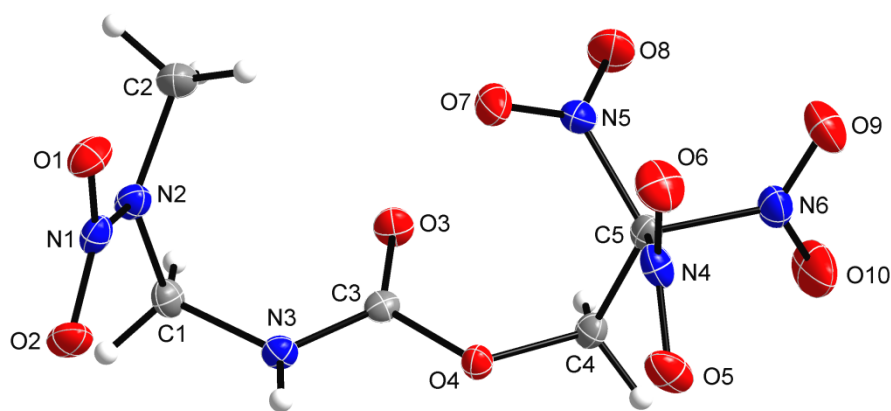


Figure 6: Crystal structure of compound **9**. Selected bond lengths [\AA] and angles [$^\circ$]: O3–C3 1.212(2), O4–C3 1.379(2), O4–C4 1.429(3), O7–N5 1.216(2), O2–N1 1.236(2), N2–N1 1.354(2), N2–C1 1.461(2), N2–C2 1.466(2), N3–C3 1.336(2), N3–C1 1.448(2), N3–H 0.76(2), N6–C5 1.541(2), C4–C5 1.516(2), O2–N1–O1 124.4(2), N3–C3–O4 110.6(3), O10–N6–C5 116.1(1), C1–N3–C3–O4 172.3(1), C2–N2–N1–O2 $-172.9(1)$.

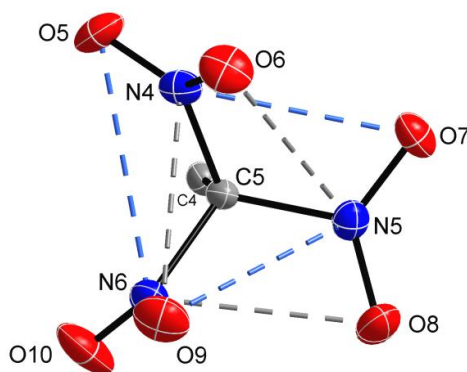


Figure 7: View along the C4–C5 bond of compound **9** displaying the conformation within the trinitroethyl moiety, and the atom distances as dashed lines well below the sum of van der Waals radii: N5...O9 2.798(2) \AA , N6...O5 3.067(2) \AA , N4...O7 2.733(2) \AA (blue), N6...O8 2.616(2) \AA , N5...O6 2.707(2) \AA , N4...O9 2.790(2) \AA (grey); ΣvdW radii: N,O = 3.07 \AA .^[26] the dihedral angles deviate considerably from the expected range ($23\text{--}67^\circ$) for the propeller-like conformation:^[27] C4–C5–N6–O10 $-2.2(2)^\circ$, C4–C5–N5–O7 $84.8(2)^\circ$, C4–C5–N4–O5 $29.0(2)^\circ$.

The structure is build up by several classical and unclassical intermolecular hydrogen bonds and electrostatic interactions. One molecule is connected to four of its neighbours by hydrogen bonds (blue dashed lines) and intercalates with a fifth neighbour by an electrostatic interaction between the nitro groups, which is found to be slightly under the sum of van der Waals radii (green dashed lines in Figure 8).

Table 8: Structural parameters for the intermolecular interactions in the crystal structure of compound **9** presented in Figure 8.

D–H···A	d (D–H) [Å]	d (H···A) [Å]	d (D–H···A) [Å]	∠ (D–H···A) [°]
C1–H5···O5(i)	0.96(2)	2.57(2)	3.112(2)	116.3(3)
C1(iii)–H5(iii)···O5				
C1–H4···O7(ii)	0.93(2)	2.75(2)	3.105(2)	103.7(2)
C1(iv)–H4(iv)···O7				
N3(i)–H6(i)···O3	0.76(2)	2.14(2)	2.897(1)	178.1(2)
N3–H6···O3(iii)				
C4–H7···O2(i)	0.94(1)	2.26(2)	3.181(1)	166.3(2)
C4(iii)–H7(iii)···O2				
Electrostatic interaction			d (X···Y) [Å]	ΣvdWaals radius ^[26]
O6···N1(v), O6(v)···N1			3.038(2)	3.07 Å
Symmetry operators: (i) 1–x, ½+y, ½–z; (ii) x, ½–y, –½+z; (iii) 1–x, –½+y, ½–z; (iv) x, ½–y, ½+z; (v) 1–x, –y, 1–z.				

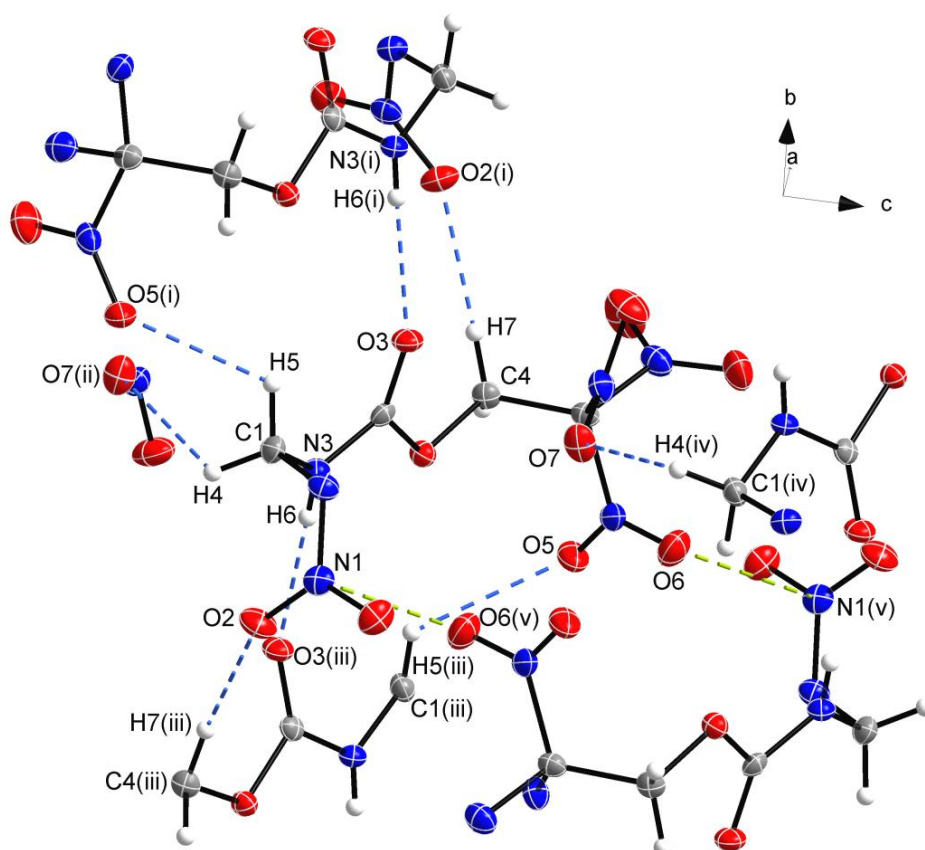


Figure 8: Intermolecular interactions presented by blue (hydrogen bonds) and green (short contact) dashed lines in the crystal structure of compound **9** for the structural parameters listed in Table 8 (methyl groups and several other atoms omitted for clarity). Symmetry operators: (i) 1–x, ½+y, ½–z; (ii) x, ½–y, –½+z; (iii) 1–x, –½+y, ½–z; (iv) x, ½–y, ½+z; (v) 1–x, –y, 1–z.

Crystal Structure of 2-Fluoro-2,2-Dinitroethyl-(2-Nitro-2-Azapropyl)-Carbamate (10)

Compound **10** crystallises as colourless blocks in the monoclinic space group $P2_1/c$ with four molecules in the unit cell and a calculated maximum density of 1.722 g cm^{-3} at $173(2) \text{ K}$. The molecular structure is shown in Figure 9. Similar to the carbamate **9** also here the carbamate unit is planar as expected and the N3–C3 bond length is shortened compared to a standard single bond (1.47 \AA),^[25] which indicates the stabilisation of the tautomeric iminol form of the carbamate unit. Differing from carbamate **9** the two functionalities are bent to opposite sides of the carbamate linker.

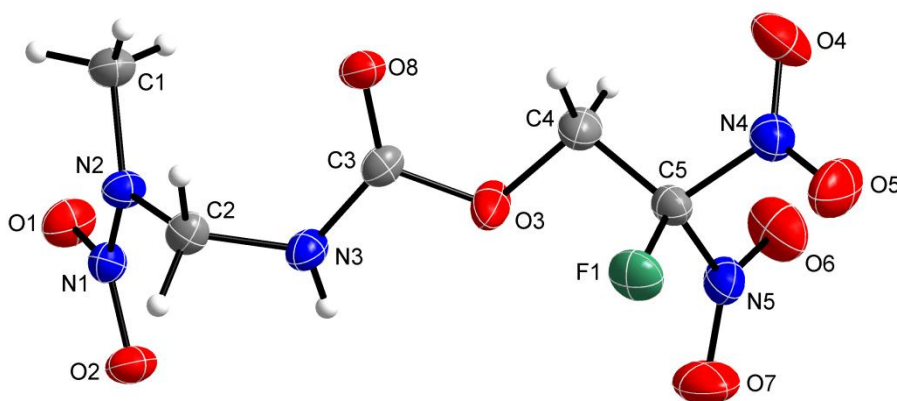


Figure 9: Crystal structure of compound **10**. Selected bond lengths [\AA] and angles [$^\circ$]: F1–C5 1.329(2), O2–N1 1.240(1), O3–C3 1.371(2), O3–C4 1.430(2), O8–C3 1.205(2), O5–N4 1.214(2), N2–N1 1.351(2), N2–C1 1.458(2), N3–C3 1.343(2), N3–H 0.77(2), N4–C5 1.527(2), C4–C5 1.504(3), O1–N1–O2 124.0(1), N3–C3–O3 109.5(2), O4–N4–C5 116.6(1), F1–C5–C4 113.9(1), C1–N2–N1–O1 9.5(2), C2–N3–C3–O3 $-176.3(1)$.

The fluorodinitromethyl group does not arrange in the propeller-like conformation described by BRILL *et al.* (C–C–N–O $23\text{--}67^\circ$)^[27] with dihedral angles of C4–C5–N5–O7 -66.5° and C4–C5–N4–O4 $19.0(2)^\circ$. Instead the nitro groups are rotated *syn* to each other (Figure 10).

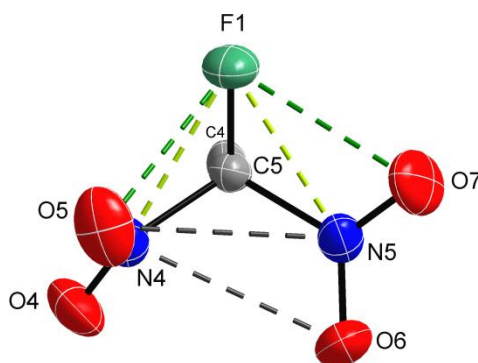


Figure 10: View along the C4–C5 bond of compound **10** displaying the conformation of the nitro groups within the fluorodinitro moiety and the atom distances as dashed lines well below the sum of van der Waals radii. Green: F1...O5 2.573(2), F1...O7 2.521(2) \AA ; yellow: F1...N4 2.301(2), F1...N5 2.302(2) \AA ; black: O5...N5 2.950(2), N4...O6 2.732(2) \AA [Σ vdW radii: (F,O) = 2.99; (F,N) = 3.02; (N,O) = 3.07 \AA].^[26]

In the crystal structure of compound **10** three intermolecular interactions are observed that might be discussed as very weak electrostatic attractions (short contacts), although showing distances well above the sum of van der Waals radii [Σ vdW radii: (C,F) = 3.17; (C,O) = 3.22 Å].^[26] They connect two molecules with opposite orientation of the carbamate unit forming chains of molecules along the *c* axis as shown in Figure 11 and are listed in Table 9.

Table 9: Structural parameters for the intermolecular interactions in the crystal structure of compound **10** presented in Figure 11.

D–H···A	d (D–H) [Å]	d (H···A) [Å]	d (D–H···A) [Å]	∠ (D–H···A) [°]
C4(i)–H8(i)···O5	0.99(2)	2.66(2)	3.501(2)	144.0(2)
C1(i)–H3(i)···F1	0.95(2)	2.73(3)	3.589(2)	150.6(2)
C2–H5···O1(i)	0.95(2)	2.63(2)	3.263(2)	124.1(2)

Symmetry operators: (i) $x, \frac{1}{2}-y, -\frac{1}{2}+z$.

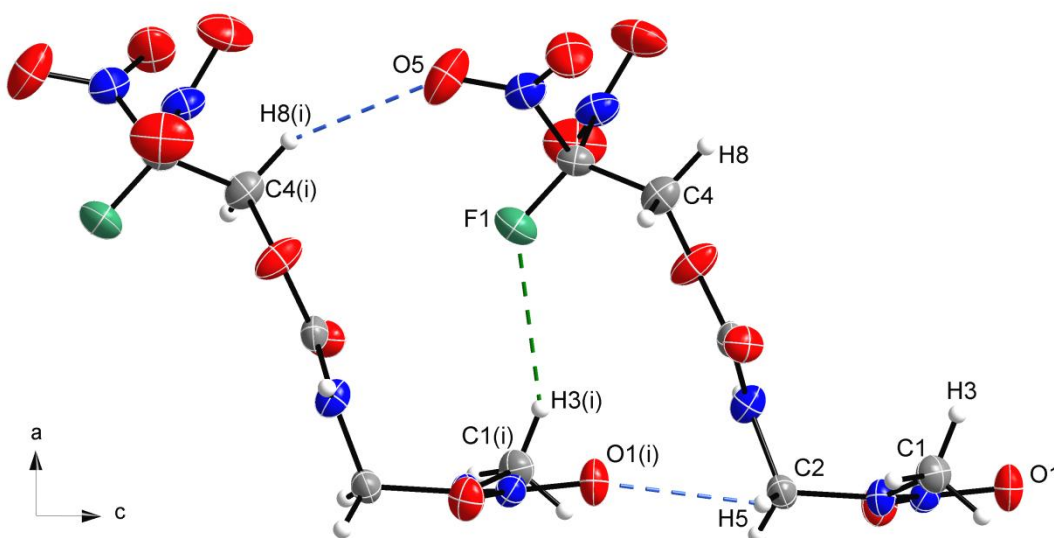


Figure 11: Three very weak intermolecular electrostatic interactions in the crystal structure of compound **10** for the structural parameters listed in Table 9 forming chains of molecules along the *c* axis. Symmetry operators: (i) $x, \frac{1}{2}-y, -\frac{1}{2}+z$.

Crystal Structure of 2,2,2-Trinitroethyl-(2-Nitro-2-Azapropyl)-N-Nitrocarbamate (11)

The nitrocarbamate (**11**) crystallises as colourless blocks in the monoclinic space group $P2_1/c$ with four molecules in the unit cell and a calculated maximum density of 1.838 g cm^{−3} at 173(2) K. The molecular structure is presented in Figure 12. It shows a weak electrostatic intramolecular interaction between O2 of the secondary nitramine group and N5 of the trinitromethyl moiety, with 2.95(1) Å clearly under the sum of van der Waals radii (Σ vdW radii: O,N = 3.07 Å).^[26] The nitrocarbamate unit shows an almost perfect planar arrangement, which is reflected in the sum of the angles around the C3 and the two nitrogen atoms N1 and N2, where the angle sum is 360.0° each as also observed in other nitrocarbamate compounds.^[18] Compared to compounds **9** and **10** the carbamate unit shows shortened C3–O5 and C3–O6 bond length and an elongated C3–N3 bond length (Figure 12). This indicates a stabilisation of the tautomeric aminon form of the carbamate unit, hence the double bond character of the C3–O5 is substantial, while the C3–N3 bond length is more likely in the

range of a standard single bond (1.47 Å).^[25] This also explains the rather elongated nitramine N3–N4 bond length in the range of a N–N single bond (1.48 Å)^[25] compared to the N1–N2 bond length, which is in the expected range for nitramines (compare X-ray diffraction section of Chapter 1). The trinitromethyl moiety is arranged in the typical propeller-like conformation for this group as described by BRILL *et al.*,^[27] which is reflected in the dihedral angles C4–C5–N–O (Figure 13). One intermolecular electrostatic interaction below the sum of van der Waals radii is observed between C3 and an adjacent O4 atom with 2.966(2) Å.

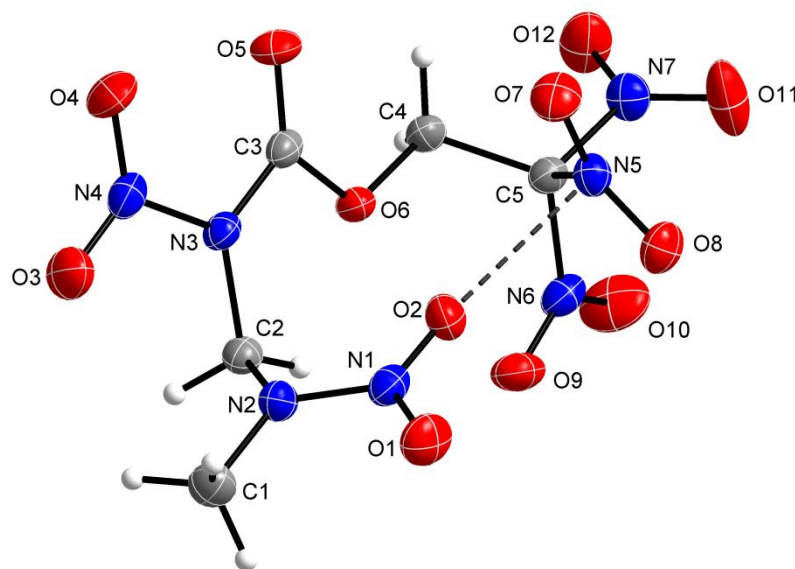


Figure 12: Crystal structure of compound **11**. Selected bond length [Å] and angles [°]: O8–N5 1.214(2), O6–C3 1.354(2), O6–C4 1.430(1), O5–C3 1.191(2), O2–N1 1.232(1), N2–N1 1.353(2), N2–C2 1.447(2), N2–C1 1.464(2), N3–C3 1.402(2), N3–N4 1.421(2), N3–C2 1.474(2), O3–N4 1.216(3), N7–C5 1.532(2), C5–C4 1.513(2), N1–N2–C2 116.7(1), O6–C3–N3 107.8(1), O6–C4–C5 108.1(1), C1–N2–N1–O2 177.9(2), N7–C5–C4–O6 –175.9(1), C3–N3–N4–O3 171.9(1), C2–N3–N4–O4 173.2(1). Intramolecular interaction: O2···N5 2.949(2) Å; Σ vdW (O,N) = 3.07 Å.^[26]

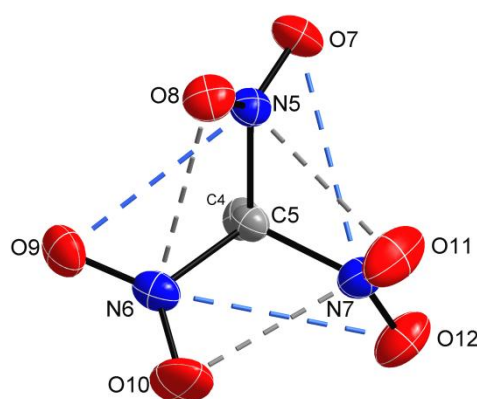


Figure 13: View along the C4–C5 bond of compound **11** displaying the propeller-like conformation within the trinitroethyl moiety, and the atom distances as dashed lines well below the sum of van der Waals radii: N5···O11 2.636(2) Å, N7···O10 2.560(2) Å, N6···O8 2.651(2) Å, N7···O7 3.029(2) Å, N5···O9 2.826(2) Å, N6···O12 3.173(2) Å; the dihedral angles almost in the expected range (23–67°) for the propeller-like conformation:^[27] C4–C5–N7–O12 –23.6(2)°, C4–C5–N6–O9 –68.9°, C4–C5–N5–O7 –34.6(3)°.

Crystal Structure of 1,3-Dinitro-1,3-Diazabutan (13)

DNDA-4 (**13**) crystallises as colourless blocks in the tetragonal space group $I4_1/acd$ with 32 molecules in the unit cell and a calculated maximum density of $1.562 \text{ g}\cdot\text{cm}^{-3}$ at 298(2) K. The molecular structure is shown in Figure 14. The N–N bond lengths are in the expected range for nitramines and the nitramine moieties are bent away from one another, thus not showing any interaction. The N1–C2–N3 angle is just in the range of the corresponding angle found in 2,4-dinitro-2,4-diazapentane [DNDA-5, $114.0(2)^\circ$].^[28] The proton at the N3 atom forms an hydrogen bond to an adjacent O2 atom, thus forming ringlike structure elements out of four molecules as presented in Figure 15.

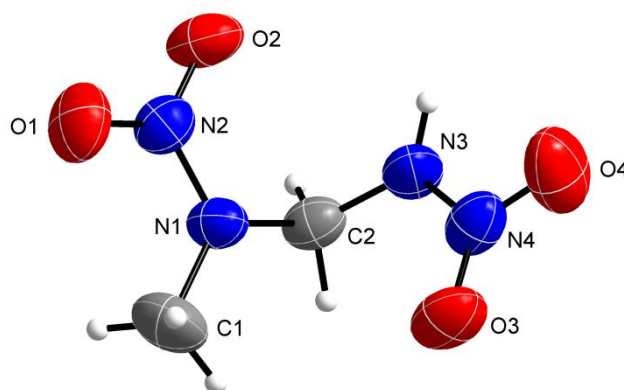


Figure 14: Crystal structure of compound **13**. Selected bond length [Å] and angles [°]: N1–N2 1.342(2), N1–C1 1.448(2), N1–C2 1.454(2), O2–N2 1.239(2), O3–N4 1.218(2), N3–N4 1.353(2), N3–C2 1.421(2), N3–H6 0.85(2), N2–O1 1.226(2), average C2–H 0.94(2), O4–N4 1.232(2), average C1–H 0.95(3); O1–N2–O2 123.9(2), O3–N4–O4 125.5(2), N3–C2–N1 114.9(1), C1–N1–N2–O1 1.3(2), C2–N1–N2–O2 –3.3(2), C2–N3–N4–O3 3.7(2).

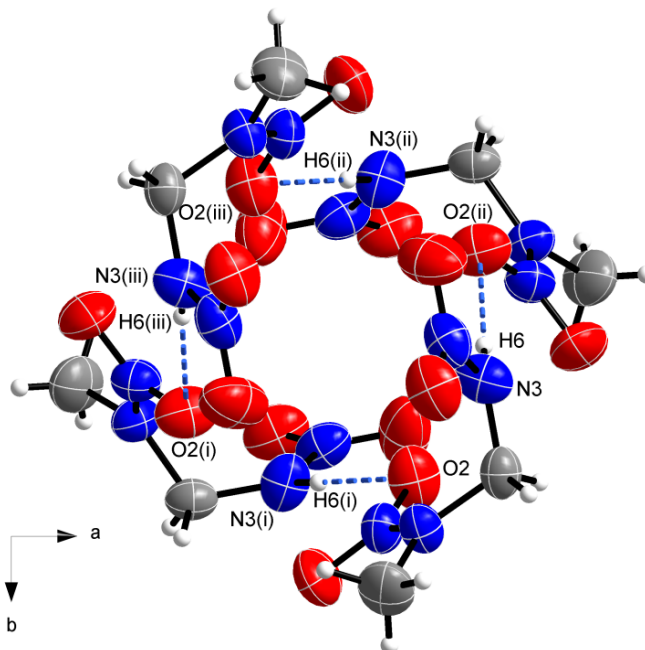


Figure 15: Hydrogen bond as blue dashed lines in the structure of compound **13** forming rings out of four molecules by view along the c axis: N3–H6 \cdots O2(ii) 0.85(2), 2.13(2), 2.974(2) Å, $173.1(2)^\circ$. Symmetry operators: (i) $-1/4+x, -1/4-y, 1/4-z$; (ii) $-1/4-x, 1/4+y, 1/4-z$; (iii) $-x, -1/2-y, z$.

2.6 Physical, Chemical and Energetic Properties

Owing to the energetic nature of the described compounds and for safety testing their sensitivities and energetic behaviour were determined. Their investigated physical and thermodynamic properties are summarised in Table 10, and the calculated detonation and combustion parameters are listed in Table 11. For convenience, their molecular structures are shown in Figure 16.

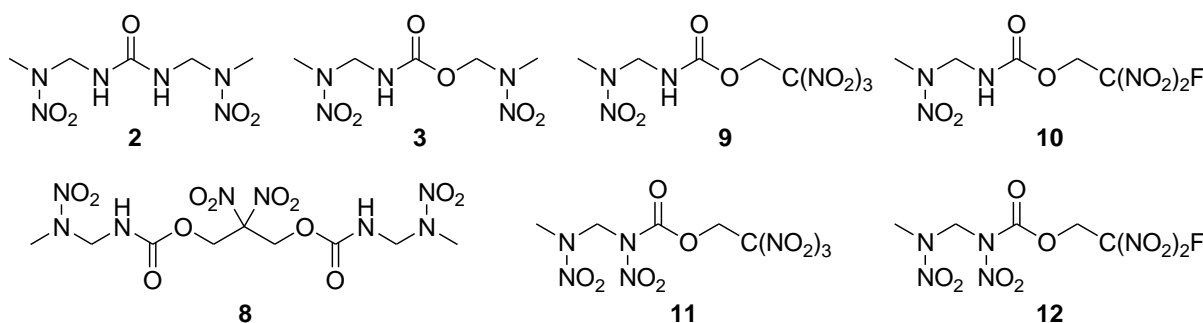


Figure 16: Molecular structures of the compounds discussed in this section with physical and thermodynamic properties and calculated performances listed in Tables 10+11.

Table 10: Physical and thermodynamic properties determined for compounds **2**, **3**, **8** and **9–12**.

	2	3	8	9	10	11	12
Formula	C ₅ H ₁₂ N ₆ O ₅	C ₅ H ₁₁ N ₅ O ₆	C ₉ H ₁₆ N ₈ O ₁₂	C ₅ H ₈ N ₆ O ₁₀	C ₅ H ₈ N ₅ O ₈ F	C ₅ H ₇ N ₇ O ₁₂	C ₅ H ₇ N ₆ O ₁₀ F
FW [g·mol⁻¹]	236.19	237.17	428.27	312.15	285.14	357.15	330.14
IS [J]^a	>40	35	35	30	>40	6	8
FS [N]^b	>360	240	240	240	324	120	144
ESD [J]^c	1.5	1.3	1.0	0.08	0.5	0.2	0.3
N [%]^d	35.58	29.53	26.16	26.92	24.56	27.45	25.46
N+O [%]^e	69.45	70.01	70.99	78.18	69.45	81.21	73.92
Ω_{CO} [%]^f	-40.6	-30.4	-18.8	5.1	-2.8	15.7	9.7
Ω_{CO2} [%]^g	-74.5	-64.1	-52.3	-20.5	-30.9	-6.7	-14.5
T_{melt} [°C]^h	150	85	117	135	70	92	62
T_{dec} [°C]ⁱ	162	180	174	183	219	147	158
ρ_{RT} [g·cm⁻³]^j	1.54	1.55	1.44	1.74	1.71	1.82	1.77
Δ_fH° [kJ·mol⁻¹]^k	-276	-426	-810	-449	-654	-316	-531
ΔU° [kJ·kg⁻¹]^l	-1048	-1682	-1786	-1343	-2199	-794	-1517

a) Impact sensitivity (BAM drophammer, method 1 out of 6);^[29–31] b) friction sensitivity (BAM friction tester, method 1 out of 6);^[31–33] c) electrostatic discharge sensitivity (OZM);^[34, 35] a–c) grain size <100 μm; d) nitrogen content; e) combined nitrogen and oxygen content; f) absolute oxygen balance assuming to the formation of CO and HF; g) absolute oxygen balance assuming to the formation of CO₂ and HF; h) melting temperature from DSC at a heating rate of 5 °C min⁻¹; i) decomposition temperature from DSC at a heating rate of 5 °C min⁻¹; j) experimentally determined density from pycnometer experiments at ambient temperature (average value from three measurements); k) heat of formation calculated at the CBS-4M level of theory;^[39] l) energy of formation calculated at the CBS-4M level of theory.^[39]

The urea derivative **2** melts at 150 °C with relatively subsequent decomposition at 162 °C, while the analogue carbamate **3** shows a rather large melting range from 85 to 180 °C. The bi-carbamate **8** shows a melting temperature of 117 °C and decomposition at 174 °C. Remarkable are the large melting ranges of the fluorine containing materials **10** and **12** with melting points considerably under 100 °C, which might be useful for melt-castable applications. As expected also their thermal stabilities are higher than for the analogue trinitroethyl derivatives **9** and **11**. The decomposition temperatures of compounds **9–12** range

from 147 °C to 219 °C, in which the carbamates **9** and **10** have considerably higher decomposition points than according nitrocarbamates **11** and **12**. However, it has to be pointed out that for compounds **2**, **3** and **8–12** no phase transitions have been observed during the DSC measurements, and that they show wax-like properties in the solid states.

The sensitivities towards impact, friction and electrostatic discharge were determined experimentally according to the standards of the German Federal Institute for Materials Research and Testing (BAM).^[31] According to the UN recommendations for the transport of dangerous goods,^[36] compounds **2** and **10** shall be classified as insensitive, compounds **3** and **8** as less sensitive, and compound **9**, **11** and **12** as sensitive towards impact. However the trend is obvious that just by introducing the additional nitro group to the carbamate units in compounds **9** and **10**, the resulting nitrocarbamates **11** and **12** become considerably more sensitive with impact sensitivities under 10 J. Also the fluorine containing materials **10** and **12** are less sensitive than their analogue trinitroethyl containing compounds **9** and **11**. With respect to the friction sensitivity only the urea derivative **2** shall be classified as insensitive, while all other compounds should be called sensitive. However, none of these compounds shows friction sensitivities under 100 N. The electrostatic discharge (ESD) test was carried out to determine whether the compounds are ignitable by the human body, which can generate up to 0.025 J of static energy.^[34, 35] All measured compounds are insensitive towards this energy. In the open flame all investigated compounds burned fast, but without deflagrating audibly. With regards of the oxygen balances, only the nitrocarbamate **11** with the highest oxygen balance can be considered as oxygen-carrier for propellant formulations. This material shows lower sensitivities than pentaerythrityltetranitrate (PETN: IS = 4 J, FS = 80 N, ESD = 0.1 J),^[37] thus meeting the requirement that is desired for novel oxidisers. The room temperature densities ρ_{RT} of the trinitroethyl containing derivatives **9** and **11** are higher compared to the analogue fluorine containing derivatives **10** and **12**, and again higher for the nitrocarbamates **11** and **12** compared to according carbamates **9** and **10** (Table 10).

The calculation of the detonation and combustion parameters was performed using the default mode with a standard set of constants (BKWG-S) in the EXPLO5 (Version 6.02) computer code^[38] and are attributed to the calculated heats of formation (CBS-4M level of theory)^[39] and densities obtained by pycnometer measurements at ambient temperature. The values of the calculation are summarised in Table 11.

The detonation performance (D_V , p_{CJ} , V_0) as well as the specific impulse I_{sp} of bisNAPurea **2** and its analogue bisNAPcarbamate **3** are comparable to each other and in the range of the values calculated for trinitrotoluene (TNT; 1.65 g·cm⁻³; $D_V = 7241$ m·s⁻¹, $p_{CJ} = 207$ kbar).^[38] However, the carbamate **3** might be interesting for further investigations as replacement for TNT owing to its large melting range, although the compound starts to decompose at 180 °C, thus 100 °C above TNT ($T_{dec} = 280$ °C)^[37] according to DSC measurements. Moreover, the impact sensitivity of compound **3** (35 J) was determined to be lower than that measured for TNT (15 J), while the friction sensitivity (240 N) is higher than that determined for TNT (>360 N).^[37]

The bi-carbamate **8** shows by far the lowest performance of all investigated compounds with a detonation velocity D_V even lower than that calculated for TNT, which might be explained by the high formula weight, its low density and the most negative heat of formation calculated at the CBS-4M level of theory of all discussed compounds (Table 10).^[39]

Table 11: Detonation and combustion parameters of compounds **2**, **3**, **8** and **9–12** calculated with the EXPLO5 computer code (Version 6.02).^[39]

	2	3	8	9	10	11	12
$-\Delta_{\text{Ex}}U^\circ$ [kJ·kg ⁻¹] ^a	4105	4172	4181	5018	4318	5949	5058
T_{det} [K] ^b	2648	2770	2970	3494	3133	4061	3605
p_{CJ} [kbar] ^c	187	182	154	283	264	328	299
D_V [m·s ⁻¹] ^d	7493	7259	6718	8118	7820	8706	8234
V_0 [L·kg ⁻¹] ^e	887	858	826	754	735	751	722
I_{sp} (neat) [s] ^f	200 (1353)	199 (1374)	203 (1641)	246 (3014)	224 (2403)	262 (3353)	253 (3222)
I_{sp} (+20 % Al) [s] ^g	245 (2374)	245 (2482)	246 (2762)	264 (3772)	253 (3198)	268 (4124)	266 (3943)
I_{sp} (+25 % Al) [s] ^g	241 (2480)	243 (2693)	243 (2844)	258 (3692)	246 (2959)	266 (4195)	258 (3850)
I_{sp} (+30 % Al) [s] ^g	237 (2702)	240 (2803)	240 (2891)	245 (3433)	238 (2994)	257 (4089)	245 (3624)
I_{sp} (+16% Al, 14% PBAN) [s] ^h	234 (2267)	233 (2326)	235 (2379)	247 (2507)	239 (2457)	255 (2818)	247 (2653)
I_{sp} (+18% Al, 12% HTPB) [s] ⁱ	239 (2305)	240 (2347)	239 (2429)	248 (2704)	236 (2509)	256 (2887)	248 (2788)

a–e) Detonation parameters calculated with EXPLO5 (V6.02)^[39] using the 'BKW EOS' equation of state with the default 'BKWG-S' set of constants; a) heat of detonation; b) detonation temperature; c) detonation pressure; d) detonation velocity; e) volume of gaseous detonation products (assuming only gaseous products). f–i) Isobaric combustion parameters calculated with EXPLO5 (V6.02)^[39] using isobaric combustion conditions, chamber pressure of 70.0 bar versus ambient pressure with equilibrium expansion conditions at the nozzle throat; isobaric combustion temperature in the combustion chamber in parentheses [K]; f) specific impulse of the neat compound; g) specific impulse of mixtures with 20–30% aluminium; h) specific impulse of mixtures with 16% aluminium, 12% polybutadiene acrylonitrile (PBAN) and 2% epoxyresin as curing agent; the analogue mixture with AP used in the Space Shuttle Programm of NASA^[40] reveals $I_{\text{sp}} = 262$ s and $T_c = 3380$ K; i) specific impulse of mixtures with 18% aluminium, 10% hydroxyterminated polybutadiene (HTPB) and 2% hexamethylene diisocyanate as curing agent; the analogue mixture with AP reveals $I_{\text{sp}} = 264$ s and $T_c = 3564$ K.

The calculated detonation parameters reveal good performances for compounds **9–12** (over 8000 m·s⁻¹) with the expected trends when compared among each other. The lowest values were obtained for the FDNE-NAP-carbamate (**10**), which are in the range of those calculated for picric acid ($\rho_{\text{RT}} = 1.77$ g·cm⁻³, $D_V = 7685$ m·s⁻¹, $p_{\text{CJ}} = 251$ kbar).^[39] Best detonation parameters were found for TNE-NAP-nitrocarbamate (**11**), which were calculated to be in the range of RDX ($\rho_{\text{RT}} = 1.80$ g·cm⁻³, $D_V = 8838$ m·s⁻¹, $p_{\text{CJ}} = 343$ kbar).^[39] The carbamate **9** and fluorine containing nitrocarbamate **12** show pretty much the same performance similar to that calculated for PETN ($\rho_{\text{RT}} = 1.78$ g·cm⁻³, 8404 m·s⁻¹, 309 kbar).^[39]

For the calculation of the isobaric combustion parameters the specific impulse I_{sp} for aluminised mixtures embedded either in polybutadiene acrylonitrile (PBAN) or in hydroxyterminated polybutadiene (HTPB) were calculated. For comparison the propellant formulation of 70% AP with 16% aluminium in 14% PBAN as used in the solid rocket boosters of the NASA Space Shuttle has been calculated to $I_{\text{sp}} = 262$ s,^[40] and the mixture with 18% aluminium in 12% HTPB as used in adjacent comparable missions has been calculated to $I_{\text{sp}} = 264$ s. The I_{sp} of compounds **2**, **3** and **8** are in the range of 233 s in PBAN and 240 s in HTPB and can be neglected as these compounds cannot be considered as oxidisers owing their rather negative oxygen balances Ω . For compounds **9–12** with multiple nitro groups and therefore improved oxygen balances Ω the values for I_{sp} are considerably higher with exception of FDNE-NAP-carbamate (**10**). The highest values for I_{sp} were obtained by formulations with the same ratios as the reference formulations with AP mentioned above. As expected owing to its high Ω the nitrocarbamate **11** achieves a I_{sp} of 255 s in PBAN, and respectively 256 s in HTPB. Hence this material almost reaches the I_{sp} of the reference formulations and yet shows decreased combustion temperatures T_c (Table 11).

2.7 Preliminary Qualitative Burning Test of TNE-NAP-Nitrocarbamate (11)

Although compound **9** does not meet all requirements such as an oxygen balance Ω of $>25\%$, the class of nitrocarbamates seems to be a good basis for further investigation on the design of oxygen-carriers for rocket propellant formulations. Therefore some preliminary qualitative combustion tests of some aluminised mixtures with TNE-NAP-nitrocarbamate (**11**), AP and ADN with and without binder were carried out. Pellets of 8 mm diameter and 2 mm height were pressed at approximately 8 bar with aluminium ($\leq 46 \mu\text{m}$) after mixing the ingredients in a mortar. As mentioned above also compound **11** shows a waxy behaviour and could be pressed with 15% aluminium without any binder to stable pellets. Furthermore compound **11** has a carbon backbone which acts as fuel during the combustion. In contrast the salts AP and ADN are very dry and porous salts and do not contain any elements that can be reduced during the combustion in addition to the aluminium. These pellets falled apart sometimes when picking them with tweezers. Therefore pellets were pressed with up to 15% polyethylene (PE, $8 \mu\text{m}$) for cohesion and better burning. In fact the aluminised pellets of AP and ADN, which were pressed without PE showed very discontinuous burning behaviour and combustion was not completed, while the burning of the aluminised pellets of compound **11** with PE resulted in carbon black residues due to the lowered oxygen balance of the formulation caused by the addiditon of PE. Best results with continuous and complete burning of the pellets were obtained by the formulations listed in Table 12. Figure 17 shows photographs of the well burning pellets at half time $t_{1/2}$ with the characteristic sparkling caused by burning aluminium particles.^[41]

Table 12: Qualitative burning behaviour of the formulations used in the pellets pressed at 8 bar for the preliminary burning tests and their ratios with and without PE.

[Ox/Al/PE] : [70/15/15]	AP	ADN	11
Burning behaviour	well	well	o.k.
Residue	no	no	yes
[Ox/Al] : [85/15]	AP	ADN	9
Burning behaviour	discontinuous	discontinuous	well
Residue	yes	yes	no
Particle sizes: AP, ADN, 9 $\leq 100 \mu\text{m}$; Al $\leq 46 \mu\text{m}$; PE $\approx 8 \mu\text{m}$.			

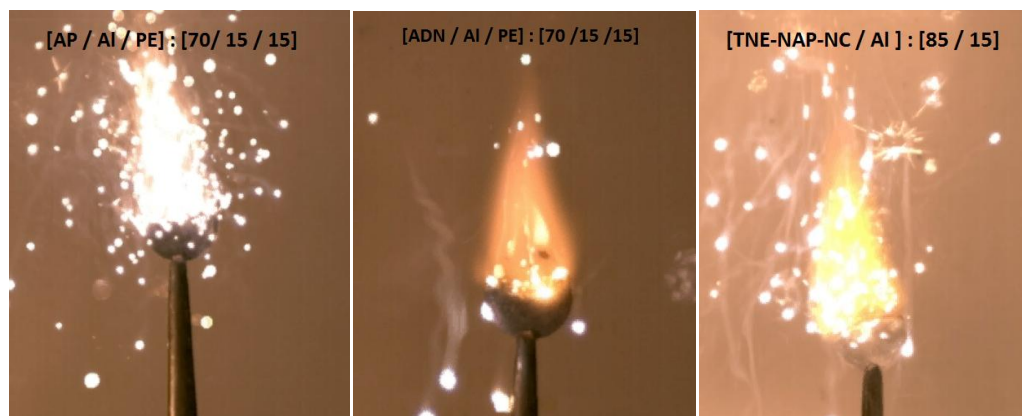


Figure 17: Photographs of the preliminary burning tests of the well burning pellets (Table 12) comprised of aluminised mixtures of AP (left) and ADN (middle) with polyethylene as binder, and TNE-NAP-NC (**11**) without binder (right).

2.8 Theoretical Evaluation of the Energetic Properties of DNDA-4 (13) as Plasticiser

Energetic plasticisers are used in propellants due to their ability to decrease glass transition temperatures of the polymeric binder of such systems, and hence induce a temperature independent combustion.^[42] They prevent the propellants degradation under extreme temperature conditions (−40 to + 50 °C), which mainly results in the loss of shoot precision, due to a lack of the combustion surface control. In the case of much larger rockets and boosters also the cracking of the polymeric matrix leads to uncontrolled combustion and therefore to pressure anomalies inside the combustion chamber.^[43] In gun propellants the mainly used binder is nitrocellulose (NC), and the best known or most employed plasticisers are nitroglycerine (NG) and diethyleneglycoldinitrate (DEGN).^[44] About 70% of the propellant world production is based on NC/NG propellants.^[45] Since 1993 a mixture of three methylene dinitramines (DNDA-57) has been investigated systematically by LANGLOTZ *et al.*^[46] as energetic plasticisers for NC and RDX based propellants, which induces the desired temperature independent combustion, but only by well defined quantities in the ternary mixture. The three molecules are 2,4-dinitro-2,4-diazapentane (DNDA-5), 2,4-dinitro-2,4-diazahexane (DNDA-6) and 3,5-dinitro-3,5-diazaheptane (DNDA-7), which can be synthesised easily by the self-condensation reaction of *N*-ethylnitramine, formaldehyde and *N*-methylnitramine in an acidic medium.^[20, 28, 47] In contrast to these secondary methyl- and ethyldinitramines, the analogue of DNDA-5 with primary nitramine groups is methylenedinitramine (MEDINA), which has been identified as an intermediate during the biodegradation of commonly used military nitramines such as RDX.^[48] It is an thermally unstable solid, whereat its decomposition is catalysed by its own products.^[49] MEDINA can be synthesised by nitration of methylenediformamide at elevated temperature.^[50]

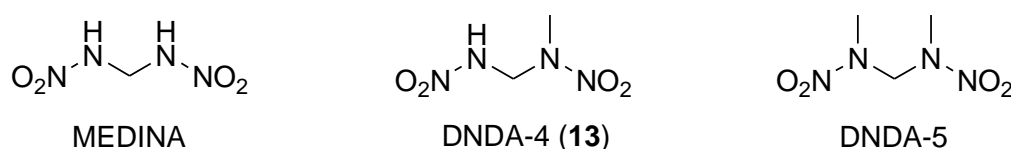


Figure 18: Molecular structures of methylenedinitramine (MEDINA), 1,3-dinitro-1,3-diazabutane (DNDA-4, **13**) and 2,4-dinitro-2,4-diazapentane (DNDA-5).

In the context of symmetrical MEDINA and DNDA-5, the energetic properties of unsymmetrical DNDA-4 (**13**) with one primary and one secondary nitramine functionality might be of interest due to different properties (Figure 18). As mentioned above compound **13** was formed unintentionally by hydrolysis of the nitrocarbamate **12** and a conventional synthesis has not been established so far (Chapter 1). Hence, only little analytical information was collected, but the calculated performance will be presented in the following.

The melting point of DNDA-4 (**13**) was estimated to be in between the melting, respectively decomposition points of MEDINA and DNDA-5 to re-calculate the heat of formation $\Delta_f H^\circ$ for the solid state (see General Procedures). The densities of the three compounds decrease in the order MEDINA > DNDA-4 > DNDA-5, which might be explained by the decreasing possibility to form hydrogen bonds with the nitramine protons. With these values the

detonation and propulsive properties were calculated using the EXPLO5 (V 6.02) computer code (Table 13).^[38] The detonation parameters show a clear trend that follows the decreasing values for the density but also the increasing carbon content. The detonation velocity as well as the detonation pressure and temperature decrease in the order MEDINA > DNDA-4 > DNDA-5. This trend is continued when considering an isobaric combustion of the neat compounds or in mixtures with 70–80% nitrocellulose (N content 13.25%), in mixtures of nitrocellulose and nitroglycerine as well as when considering these compounds as oxidisers in composite propellants with aluminium and HTPB. The specific impulses decrease in the same order. However, the development of a convenient synthesis route for compound **13** to obtain enough material should be focused on, so that the experimental properties can be determined. Especially the glass transition point of the compound for application as plasticiser should be of very first interest.

Table 13: Energetic properties known so far for MEDINA,^[51] DNDA-4 (**13**) and DNDA-5,^[20] and detonation and propulsive performance calculated with EXPLO5 (V6.02).^[38]

	MEDINA	DNDA-4 (13)	DNDA-5
Formula	CH ₄ N ₄ O ₄	C ₂ H ₆ N ₄ O ₄	C ₃ H ₈ N ₄ O ₄
FW [g·mol⁻¹]	136.07	150.09	164.12
N [%]^a	41.18	37.33	34.14
N+O [%]^b	88.21	79.97	73.13
Ω_{CO} [%]^c	11.8	-10.7	-29.2
Ω_{CO2} [%]^c	0.0	-32.0	-58.5
T_{melt} [°C]^d	105 (with dec.)	75 (est.)	54 (with dec.)
T_{GT} [°C]^e	unknown	unknown	-44
ρ_{RT} [g·cm⁻³]^f	1.74 ^[51]	1.56	1.49
Δ_fH° [kJ·mol⁻¹]^g	-28	-34	-33
ΔU° [kJ·kg⁻¹]^h	-98	-113	-79
-Δ_{Ex}U° [kJ·kg⁻¹]ⁱ	6135	5630	5540
T_{det} [K]^j	4038	3619	3386
p_{CJ} [kbar]^k	328	244	208
D_V [m·s⁻¹]^l	9008	8046	7696
V₀ [L·kg⁻¹]^m	896	900	910
I_{sp} (neat) [s]ⁿ	271 (3270)	258 (2833)	235 (2089)
I_{sp} (+80% NC) [s]^o	244 (2960)	239 (2761)	234 (2590)
I_{sp} (+70% NC) [s]^o	249 (3051)	241 (2770)	234 (2517)
I_{sp} (+40% NC, +40% NG) [s]^p	260 (3277)	258 (3219)	255 (3124)
I_{sp} (+18% Al, +12% HTPB) [s]^q	268 (2981)	257 (2419)	254 (2413)

a) Nitrogen content; b) combined nitrogen and oxygen content; c) oxygen balance assuming the formation of CO and CO₂; d) melting point according the literature or DSC measurement; e) glass transition point according to the literature; f) density from the crystal structure; g) calculated heat of formation at the CBS-4M level of theory; h) calculated internal energy of formation at the CBS-4M level of theory.

i–m) Detonation parameters calculated with EXPLO5 (V6.02) using the 'BKW EOS' equation of state with the default 'BKWG-S' set of constants; i) heat of detonation; j) detonation temperature; k) detonation pressure; l) detonation velocity; m) volume of gaseous detonation products (assuming only gaseous products).

n–p) Isobaric combustion parameters calculated with EXPLO5 (V6.02) using isochoric combustion conditions, chamber pressure of 70.0 bar versus ambient pressure with equilibrium expansion conditions at the nozzle throat; isobaric combustion temperature in the combustion chamber in parentheses [K]; n) specific impulse of the neat compound; o) specific impulse of mixtures with 70–80% nitrocellulose with 13.25% nitrogen content as a common monobased propellant; p) specific impulse of a mixtures with 40% nitrocellulose with 13.25% nitrogen content and 40% nitroglycerine as a common double-base propellant; q) specific impulse of a mixture with 70% of the compound, 18% aluminium, 10% HTPB and 2% hexamethylene diisocyanate, thus using the compound as oxidiser.

2.9 Summary, Conclusions and Outlook

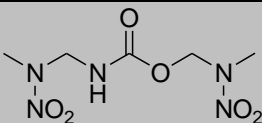
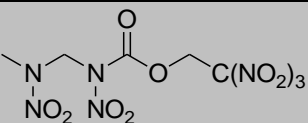
The goal of this study was the preparation and characterisation of hitherto unknown carbamate derivatives by addition reactions of alcohols to the parent 2-nitro-azapropyl isocyanate described in Chapter 1. The reaction to the latter with water also furnished one symmetrically substituted urea derivative. The addition of oxygen rich alcohols such as trinitroethanol and fluorodinitroethanol yielded asymmetrically substituted carbamates, which could be further nitrated at the nitrogen atom of the carbamate unit forming the corresponding nitrocarbamates. All compounds were fully characterised by various analytical methods including multinuclear (^1H , ^{13}C , ^{14}N and ^{19}F) NMR spectroscopy and most of them were investigated by single crystal X-ray diffraction. The sensitivities of all compounds towards impact, friction and electrostatic discharge were determined.

The compounds detonation parameters were calculated and revealed performances that are comparable with those calculated for commonly used explosives ranging from picric acid to RDX. Symmetrically substituted *O,N*-bis-(2-nitro-2-azapropyl)carbamate (**3**) shows a melting point below 100 °C with a large melting range. This fact in combination with its low sensitivities and wax-like properties in the solid state might make this material interesting for further investigation as an alternative to toxic 2,4,6-trinitrotoluene (TNT).

In order to evaluate the suitability of the oxygen rich materials as oxidisers for solid composite propellants the specific impulses I_{sp} and combustion temperatures T_{C} of the neat compounds, compositions with 20–30 % aluminium, and aluminised formulations embedded in two different commonly used polybutadiene based binders were calculated and evaluated. In this context the aluminised mixtures of 2,2,2-trinitroethyl-(2-nitro-2-azapropyl)-nitrocarbamate (**11**) show the best performance with specific impulses I_{sp} almost achieving the performance of commonly used AP formulations, although the material does not meet all the requirements determined for novel oxidisers. Therefore it is recommended to further investigate the thermally stable carbamate derivatives in combination with the trinitroethyl or other oxygen rich moieties.

The development of a convenient synthesis for DNDA-4 (**13**) out of 2-nitro-2-azapropyl amine (Chapter 1) is recommended in order to fully characterise it and determine its glass transition point and therefore its suitability as energetic plasticiser.

Table 14: Molecular structures of the promising compounds **3** and **11** with their characteristic properties, calculated performances and possible applications.

	3	11
Molecular structure		
I_{S} [J]	35	6
F_{S} [N]	240	120
T_{melt} [°C]	85	92
T_{dec} [°C]	180	147
D_{V} [m·s $^{-1}$]	7259	8706
p_{CJ} [kbar]	182	328
I_{sp} (Al+HTPB) [s]	240	256
Possible applications	melt-castable explosive	oxidiser / propellant

2.10 Experimental Section

***N,N'*-Bis-(2-nitro-2-azapropyl)-urea (2):** 2-Nitro-2-azapropyl chloride (500 mg, 4.0 mmol) was added to a stirred suspension of silver cyanate (700 mg, 4.7 mmol) in dry diethyl ether (50 mL) in the dark and under an argon atmosphere. The mixture was stirred overnight at room temperature.^[19] The precipitate was removed by filtration under an argon atmosphere and a mixture of H₂O (36 mg, 0.36 mL, 2.0 mmol) in absolute Et₂O (20 mL) was added to the resulting solution of 2-nitro-2-azapropyl isocyanate **1**. It was stirred for an additional 12 h at ambient temperature. Then the solvent was evaporated under reduced pressure to yield a colourless solid. Recrystallisation from dichloromethane (20 mL) furnished the urea derivative **2** (440 mg, 1.9 mmol) as colourless crystals (two-step yield 47%).

DSC (T_{onset}): $T_{\text{melt}} = 150\text{ }^{\circ}\text{C}$, $T_{\text{dec}} = 162\text{ }^{\circ}\text{C}$; **¹H NMR** (CDCl₃): $\delta = 6.05$ (t, $^3J_{\text{HH}} = 6.5\text{ Hz}$, 1 H, NH), 5.05 (d, $^3J_{\text{H-H}} = 6.5\text{ Hz}$, 4 H, CH₂), 3.47 (s, 6 H, CH₃) ppm; **¹³C{¹H} NMR** (CDCl₃): $\delta = 156.8$ (CO), 57.2 (CH₂), 39.1 (CH₃) ppm; **¹⁴N{¹H} NMR** (CDCl₃): $\delta = -28.0$ (NNO₂) ppm; **EA**: C₅H₁₂N₆O₅ (236.19 g·mol⁻¹): calcd. C 25.43, H 5.12, N 35.58; found C 25.85, H 4.98, N 35.14 %; **IR**: $\tilde{\nu}$ (rel. int.) = 3331 (m), 3039 (vw), 2994 (vw), 2949 (vw), 1651 (s), 1568 (s), 1502 (vs), 1460 (s), 1445 (s), 1415 (s), 1390 (m), 1345 (s), 1286 (vs), 1215 (vs), 1122 (s), 1052 (s), 1002 (vs), 982 (vs), 895 (m), 835 (s), 764 (vs), 701 (s) cm⁻¹; **Raman** (200 mW): $\tilde{\nu}$ (rel. int.) = 3336 (15), 3039 (50), 2996 (100), 2949 (75), 1654 (10), 1418 (21), 1282 (23), 836 (69), 609 (11) cm⁻¹; **MS** (DEI⁺): $m/z = 237.1$ [M+H⁺], 161.1, [M-NO₂NHCH₃⁺]; **drophammer**: >40 J, **friction tester**: >360 N, **ESD**: 1.5 J; **grain size**: <100 μm .

***O,N*-Bis-(2-nitro-2-azapropyl)-carbamate (3):** 2-Nitro-2-azapropyl chloride (500 mg, 4.0 mmol) was added to a stirred suspension of silver cyanate (700 mg, 4.7 mmol) in dry diethyl ether (50 mL) in the dark and under an argon atmosphere. The mixture was stirred overnight at room temperature.^[19] The precipitate was removed by filtration under argon atmosphere and anhydrous 2-nitro-2-azapropanol (**4**, 300 mg, 4.0 mmol) was added to the resulting solution of 2-nitro-2-azapropyl isocyanate (**1**). The mixture was stirred overnight at room temperature. Then the solvent was evaporated under reduced pressure and washed with water (3 \times 50 mL) to yield a colourless solid. It was re-crystallised from methanol (30 mL) to furnish carbamate **6** (330 mg, 1.6 mmol) as colourless crystals (two-step yield 41%).

DSC (T_{onset}): $T_{\text{melt}} = 85\text{ }^{\circ}\text{C}$, $T_{\text{dec}} = 180\text{ }^{\circ}\text{C}$. **¹H NMR** (CDCl₃): $\delta = 6.04$ (br, 1 H, NH), 5.72 (s, 2 H, OCH₂), 5.04 (d, $^3J_{\text{H-H}} = 6.9\text{ Hz}$, 2 H, CH₂NH), 3.47 (s, 3 H, OCH₂N(NO₂)CH₃), 3.45 (s, 3 H, NHCH₂N(NO₂)CH₃) ppm; **¹³C{¹H} NMR** (CDCl₃): $\delta = 155.7$ (CO), 73.9 (OCH₂), 57.9 (CH₂NH), 39.3 (OCH₂N(NO₂)CH₃), 38.6 (NHCH₂N(NO₂)CH₃) ppm; **¹⁴N{¹H} NMR** (CDCl₃): $\delta = -29$ (NHCH₂NNO₂), -31 (OCH₂NNO₂) ppm; **EA**: C₅H₁₁N₅O₆ (237.17 g·mol⁻¹): calcd. C 25.32, H 4.67, N 29.53; found C 25.35, H 4.78, N 29.44 %; **IR**: $\tilde{\nu}$ (rel. int.) = 3404 (w), 2954 (vw), 1728 (m), 1503 (s), 1469 (s), 1295 (vs), 1212 (vs), 1120 (m), 1044 (m), 1004 (s), 947 (vs), 884 (m), 836 (m), 782 (m), 765 (s) cm⁻¹; **Raman** (200 mW): $\tilde{\nu}$ (rel. int.) = 3019 (100), 2986 (97), 1708 (9), 1457 (17), 1295 (21), 1049 (9), 1001 (8), 839 (48), 673 (7), 612 (10) cm⁻¹; **MS** (DCI⁺): $m/z = 238.1$ [M+H⁺], 161.1, [M-NO₂NHCH₃⁺], 89.1 [M-(NO₂NHCH₃)₂⁺]; **drophammer**: 35 J; **friction tester**: 240 N; **ESD**: 1.25 J; **grain size**: <100 μm .

1,3-Bis-(2-nitro-2-azapropyl-carbamate)-2,2-dinitropropane (8): 500 mg 2-Nitro-2-azapropyl chloride (4.0 mmol) was added to a stirred suspension of silver cyanate (700 mg, 4.7 mmol) in dry diethyl ether (50 mL) in the dark and under an argon atmosphere. The mixture was stirred overnight at room temperature.^[19] The precipitate was removed by filtration under argon atmosphere and 270 mg anhydrous 2,2-dinitropropan-1,3-diol (**5**, 1.6 mmol) was added to the resulting solution of 2-nitro-2-azapropyl isocyanate **1**. The mixture was stirred overnight at room temperature. Then the solvent was evaporated under reduced pressure and washed with water (3 × 50 mL) to yield a pale yellow solid. Purification by column chromatography (Silica, EtOAc, $R_f = 0.8$) furnished 310 mg of compound **8** (1.3 mmol, 45%) as colourless solid.

DSC (T_{onset}): $T_{\text{melt}} = 117\text{ }^{\circ}\text{C}$, $T_{\text{dec}} = 174\text{ }^{\circ}\text{C}$; **^1H NMR** (d_6 -acetone) $\delta = 7.92$ (br, 2 H, NH), 5.11 (d, 4 H, CH_2NH , $^3J_{\text{H-H}} = 6.4$ Hz), 5.09 (s, 4 H, OCH_2), 3.39 (s, 6 H, CH_3) ppm; **^{13}C NMR** (d_6 -acetone) $\delta = 155.6$ (CO), 115.5 ($\text{C}(\text{NO}_2)_2$), 62.2 (CH_2NH), 58.7 (OCH_2), 39.2 (CH_3) ppm; **^{14}N NMR** (d_6 -acetone) $\delta = -17$ ($\text{C}(\text{NO}_2)_2$), -28 (NNO_2) ppm; **IR**: $\tilde{\nu}$ (rel. int.) = 3233 (m, N-H), 2971 (w), 2880 (vw), 1731 (m, C=O), 1587 (m, N- NO_2), 1568 (m, C- NO_2), 1530 (m), 1504 (m), 1473 (w), 1460 (w), 1418 (w), 1347 (m, C- NO_2), 1317 (s), 1259 (ms, N- NO_2), 1220 (ms), 1138 (vw), 1100 (w), 1082 (w), 1067 (m), 1023 (vs), 962 (w), 922 (m), 888 (vw), 874 (w), 858 (w), 842 (m), 799 (m), 762 (s), 692 (m), 670 (s) cm^{-1} ; **Raman** (200 mW): $\tilde{\nu}$ (rel. int.) = 3025 (50), 2974 (65), 2907 (43), 1733 (18), 1590 (18), 1451 (22), 1423 (38), 1352 (10), 1308 (30), 1260 (19), 1226 (16), 1094 (15), 1049 (19), 1003 (29), 922 (10), 851 (65), 841 (100), 707 (10), 672 (11), 618 (14), 551 (8), 487 (9), 421 (22), 235 (19) cm^{-1} ; **MS** (DCI^+): $m/z = 429.0$ [$\text{M}+\text{H}^+$]; **BAM drophammer**: 35 J; **friction tester**: 240 N; **ESD**: 1.0 J.

2,2,2-Trinitroethyl-(2-nitro-2-azapropyl)-carbamate (9): To a stirred suspension of silver cyanate (700 mg, 4.7 mmol) in dry diethyl ether (50 mL) in a 100 mL Schlenk flask was added **1** (500 mg, 4.0 mmol) with exclusion of light and under an argon atmosphere. The mixture was stirred overnight at ambient temperature.^[19] The precipitate was removed by filtration under an argon atmosphere, and to the resulting solution of isocyanate **1** was added anhydrous 2,2,2-trinitroethanol (**6**, 600 mg, 3.3 mmol). The mixture was stirred overnight at ambient temperature, and the solvent was evaporated under reduced pressure to produce a light yellow liquid, which was then washed with cold water until the yellow colour of 2,2,2-trinitroethanol (**6**) disappeared. Recrystallisation from dichloromethane yielded compound **5** (500 mg, 1.6 mmol, two-step yield 40%) as colourless crystals.

DSC (T_{onset}): $T_{\text{melt}} = 135\text{ }^{\circ}\text{C}$, $T_{\text{dec}} = 183\text{ }^{\circ}\text{C}$; **^1H NMR** (d_6 -acetone): $\delta = 8.13$ (br, 1 H, NH), 5.79 (s, 2 H, $\text{CH}_2\text{C}(\text{NO}_2)_3$), 5.15 (d, $^3J_{\text{H-H}} = 6.3$ Hz, 2 H, CH_2NH), 3.41 (s, 3 H, CH_3) ppm; **$^{13}\text{C}\{^1\text{H}\}$ NMR** (d_6 -acetone): $\delta = 154.3$ (CO), 124.6 ($\text{C}(\text{NO}_2)_3$), 61.5 (CH_2NH), 57.9 ($\text{CH}_2\text{C}(\text{NO}_2)_3$), 38.1 (CH_3) ppm; **$^{14}\text{N}\{^1\text{H}\}$ NMR** (d_6 -acetone): $\delta = -29$ (NNO_2), -33 ($\text{C}(\text{NO}_2)_3$) ppm; **EA**: $\text{C}_5\text{H}_8\text{N}_6\text{O}_{10}$ (312.15 $\text{g}\cdot\text{mol}^{-1}$): calcd. C 19.24, H 2.58, N 26.92; found C 20.02, H 2.71, N 26.87 %; **IR**: $\tilde{\nu}$ (rel. int.) = 3318 (m, N-H), 3034 (vw), 2981 (vw), 2960 (vw), 1754 (w), 1729 (s), 1599 (vs), 1580 (s), 1542 (m), 1516 (s), 1467 (m), 1451 (m), 1419 (s), 1341 (m), 1299 (vs), 1259 (s), 1222 (vs), 1136 (m), 1099 (m), 1041 (s), 1026 (s), 1005 (s), 903 (w), 867 (m), 854 (m), 842 (m), 802 (vs), 787 (s), 768 (vs), 723 (w), 689 (s), 668 (s), 662 (s), 659 (s) cm^{-1} ; **Raman** (300 mW): $\tilde{\nu}$ (rel. int.) = 3321 (17), 3041 (62), 3000 (100), 2985 (97), 2953 (60), 1732 (11), 1617 (17), 1421 (25), 1384 (9), 1350 (22), 1306 (31), 1225 (9), 1045 (8), 1027 (8), 1004 (14), 855 (56), 844 (49), 608 (8), 554 (7), 429 (10) cm^{-1} ; **MS**

(DCI⁺): $m/z = 313.1$ [M+H⁺]; (DEI⁺): $m/z = 266.2$ [M-NO₂⁺]; **drophammer**: 30 J; **friction tester**: 240 N; **ESD**: 0.08 J; **grain size**: <100 μm .

2-Fluoro-2,2-dinitroethyl-(2-nitro-2-azapropyl)-carbamate (10): To a stirred suspension of silver cyanate (700 mg, 4.7 mmol) in dry diethyl ether (50 mL) was added **1** (500 mg, 4.0 mmol) with the exclusion of light and under an argon atmosphere. The mixture was stirred overnight at ambient temperature.^[19] The precipitate was removed by filtration under an argon atmosphere, and to the resulting solution of **2** was added 2-fluoro-2,2-dinitroethanol (430 mg, 2.8 mmol). The mixture was stirred overnight at ambient temperature, and the solvent was evaporated under reduced pressure to produce a colourless liquid. Upon the addition of water (5 mL), the crude product **6** precipitated. The solid was collected by filtration and washed with cold water. Re-crystallisation from acetone or dichloromethane yielded carbamate **6** (570 mg, 2.0 mmol, two-step yield 50%) as colourless crystals.

DSC (T_{onset}): $T_{\text{melt}} = 70$ °C, $T_{\text{dec}} = 219$ °C; **¹H NMR** (d_6 -acetone): $\delta = 8.00$ (br, 1 H, NH), 5.47 (d, $^3J_{\text{H-F}} = 16.2$ Hz, 2 H, CH₂C(NO₂)₂F), 5.12 (d, $^3J_{\text{H-H}} = 6.3$ Hz, 2 H, CH₂NH), 3.40 (s, 3 H, CH₃) ppm; **¹³C{¹H} NMR** (d_6 -acetone): $\delta = 155.5$ (CO), 120.9 (d, $J_{\text{C-F}} = 292.3$ Hz, C(NO₂)₂F), 62.1 (d, $^2J_{\text{C-F}} = 20.1$ Hz, CH₂C(NO₂)₂F), 58.8 (CH₂NH), 39.0 (CH₃) ppm; **¹⁴N{¹H} NMR** (d_6 -acetone): $\delta = -23$ (br, C(NO₂)₂F), -28 (NNO₂) ppm; **¹⁹F NMR** (d_6 -acetone): $\delta = -112.0$ (br, CF) ppm; **EA**: C₅H₈FN₅O₈ (285.14 g·mol⁻¹): calcd. C 21.06, H 2.83, N 24.56; found C 21.14, H 3.09, N 24.48 %; **IR**: $\tilde{\nu}$ (rel. int.) = 3361 (m), 2981 (vw), 2361 (m), 2341 (m), 1735 (s), 1599 (vs), 1523 (vs), 1465 (m), 1446 (m), 1419 (w), 1383 (vw), 1341 (w), 1311 (vs), 1260 (m), 1212 (s), 1150 (m), 1114 (m), 1041 (m), 1017 (s), 910 (w), 896 (m), 850 (m), 843 (m), 792 (s), 773 (s), 766 (vs), 696 (w), 669 (m) cm⁻¹; **Raman** (200 mW): $\tilde{\nu}$ (rel. int.) = 3367 (15), 3356 (15), 3044 (52), 3027 (50), 2997 (100), 2960 (96), 2881 (78), 1736 (20), 1604 (15), 1591 (20), 1448 (30), 1418 (20), 1379 (29), 1359 (17), 1314 (20), 1245 (15), 1221 (15), 1056 (25), 1005 (18), 912 (15), 899 (15), 852 (70), 774 (15), 418 (14) cm⁻¹; **MS** (DEI⁺): $m/z = 286.1$ [M+H⁺], 239.1 [M-NO₂⁺], 210.1 [M-CH₃NNO₂⁺]; **drophammer**: 40 J; **friction tester**: 324 N; **ESD**: 0.5 J; **grain size**: <100 μm .

2,2,2-Trinitroethyl-(2-nitro-2-azapropyl)-nitrocarbamate (11): A 50 mL two-necked reaction flask equipped with a thermometer was charged with trifluoroacetic anhydride (10 mL) and cooled to 0 °C. Fuming nitric acid (2 mL, 47.9 mmol) was added slowly with care taken to ensure that the temperature did not exceed 5 °C. Compound **9** (400 mg, 1.3 mmol) was added to the reaction mixture over 30 min as the temperature was maintained below 10 °C. The mixture was stirred for an additional 2 h; the reaction mixture was warmed to ambient temperature over the last 30 min. The liquids were removed into a cooling trap (N₂) under reduced pressure. The colourless residue was washed with water (50 mL) and re-crystallised from dichloromethane (5 mL) yielding nitrocarbamate **11** (300 mg, 0.8 mmol, 64% yield) as colourless crystals.

DSC (T_{onset}): $T_{\text{melt}} = 92$ °C, $T_{\text{dec}} = 147$ °C; **¹H NMR** (d_6 -acetone): $\delta = 6.17$ (s, 2 H, OCH₂), 6.05 (s, 2 H, NCH₂N), 3.52 (s, 3 H, CH₃) ppm; **¹³C{¹H} NMR** (d_6 -acetone): $\delta = 148.0$ (CO), 122.9 (C(NO₂)₃), 64.4 (CH₂N), 63.5 (OCH₂), 39.2 (CH₃) ppm; **¹⁴N{¹H} NMR** (d_6 -acetone): $\delta = -30$ (2 NNO₂), -34 (C(NO₂)₃) ppm; **EA**: C₅H₇N₇O₁₂ (357.15 g·mol⁻¹): calcd. C 16.81, H 1.98, N 27.45; found C 16.89, H 1.90, N 27.21 %; **IR**: $\tilde{\nu}$ (rel. int.) = 3020 (w), 2360 (w), 2341 (w), 1731 (m), 1599 (s), 1508 (s), 1419 (m), 1341 (w), 1300 (vs), 1260 (s), 1223 (s), 1026

(vs), 867 (w), 801 (vs), 769 (vs), 669 (s) cm^{-1} ; **Raman** (300 mW): $\tilde{\nu}$ (rel. int.) = 3060 (35), 3019 (81), 2973 (100), 2901 (21), 1789 (09), 1610 (18), 1440 (8), 1382 (9), 1350 (8), 1307 (8), 1241 (21), 1095 (8), 1025 (7), 890 (11), 857 (69), 422 (21) cm^{-1} ; **MS** (DCI⁺): m/z = 358 [M+H⁺], 237 [M-(NO₂)NCH₃⁺]; **drophammer**: 6 J; **friction tester**: 120 N; **ESD**: 0.2 J; **grain size**: <100 μm .

2-Fluoro-2,2-dinitroethyl-(2-nitro-2-azapropyl)-nitrocarbamate (12): A 100 mL two-necked reaction flask equipped with a thermometer was charged with acetic anhydride (8 mL) and cooled to 0 °C. Fuming nitric acid (2 mL, 47.9 mmol) was added slowly with care taken to ensure that the temperature did not exceed 5 °C. Compound **10** (400 mg, 1.4 mmol) was added to the reaction mixture over 20 min as the temperature was maintained below 10 °C. The mixture was stirred for 90 min; the reaction mixture was warmed to ambient temperature over the last 30 min. The reaction mixture was then poured onto ice water (20 mL) and extracted with dichloromethane. The organic layer was dried over sodium sulfate, and the solvent was removed under reduced pressure. The remaining colourless solid was re-crystallised from dichloromethane yielding compound **8** (360 mg, 1.1 mmol, 80% yield) as a colourless solid.

DSC (T_{onset}): T_{melt} = 62 °C, T_{dec} = 158 °C; **¹H NMR**: δ = 6.04 (s, 2 H, NCH₂N), 5.80 (d, $^3J_{\text{H-F}}$ = 15.6 Hz, 2 H, CH₂C(NO₂)₂F), 3.52 (s, 3 H, CH₃) ppm; **¹³C{¹H} NMR**: δ = 148.3 (CO), 119.2 (d, $J_{\text{C-F}}$ = 292.9 Hz, C(NO₂)₂F), 64.2 (NCH₂N), 63.5 (d, $^2J_{\text{C-F}}$ = 19.2 Hz, CH₂C(NO₂)₂F), 39.1 (CH₃) ppm; **¹⁴N{¹H} NMR**: δ = -25 (br, C(NO₂)₂F), -30 (2 NNO₂) ppm; **¹⁹F NMR**: δ = -111.4 (br, CF) ppm; **EA**: C₅H₇FN₆O₁₀ (330.14 g·mol⁻¹): calcd. C 18.19, H 2.14, N 25.46; found C 18.43, H 2.08, N 25.09 %; **EA**: C₅H₇FN₆O₁₀ (330.14 g·mol⁻¹): calcd. C 18.19, H 2.14, N 25.46; found C 18.43, H 2.08, N 25.09 %; **IR**: $\tilde{\nu}$ (rel. int.) = 3051 (vw), 2963 (vw), 1795 (m), 1758 (m), 1600 (vs), 1597 (s), 1525 (s), 1470 (w), 1427 (m), 1401 (m), 1388 (w), 1361 (w), 1331 (s), 1309 (s), 1293 (s), 1263 (s), 1241 (vs), 1217 (m), 1178 (s), 1149 (s), 1121 (s), 1094 (m), 1074 (w), 1026 (m), 995 (w), 953 (m), 920 (s), 910 (m), 869 (w), 857 (m), 846 (s), 797 (vs), 764 (s), 738 (m), 728 (vs), 672 (m), 657 (s) cm^{-1} ; **Raman** (300 mW): $\tilde{\nu}$ (rel. int.) = 3052 (62), 3006 (78), 2900 (100), 2896 (17), 1833 (11), 1762 (12), 1592 (16), 1535 (5), 1452 (8), 1390 (12), 1363 (16), 1336 (16), 1313 (10), 1283 (6), 1259 (10), 1032 (11), 859 (51), 660 (4), 610 (12), 420 (10) cm^{-1} ; **MS** (DCI⁺): m/z = 331.2 [M+H⁺]; **drophammer**: 8 J; **friction tester**: 144 N; **ESD**: 0.3 J; **grain size**: <100 μm .

1,3-Dinitro-1,3-diazabutane (13): The attempted re-crystallisation of compound **12** in acidified (1M HCl) acetone yielded crystals of compound **13** suitable for X-ray diffraction due to hydrolysis.

2.11 References

- [1] B. Aas, M. A. Kettner, T. M. Klapötke, M. Sućeska, C. Zoller, *Eur. J. Inorg. Chem.* **2013**, 2013(35), 6028–6036.
- [2] M. A. Kettner, T. M. Klapötke, T. G. Müller, M. Sućeska, *Eur. J. Inorg. Chem.* **2014**, 4756–4771.
- [3] a) T. M. Klapötke, *Chemie der hochenergetischen Materialien*, de Gruyter, Berlin, New York, **2009**; b) T. M. Klapötke, *Chemistry of High-Energy Materials*, 2nd Eng. ed., de Gruyter, Berlin, New York, **2011**.
- [4] K. P. C. Vollhardt, *Organische Chemie*, 1. Aufl., Weinheim, Basel, Cambridge, New York, VCH, **1988**.
- [5] a) W. F. Gum, W. Riese, H. Ulrich, *Reaction Polymers-Chemistry, Technology, Applications, Markets*, Carl Hanser Publishers, **1992**; b) G. Oertel, L. Abel, *Polyurethane*, Hanser Verlag, **1993**; c) U. Meier-Westhues, *Polyurethane*, Vincentz Network GmbH, **2007**.
- [6] a) M. B. Frankel, *Tetrahedron* **1963**, 19, 213–217; b) M. B. Frankel, Aerojet-General Cooperation, *US 3109020*, **1963**; c) M. E. Hill, *US 3306939*, 1967; d) M. J. Kamlet, K. G. Shipp, M. E. Hill, *US 3388147*, **1968**.
- [7] a) M. E. Sitzmann, W. H. Gilligan, *US 4705899*, **1987**; b) M. E. Hill, *US 3375266*, **1968**.
- [8] a) A. B. Sheremetev, B. Aleksei, I. L. Yudin, *Mendeleev Commun.* **2005**, 15(5), 204–205; b) M. A. Epishina, I. V. Ovchinnikov, A. S. Kulikov, N. N. Makhova, V. A. Tartakovsky, *Mendeleev Commun.* **2011**, 21(1), 21–23.
- [9] a) M. Göbel, T. M. Klapötke, *Acta Crystallogr. C* **2008**, C64(2), 58–60; b) T. M. Klapötke, B. Krumm, R. Moll, S. F. Rest, *Z. Anorg. Allg. Chem.* **2011**, 637, (14–15), 2103–2110; c) T. M. Klapötke, B. Krumm, R. Moll, S. F. Rest, M. Sućeska, *Z. Naturforsch.* **2014**, 69b, 8–16.
- [10] A. Baumann, A. Erbacher, C. Evangelisti, T. M. Klapötke, B. Krumm, S. F. Rest, M. Reynders, V. Sproll, *Chem. Eur. J.* **2013**, 19, 15627–15638.
- [11] T. M. Klapötke, B. Krumm, R. Moll, S. F. Rest, W. Schnick, M. Seibald, *J. Fluor. Chem.* **2013**, 156, 253–261.
- [12] R. Schenck, G. A. Wetterholm, *SE 148217 C1*, **1954**.
- [13] <http://www.appbv.nl/> (accessed: 19.03.2015)
- [14] T. L. Davis, K. C. Blanchard, *J. Am. Chem. Soc.* **1929**, 51(6), 1790–1800.
- [15] M. E. Sitzmann, W. H. Gilligan, *J. Org. Chem.* **1985**, 50(26), 5879–5881.
- [16] S. F. Rest, *private communication*.
- [17] O. A. Luk'yanov, G. V. Pokhvisneva, *Russ. Chem. Bull.* **1992**, 41, 1286.
- [18] Q. J. Axthammer, T. M. Klapötke, B. Krumm, R. Moll, S. F. Rest, *Z. Anorg. Allg. Chem.* **2014**, 640(1), 76–83.
- [19] B. Unterhalt, F. Leiblein, *Arch. Pharm.* **1979**, 312(2), 159–164.
- [20] D. Spitzer, S. Braun, M. R. Schäfer, F. Cizek, *Propellants Explos. Pyrotech.* **2003**, 28(2), 58–64.
- [21] H.-O. Kalinowski, S. Berger, S. Braun, *¹³C NMR-Spektroskopie*, Georg Thieme Verlag, Stuttgart, New York, **1984**.
- [22] M. Witanowski, L. Stefaniak, G. A. Webb, *Annual Reports on NMR Spectroscopy*, Vol. 25, Academic Press Inc., London, **1993**.
- [23] T. M. Klapötke, B. Krumm, R. Moll, *Chem. Eur. J.* **2013**, 19, 12113–12123.
- [24] a) M. Hesse, H. Meier, B. Zeeh, *Spektroskopische Methoden in der organischen Chemie*, Georg Thieme Verlag KG, Stuttgart, **2005**; b) G. Socrates, *Infrared and Raman Characteristic Group Frequencies: Tables and Charts*, 3rd ed., Wiley, New York, **2004**.

- [25] A. F. Holleman, *Lehrbuch der Anorganischen Chemie*, 101st ed., Walter de Gruyter GmbH & Co., Berlin, New York, **1995**.
- [26] A. Bondi, *J. Phys. Chem.* **1964**, 68, 441–451.
- [27] Y. Oyumi, T. B. Brill, A. L. Rheingold, *J. Phys. Chem.* **1985**, 89, 4824–4828.
- [28] D. Spitzer, B. Wanders, M. R. Schafer, R. Welter, *J. Mol. Struct.* **2003**, 644, 37–48.
- [29] *NATO Standardization Agreement (STANAG) on Explosives*, Impact Tests, no. 4489, 1st ed., Sept. 17, **1999**.
- [30] *WIWEB-Standardarbeitsanweisung 4-5.1.02, Ermittlung der Explosionsgefährlichkeit, hier der Schlagempfindlichkeit mit dem Fallhammer*, Nov. 08, **2002**.
- [31] a) Bundesanstalt für Materialforschung (BAM), <http://www.bam.de>, which lays down test methods pursuant to Regulation (EC) No. 1907/2006 of the European Parliament and of the Council on the Evaluation, Authorisation and Restriction of Chemicals (REACH), ABl. L142, **2008**; b) T. M. Klapötke, B. Krumm, N. Mayr, F. X. Steemann, G. Steinhauser, *Safety Science* **2010**, 48, 28–34.
- [32] *NATO Standardization Agreement (STANAG) on Explosives*, Friction Tests, no. 4487, 1st ed., Aug. 22, **2002**.
- [33] *WIWEB-Standardarbeitsanweisung 4-5.1.03, Ermittlung der Explosionsgefährlichkeit, hier der Reibempfindlichkeit mit dem Reibeapparat*, Nov. 08, **2002**.
- [34] *NATO Standardization Agreement (STANAG) on Explosives, Electrostatic Discharge Sensitivity Tests*, no. 4490, 1st ed., Feb. 19, **2001**.
- [35] <http://www.ozm.cz/en/sensitivity-tests/esd-2008a-small-scaleelectrostatic-spark-sensitivity-test/>.
- [36] a) *Test methods according to the UN Manual of Tests and Criteria, Recommendations on the Transport of Dangerous Goods*, United Nations Publication, New York, Geneva, 4th revised ed., **2003**: Impact: insensitive >40 J, less sensitive ≥ 35 J, sensitive ≥ 4 J, very sensitive ≤ 3 J; friction: insensitive >360 N, less sensitive: 360 N, sensitive <360 N and >80 N, very sensitive ≤ 80 N, extremely sensitive ≤ 10 N; b) www.reichel-partner.de.
- [37] J. F. Köhler, R. Meyer, A. Homburg, *Explosivstoffe*, 10. Aufl., Wiley-VCH Verlag GmbH & Co. KGaA, Weinheim, **2008**.
- [38] a) EXPLO5, Version 6.02, M. Sućeska, Zagreb, Croatia, **2014**; b) M. Sućeska, *Propellants Explos. Pyrotech.* **1991**, 16, 197–202; c) M. Sućeska, *Propellants Explos. Pyrotech.* **1999**, 24, 280–285; d) M. Suceka, H. G. Ang, H. Y. Chan, *Mater. Sci. Forum* **2011**, 673, 47–52.
- [39] a) GAUSSIAN09W, Version 7.0, M. J. Frisch, G. W. Trucks, H. B. Schlegel, G. E. Scuseria, M. A. Robb, J. R. Cheeseman, G. Scalmani, V. Barone, B. Mennucci, G. A. Petersson, H. Nakatsuji, M. Caricato, X. Li, H. P. Hratchian, A. F. Izmaylov, J. Bloino, G. Zheng, J. L. Sonnenberg, M. Hada, M. Ehara, K. Toyota, R. Fukuda, J. Hasegawa, M. Ishida, T. Nakajima, Y. Honda, O. Kitao, H. Nakai, T. Vreven, J. A. Montgomery Jr., J. E. Peralta, F. Ogliaro, M. Bearpark, J. J. Heyd, E. Brothers, K. N. Kudin, V. N. Staroverov, R. Kobayashi, J. Normand, K. Raghavachari, A. Rendell, J. C. Burant, S. S. Iyengar, J. Tomasi, M. Cossi, N. Rega, J. M. Millam, M. Klene, J. E. Knox, J. B. Cross, V. Bakken, C. Adamo, J. Jaramillo, R. Gomperts, R. E. Stratmann, O. Yazyev, A. J. Austin, R. Cammi, C. Pomelli, J. W. Ochterski, R. L. Martin, K. Morokuma, V. G. Zakrzewski, G. A. Voth, P. Salvador, J. J. Dannenberg, S. Dapprich, A. D. Daniels, Ö. Farkas, J. B. Foresman, J. V. Ortiz, J. Cioslowski, D. J. Fox, Gaussian, Inc., Wallingford CT, **2009**; b) GAUSS-VIEW 5, Version 5.0.8, T. K. R. Dennington, J. Millam, Semichem Inc., Shawnee Mission, **2009**.
- [40] a) NASA, Space Shuttle News Reference, 2-20-22-21, <http://de.scribd.com/doc/-17005716/NASA-Space-Shuttle-News-Reference-1981>; b) NASA, press release: STS-122 The Voyage of Columbus, **2008**, 82–84.

- [41] a) Luigi T. DeLuca, F. Maggi, S. Dossi, V. Weiser, A. Franzin, V. Gettwert, *Huozhayao Xuebao/Chinese Journal of Explosives and Propellants* **2013**, 12(6),1–14; b) E. Bucci, S. Cianfanelli, A. Tamburini, S. Dossi, M. Fassina, F. Maggi, L. Galfetti, L. T. DeLuca, G. Marra, L. Meda, A. Congiu, S. Perucchini, *A Systematic Characterisation of Aluminium Metal Powder in Use in Solid Rocket Motors*, Proceedings of the International Workshop on New Energetic Materials and Propulsion Techniques for Space Exploration, 9–10 June, Milan, Italy, **2014**.
- [42] a) T. M. Klapötke, *Chemie der hochenergetischen Materialien*, de Gruyter, Berlin, New York, **2009**; b) T. M. Klapötke, *Chemistry of High-Energy Materials*, 2nd Eng. ed., de Gruyter, Berlin, New York, **2011**.
- [43] G. P. Sutton, *Rocket Propulsion Elements*, 7th ed., John Wiley & Sons, **2001**.
- [44] H. G. Ang, S. Pisharath, *Energetic Polymers*, 1st ed., Wiley-VCH, Weinheim, **2012**.
- [45] T. Urbanski, *Production of nitroglycerine, Chemistry and Technology of Explosives*, 2, **1984**.
- [46] W. Langlotz, D. Diehl, I.C.T. Mueller, *WO 98/34891*, **1998**.
- [47] a) D. Spitzer, H. Ritter, S. Braun, Rapport ISL, S-R111/**2001**; b) D. Spitzer, B. Wanders, Rapport ISL, S-R124/**2001**.
- [48] A. Halasz, J. Spain, L. Paquet, C. Beaulieu, J. Hawari, *Environ. Sci. Technol.* **2002**, 36(4), 633–638.
- [49] a) A. H. Lamberton, C. Lindley, J. C. Speakman, *J. Chem. Soc.* **1949**, 1650–1656; b) M. C. Tobin, C. Marvin, J. P. Fowler, H. A. Hoffman, C. W. Sauer, *J. Am. Chem. Soc.* **1954**, 76, 3249–3253.
- [50] R. C. Brian, A. H. Lamberton, *J. Chem. Soc.* **1949**, 1633–1635; b) C. W. Sauer, R. P. Follett, *J. Am. Chem. Soc.* **1955**, 77, 2560–2561.
- [51] J. Krc (Jr.), *Anal. Chem.* **1958**, 30(7), 1301–1302.

CHAPTER 3**POLYNITROTETRAZOLES**

This chapter deals with the preparation of two 5-(polynitromethyl)-tetrazole derivatives and further alkylation of the ring system. Simultaneously and independently some of the work presented in this chapter was also carried out by K. O. CHRISTE and R. HAIGES. In this context, the crystal structures of ammonium 5-(trinitromethyl)tetrazolate and its two precursors have been published by:

R. Haiges, K. O. Christe

“Energetic High-Nitrogen Compounds: 5-(Trinitromethyl)-2*H*-tetrazole and -tetrazolates, Preparation, Characterisation, and Conversion into 5-(Dinitromethyl)tetrazoles”^[1]

Nevertheless similar results on these three molecules will be presented in this chapter. The alkylation of the 5-(polynitromethyl)-tetrazole derivatives has been presented as poster at the workshop ‘NTREM 2014’:

J. Feierfeil, M. A. Kettner, T. M. Klapötke,* M. Sućeska, S. Wunder

“Synthesis and Characterisation of Alkylated Trinitromethyl- and Fluorodinitromethyl-tetrazoles”^[2]

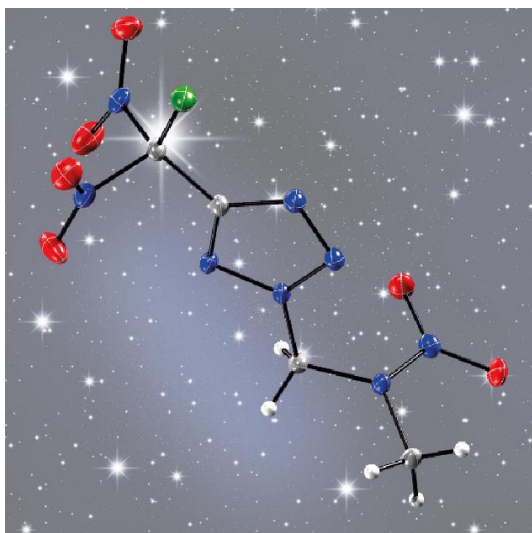
The main part of this chapter is reproduced with permission from:

M. A. Kettner, T. M. Klapötke*

“New Polynitrotetrazoles”^[3]

DOI: 10.1002/chem.201405659

Copyright 2015 Chemistry - A European Journal



3.1 Introduction

Polynitroazoles are important and common compounds in the research of energetic materials.^[4] The design of new materials includes strategies based on tetrazoles,^[5] triazoles,^[6] furazanes,^[7] *N*-oxides,^[8] furoxanes^[9] and tetrazines.^[10] Their high nitrogen contents lead to large amounts of N₂ during combustion causing high detonation velocities and pressures.^[4] Tetrazole derivatives are of special interest owing to the highest nitrogen content of these five-membered heterocycles (Figure 1). Five-substituted tetrazoles are easily accessible through treatment of organic nitriles with sodium azide.^[11] Several derivatives with oxygen containing moieties such as nitro groups, nitrate esters or nitramines at the 5-position were investigated within our group and are suitable for various energetic applications. For instance, derivatives of 5-nitro-^[12] and 5-nitriminotetrazoles^[13] for gas-generating applications, or energetic polymers based on tetrazoles.^[14] Moreover tetrazole derivatives with perfluorinated alkyl groups were investigated as ingredients in MTV (magnesium, teflon, viton) decoy flares.^[15]

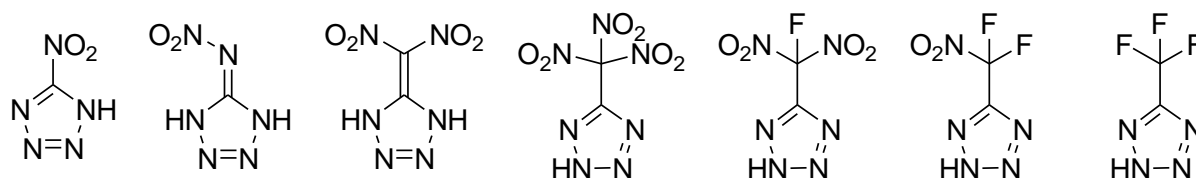


Figure 1: Some examples of 5-substituted polynitro- and polyfluoro-tetrazoles.

The trinitromethyl and fluorodinitromethyl functionalities have proven to be useful functional groups in the synthesis of high performing explosives as well as novel oxidisers for high tech propellants.^[16] The combined high nitrogen and oxygen contents of this group allow full oxidation of fuels within the molecule leading to high performances. Additionally, the large dipole moment within the nitro and fluorine groups gives rise to extensive inter- and intramolecular interactions resulting in high densities, which also affect the performance advantageously.^[17]

The syntheses of 5-trinitromethyl- and 5-fluorodinitromethyl-2*H*-tetrazole and some of their salts were first published in 1981 by GRAKAUSKAS *et al.*^[18] and FOKIN *et al.*,^[19] respectively. They used the corresponding polynitroacetonitriles^[20] for the 1,3-dipolar ring-closure reaction with trimethylsilyl azide or sodium azide. However, all starting materials are hazardous chemicals. A more convenient and ‘greener’ route to the trinitromethyl derivative was introduced by CHRISTE and HAIGES by decarboxylative nitration of the corresponding methyl carboxylic acid furnishing high yields.^[11] Owing to their high oxygen content these compounds can be considered as solid oxygen carriers in solid rocket propellants, replacing or partially replacing currently used ammonium perchlorate (AP).^[4] AP has been identified as toxic to humans thyroid gland^[21] and amphibians.^[22] Additionally, the decomposition product hydrogen chloride, which is produced in large amounts during a rocket launch, is environmentally critical.^[23] This visible and detectable expulsion affects guidance systems adversely, and is also unfavourable for tactical missiles.^[24] However, the very high mechanical sensitivities of 5-trinitromethyl- and 5-fluorodinitromethyl-2*H*-tetrazole and their

salts make these compounds inoperable concerning agitation and processing of propellant formulations. The alkylation described in this chapter – besides some additional tetrazolate salts – was carried out to overcome some problematic issues of the known polynitromethyl tetrazole derivatives:

- the acidities associated with cyclic nitroazoles
- their low thermal stabilities and
- their very high sensitivities towards impact and friction.

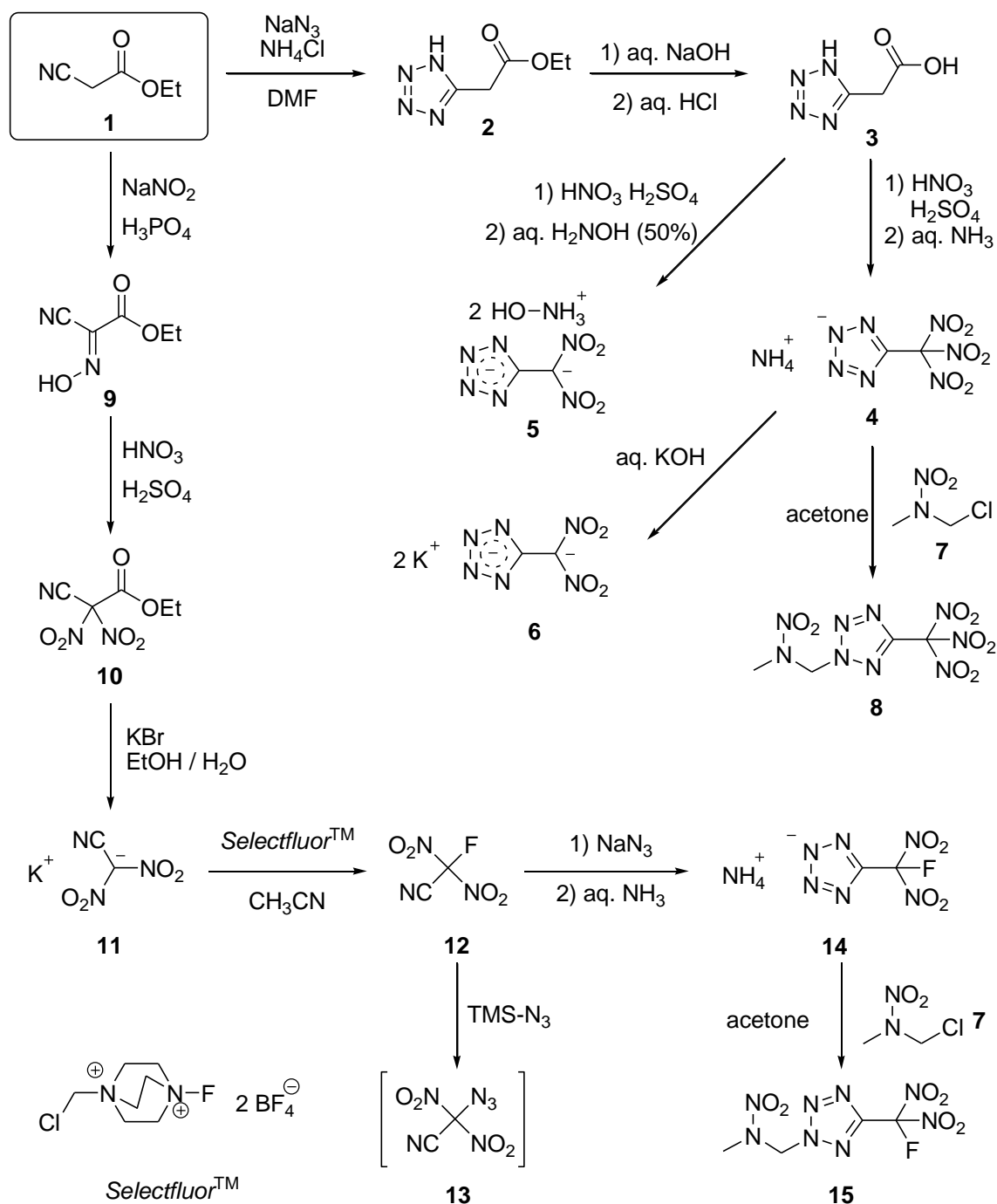
As known from other 5-substituted tetrazole derivatives the methylation can significantly lower the sensitivities.^[12, 13] However, to maintain the energetic character and by trying to keep the oxygen balance as high as possible, the secondary nitramine moiety was chosen to be incorporated to these tetrazoles.^[25]

3.2 Syntheses

All syntheses described in this chapter started from commercially available ethyl 2-cyanoacetate (**1**) and are depicted in Scheme 1. The literature known synthesis of ammonium 5-(trinitromethyl)-2*H*-tetrazolate (**4**, AmTNMTz) started with the tetrazole ring closing reaction at the cyano group of ethyl 2-cyanoacetate (**1**) with ammonium chloride and sodium azide in dimethylformamide yielding ethyl 2-(1*H*-tetrazol-5-yl)-acetate (**2**).^[26] This step was followed by saponification of the ethyl ester to give the free carboxylic acid **3**.^[27] AmTNMTz (**4**) was then furnished by decarboxylative nitration of 5-(tetrazol-1*H*-yl)-acetic acid (**3**) and worked-up by treatment with aqueous ammonia (25%).^[1, 26, 27] The work-up with aqueous hydroxylammonia (50%) yielded dihydroxylammonium 5-(dinitromethylide)-tetrazolate (**5**). During the work with compound **4** also crystals of dipotassium 5-(dinitromethylide)-tetrazolate (**6**)^[28] were isolated from the reaction of compound **4** with concentrated potassium hydroxide solution (10M). The conversion of the free acid 5-(trinitromethyl)-2*H*-tetrazole with aqueous hydroxylamine and hydrazine yielding the corresponding mono hydroxylammonium and hydrazinium dinitromethylide salts has been reported previously.^[1] However, the dihydroxylammonium 5-(dinitromethylide)-tetrazolate (**5**) is not mentioned in the literature to the best of our knowledge. In this chapter its crystal structure and its calculated energetic properties are presented. The alkylation of the tetrazolate **4** was carried out by treatment with 2-nitro-2-azapropyl chloride (**7**)^[29] in anhydrous acetone yielding 2-(2-nitro-2-azapropyl)-5-(trinitromethyl)-2*H*-tetrazole (**8**) as colourless crystals in good yield of 78%.

For the synthesis of 5-(fluorodinitromethyl)-2*H*-tetrazolate (**14**) first the dinitromethyl moiety was introduced by the literature known synthesis of potassium dinitroacetonitrile (**11**) from ethyl 2-cyanoacetate (**1**) via compounds **9** and **10**.^[30–32] The formation of ethyl (hydroxyimino)cyanoacetate (**9**) facilitates the nitration yielding ethyl cyanodinitroacetate (**10**) in quantitative yield.^[30, 31] Subsequent treatment with potassium bromide furnishes potassium dinitroacetonitrile (**11**) in good yield and purity.^[32] The overall yield from compound **1** to **11** was 72%.

Differing from the literature the fluorination of potassium dinitroacetonitrile (**11**) was performed with *Selectfluor*TM (instead of 25% F₂ in He) in anhydrous acetonitrile at ambient temperature in a closed vessel. Fluorodinitroacetonitrile (**12**)^[20] was not isolated due to its high volatility. When the reaction mixture turned colourless, the solution containing compound **12** was distilled into a cooling trap (−78 °C) and compound **12** was identified by



Scheme 1: Syntheses of compounds **4–6**, **8**, **14** and **15** starting from commercially available ethyl cyanoacetate **1**. Compounds **2** (61%),^[26] **3** (73%),^[27] **4** (91%),^[11] **9** (98%),^[31] **10** (98%)^[31] and **11** (75%)^[32] were synthesised according to the literature known procedures. The salts **5** (13%) and **6** (77%) were synthesised from compound **3**. The 2-steps yield of compound **14** from **11** was 32%. The alkylation of compounds **4** and **14** with 2-nitro-2-azapropyl chloride (**7**)^[29] yielded the compounds **8** and **15** each with 78%.

multinuclear NMR measurements from the acetonitrile solution. Subsequently, sodium azide was added to the solution and the reaction mixture was stirred at ambient temperature in a closed vessel.^[19] The progress of the 1,3-dipolar ring-closure reaction was monitored by ^{19}F NMR spectroscopy. After an acidic work-up and treatment with aqueous ammonia (25%) ammonium 5-(fluorodinitromethyl)-2*H*-tetrazolate (**14**) was isolated in acceptable yield of 32% (two steps from compound **11**). If trimethylsilyl azide is used instead of sodium azide as known from the literature,^[18] with heating the risk of the formation of undesired side products including azidodinitro acetonitrile (**13**) is given. In fact, ^{19}F NMR experiments out of this reaction mixture confirmed the generation of more than three species even without heating, and ring-closing reactions were continued with sodium azide. The alkylation of compound **14** was performed analogous to compound **8** with 2-nitro-2-azapropyl chloride (**7**)^[29] in anhydrous acetone, furnishing according 2-(2-nitro-2-azapropyl)-5-(fluoro-dinitromethyl)-2*H*-tetrazole (**15**) as colourless crystalline solid in good yield of 78%. Compounds **4** and **14** were alkylated exclusively in the β -position of the tetrazole ring due to the strong directing effect of the polynitromethyl groups.^[33]

3.3 Multinuclear NMR Spectroscopy

Compounds **4**, **6**, **8**, **14** and **15** were investigated by multinuclear NMR spectroscopy in D_2O (**4**) and *d*6-acetone (**14**, **8–12**) (Table 1). The signals of the hydrogen atoms of the ammonium cations of compounds **4** and **14** are shifted to $\delta = 7.22$ and 8.42 ppm in the ^1H NMR spectra. The chemical shifts of the methyl and methylene groups in compounds **8** and **15** are observed in the expected ranges in the ^1H and $^{13}\text{C}\{^1\text{H}\}$ NMR spectra. The $^{13}\text{C}\{^1\text{H}\}$ signals of the tetrazole carbon atoms are observed in the narrow range of $\delta = 150.8(\text{14})\text{--}155.2(\text{5})$ ppm, and are splitted into doublets for the fluorine containing compounds **14** and **15** due to $^2J_{\text{C-F}}$ coupling with coupling constants of 23.0 Hz (**14**) and 25.4 Hz (**15**). The signals of the polynitro carbon atoms are observed in the range of $\delta = 115.4(\text{15})\text{--}128.5(\text{5})$ ppm, and are splitted into doublets for the fluorine containing compounds **14** and **15** due to $^1J_{\text{C-F}}$ coupling with coupling constants of 284.7 Hz (**14**) and 282.9 Hz (**15**).^[34] Compound **6** was identified on the basis of the literature known ^{13}C NMR chemical shifts.^[28]

In the $^{14}\text{N}\{^1\text{H}\}$ NMR spectra the signals of the nitro groups at the nitramine moiety are observed at $\delta = -33$ ppm for compound **8** and at $\delta = -32$ ppm for compound **15**. The signals of the polynitro groups are observed in the range between $\delta = -23(\text{5})$ and $-37(\text{8})$ ppm, and are splitted into doublets for the fluorine containing compounds **14** and **15** according to $^2J_{\text{15N-F}}$ (**14**) and $^2J_{\text{14N-F}}$ (**15**) coupling with coupling constants of 16.5 Hz (**14**) and 10 Hz (**15**).^[35]

The ^{15}N NMR spectra of the ammonium salts **4** and **14** were recorded. They show additionally the signals for the nitrogen atoms of the tetrazole rings [$\delta(\text{N}_\alpha) = 9.6(\text{14})$ and $11.8(\text{4})$ ppm; $\delta(\text{N}_\beta) = -57.5(\text{14})$ and $-51.8(\text{4})$ ppm]. The nitrogen NMR signals of the ammonium cation are found at $\delta = -362.2(\text{14})$ and $-362.8(\text{4})$ ppm.^[35]

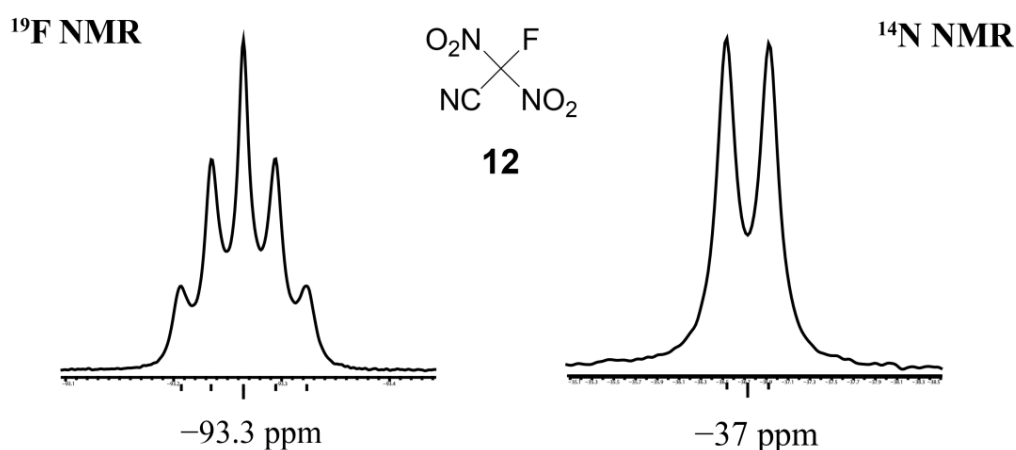
Table 1: Multinuclear NMR chemical shifts δ of compound **4** in D₂O, and compounds **6**, **8**, **14** and **15** in *d*6-acetone [ppm].

Nucleus	Assignment	4	6	8	14	15
¹ H	CH ₃	—	—	3.70	—	3.68
	CH ₂	—	—	7.00	—	6.96
	NH ₄ ⁺	7.22 (br)	—	—	8.42 (br)	—
¹³ C{ ¹ H}	CH ₃	—	—	38.6	—	38.6
	CH ₂	—	—	67.6	—	67.3
	C(NO ₂) _x F _y	127.9	128.5	121.2	119.9(d)	115.4(d)
	C _{Tz}	152.2	155.2	152.3	150.8(d)	153.7(d)
¹⁴ N	NVO ₂	—	—	−33	—	−32
	C(NO ₂) _x F _y	−28.3*	−23	−37	−20.6(d)*	−27(d)
	N _α	11.8*	—	—	9.6*	—
	N _β	−51.8*	—	—	−57.5*	—
¹⁹ F	NH ₄ ⁺	−362.8*	—	—	−362.2*	—
	CF	—	—	—	−95.5 (br)	−99.6 (br)

(br) broad; x = 2, 3; y = 0, 1; (d) doublet; * from ¹⁵N NMR measurement.

In the ¹⁹F NMR spectrum the fluorine signal of compound **14** is observed at $\delta = -95.5$ ppm and the signal of compound **15** is found at $\delta = -99.6$ ppm, both as broad singlets indicating multiplets.

The intermediate fluorodinitroacetonitrile (**12**), which was not isolated, was identified by ¹⁴N and ¹⁹F NMR spectroscopy from the acetonitrile solution (Figure 2). Its ¹⁴N NMR spectrum shows the signal of the two nitro groups at $\delta = -37$ ppm as a doublet due to a ²J_{14N-F} coupling of 11 Hz. The broad signal of the reaction solvent acetonitrile at $\delta = -132$ ppm overlies the signal of the nitrile group that is expected to be in this range. In the ¹⁹F NMR spectrum the signal is observed at $\delta = -93.3$ ppm, splitted into a quintet due to coupling with two ¹⁴N nuclei (²J_{F-14N} = 11 Hz).

**Figure 2:** NMR spectra of compound **12**. Left: ¹⁹F NMR spectrum, ²J_{F-14N} = 11 Hz; right: ¹⁴N NMR spectrum, ²J_{14N-F} = 11 Hz.

3.4 Vibrational Spectroscopy

The alkylated 5-(polynitromethyl)-tetrazoles **8** and **15** were also investigated by IR and Raman spectroscopy (Table 2).^[36] The spectra of compound **8** shows the stretching modes of the methyl and methylene groups [$\nu(\text{C-H})$, $\nu_s(\text{CH}_3)$ and $\nu_{as}(\text{CH}_3)$] in the range of $\tilde{\nu} = 3068\text{--}2883\text{ cm}^{-1}$. The absorption bands in the range of $\tilde{\nu} = 1468\text{--}1420\text{ cm}^{-1}$ can be attributed to the deformation vibrations δ of the methyl and methylene groups. At $\tilde{\nu} = 1540$ and 1258 cm^{-1} the asymmetric ν_{as} and symmetric stretching ν_s vibrations of the trinitromethyl moiety are observed. The nitramine unit shows the asymmetric stretching vibration ν_{as} at $\tilde{\nu} = 1598\text{ cm}^{-1}$ and the symmetric stretching vibration ν_s at $\tilde{\nu} = 1299\text{ cm}^{-1}$. The Raman spectrum additionally shows the stretching mode ν of the C=N bond at $\tilde{\nu} = 1487\text{ cm}^{-1}$.

Table 2: IR and Raman vibrations of the alkylated 5-(polynitromethyl)-tetrazoles **8** and **15** [cm^{-1}].

Vibration	8		15	
	IR	Raman	IR	Raman
$\nu(\text{CH}_2/\text{CH}_3)$	3068	3069	3050	3051
	3007	3008	3004	3004
	2883	2890	2966	2970
$\delta(\text{CH}_2)$	1468	—	1460	1466
	1447	—	—	1436
	1420	1421	1427	—
$\nu_{as}(\text{NO}_2)$	1540	1540	1536	1552
$\nu_s(\text{NO}_2)$	1258	1260	1260	1276
$\nu_{as}(\text{N-NO}_2)$	1598	1607	1595	1590
$\nu_s(\text{N-NO}_2)$	1299	1304	1304	1304
$\nu(\text{C-F})$	—	—	1260	1276
$\nu(\text{C=N})$	—	1487	—	1503

The spectra of compound **15** displays the stretching modes of the methyl and methylene groups [$\nu(\text{C-H})$, $\nu_s(\text{CH}_3)$ and $\nu_{as}(\text{CH}_3)$] in the range of $\tilde{\nu} = 3050\text{--}2966\text{ cm}^{-1}$. The absorption bands in the range of $\tilde{\nu} = 1460\text{--}1427\text{ cm}^{-1}$ can be assigned to the deformation vibrations δ of the methyl and methylene groups. At $\tilde{\nu} = 1536$ and 1260 cm^{-1} the asymmetric ν_{as} and symmetric stretching ν_s vibrations of the nitro groups in the fluorodinitromethyl moiety can be observed. The nitramine moiety shows the asymmetric stretching vibration ν_{as} at $\tilde{\nu} = 1595\text{ cm}^{-1}$ and the symmetric stretching vibration ν_s at $\tilde{\nu} = 1304\text{ cm}^{-1}$. The C-F stretching vibration is observed at $\tilde{\nu} = 1260\text{ cm}^{-1}$. The Raman spectrum additionally shows the stretching vibration ν of the C=N bond at $\tilde{\nu} = 1503\text{ cm}^{-1}$.

3.5 X-ray Crystal Structures

Single crystals suitable for low temperature X-ray diffraction measurements were obtained from a dimethylformamide solution of compound **2**, from an aqueous acetic acid solution of compound **3**, from a 1:1 toluene/ethyl acetate mixture of compounds **4** and **14**, and from a 1:1 methanol/dichloromethane mixture of compounds **8** and **15**. Compound **5** crystallised from an aqueous KOH solution and compound **6** from an aqueous hydroxylammonia solution. The structures of compounds **2**, **3** and **4** were already published by CHRISTE and HAIGES in 2013 as mentioned above.^[1] Nevertheless the data obtained within the group of KLAPÖTKE were submitted to the Cambridge Crystallographic Database as private communication as they were measured under different conditions and are also discussed in this subchapter. All relevant crystallographic and structural refinement data are listed in Tables 3 and 4. The refined atom positions and anisotropic thermal displacement parameters are listed in the Appendix 3.10.

Table 3: Crystal structure parameters of the precursors **2** and **3** of AmTNMTz (**4**), and Hx₂DNMTz (**5**). Standard deviations are given in parentheses.

	2	3	4	5
Refined formula	C ₅ H ₈ N ₄ O ₂	C ₃ H ₄ N ₄ O ₂	C ₂ H ₄ N ₈ O ₆	C ₂ H ₈ N ₈ O ₆
Formula weight [g·mol⁻¹]	156.14	128.09	236.10	240.13
Crystal dimensions [mm]	0.37×0.35×0.02	0.18×0.05×0.04	0.33×0.17×0.15	0.48×0.20×0.05
Crystal description	colourless plate	colourless rod	colourless block	yellow plate
Crystal system	orthorhombic	monoclinic	triclinic	orthorhombic
Space group	<i>Pca</i> 2 ₁	<i>P</i> 2 ₁ / <i>c</i>	<i>P</i> -1	<i>Ima</i> 2
<i>a</i> [Å]	9.786(1)	7.204(1)	7.056(1)	8.262(2)
<i>b</i> [Å]	11.046(1)	7.319(2)	7.367(1)	19.397(1)
<i>c</i> [Å]	6.598(1)	10.014(2)	9.168(1)	6.237(2)
α [°]	90	90	104.81(1)	90
β [°]	90	102.80(1)	91.80(1)	90
γ [°]	90	90	109.11(1)	90
<i>V</i> [Å³]	713.3(2)	514.9(2)	431.8(1)	999.6(1)
<i>Z</i>	4	4	2	4
ρ_{calcd} [g·cm⁻³]	1.454	1.653	1.816	1.596
μ [mm⁻¹]	0.115	0.140	0.175	0.152
temperature [K]	173(2)	123(2)	173(2)	173(2)
θ range [°]	4.16–26.97	3.48–26.00	4.32–26.00	4.20–28.27
<i>F</i>(000)	328	264	240	496
dataset <i>h</i>	−9 ≤ <i>h</i> ≤ 12	−8 ≤ <i>h</i> ≤ 8	−8 ≤ <i>h</i> ≤ 8	−11 ≤ <i>h</i> ≤ 11
dataset <i>k</i>	−14 ≤ <i>k</i> ≤ 14	−9 ≤ <i>k</i> ≤ 9	−9 ≤ <i>k</i> ≤ 9	−25 ≤ <i>k</i> ≤ 25
dataset <i>l</i>	−8 ≤ <i>l</i> ≤ 8	−11 ≤ <i>l</i> ≤ 12	−11 ≤ <i>l</i> ≤ 11	−8 ≤ <i>l</i> ≤ 8
reflections measured	3761	9607	4323	8409
reflections independent	1533	995	1679	1320
reflections unique	1384	899	1402	1258
<i>R</i>_{int}	0.0327	0.0260	0.0273	0.0287
<i>R</i>₁, <i>wR</i>₂ (2σ data)	0.0299, 0.0663	0.0276, 0.0657	0.0336, 0.0695	0.0261, 0.0692
<i>R</i>₁, <i>wR</i>₂ (all data)	0.0360, 0.0698	0.0315, 0.0683	0.0444, 0.0756	0.0277, 0.0704
Data/restraints/parameters	1533/1/132	995/0/98	1679/0/157	1320/1/121
GOOF on <i>F</i>²	1.055	1.062	1.087	1.073
Residual electron density	−0.198/0.179	−0.175/0.229	−0.215/0.278	−0.175/0.336
CCDC number	1049186	1049187	1049188	not deposited

Table 4: Crystal structure parameters of K₂DNMTz (**6**), NAP-TNMTz (**8**), AmFDNMTz (**14**) and NAP-FDNMTz (**15**). Standard deviations are given in parentheses.

	6	8	14	15
Refined formula	K ₂ C ₂ N ₆ O ₄	C ₄ H ₅ N ₉ O ₈	C ₂ H ₄ N ₇ O ₄ F	C ₄ H ₅ N ₈ O ₆ F
Formula weight [g·mol⁻¹]	250.26	307.14	209.10	280.13
Crystal dimensions [mm]	0.40×0.60×0.05	0.40×0.19×0.08	0.30×0.10×0.05	0.30×0.16×0.09
Crystal description	yellow rod	colourless plate	colourless plate	colourless needle
Crystal system	orthorhombic	orthorhombic	monoclinic	monoclinic
Space group	<i>Pbcn</i>	<i>Pbca</i>	<i>P2₁/c</i>	<i>P2₁/c</i>
<i>a</i> [Å]	9.170(1)	5.940(1)	14.008(9)	5.850(1)
<i>b</i> [Å]	9.074(1)	18.673(1)	8.990(1)	15.300(1)
<i>c</i> [Å]	9.262(1)	20.484(1)	13.979(4)	12.199(1)
α [°]	90	90	90	90
β [°]	90	90	115.40(8)	97.00(1)
γ [°]	90	90	90	90
<i>V</i> [Å³]	770.7(1)	2272.0(1)	1590.1(15)	994.8(1)
<i>Z</i>	4	8	8	4
ρ_{calcd} [g·cm⁻³]	2.157	1.796	1.747	1.870
μ [mm⁻¹]	1.230	0.171	0.173	0.182
temperature [K]	100(2)	100(2)	113(2)	100(2)
θ range [°]	4.40–25.98	4.11–26.00	4.12–25.99	4.15–26.00
<i>F</i>(000)	496	1248	1696	568
dataset <i>h</i>	$-7 \leq h \leq 11$	$-7 \leq h \leq 6$	$-17 \leq h \leq 17$	$-7 \leq h \leq 7$
dataset <i>k</i>	$-11 \leq k \leq 11$	$-23 \leq k \leq 23$	$-11 \leq k \leq 11$	$-18 \leq k \leq 18$
dataset <i>l</i>	$-11 \leq l \leq 11$	$-25 \leq l \leq 25$	$-17 \leq l \leq 17$	$-13 \leq l \leq 12$
reflections measured	3577	16301	13741	7248
reflections independent	749	2205	3108	1933
reflections unique	651	1762	2633	1658
<i>R</i>_{int}	0.0271	0.0510	0.0331	0.0231
<i>R</i>1, <i>wR</i>2 (2σ data)	0.0218, 0.0486	0.0368, 0.0857	0.0302, 0.0688	0.0270, 0.0613
<i>R</i>1, <i>wR</i>2 (all data)	0.0284, 0.0517	0.0502, 0.0938	0.0385, 0.0732	0.0338, 0.0651
Data/restraints/parameters	749/0/65	2205/0/210	3108/0/250	1933/0/192
GOOF on <i>F</i>²	1.098	1.038	1.025	1.035
Residual electron density	−0.239/0.351	−0.160/0.239	−0.223/0.314	−0.215/0.314
CCDC number	1026523	974783	956909	974784

Crystal Structure of Ethyl 5-(Tetrazol-1*H*-yl)-Acetic Ester (**2**)

Ethyl 5-(tetrazol-1*H*-yl)-acetic ester (**2**) crystallises as colourless plates in the orthorhombic space group *Pca*2₁ with four molecules in the unit cell and a calculated maximum density of 1.454 g·cm⁻³ at 173(2) K. It shows an intramolecular hydrogen bond between N4 of the tetrazole ring and O1 of the carboxyl group (Figure 3). N4 also interacts intermolecularly with N1 of the next tetrazole ring, thus forming chains of tetrazole rings along the *a* axis (Figure 4, Table 5).

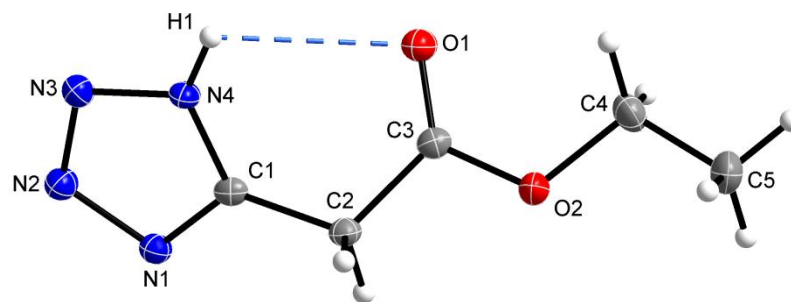


Figure 3: Crystal structure of compound **2**; selected bond length [\AA] and angles [$^\circ$]: O1–C3 1.206(2), O2–C3 1.341(2), N4–H1 0.86(2), N2–N3 1.295(2), C1–C2 1.486(2); C1–N4–H1 132.6(1), N3–N4–H1 118.0(1), N1–N2–N3–N4 $-0.2(2)$, C1–N4–N3–N2 $0.0(2)$, C4–O2–C3–O1 $-2.0(2)$.

Table 5: Structural parameters of the intra- and intermolecular hydrogen bonds in the crystal structure of compound **2** presented in Figures 3 and 4.

D–H \cdots A	d (D–H) [\AA]	d (H \cdots A) [\AA]	d (D–H \cdots A) [\AA]	\angle (D–H \cdots A) [$^\circ$]
N4–H1 \cdots O1	0.86(2)	2.62(2)	2.893(2)	99.9(3)
N4–H1 \cdots N1(i)	0.86(2)	2.00(2)	2.831(2)	162.0(2)
N4(i)–H1(i) \cdots N1(ii)				
Symmetry operators: (i) $-\frac{1}{2}+x, 1-y, z$; (ii) $-1+x, y, z$.				

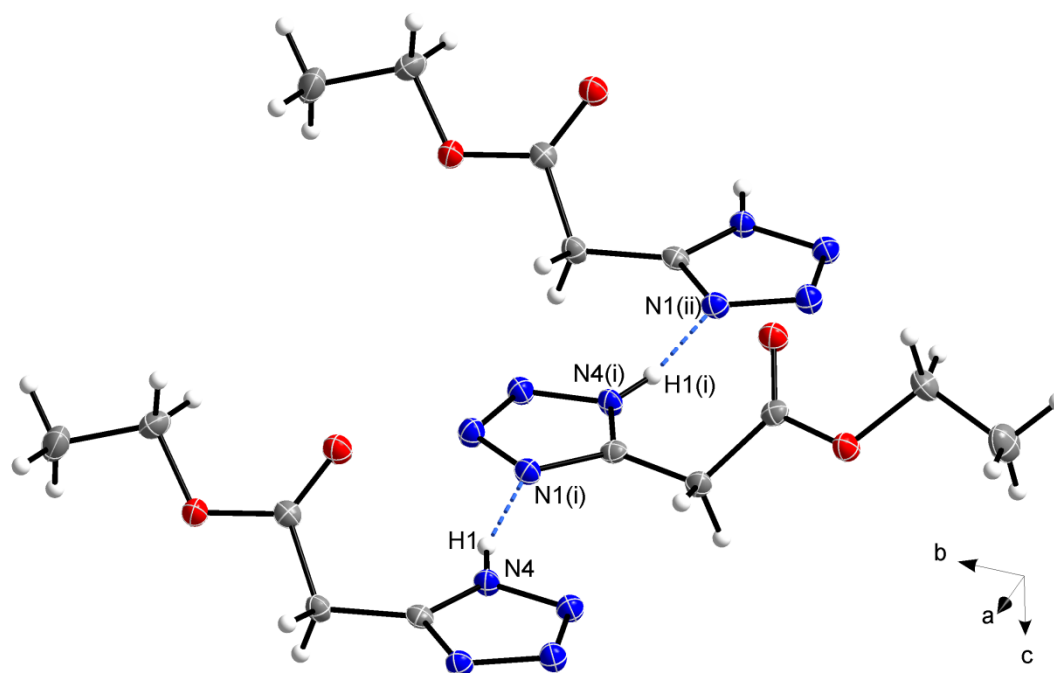


Figure 4: Tetrazole chains connected by hydrogen bonds along the a axis in the crystal structure of compound **2** for the structural parameters listed in Table 5. Symmetry operators: (i) $-\frac{1}{2}+x, 1-y, z$; (ii) $-1+x, y, z$.

Crystal Structure of 5-(Tetrazol-1*H*-yl)-Acetic Acid (**3**)

5-(tetrazol-1*H*-yl)-acetic acid (**3**) crystallises as colourless rods in the space group $P2_1/c$ with four molecules per unit cell and a calculated maximum density of $1.239 \text{ g}\cdot\text{cm}^{-3}$ at $123(2) \text{ K}$ (Figure 5).

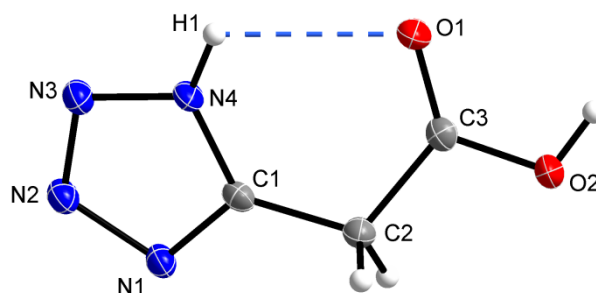


Figure 5: Crystal structure of compound **3**; selected bond length [\AA] and angles [$^\circ$]: O1–C3 1.203(2), O2–C3 1.322(1), O2–H 0.86(2), C2–C1 1.486(2), N2–N3 1.288(2), N4–H1 0.87(2), C1–N4–H1 132.5(1), N3–N4–H1 118.1(1), O1–C3–O2 123.9(1), C3–O2–H4 107.8(1), N1–N2–N3–N4 0.0(1), C1–N4–N3–N2 0.2(1), N4–C1–N1–N2 0.3(1).

Table 6: Structural parameters of the intra- and intermolecular hydrogen bonds in the crystal structure of compound **2** presented in Figures 5 and 6.

D–H \cdots A	d (D–H) [\AA]	d (H \cdots A) [\AA]	d (D–H \cdots A) [\AA]	\angle (D–H \cdots A) [$^\circ$]
N4–H1 \cdots O1	0.87(2)	2.31(1)	2.729(2)	109.4(1)
N4–H1 \cdots N1(i)				
N4(iii)–H1(iii) \cdots N1	0.87(2)	2.04(2)	2.869(2)	159.2(2)
N4(ii)–H1(ii) \cdots N1(iv)				
O2(ii)–H2(ii) \cdots N2				
O2(iv)–H2(iv) \cdots N2(i)	0.86(2)	1.92(2)	2.753(1)	164.8(2)

Symmetry operators: (i) $x, \frac{1}{2}-y, -\frac{1}{2}+z$; (ii) $1+x, \frac{1}{2}-y, \frac{1}{2}+z$; (iii) $x, \frac{1}{2}-y, \frac{1}{2}+z$; (iv) $1+x, y, z$.

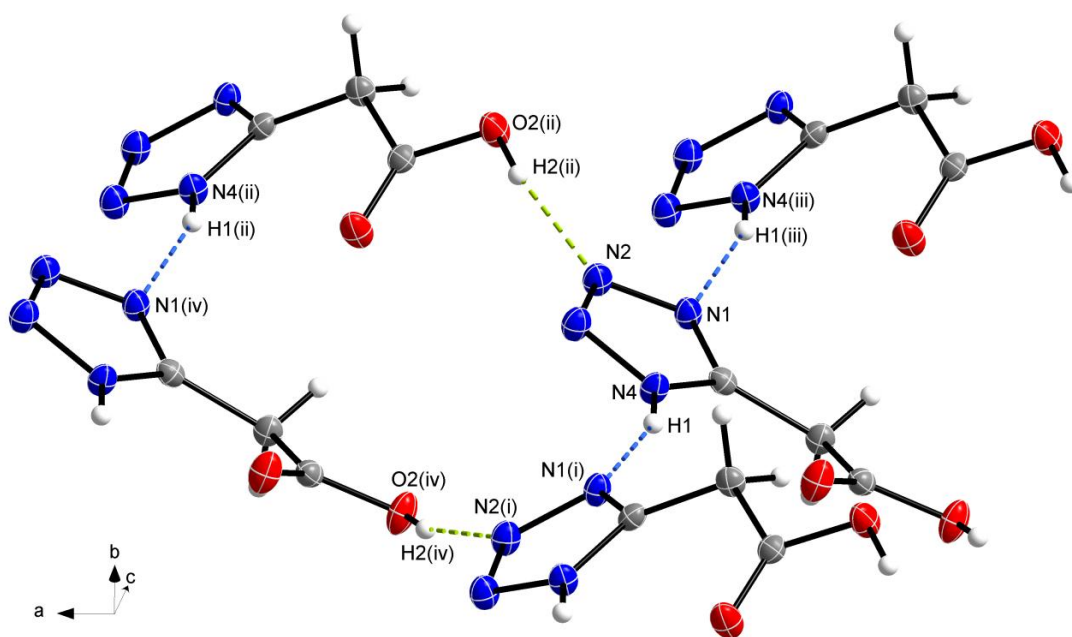


Figure 6: Intermolecular hydrogen bonds forming tetrazole chains along the c axis (blue dashed lines) that are linked through the carboxylic acid group (yellow dashed lines) with each other. Structural parameters are listed in Table 6. Symmetry operators: (i) $x, \frac{1}{2}-y, -\frac{1}{2}+z$; (ii) $1+x, \frac{1}{2}-y, \frac{1}{2}+z$; (iii) $x, \frac{1}{2}-y, \frac{1}{2}+z$; (iv) $1+x, y, z$.

Crystal Structure of Ammonium 5-(Trinitromethyl)-2H-Tetrazolate (4)

Ammonium 5-(trinitromethyl)-tetrazolate (**4**) crystallises as colourless blocks in the triclinic space group $P\bar{1}$ with two formulas in the unit cell and a calculated maximum density of $1.816 \text{ g}\cdot\text{cm}^{-3}$ at 173(2) K. Figure 7 shows the asymmetric unit in the crystal structure of compound **4**.

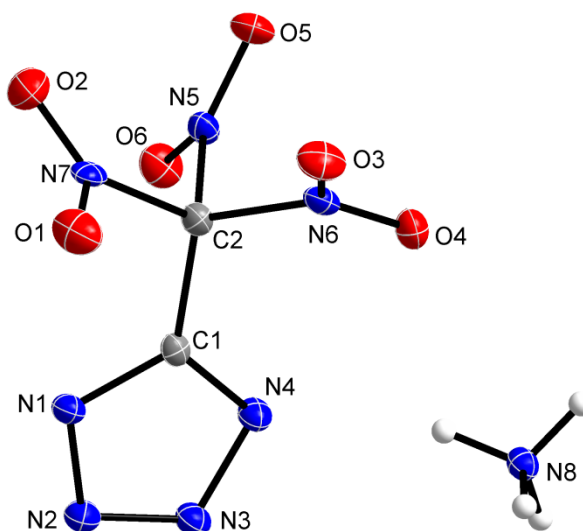


Figure 7: Crystal structure of compound **4**. Selected bond lengths [\AA] and angles [$^\circ$]: average N–O 1.211(2), N1–C1 1.335(2), N1–N2 1.340(2), N2–N3 1.326(2), N3–N4 1.337(2), N4–C1 1.337(2), N5–C2 1.547(2), N6–C2 1.539(2), N7–C2 1.556(2), C1–C2 1.485(2), average N8–H 0.92(1); N1–C1–N4 113.1(1), average O–N–O 128.6(1), N3–N4–C1–N1 0.3(2), C1–C2–N6–O4 59.3(2), C1–C2–N7–O1 61.9(2), C1–C2–N5–O6 17.8(2), N4–C1–C2–N7 $-178.0(2)$.

The C1–C2 bond length [1.485(2) \AA] is shorter than a common C–C single bond (1.54 \AA).^[37] The C2–N bonds to the nitro groups are slightly elongated [1.539(2)–1.556(2) \AA]. The N–O bond lengths and O–N–O angles of all nitro groups are in the expected ranges [1.201(2)–1.218(2) \AA]. The bond lengths and angles within the five-membered ring are also in the expected range. The trinitromethyl group arranges into the characteristic propeller-like motif, which is reflected in the dihedral angles C1–C2–N6–O4 of 59.3(2) $^\circ$ and C1–C2–N7–O1 of 61.9(2) $^\circ$. Only the C1–C2–N5–O6 torsion angle of 17.8(2) $^\circ$ deviates from the typical range for this conformation (23–67 $^\circ$) as described by BRILL *et al.*, although this nitro group does not interact with the atoms of the tetrazole ring.^[38] This conformation results in atom distances between the nitro groups well below the sum of van der Waals radii caused by sterical hindrance and electrostatic attraction. The oxygen atoms O1 and O4 also interact with the nitrogen atoms N1 and N4 of the five-membered ring (Figure 8). Every nitrogen atom of the tetrazole ring is involved in hydrogen bonds with the adjacent ammonium cations (Figure 9, Table 7).

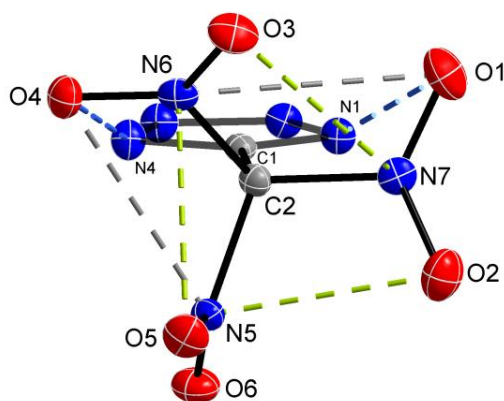


Figure 8: View along the C1–C2 bond showing the propeller-like conformation of the nitro groups with atom distances well below the sum of van der Waals radii: N6...O5 2.618(2), N5...O2 2.553(2), N7...O3 2.685(2) Å (yellow dashed lines); N6...O1 2.910(2), N5...O4 2.789(2) Å (grey dashed lines); short contacts to the tetrazole as blue dashed lines: O1...N1 2.865(2), O4...N4 2.899(2) Å; $\Sigma \text{vdW (O,N)} = 3.07$ Å.^[39]

Table 7: Structural parameters of the intermolecular hydrogen bonds in the crystal structure of compound **4** presented in Figure 9.

D–H...A	d (D–H) [Å]	d (H...A) [Å]	d (D–H...A) [Å]	\angle (D–H...A) [°]
N8(i)–H4(i)...N1	0.89(2)	2.23(2)	3.032(2)	149.0(2)
N8(ii)–H2(ii)...N2	0.90(2)	2.06(2)	2.960(2)	174.6(2)
N8(iii)–H3(iii)...N3	0.93(2)	2.02(2)	2.944(2)	175.3(2)
N8–H1...N4	0.92(2)	2.07(3)	2.942(2)	157.5(2)
Symmetry operators: (i) $1-x, 1-y, -z$; (ii) $x, -1+y, z$; (iii) $-x, 1-y, -z$.				

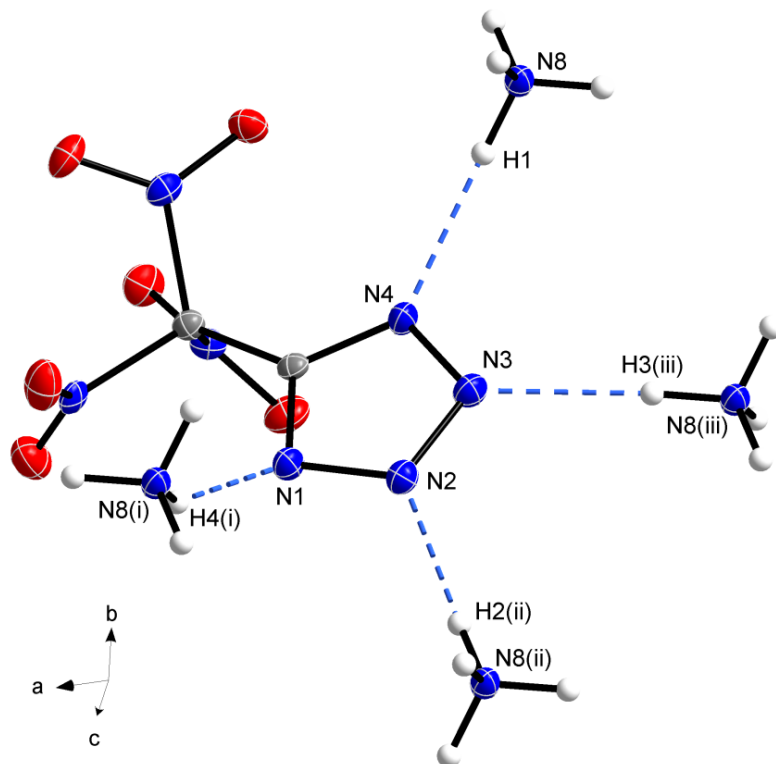


Figure 9: Coordination sphere of the tetrazole ring. Every nitrogen atom of the ring contacts ammonium cations through hydrogen bonds for the structural parameters listed in Table 7. Symmetry operators: (i) $1-x, 1-y, -z$; (ii) $x, -1+y, z$; (iii) $-x, 1-y, -z$.

Crystal Structure of Dihydroxylammonium 5-(Dinitromethylide)-Tetrazolate (5)

Dihydroxylammonium 5-(dinitromethylide)-tetrazolate (**5**) crystallises as yellow rods in the orthorhombic space group *Ima2* with four formulas in the unit cell and a calculated maximum density of 1.596 g·cm⁻³ at 173(2) K. One of the hydroxylammonium cations is disordered (Figure 10), which makes refinement taking into account the corresponding protons problematic. However, the structure of the anion can be determined without residual electron density nearby the nitrogen atoms of the tetrazolate ring and the carbon atom of the dinitromethylide group. This indicates the presence of the dianion with two hydroxylammonium cations in the crystal. The protons shown in Figure 10 were all calculated and therefore their possible interactions cannot be discussed. The structure of the dianion is almost planar, which is reflected in the dihedral angles [C1–C2–N3–O2 –178.5(1)°, N2–N2–N1–C1 0.1(2)°, N1–C1–C2–N3 0.4(2)°]. The C1–C2 bond length of 1.466(2) Å and the C1–N1 of 1.349(1) Å correspond to literature known structures of dianionic salts.^[40]

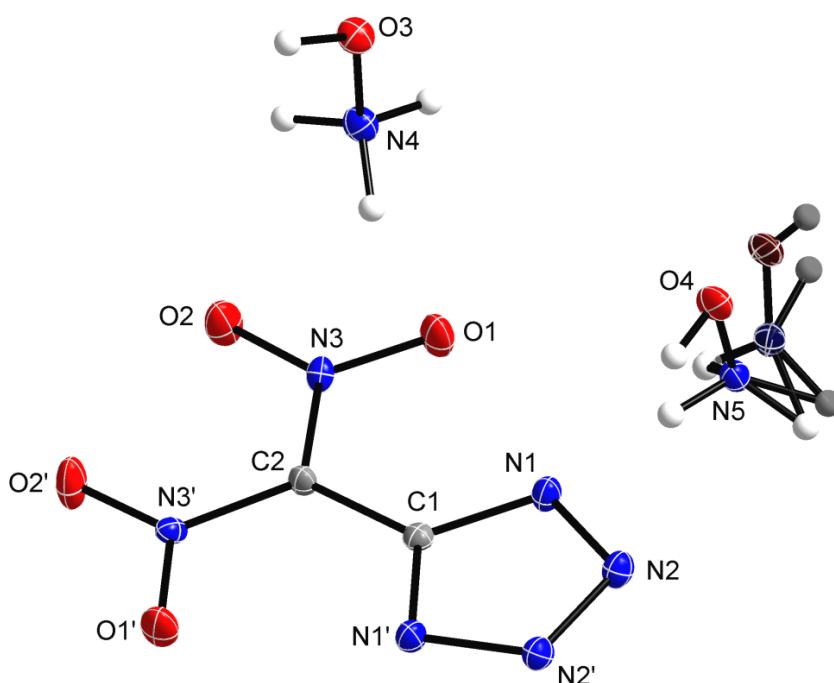


Figure 10: Crystal structure of compound **5**. Selected bond length [Å] and angles [°]: C1–C2 1.466(2), C1–N1 1.349(1), N1–N2 1.340(1), C2–N3 1.415(2), N3–O1 1.242(2), N3–O2 1.240(1), N2–N2' 1.308(2); C1–N1–N2 104.9(2), N1–C1–C2 124.7(2), C1–C2–N3 120.5(2), O1–N3–O2 120.9(2).

Crystal Structure of Dipotassium 5-(Dinitromethylide)-Tetrazolate (6)

Dipotassium 5-(dinitromethylide)-tetrazolate (**6**) crystallises as yellow rods in the orthorhombic space group *Pbcn* with four formulas in the unit cell and a calculated maximum density of $2.157 \text{ g}\cdot\text{cm}^{-3}$ at 100(2) K (Figure 11). To the best of our knowledge, only the crystal structure of the monopotassium salt is known so far,^[1] which mainly differs in the orientation of the dinitromethyl group relative to the five-membered ring. Whereas in the monopotassium salt the anion is almost planar with a C1–C2 bond length of $1.449(1) \text{ \AA}$,^[1] in the structure of the dipotassium salt **6** the dinitromethyl moiety is rotated out of the tetrazole plane with a N1–C1–C2–N3' torsion angle of $93.5(2)^\circ$ and a C1–C2 bond length of $1.463(4) \text{ \AA}$. This indicates, that the negative charge of the dinitromethyl group is not delocalised into the tetrazole ring. The C1–C2 bond length in the structure of the free acid dihydro-(dinitromethylene)-tetrazole is even shorter with $1.418(2) \text{ \AA}$ and the molecule is completely planar.^[40]

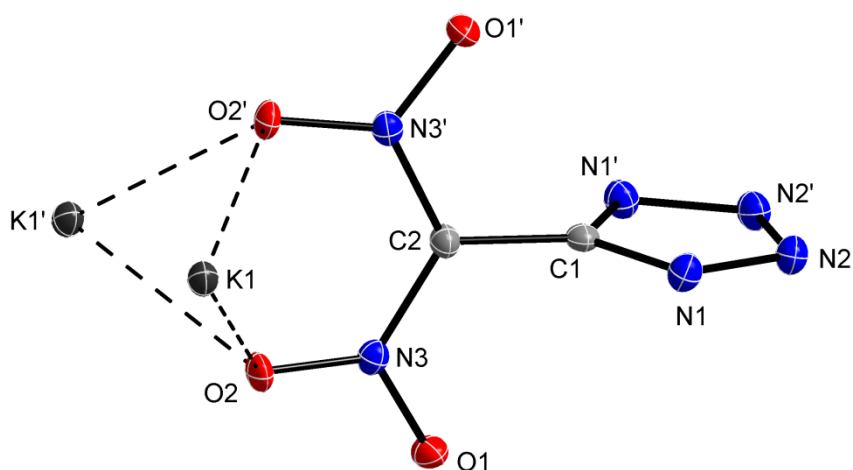


Figure 11: Crystal structure of compound **6**. Selected atom distances, bond lengths [\AA] and angles [$^\circ$]: K1 \cdots O2 $2.997(2)$, K1 \cdots O2' $2.903(2)$; C1–C2 $1.463(4)$, C1–N1 $1.337(2)$, N1–N2 $1.344(3)$, C2–N3 $1.384(1)$, N3–O1 $1.264(2)$, N3–O2 $1.250(1)$; O2–K1–O2' $52.1(2)$, K1 \cdots O2 \cdots K1' $101.0(2)$, O1–N3–O2 $120.2(1)$, O2–N3–C2 $123.4(1)$, O1–N3–C2 $116.4(2)$, N3–C2–N3' $120.8(1)$, O1–N3–C2 $116.4(1)$, N1–C1–N1' $111.9(1)$, N1–C1–C2–N3' $93.5(2)$, N1–C1–C2–N3 $-86.5(2)$. Symmetry operator: ') $\frac{1}{2}-x, -\frac{1}{2}+y, z$.

The crystal structure of compound **6** is mainly build up by one repetitive motif illustrated in Figure 12. It forms chains along the *b* axis that run in both directions and in which the molecules are rotated by 90° with respect to each other. Every nitrogen atom of the ring and all oxygen atoms of the nitro groups are involved in ionic contacts to the potassium cations with distances ranging between $2.750(1)$ and $2.830(2) \text{ \AA}$.

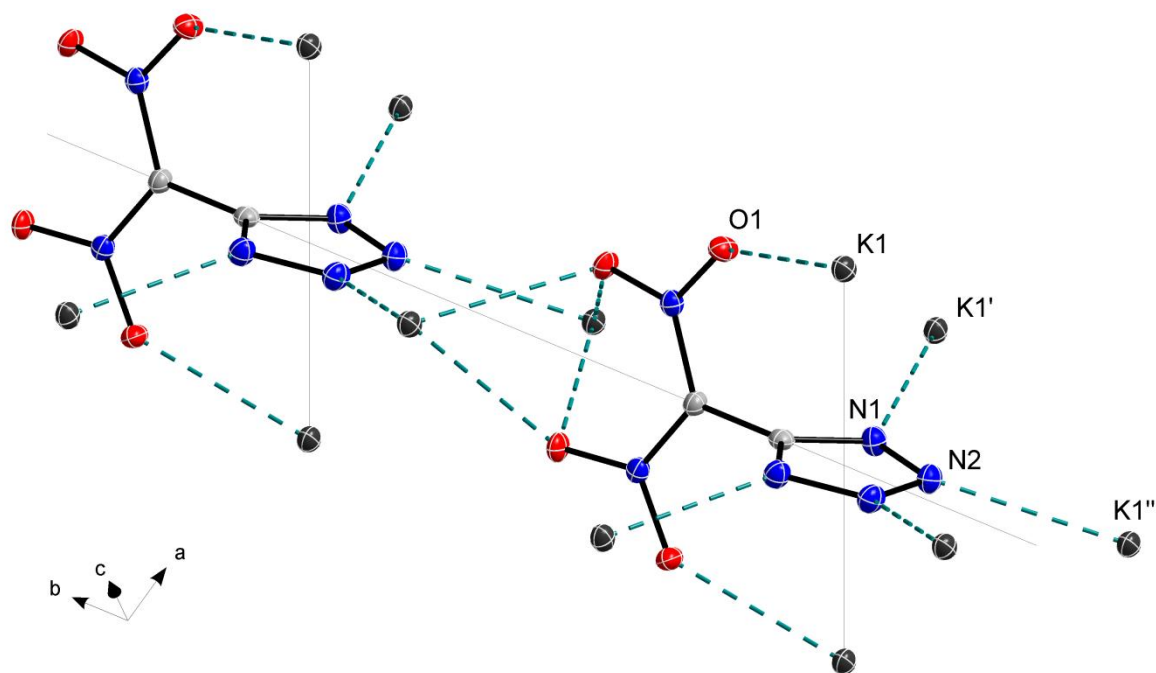


Figure 12: Arrangement of the molecules forming chains along the *b* axis in the crystal structure of compound **6**. Selected atom distances [Å]: O1...K1 2.750(1), N1...K1' 2.774(2), N2...K1'' 2.830(2).

Crystal Structure of Ammonium 5-(Fluorodinitromethyl)-2H-Tetrazolate (14)

Ammonium 5-(fluorodinitromethyl)-2*H*-tetrazolate (**14**) crystallises in the monoclinic space group $P2_1/c$ with eight formulas per unit cell and a calculated maximum density of $1.747 \text{ g}\cdot\text{cm}^{-3}$ at 113(2) K. The structure displays two crystallographically independent 5-(fluorodinitromethyl)-2*H*-tetrazolate anions and ammonium cations in the asymmetric unit (Figure 13). In the anions the C–F bond lengths are slightly shorter than the common single C–F bond length (1.36 Å). The C–NO₂ bond lengths are elongated as compared to the average value of a single C–N bond length (1.47 Å).^[37] The average N–O bond lengths and O–N–O angles are in the range of common nitro groups. The C–C bond lengths are in between the common single (1.54 Å) and double bond (1.33 Å).^[37] The bond lengths and angles within the five-membered rings are in the expected range.

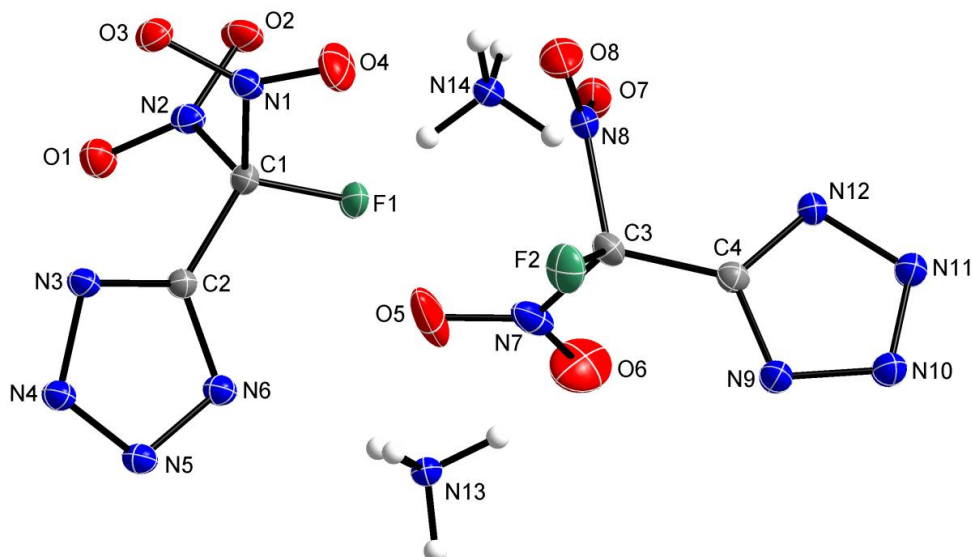


Figure 13: Asymmetric unit in the crystal structure of compound **14**. Selected bond lengths [Å] and angles [°]: N1–O3 1.219 (2), N1–O4 1.210 (2), N2–O1 1.208(2), N2–O2 1.227(2), C1–C2 1.481(3), C3–C4 1.478(2), C1–F1 1.337(2), C3–F2 1.328(3), C1–N1 1.539(2), C1–N2 1.544(2), C2–N3 1.334(2), C2–N6 1.335(2), N3–N4 1.343(2), N4–N5 1.323(1), N5–N6 1.342(2); O1–N2–O2 127.7(1), O3–N1–O4 127.5(1), O1–N2–C1 117.4(1), O2–N2–C1 115.1(1), N1–C1–F1 108.0(1), N2–C1–F1 105.6(1), N1–C1–N2 103.6(1), F1–C1–C2 113.3(1), N3–C2–C1 124.7(1), N4–N5–N6–C2 0.0(1).

It is remarkable that the C–C–N–O torsion angles of both molecules [C2–C1–N1–O3 $-72.4(1)^\circ$, C2–C1–N2–O1 $3.3(1)^\circ$, C4–C3–N8–O7 $71.8(2)^\circ$, C4–C3–N7–O6 $-15.6(2)^\circ$] are not in the typical range for the propeller-like conformation of polynitromethyl moieties ($23\text{--}67^\circ$) described by BRILL *et al.*^[38] Instead the nitro groups are rotated *syn* to each other. This orientation results in intramolecular interactions with N \cdots O, F \cdots O and F \cdots N distances well below the sum of van der Waals radii as depicted in Figure 14.^[39]

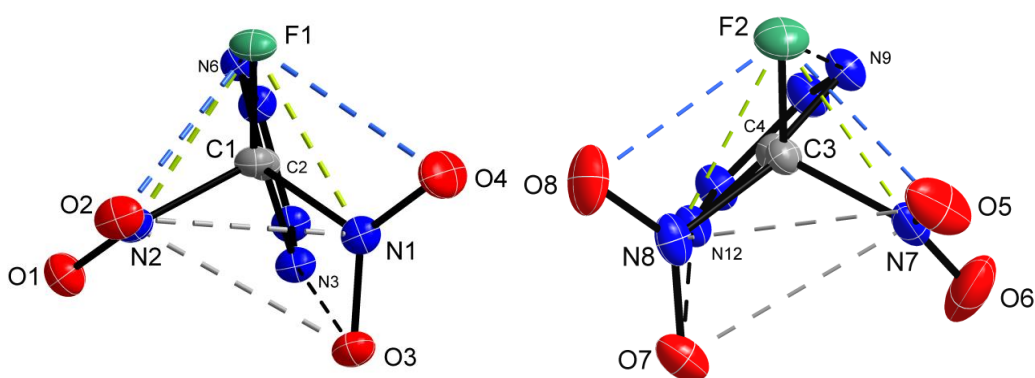


Figure 14: Views along the C1–C2 (left) and C3–C4 (right) bonds of compound **14** illustrating the geometry of the fluorodinitromethyl groups with its intramolecular interactions well below the Σ vdW radii: F1 \cdots O2 2.637(2), F1 \cdots O4 2.544(2), F2 \cdots O5 2.567(2), F2 \cdots O8 2.517 Å (blue dashed lines); F1 \cdots N1 2.329(2), F1 \cdots N2 2.298(2), F2 \cdots N7 2.301(2), F2 \cdots N8 2.320(2) Å (yellow dashed lines); N1 \cdots O2 2.796(2), N2 \cdots O3 2.683(2), N7 \cdots O7 2.694(3), N8 \cdots O5 2.901(3) Å (grey dashed lines); F1 \cdots N6 2.739(3), N3 \cdots O3 2.979(3), F2 \cdots N9 2.871(2), N12 \cdots O7 2.966(3) Å (black dashed lines); Σ vdW: (F,O) = 2.99, (N,O) = 3.07, (F,N) = 3.02 Å.^[39]

The solid state structure of compound **14** consists of ammonium cations and 5-(fluorodinitromethyl)-2*H*-tetrazolate anions that are associated through hydrogen bonds (Figure 15). Similar to the trinitromethyl derivative **4** all nitrogen atoms of the tetrazole rings participate in those. The fluorine atoms form intermolecular short contacts with distances below the sum of van der Waals radii [F1...O5 2.871(2), F2...O2(iii) 2.853(3) Å; Σ vdW: (O,F) = 2.99 Å].^[39] In addition, the typical electrostatic interactions between the nitro groups slightly under the sum of van der Waals radii are observed. One of those [N8...O4 3.024(2) Å] is shown in Figure 15.

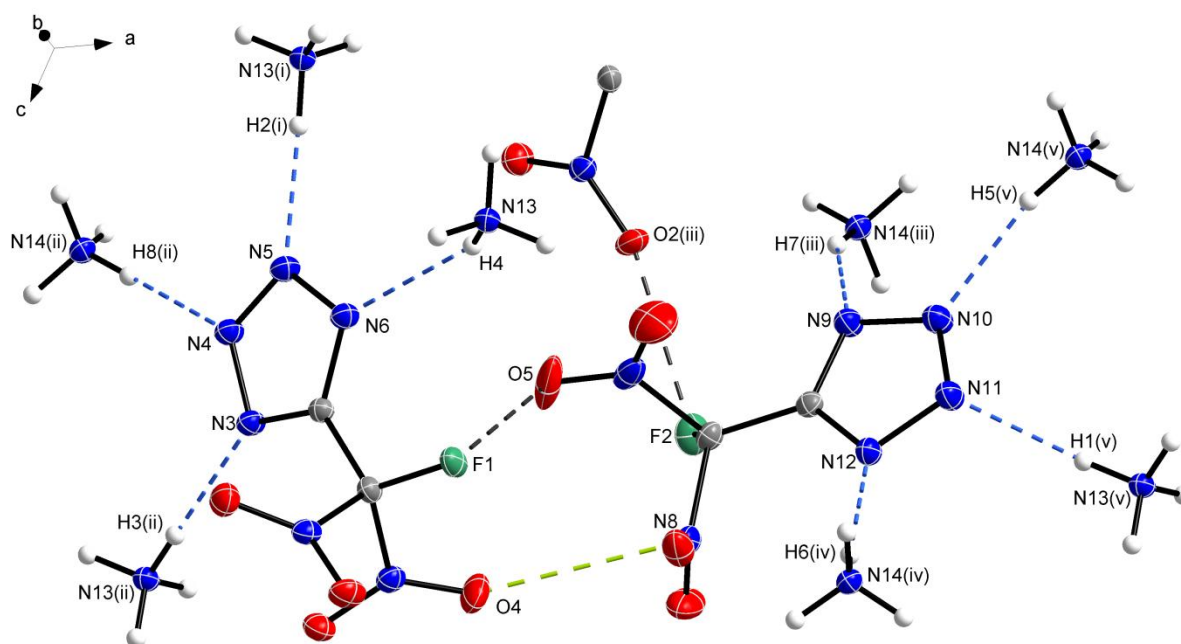


Figure 15: Hydrogen bonds as blue dashed lines and electrostatic interactions as grey and yellow dashed lines in the crystal structure of compound **14** for the structural parameters listed in Table 8. Symmetry operators: (i) $-x, 1-y, -z$; (ii) $-x, -1/2+y, 1/2-z$; (iii) $x, 1/2-y, -1/2+z$; (iv) $1-x, 1-y, 1-z$; (v) $1-x, -1/2+y, 1/2-z$.

Table 8: Structural parameters of the interactions in the crystal structure of compound **14** presented in Figure 15.

D–H...A	d (D–H) [Å]	d (H...A) [Å]	d (D–H...A) [Å]	\angle (D–H...A) [°]
N13(ii)–H3(ii)···N3	0.93(2)	2.02(2)	2.918(3)	164.1(1)
N14(ii)–H8(ii)···N4	0.89(1)	2.13(2)	3.015(3)	173.2(2)
N13(i)–H2(i)···N5	0.92(2)	1.99(2)	2.907(2)	177.0(2)
N13–H4···N6	0.88(2)	2.31(2)	3.053(2)	141.9(1)
N14(iii)–H7(iii)···N9	0.88(1)	2.14(2)	2.949(2)	152.6(1)
N14(v)–H5(v)···N10	0.92(2)	2.08(2)	2.981(2)	168.9(2)
N13(v)–H1(v)···N11	0.92(1)	2.07(2)	2.976(3)	170.2(2)
N14(iv)–H6(iv)···N12	0.92(2)	2.14(2)	3.019(2)	160.7(3)
Electrostatic interactions			d (X...Y) [Å]	Σ vdW radius ^[39]
O4...N8			3.024(3)	3.07
F1...O5			2.871(2)	2.99
F2...O2(iii)			2.853(3)	2.99
Symmetry operators: (i) $-x, 1-y, -z$; (ii) $-x, -1/2+y, 1/2-z$; (iii) $x, 1/2-y, -1/2+z$; (iv) $1-x, 1-y, 1-z$; (v) $1-x, -1/2+y, 1/2-z$.				

Crystal Structure of 2-(2-Nitro-2-Azapropyl)-5-(Trinitromethyl)-2H-Tetrazole (8)

2-(2-Nitro-2-azapropyl)-5-(trinitromethyl)-2H-tetrazole (**8**) crystallises as colourless plates in the orthorhombic space group *Pbca* with eight molecules in the unit cell and a calculated maximum density of 1.796 g·cm⁻³ at 100(2) K (Figure 16).

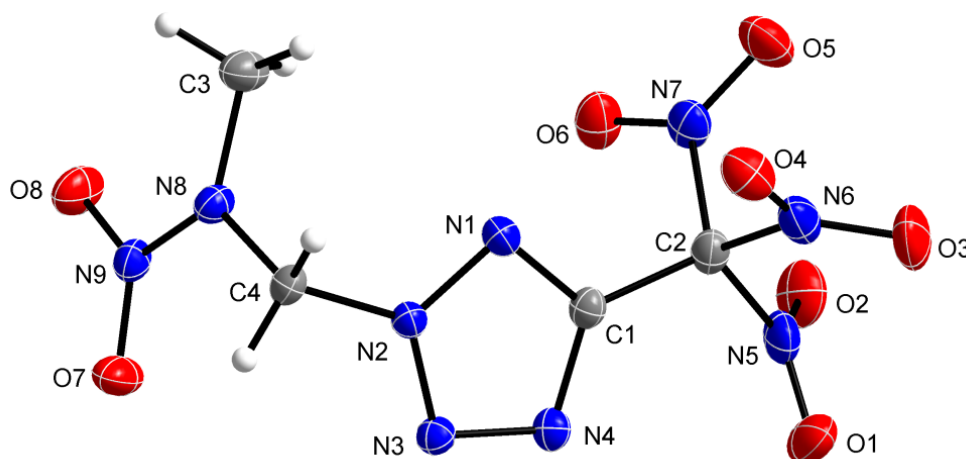


Figure 16: Crystal structure of compound **8**. Selected bond lengths [Å] and angles [°]: C1–C2 1.488(2), N5–C2 1.523(2), N6–C2 1.538(2), N7–C2 1.544(2), O1–N5 1.208(1), O3–N6 1.213(2), O6–N7 1.210(2), N3–N4 1.316(2), N8–N9 1.366(2), O7–N9 1.227(2); N2–C4 1.471(2); O4–N6–O3 127.7(2), C4–N8–C3 122.5(2), C4–N8–N9–O7 –6.9(2), O1–N5–C2–C1 62.4(2), O4–N6–C2–C1 40.8(2), O6–N7–C2–C1 39.2(2).

The C1–C2 bond length with 1.488(2) Å is shorter than a common C–C single bond (1.54 Å).^[37] The C2–N bonds to the nitro groups are slightly elongated [1.523(2)–1.544(2) Å]. The N–O bond lengths of all nitro groups are in the expected range [1.208(1)–1.227(2) Å].

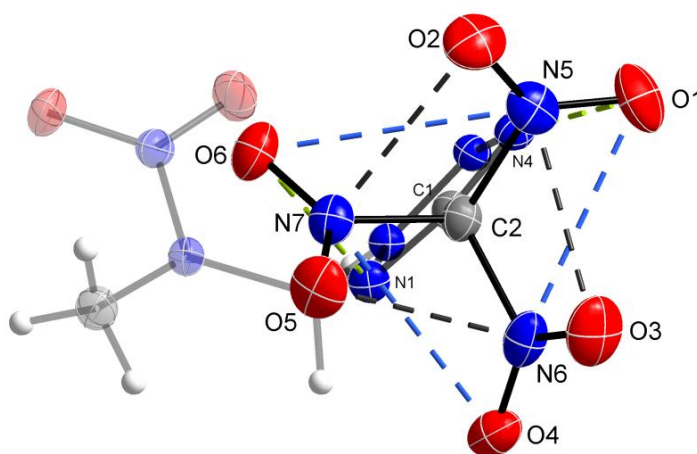


Figure 17: View along the C2–C1 bond displaying the propeller-like conformation of the nitro groups with its intramolecular interactions: N5...O3 2.622(3), N6...O5 2.546(2), N7...O2 2.543(2) Å (grey dashed lines), N5...O6 3.038(2), N7...O4 2.973(2), N6...O1 2.866(2) Å (blue dashed lines), O1...N4 2.857(2), O6...N1 2.941(2) Å (yellow dashed lines); ΣvdW : (N,O) = 3.07 Å.^[39]

The trinitromethyl group arranges into the typical propeller-like orientation as found in many trinitromethyl containing compounds with several intramolecular steric and electrostatic interactions between the nitro groups well below the sum of van der Waals radii (Figure 17).^[38, 39] This is also reflected in the torsion angles [O1–N5–C2–C1 62.4(2)°, O4–N6–C2–C1 40.8(2)°, O6–N7–C2–C1 39.2(2)°], which are in the range for this propeller-like structure of polynitromethyl moieties described by BRILL *et al.* (23–67°).^[38] The sterical hindrance also causes interactions of the oxygen atoms O1 and O6 with the α nitrogen atoms N4 and N1 of the tetrazole ring well below the sum of van der Waals radii (yellow dashed lines in Figure 17).

The crystal structure is build up by multiple hydrogen bonds, whereby all hydrogen atoms participate and connect one molecule to six of its neighbours as depicted in Figure 18. The structural parameters of the hydrogen bonds are listed in Table 9.

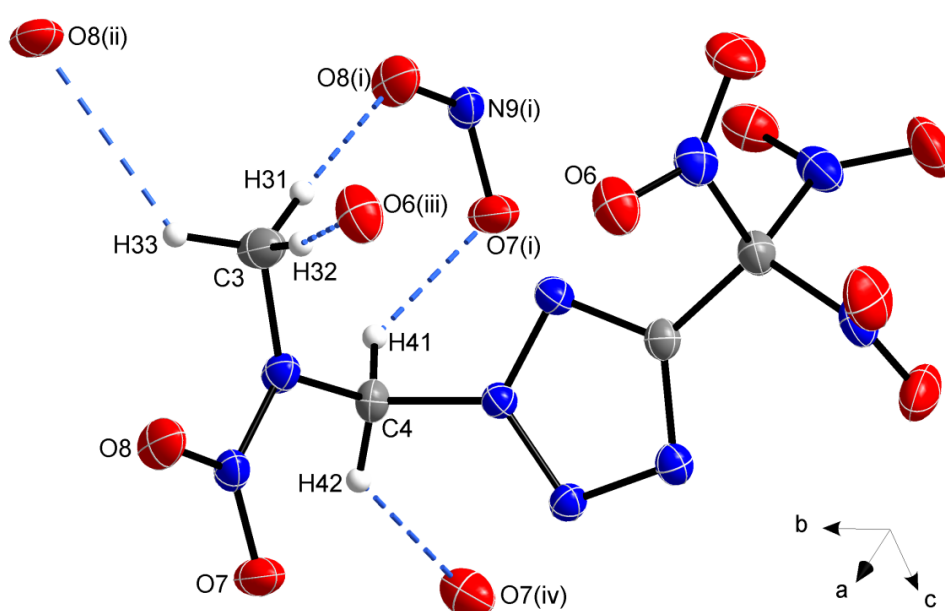


Figure 18: Intermolecular hydrogen bonds presented by blue dashed lines in the crystal structure of compound **8** for the structural parameters given in Table 9. Symmetry operators: (i) $-1+x, y, z$; (ii) $-1/2+x, 1/2-y, -z$; (iii) $1-x, -y, -z$; (iv) $-1/2+x, y, 1/2-z$.

Table 9: Structural parameters of the hydrogen bonds in the crystal structure of compound **8** presented in Figure 18.

D–H···A	d (D–H) [Å]	d (H···A) [Å]	d (D–H···A) [Å]	\angle (D–H···A) [°]
C3–H31···O8'	0.95(2)	2.54(1)	3.479(3)	167.3(9)
C4–H41···O7'	0.95(2)	2.50(1)	3.348(2)	149.5(5)
C3–H33···O8'''	0.94(2)	2.58(2)	3.307(3)	133.6(8)
C3–H32···O6'''	0.95(3)	2.57(2)	3.501(2)	167.1(1)
C4–H42···O7''''	0.94(2)	2.39(2)	3.084(3)	130.7(5)
Symmetry operators: (i) $-1+x, y, z$; (ii) $-1/2+x, 1/2-y, -z$; (iii) $1-x, -y, -z$; (iv) $-1/2+x, y, 1/2-z$.				

Crystal Structure of 2-(2-Nitro-2-Azapropyl)-5-(Fluorodinitromethyl)-2H-Tetrazole (15)

2-(2-Nitro-2-azapropyl)-5-(fluorodinitromethyl)-2H-tetrazole (**15**) crystallises as colourless needles in the monoclinic space group $P2_1/n$ with four molecules in the unit cell and a calculated maximum density of $1.870 \text{ g}\cdot\text{cm}^{-3}$ at 100(2) K (Figure 19). The C1–C2 bond is shorter than a common C–C single bond (1.54 Å)^[37] but with $1.492(2) \text{ Å}$ it is slightly elongated in comparison to the corresponding bond in the analogous compound **8**. The C2–F1 bond is slightly shorter [$1.313(2) \text{ Å}$] than common C–F bonds (1.36 Å).^[37] The C2–N bonds to the nitro groups are elongated [$1.551(2)$ and $1.557(2) \text{ Å}$]. As expected the average N–O bond lengths of the nitro groups [$1.208(2)$ – $1.212(2) \text{ Å}$] show substantial double bond character (standard double N=O bond: 1.17 Å).^[37]

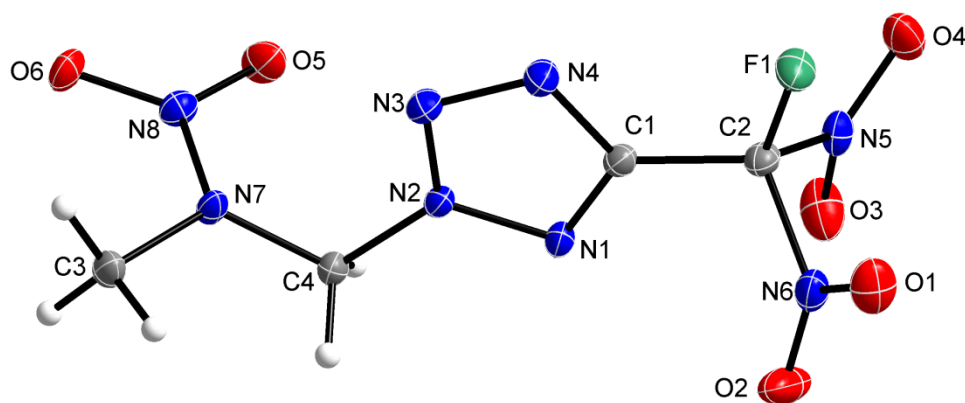


Figure 19: Crystal structure of compound **15**. Selected bond lengths [Å] and angles [$^\circ$]: C1–C2 $1.492(2)$, F1–C2 $1.313(2)$, N6–C2 $1.557(2)$, N5–C2 $1.551(2)$, N7–N8 $1.363(1)$, N3–N4 $1.321(2)$, O3–N5 $1.208(2)$, O2–N6 $1.210(2)$, O5–N8 $1.234(1)$, N7–C3 $1.461(2)$, N2–C4 $1.486(2)$; O4–N5–O3 $127.7(1)$, C4–N7–C3 $123.0(1)$, C4–N7–N8 $116.6(1)$, N4–C1–C2–F1 $0.4(1)$, C1–C2–N6–O2 $53.6(2)$, O3–N5–C2–C1 $59.9(1)$.

Differing from the starting material **14** the orientation of the fluorodinitromethyl moiety shows the propeller-like conformation, here with C1–C2–N–O torsion angles [C1–C2–N5–O3 $-59.9(2)^\circ$, C1–C2–N6–O2 $53.6(1)^\circ$] in the typical range for the propeller-like structure as described by BRILL *et al.* (23 – 67°).^[38] The fluorine atom strongly stabilises this orientation by interacting with the oxygen atoms O1 and O4 of the nitro groups (blue dashed lines in Figure 20) and the nitrogen atoms N5 and N6 of the nitro groups (yellow dashed lines in Figure 20). Also the N...O distances between the nitro groups are clearly under the sum of van der Waals radii (grey dashed lines in Figure 20).^[39] The sterical hindrance also causes atom distances well below the sum of van der Waals radii between the fluorodinitromethyl unit and the nitrogen atoms of the tetrazole ring. O2...N1 and O3...N1 are highlighted as red dashed lines in Figure 20, and the fluorine atom F1 contacts N4 of the ring.

The structure of compound **15** is built up by extensive hydrogen bonding. Similar to compound **8** all hydrogen atoms participate in those hydrogen bonds and connect one molecule to eight of its neighbours (Figure 21, Table 10). Differing from compound **8** the tetrazole rings are orientated parallelly to each other.

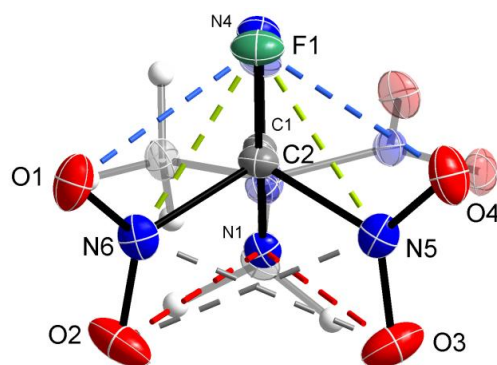


Figure 20: View along the C2–C1 bond displaying the propeller-like arrangement of the fluorodinitromethyl group with its intramolecular interactions as dashed lines: F1...O4 2.480(1), F1...O1 2.481(1) Å (blue), F1...N5 2.315(1), F1...N6 2.315(2) Å (yellow), N5...O2 2.941(1), N6...O3 2.883(1) Å (grey); N1...O2 2.945(2), N1...O3 2.971(1) Å (red); F1...N4 2.676(1) Å; Σ vdW: (F,O) = 2.99, (F,N) = 3.02, (N,O) 3.07 Å.^[39]

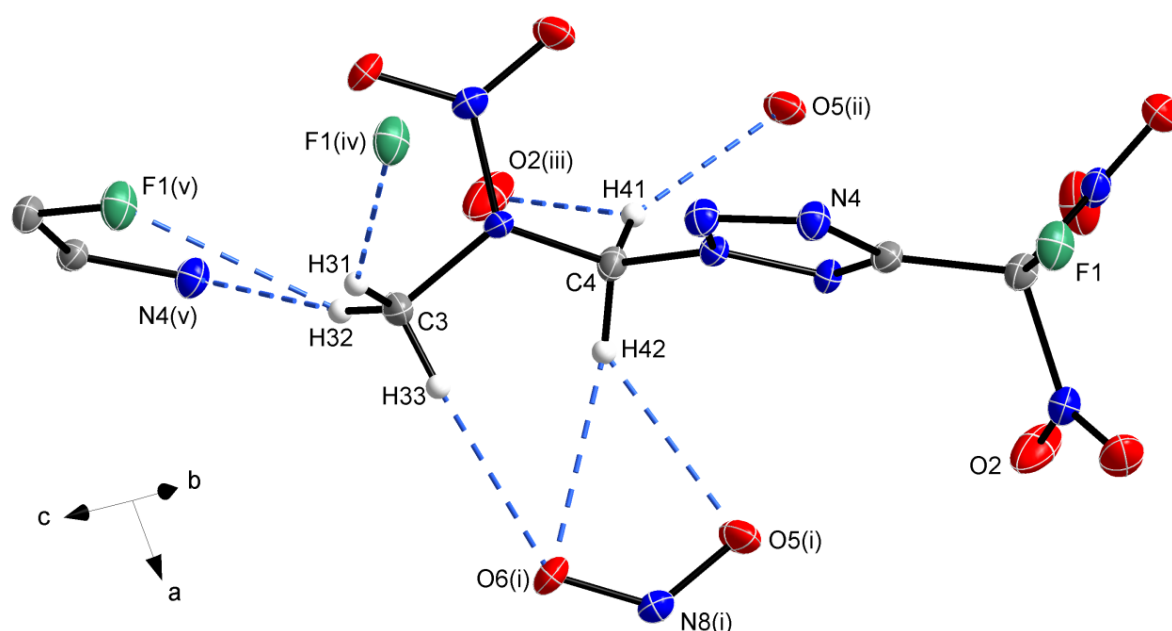


Figure 21: Intermolecular hydrogen bonds presented by blue dashed lines in the crystal structure of compound **15** for the structural parameters listed in Table 10. Symmetry operators: (i) $1+x, y, z$; (ii) $-x, -y, 1-z$; (iii) $1-x, -y, 1-z$; (iv) $-\frac{1}{2}+x, \frac{1}{2}-y, \frac{1}{2}+z$; (v) $\frac{1}{2}-x, -\frac{1}{2}+y, 1\frac{1}{2}-z$.

Table 10: Structural parameters of the hydrogen bonds in the crystal structure of compound **15** presented in Figure 20.

D–H...A	d (D–H) [Å]	d (H...A) [Å]	d (D–H...A) [Å]	\angle (D–H...A) [°]
C4–H42...O5(i)	0.98(2)	2.50(2)	3.287(1)	137.5(4)
C4–H42...O6(i)	0.98(2)	2.57(2)	3.479(2)	155.0(3)
C3–H33...O6(i)	0.97(2)	2.47(2)	3.382(2)	157.9(5)
C4–H41...O5(ii)	0.95(1)	2.41(2)	3.270(2)	150.4(1)
C4–H41...O2(iii)	0.95(1)	2.64(1)	3.239(1)	122.0(5)
C3–H31...F1(iv)	0.94(2)	2.69(2)	3.460(1)	139.8(2)
C3–H32...F1(v)	0.98(2)	2.70(2)	3.264(2)	117.3(2)
C3–H32...N4(v)	0.98(2)	2.66(2)	3.623(2)	170.4(4)
Symmetry operators: (i) $1+x, y, z$; (ii) $-x, -y, 1-z$; (iii) $1-x, -y, 1-z$; (iv) $-\frac{1}{2}+x, \frac{1}{2}-y, \frac{1}{2}+z$; (v) $\frac{1}{2}-x, -\frac{1}{2}+y, 1\frac{1}{2}-z$.				

3.6 Physical, Chemical and Energetic Properties

Owing to the energetic nature of all described compounds **4**, **5**, **6**, **8**, **14** and **15** and for initial safety testing their sensitivities and energetic behaviour were investigated. The investigated physical and thermodynamic properties are summarised in Table 11, and the calculated detonation and combustion parameters are listed in Table 12. For convenience, the molecular structures are shown in Figure 22.

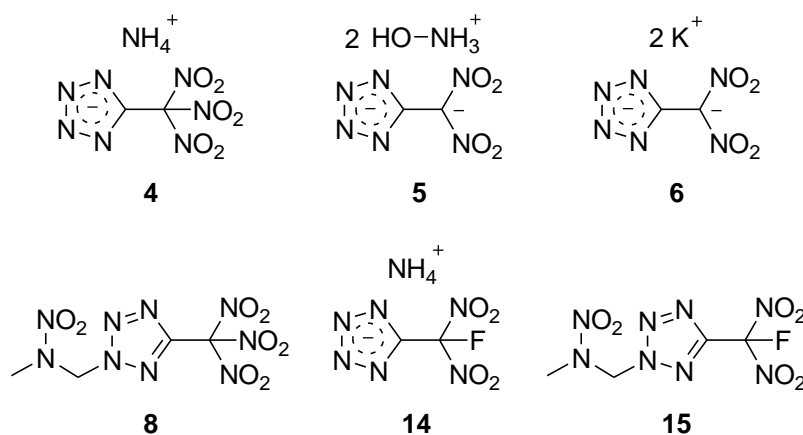


Figure 22: Molecular structures of the compounds discussed in this section with physical and thermodynamic properties and calculated performances listed in Tables 11+12.

Table 11: Physical and thermodynamic data for compounds **4**, **5**, **6**, **8**, **14** and **15**.

	4	5	6	8	14	15
Formula	C ₂ H ₄ N ₈ O ₆	C ₂ H ₈ N ₈ O ₆	K ₂ C ₂ N ₆ O ₄	C ₄ H ₅ N ₉ O ₈	C ₂ H ₄ N ₇ O ₄ F	C ₄ H ₅ N ₈ O ₆ F
FW [g·mol⁻¹]	236.10	240.13	250.28	307.17	209.10	280.13
IS [J]^a	2	1*	4	3	1	2
FS [N]^b	8	80*	144	40	16	36
ESD [J]^c	0.05	n. d.	0.1	0.1	0.1	0.1
grain size [μm]	<100	<100	100–500	100–500	<100	100–500
N [%]^d	47.46	46.66	33.58	41.04	46.89	40.00
N+O [%]^e	88.12	86.64	59.15	82.71	77.50	74.27
Ω_{CO} [%]^f	13.5	0.0	6.4	7.8	0.0	–2.9
Ω_{CO2} [%]^f	0.0	–13.3	–6.4	–13.0	–15.3	–25.7
T_{melt} [°C]^g	–	–	284	87	–	46
T_{dec} [°C]^h	128	164	291	134	166	184
ρ_{RT} [g·cm⁻³]ⁱ	1.78	1.54	2.13	1.75	1.70	1.83
Δ_fH° [kJ·mol⁻¹]^j	231.4	248.6	–335	313.9	6.7	98.3
ΔU° [kJ·kg⁻¹]^k	1074.7	1148.7	–1289	1110.8	126.9	439.4

a) Impact sensitivity (BAM drophammer, method 1 out of 6);^[42–44] b) friction sensitivity (BAM friction tester, method 1 out of 6);^[44–46] *) one test due to lack of compound; c) electrostatic discharge sensitivity (OZM);^[47,48] d) nitrogen content; e) combined nitrogen and oxygen content; f) absolute oxygen balance assuming the formation of CO or CO₂ and HF; g) melting temperature from DSC at a heating rate of 5 °C min⁻¹; h) decomposition temperature from DSC at a heating rate of 5 °C min⁻¹; i) density measured with pycnometer at ambient temperature; j) calculated heat of formation at the CBS-4M level of theory; k) internal energy of formation.

The ammonium salts **4** and **14** as well as the dihydroxylammonium salt **5** decompose without melting at 128, 164 and 166 °C, respectively. Also the dipotassium salt **6** decomposes subsequently after melting (284 °C) at 291 °C. In contrast the alkylated tetrazoles show melting areas of about 50 °C for the trinitromethyl derivative **8**, and about 140 °C for the

fluorodinitromethyl derivative **15**. This fact might be explained by more hydrogen bonding within the structures and is observed for many compounds containing this secondary nitramine moiety.^[41] Comparing the decomposition temperatures of compounds **8** and **15** with the parent ammonium salts **4** and **14**, the thermal stability got improved only slightly, thus indicating that the thermal decomposition of these compounds is strongly dependent on, or starts at the polynitromethyl groups.

The sensitivities towards impact, friction and electrostatic discharge were determined experimentally according to the standards of the German Federal Institute for Materials Research and Testing (BAM).^[44] According to the UN recommendations for the transport of dangerous goods,^[49] all compounds **4–6**, **8**, **14** and **15** shall be classified as sensitive or very sensitive towards impact, and with exception of the dipotassium salt **6** as very or extremely sensitive towards friction. It has to be mentioned that the sensitivities of compound **4** determined by CHRISTE and HAIGES are lower (IS = 6 J, FS = 20 N).^[1] This difference might be explained by the accuracy of the measurements (see the General Procedures section for more information). The alkylation of compounds **4** and **14** to give compounds **8** and **15** improved their impact sensitivities only by 1 J each, and their friction sensitivities by 20–30 N. This again indicates that also the sensitivities towards mechanical stimuli, which can be understood as thermal stress (inducing “hot-spots”),^[50] are dependent on the polynitromethyl moieties in these molecules that are fixed in the propeller-like conformation (see X-ray diffraction section).^[38]

Comparing the impact sensitivities of the analogous compounds **4** with **14**, and **8** with **15** (trinitromethyl versus fluorodinitromethyl), it stands out that the fluorine containing compounds are more sensitive than their corresponding trinitromethyl containing materials. The difference within each pair is only marginal with 1 J, however, this result stands in contrast to KAMLETs theory, that trinitromethyl containing materials are more sensitive towards impact than their fluorodinitromethyl containing analogues, due to the more restricted rotation of the C–NO₂ bonds.^[51]

The electrostatic discharge (ESD) test was carried out to determine whether the compounds are ignitable by the human body, which can generate up to 0.025 J of static energy.^[47, 48] All measured compounds are insensitive towards this energy.

With exception of the dipotassium salt **6** the very high combined nitrogen and oxygen contents ranging from 74.46 to 88.12% might make these tetrazole derivatives interesting for gas generating applications. The trinitromethyl derivatives **4** and **8** show positive oxygen balances assuming the formation of carbon monoxide, as required for oxygen carriers in solid rocket propellants. The densities as obtained from ambient temperature pycnometer measurements range between 1.70 and 1.83 g·cm⁻³. Compound **6** has a density of 2.13 g·cm⁻³. The heats of formation were computed by *ab initio* calculations at the CBS-4M level of theory.^[52] All compounds except the dipotassium salt **6** show positive heats of formation with the highest value of 313.9 kJ·mol⁻¹ calculated for compound **8**.

The detonation and combustion parameters of compounds **4–6**, **8**, **14** and **15** were computed with the EXPLO5 computer code (Version 6.02),^[53] based on the calculated heats of formation and attributed to the corresponding densities at ambient temperature. The results are summarised in Table 12. The detonation velocities and pressures of all these tetrazole derivatives are comparable with those calculated for HMX (1,3,5,7-tetranitro-1,3,5,7-tetraoctane, 9235 m·s⁻¹, 388 kbar), RDX (1,3,5-trinitroperhydro-1,3,5-triazine, 8838 m·s⁻¹,

343 kbar) and PETN (pentaerythrithyltetranitrate, 8404 m·s⁻¹, 309 kbar).^[53] These calculated values for known explosives stand in agreement with the literature known values.^[54] The lowest detonation performance was calculated for dihydroxylammonium 5-(dinitromethylide)-tetrazolate **5**, and the highest for ammonium 5-(fluorodinitromethyl)-tetrazolate **6**. Despite the fact that these compounds reveal rather high sensitivities, they are all very high performing and oxygen-rich explosives. The dipotassium salt **6** reveals a rather high detonation velocity of about 9100 m·s⁻¹ while being thermally stable up to 280 °C. With sensitivities (IS = 4 J, FS = 144 N, ESD = 0.1 J) in the range of PETN (IS = 4 J, FS = 80 N, ESD = 0.1 J),^[54] it might also be a good detonator material with improved performance and thermal stability compared to PETN.

Table 12: Detonation and combustion parameters of compounds **4–6**, **8**, **14** and **15** calculated with the EXPLO5 (Version 6.02) computer code.^[53]

	4	5	6	8	14	15
$-\Delta_{\text{Ex}}U^\circ$ [kJ·kg ⁻¹] ^a	6190	6272	4049	6016	5540	5394
T_{det} [K] ^b	4346	4178	2901	4291	3734	3783
p_{CJ} [kbar] ^c	341	274	289	334	299	342
D_V [m·s ⁻¹] ^d	9058	8358	9137	8704	8476	8773
V_0 [L·kg ⁻¹] ^e	826	294	346	774	801	728
I_{sp} (neat) [s] ^f	270 (3431)	283 (3433)	172 (2697)	273 (3551)	259 (3306)	259 (3328)
I_{sp} (+20 % Al) [s] ^g	275 (4252)	288 (3982)	196 (2993)	274 (4094)	263 (3739)	253 (3440)
I_{sp} (+25 % Al) [s] ^g	270 (4233)	282 (3935)	193 (3041)	261 (3937)	251 (3511)	248 (3139)
I_{sp} (+30 % Al) [s] ^g	258 (4081)	268 (3771)	188 (3075)	248 (3670)	242 (3190)	240 (3082)
I_{sp} (+16% Al, 14% PBAN) [s] ^h	258 (2892)	266 (2815)	189 (2317)	253 (2828)	244 (2724)	244 (2775)
I_{sp} (+10% Al, 14% PBAN) [s] ⁱ	260 (2921)	266 (2744)	173 (1937)	256 (2760)	245 (2490)	246 (2563)
I_{sp} (+18% Al, 12% HTPB) [s] ^j	260 (2949)	268 (2888)	189 (2360)	254 (2901)	246 (2902)	246 (2928)
I_{sp} (+12% Al, 12% HTPB) [s] ^k	266 (3048)	272 (2844)	182 (2289)	258 (2862)	249 (2734)	250 (2774)

a–e) Detonation parameters calculated with EXPLO5 (V6.02) using the 'BKW EOS' equation of state with the default 'BKWG-S' set of constants;^[53] a) heat of detonation; b) detonation temperature; c) detonation pressure; d) detonation velocity; e) volume of gaseous detonation products (assuming only gaseous products).
f–h) Isobaric combustion parameters calculated with EXPLO5 (V6.02) using isobaric combustion conditions, chamber pressure of 70.0 bar versus ambient pressure with equilibrium expansion conditions at the nozzle throat;^[53] isobaric combustion temperature in the combustion chamber in parentheses [K]; f) specific impulse of the neat compound; g) specific impulse of mixtures with 20–30% aluminium; h) specific impulse of mixtures with 70% oxidiser, 16% aluminium, 12% polybutadiene acrylonitrile (PBAN) and 2% epoxyresin as curing agent; the analogue mixture with AP used in the Space Shuttle Programm of NASA^[55] reveals $I_{\text{sp}} = 262$ s and $T_c = 3380$ K; i) higher specific impulse values achieve mixtures in PBAN with 76% oxidiser, 10% aluminium and 2% epoxyresin; j) specific impulse of mixtures with 18% aluminium, 10% hydroxyterminated polybutadiene (HTPB) and 2% hexamethylene diisocyanate as curing agent; the analogue mixture with AP reveals $I_{\text{sp}} = 264$ s and $T_c = 3564$ K; k) higher specific impulse values achieve mixtures in HTPB with 76% oxidiser, 12% aluminium and 2% hexamethylene diisocyanate.

The isobaric combustion in a chamber with 70 bar inner pressure against atmosphere was also calculated using the EXPLO5 (Version 6.02) computer code.^[53] The dipotassium salt **6** is omitted from this discussion as the specific impulse values are too low for comparison due to the potassium atoms. The trinitromethyl containing derivatives **4** and **8** and dihydroxylammonium 5-(dinitromethylide)-tetrazolate **5** show by far the highest specific impulse values as neat compounds as well as in their aluminised (20–30%) mixtures [248(**8**)–288(**5**) s]. When the mixtures are embedded in the polybutadiene binders (PBAN or HTPB),

for all discussed compounds the oxidiser/aluminium ratios of the corresponding AP mixtures (PBAN: 70/16/14; HTPB: 70/18/12) need to be updated. Higher specific impulse I_{sp} values are achieved when using approximately 6% more oxidiser, thus in mixtures with ratios of 76/10/14 in PBAN and 76/12/12 in HTPB. Compounds **4** and **8** show I_{sp} values in the range the original NASA compositions with AP (262–264 s depending on polymeric matrix).^[55, 56] In contrast, the I_{sp} values of compound **5** exceed the AP mixtures by 4–8 s while showing about 400–500 K lower temperatures in the combustion chamber. As a rule of thumb an increase of the value for I_{sp} by 20 s leads empirically to a doubling of the usual carried payload (satellite or warhead) of a rocket.^[4] The I_{sp} values of the fluorine containing materials **14** and **15** in the aluminised mixtures embedded in the polymers PBAN and HTPB are about 10–14 s below the maximum values of AP (262–264 s).^[55, 56] However, these compounds might also be useful for applications that require the toxicity of the assumed toxic fluorine containing combustion products such as agent defeat weapons.^[4]

3.7 Summary, Conclusions and Outlook

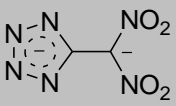
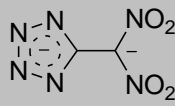
The goal of this study was the alkylation of two 5-(polynitromethyl)-2*H*-tetrazoles with the 2-nitro-2-azapropyl moiety. Two further salts derived from 5-(dinitromethylide)-tetrazolate were synthesised. All compounds during the synthesis routes were fully characterised by various analytical methods including multinuclear (^1H , ^{13}C , ^{14}N , ^{15}N and ^{19}F) NMR spectroscopy and were investigated by single crystal X-ray diffraction giving interesting insights about the structural conformation of the trinitromethyl and fluorodinitromethyl groups. The sensitivities of all compounds towards impact, friction and electrostatic discharge were determined according to BAM standard methods and characterised according to the UN recommendations. The compounds detonation and combustion parameters were calculated and some compounds revealed promising performances (Table 13). From this combined experimental, theoretical and comparative study the following conclusions can be drawn:

- The treatment of 5-(trinitromethyl)-tetrazole with strong nucleophilic bases such as concentrated potassium hydroxide and hydroxylamine (or hydrazine)^[1] subtracts one of the nitro groups yielding corresponding salts of the dianion 5-(dinitromethylide)-tetrazolate. The investigated dipotassium and dihydroxylammonium salts show promising detonation and combustion performances.
- The alkylation of the 5-(polynitromethyl)-substituted tetrazoles is very selective at the β position of the ring system.
- The alkylation barely affects the impact sensitivity, but the friction sensitivity gets slightly improved.
- The target alkylated compounds have a large melting area and higher decomposition points than the starting ammonium salts, which have no melting points.
- Comparing the trinitromethyl compounds with the fluorodinitromethyl compounds, the latter show slightly lower sensitivities, higher decomposition points and the alkylated

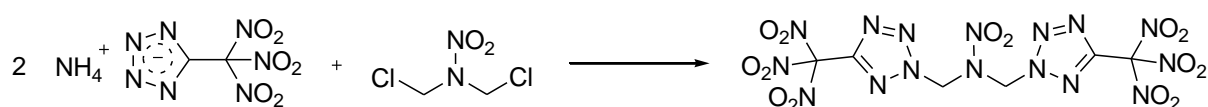
fluorine containing compound shows a much larger melting area than the alkylated trinitromethyl containing compound.

- The calculated heats of formation for the trinitromethyl-containing compounds are more endothermic than those of the fluorine containing compounds. Moreover, they are higher endothermic for the corresponding alkylated compounds.
- All calculated detonation parameters are comparable with those calculated for commonly used explosives ranging from PETN to HMX.
- The dipotassium 5-(dinitromethylide)-tetrazolate **6** reveals desirable detonation parameters while being thermally stable up to 280 °C and shows sensitivities in the range of PETN, thus providing an alternative primary explosive or detonator material.
- The calculated specific impulses I_{sp} of the trinitromethyl containing compounds are in the range of the maximum value of aluminised mixtures of AP, and are considerably higher than those of the fluorodinitromethyl containing compounds.
- The calculated specific impulse I_{sp} of the dihydroxylammonium 5-(dinitromethylide)-tetrazolate **5** and compositions thereof achieve by far the highest values, which are about 8 s higher than the values of aluminised mixtures of AP. Therefore it would be of interest to re-synthesise this material for full characterisation and further investigations.

Table 14: Molecular structures of the promising compounds **5** and **6** with their characteristic properties, calculated performances and possible applications.

	5	6
Molecular structure	2 HO-NH_3^+ 	2 K^+ 
IS [J]	1	4
FS [N]	80	144
T_{dec} [°C]	164	291
ρ_{RT} [g·cm ⁻³]	1.76	2.13
D_V [m·s ⁻¹]	9215	9137
p_{CJ} [kbar]	361	289
I_{sp} (Al+HTPB) [s]	272	182
Possible applications	oxidiser/propellant	primary explosive

Owing to these promising properties and although the sensitivities towards mechanical stimuli of all compounds discussed in this chapter are rather high, for future work it is recommended to further investigate alkylated derivatives of 5-(trinitromethyl)-2*H*-tetrazole. For instance, reactions that combine two or more of these tetrazole derivatives with an appropriate linker may furnish new molecules with interesting properties and performances (Scheme 2).



Scheme 2: The linkage of two 5-(trinitromethyl)-2*H*-tetrazoles by a secondary nitramine might be a good example for future work.

3.8 Experimental

Ethyl 2-(1*H*-tetrazol-5-yl)acetate (2):^[26] 20.2 g ethyl 2-cyanoacetate (**1**, 0.179 mmol), 12.3 g sodium azide (0.189 mmol) and 10.1 g ammonium chloride (0.189 mmol) were dissolved in dimethylformamide (130 mL) and stirred at room temperature for 5 h. The reaction mixture was concentrated to the half of the original volume and water (50 mL) was added to dissolve the formed precipitate. The resulting mixture was acidified to pH = 2 with hydrochloric acid. The suspension was filtered, cooled to 4 °C and filtered again yielding 17.0 g of compound **2** (0.11 mmol, 61%) as colourless crystalline solid.

DSC (T_{onset}): $T_{\text{melt}} = 124$ °C; **¹H NMR** (d_6 -acetone): $\delta = 1.21$ (t, $^3J_{\text{H-H}} = 7.3$ Hz, CH_3), 3.40 (br, CN_4H), 4.16 (s, $\text{CH}_2\text{CN}_4\text{H}$), 4.17 (q, $^3J_{\text{H-H}} = 7.3$ Hz, CH_2) ppm; **¹³C{¹H} NMR** (d_6 -acetone): $\delta = 14.4$ (CH_3CH_2), 30.5 ($\text{CH}_2\text{CO}_2\text{Et}$), 62.3 (CH_3CH_2), 168.5 (CN_4H) ppm; **IR**: $\tilde{\nu}$ (rel. int.) = 3473 (m), 3132 (m), 3022 (m), 2997 (s), 2987 (s), 2974 (s), 2941 (m), 2911 (s), 2871 (m), 2798 (m), 2733 (m), 2688 (m), 2611 (w), 2461 (w), 1745 (s), 1703 (w), 1567 (m), 1480 (m), 1454 (m), 1438 (m), 1395 (s), 1382 (s), 1333 (s), 1249 (m), 1220 (s), 1199 (s), 1161 (w), 1105 (m), 1051 (s), 1034 (s), 942 (s), 882 (m), 807 (w), 787 (m); 723 (w), 711 (w), 684 (m) cm^{-1} ; **Raman** (80 mW): $\tilde{\nu}$ (rel. int.) = 2978 (75), 2942 (100), 2915 (23), 2876 (18), 1751 (15), 1567 (6), 1456 (13), 1397 (9), 1384 (7), 1339 (11), 1259 (11), 1201 (5), 1113 (9), 1091 (15), 1052 (10), 949 (5), 885 (15), 713 (6), 687 (4) cm^{-1} .

2-(1*H*-tetrazol-5-yl)acetic acid (3):^[27] 1.0 g ethyl 2-(1*H*-tetrazol-5-yl)acetate (**2**, 6.40 mmol) was dissolved in methanol (5 mL), followed by the addition of methanolic sodium hydroxide solution (3M, 4 mL). The mixture was heated to reflux for 4 h, whereafter the solvent was removed under reduced pressure. The residue was dissolved in a small amount of water and acidified with concentrated hydrochloric acid to pH \approx 1. After extraction with ethyl acetate (5 \times 20 mL) 600 mg of compound **3** (4.68 mmol, 73%) was obtained as colourless crystals.

¹H NMR (D_2O): $\delta = 3.75$ (s, 2 H, CH_2), 4.17 (br, 1 H, OH) ppm; **¹³C{¹H} NMR** (D_2O): $\delta = 29.3$ (CH_2), 150.9 (CCH_2), 171.2 (CO) ppm.

Ammonium 5-(trinitromethyl)-2*H*-tetrazolate (4):^[1] 8.3 mL sulfuric acid (96%) was cooled to -10 °C and 2.5 mL nitric acid (100%) was added dropwise. 400 mg 2-(1*H*-tetrazol-5-yl)acetic acid (**3**, 3.12 mmol) was added slowly in small portions. The reaction mixture was allowed to warm up to room temperature and was stirred for 16 h. The mixture was poured on 20 g of ice, extracted with dichloromethane (4 \times 50 mL) and dried over sodium sulfate. After concentration of the solution under reduced pressure, 1 mL aqueous ammonia (25%) was added and the solvent was removed under reduced pressure. The residue was re-crystallised from ethyl acetate/toluene (1:1) yielding 670 mg of the tetrazolate **4** (2.83 mmol, 91%) as yellowish crystals.

DSC (T_{onset}): $T_{\text{dec}} = 128$ °C; **¹H NMR** (D_2O): $\delta = 7.22$ (br, 4 H, NH_4) ppm; **¹³C{¹H} NMR** (D_2O): $\delta = 152.2$ (C_{Tz}), 127.9 ($\text{C}(\text{NO}_2)_3$) ppm; **¹⁵N{¹H} NMR** (D_2O): $\delta = 11.8$ (N_α), -28.3 (NO_2), -51.8 (N_β), -362.8 (NH_4^+) ppm; **EA**: $\text{C}_2\text{H}_4\text{N}_8\text{O}_6$ (236.10 $\text{g}\cdot\text{mol}^{-1}$) calcd: C, 10.17, H, 1.71, N, 47.46; found: C, 10.46, H, 1.83, N, 46.91 %; **IR**: $\tilde{\nu}$ (rel. int.) = 3172 (w), 2981 (m), 2878 (m), 1696 (w), 1623 (w), 1603 (m), 1587 (s), 1527 (w), 1456(s), 1440 (s), 1391 (m), 1356 (w), 1314 (w), 1284 (m), 1204 (w), 1106 (s), 1045 (w), 1021 (w), 988 (m), 843 (s), 800

(vs), 748 (w), 733 (m), 688 (w) cm^{-1} ; **Raman** (200 mW): $\tilde{\nu}$ (rel. int.) = 2999 (20), 2870 (16), 1711 (8), 1696 (7), 1619 (34), 1597 (10), 1524 (5), 1434 (100), 1357 (21), 1293 (16), 1207 (18), 1148 (6), 1109 (23), 1072 (30), 1021 (21), 990 (28), 952 (39), 846 (46), 821 (22), 641 (6) cm^{-1} ; **MS** (FAB⁻): m/z = 218.1 [$\text{C}_2\text{N}_7\text{O}_6$]⁻; (FAB⁺): m/z = 18.1 [NH_4]⁺; **drophammer**: 2 J; **friction tester**: 8 N; **ESD**: 0.05 J; **grain size**: <100 μm .

Dihydroxylammonium 5-(dinitromethylide)-tetrazole (5): 6.6 mL sulfuric acid (96%) was cooled to $-10\text{ }^\circ\text{C}$ and 2.0 mL nitric acid (100%) was added dropwise. 400 mg 2-(1*H*-tetrazol-5-yl)acetic acid (**3**, 3.12 mmol) was added slowly in small portions. The reaction mixture was allowed to warm up to room temperature and was stirred for 16 h. The mixture was poured on 25 g of ice, extracted with dichloromethane ($4 \times 50\text{ mL}$) and dried over sodium sulfate. After concentration of the solution under reduced pressure, 1 mL aqueous hydroxylammonia (50%) was added and the solvent was removed under reduced pressure. The residue was re-crystallised from ethyl acetate/toluene (1:1) yielding 100 mg of the tetrazolate **5** (0.40 mmol, 13%) as yellow crystals.

DSC (T_{onset}): T_{dec} = $164\text{ }^\circ\text{C}$; **drophammer**: 1 J; **friction tester**: 80 N; **grain size**: 100 μm .

Dipotassium 5-(dinitromethylide)-tetrazolate (6): A solution of 0.5 g (2.12 mmol) of compound **4** in water (100 mL) was acidified with hydrochloric acid until pH = 2 was reached and extracted with dichloromethane ($4 \times 40\text{ mL}$). The organic phases were dried over sodium sulfate and the solvent evaporated under reduced pressure. The residue was treated with an aqueous solution of KOH (10M) overnight, the solvent was evaporated under reduced pressure and the residue is re-crystallised in a 1:1 mixture of ethyl acetate and toluene (20 mL) yielding 410 mg of the dipotassium salt **6** (1.64 mmol, 77%) as colourless crystals.

DSC (T_{onset}): T_{melt} = $284\text{ }^\circ\text{C}$, T_{dec} = $291\text{ }^\circ\text{C}$; $^{13}\text{C}\{^1\text{H}\}$ **NMR** (d_6 -acetone): δ = 155.2 (C_{Tz}), 128.5 ($\text{C}(\text{NO}_2)_2$); ^{14}N **NMR** (d_6 -acetone) δ = -23 (NO_2); **drophammer**: 4 J; **friction tester**: 160 N; **ESD**: 0.1 J; **grain size**: 100–500 μm .

2-(2-nitro-2-azapropyl)-5-(trinitromethyl)-tetrazole (8): 130 mg 2-nitro-2-azapropyl chloride (**7**, 1.04 mmol), was added to a solution of 250 mg ammonium 5-(trinitromethyl)-tetrazolate (**4**, 1.06 mmol) in anhydrous acetone (10 mL). The solution was stirred overnight at ambient temperature. Precipitated ammonium chloride was filtered off and washed with dichloromethane. Water (10 mL) was added to the filtrate and the mixture was extracted with dichloromethane ($4 \times 10\text{ mL}$). The combined organic phases were dried over sodium sulfate and the solvent was concentrated to 2 mL under reduced pressure. Methanol (2 mL) was added to the residue and the 1:1 mixture was kept at $8\text{ }^\circ\text{C}$ overnight whereas 250 mg of the desired compound **8** crystallised as colourless crystals (0.81 mmol, 78%).

DSC ($5\text{ }^\circ\text{C min}^{-1}$): T_{melt} = $87\text{ }^\circ\text{C}$, T_{dec} = $134\text{ }^\circ\text{C}$; ^1H **NMR** (d_6 -acetone): δ = 7.00 (s, 2H, CH_2), 3.70 (s, 3H, CH_3) ppm; $^{13}\text{C}\{^1\text{H}\}$ **NMR** (d_6 -acetone): δ = 152.3 (C_{Tz}), 121.2 ($\text{C}(\text{NO}_2)_3$), 67.6 (CH_2), 38.6 (CH_3) ppm; ^{14}N **NMR** (d_6 -acetone): δ = -33 (NNO_2), -37 ($\text{C}(\text{NO}_2)_3$) ppm; **EA** ($\text{C}_4\text{H}_5\text{N}_9\text{O}_8$, 307.17): calc.: C 15.64, H 1.64, N 41.04 %; found: C 18.43, H 2.08, N 25.09 %; **IR**: $\tilde{\nu}$ (rel. int.) = 3068 (w), 3007 (w), 2883 (w), 1623 (m), 1598 (s), 1540 (s), 1468 (m), 1447 (m), 1420 (m), 1384 (w), 1331 (m), 1299 (s), 1258 (s), 1198 (m), 1132 (m), 1101 (w), 1044 (m), 1010 (s), 987 (m), 961 (w), 943 (m), 857 (w), 843 (s), 821 (w), 798 (s), 760 (s), 734 (m), 690 (m), 654 (w) cm^{-1} ; **Raman** (300 mW): $\tilde{\nu}$ (rel. int.) = 3069 (34), 3038 (34), 3008 (100),

2963 (72), 2890 (20), 2859 (12), 1627 (20), 1608 (26), 1541 (9), 1487 (60), 1422 (18), 1398 (30), 1347 (12), 1305 (21), 1261 (42), 1134 (8), 1046 (27), 989 (29), 962 (30), 946 (40), 859 (86), 845 (61), 803 (7), 770 (10), 691 (8), 656 (10), 604 (17) cm^{-1} ; **MS** (FAB[−]): m/z = 306.4 [$\text{M}-\text{H}^-$]; **drophammer**: 3 J; **friction tester**: 40 N; **ESD**: 0.1 J; **grain size**: 100–500 μm .

Ethyl (hydroxyimino)cynoacetate (9):^[31] 17.5 g ethyl cyanoacetate (**1**, 16.5 mL, 155 mmol) was suspended in a vigorously stirred solution of 21.4 g sodium nitrite (310 mmol) in water (125 mL). The solution was ice-cooled and 11.0 g of phosphoric acid (85%) was added dropwise in such manner that the pH was maintained at approximately 4–5 and the temperature did not rise above 40 °C, which took about 30 min. The reaction mixture was stirred at 30 °C for additional 30 min. The temperature was risen to 50 °C before it was acidified with 12.7 mL concentrated hydrochloric acid. Then the mixture was cooled slowly to −5 °C, compound **9** precipitated and was collected by filtration. Even more product **9** was recovered from the solution by extraction with diethyl ether (3 × 50 mL). Drying under reduced pressure yielded 21.6 g of compound **9** (152 mmol, 98%) as colourless solid.

¹H NMR (*d6*-acetone): 4.35 (q, $^3J_{\text{H-H}} = 7.0$ Hz, 2H, CH_2), 3.28 (br, 1H, OH), 1.32 (t, $^3J_{\text{H-H}} = 7.0$ Hz, 3H, CH_3) ppm; **¹³C{¹H} NMR** (*d6*-acetone): 159.2 (COO), 127.6 (CNOH), 108.9 (CN), 63.5 (CH_2), 14.2 (CH_3) ppm; **¹⁴N{¹H} NMR** (*d6*-acetone): −6 (CNOH), −105 (CN) ppm.

Ethyl dinitrocynoacetate (10):^[31] 18 mL of concentrated sulfuric acid was ice-cooled and 7 mL concentrated nitric acid was added dropwise maintaining the temperature below 5 °C. 10.0 g of compound **9** (70.4 mmol) was added in small portions to the reaction mixture at the same temperature (below 5 °C). It was stirred for 1.5 hours at 15–20 °C, whereat two layers formed. The lower layer of acids was drained and quenched. The upper layer was dissolved in dichloromethane and washed with water (3 × 50 mL). The organic phase was dried over sodium sulfate, filtered and concentrated under reduced pressure yielding 14.0 g of compound **10** (69.0 mmol, 98%) as yellowish oil.

¹H NMR (CDCl_3) δ = 4.61 (q, $^3J_{\text{C-H}} = 7.2$ Hz, 2H, OCH_2CH_3), 1.46 (t, $^3J_{\text{C-H}} = 7.2$ Hz, 3H, OCH_2CH_3) ppm; **¹³C{¹H} NMR** (CDCl_3) δ = 152.3 (CO), 109.3 ($\text{C}(\text{NO}_2)_2$), 105.7 (CN), 68.8 (OCH_2CH_3), 13.6 (OCH_2CH_3) ppm; **¹⁴N{¹H} NMR** (CDCl_3) δ = −37 ($\text{C}(\text{NO}_2)_2$), −102 (CN) ppm.

Potassium dinitroacetonitrile (11):^[32] 5.5 g of the crude ethyl cyanodinitroacetate (**10**, 27.1 mmol) was dissolved in ethanol (11.3 mL) and added dropwise to a cooled solution of 3.83 g potassium bromide (32.2 mmol) in water (8.0 mL). The reaction mixture was stirred at room temperature for 1 h, then cooled to 0 °C, filtrated and re-crystallised from acetone to yield 3.4 g of compound **11** (20.3 mol, 75%) as yellow crystalline solid.

¹³C{¹H} NMR (D_2O) δ = 112.9 (CN) ppm; **¹⁴N{¹H} NMR** (D_2O) δ = −24 (NO_2), −110 (CN) ppm; **EA** ($\text{C}_2\text{KN}_3\text{O}_4$): calc.: C 14.20, N 24.84 %; found: C 14.33, N 24.64 %; **IR**: $\tilde{\nu}$ (rel. int.) = 2234 (m), 1500 (s), 1428 (m), 1368 (vw), 1253 (vs), 1242 (vs), 1155 (s), 856 (m), 773 (m), 745 (s) cm^{-1} ; **Raman** (200 mW): $\tilde{\nu}$ (rel. int.) = 2236 (100), 1496 (8), 1424 (13), 1360 (45), 1292 (3), 1257 (26), 1247 (16), 1213 (60), 1148 (27), 858 (50), 775 (2), 571 (2) cm^{-1} ; **MS** (high res., FAB[−]): m/z = 130.1 [$\text{C}_2\text{HN}_3\text{O}_4^-$], 120.0 [$\text{C}_2\text{N}_3\text{O}_4^-$].

Ammonium 5-(fluorodinitromethyl)-tetrazolate (14): 10.0 g (28.4 mmol) *Selectfluor*TM was added to a yellow solution of 3.0 g potassium dinitroacetonitrile (**11**, 17.7 mmol) in anhydrous acetonitrile (100 mL) and the mixture was stirred until the reaction mixture turned colourless (2–3 h). The reaction mixture was distilled (82 °C) by means of an additional argon flow and a cooling trap (–78 °C) and fluorodinitroacetonitrile (**12**) was detected by multinuclear NMR spectroscopy in the resulting acetonitrile solution.

(**12**): ¹⁴N{¹H} NMR (*d6*-acetone) $\delta = -37$ (d, ²J_{14N-F} = 11 Hz, NO₂); ¹⁹F NMR (*d6*-acetone) $\delta = -93.3$ (q, ²J_{F-14N} = 11 Hz, C(NO₂)₂F) ppm.

To the acetonitrile solution containing compound **12** was added 1.48 g (22.8 mmol) sodium azide (or 3 mL trimethylsilyl azide). The reaction mixture was stirred in a barred flask at ambient temperature overnight and additional 12 h at 50 °C. The solvent was evaporated under reduced pressure and the remaining yellow oil was treated with water for 2 h. The solution was filtered off and the water was evaporated again under reduced pressure. The resulting brownish oil was stirred with 4 mL aqueous ammonia (25 %) for 30 min. The solvent was evaporated and the resulting tan solid was re-crystallised in a 1:1 mixture of ethyl acetate and toluene (10 mL) yielding 1.18 g (5.7 mmol, 2 steps yield from **11**: 32 %) ammonium 5-(fluorodinitromethyl)-2*H*-tetrazolate (**6**) as colourless crystals.

(**14**): DSC (*T*_{onset}): *T*_{dec} = 166 °C; ¹H NMR (*d6*-acetone) $\delta = 8.42$ (br. s, 4 H, NH₄); ¹³C{¹H} NMR (*d6*-acetone) $\delta = 150.8$ (d, ²J_{C-F} = 23.0 Hz, C_{Tz}), 119.9 (d, ¹J_{C-F} = 284.7 Hz, C(NO₂)₂F); ¹⁵N{¹H} NMR (*d6*-acetone) $\delta = 9.6$ (N_α), –20.6 (d, ²J_{15N-F} = 16.5 Hz, NO₂), –57.5 (N_β), –362.2 (NH₄⁺); ¹⁹F NMR (*d6*-acetone) $\delta = -95.5$ (br. s, CF) ppm; EA (C₂H₄N₇O₄F): calc.: C 11.49, H 1.93, N 46.89 %; found: C 11.90, H 1.99, N 46.49 %; IR: $\tilde{\nu}$ (rel. int.) = 3192 (m), 3026 (m), 2873 (m), 2806 (m), 1924 (vw), 1685 (vw), 1605 (vs), 1595 (vs), 1457 (vs), 1424 (s), 1408 (m), 1361 (w), 1310 (m), 1238 (s), 1190 (s), 1160 (w), 1152 (w), 1099 (s), 1066 (vw), 1046 (w), 982 (vs), 947 (w), 836 (vs), 798 (vs), 740 (w), 704 (w); Raman (200 mW): $\tilde{\nu}$ (rel. int.) = 3033 (52), 2902 (38), 1683 (10), 1607 (32), 1471 (100), 1362 (43), 1317 (15), 1213 (10), 1190 (50), 1160 (17), 1101 (39), 1068 (20), 984 (53), 949 (60), 838 (70), 803 (10), 651 (8), 530 (7), 444 (16) cm^{–1}; MS (high res., FAB⁺): *m/z* = 190.99 [C₂N₆O₄F]⁺; drophammer: 1 J; friction tester: 16 N; ESD: 0.1 J; grain size: <100 μm.

2-(2-Nitro-2-azapropyl)-5-(fluorodinitromethyl)-tetrazole (15): 150 mg 2-nitro-2-azapropyl chloride (**7**, 1.20 mmol) were added to a solution of 250 mg ammonium 5-(fluorodinitromethyl)-tetrazolate (**14**, 1.20 mmol) in anhydrous acetone (10 mL). The solution was stirred overnight at ambient temperature. Precipitated ammonium chloride was filtered off and washed with dichloromethane. Water (10 mL) was added to the filtrate and the mixture was extracted with dichloromethane (4 × 10 mL). The combined organic phases were dried over sodium sulfate and the solvent was concentrated to 2 mL under reduced pressure. Methanol (2 mL) was added to the residue, and the 1:1 mixture was kept at 8 °C overnight whereas 260 mg of the desired compound **15** crystallised as colourless crystals (0.93 mmol, 78 %).

DSC (*T*_{onset}): *T*_{melt} = 46 °C, *T*_{dec} = 184 °C; ¹H NMR (*d6*-acetone): $\delta = 6.96$ (s, 2H, CH₂), 3.69 (s, 3H, CH₃) ppm; ¹³C{¹H} NMR (*d6*-acetone): $\delta = 153.7$ (d, ²J_{CF} = 25.4 Hz, C_{Tz}), 115.4 (d, ¹J_{CF} = 282.9 Hz, C(NO₂)₂F), 67.3 (CH₂), 38.6 (CH₃) ppm; ¹⁴N{¹H} NMR (*d6*-acetone): $\delta = -27$ (d, ²J_{14NF} = 10 Hz, C(NO₂)₂F), –32 (s, NNO₂) ppm; ¹⁹F NMR (*d6*-acetone): $\delta = -99.6$ (br, CF); EA (C₄H₅N₈O₆F, 280.13): calc.: C 17.15, H 1.80, N 40.00 %; found: C 18.43, H 2.08, N

25.09 %; **IR**: $\tilde{\nu}$ (rel. int.) = 3050 (w), 3005 (w), 2967 (w), 1626 (s), 1595 (m), 1537 (s), 1461 (m), 1427 (w), 1409 (w), 1349 (m), 1325 (w), 1305 (m), 1260 (s), 1164 (m), 1084 (m), 1054 (w), 1039 (s), 963 (s), 871 (w), 835 (s), 804 (s), 765 (s), 722 (s), 684 (s), 664 (m) cm^{-1} ; **Raman** (300 mW): $\tilde{\nu}$ (rel. int.) = 3069 (34), 3038 (34), 3008 (100), 2963 (72), 2890 (20), 2859 (12), 1627 (20), 1608 (26), 1541 (9), 1487 (60), 1422 (18), 1398 (30), 1347 (12), 1305 (21), 1261 (42), 1134 (8), 1046 (27), 989 (29), 962 (30), 946 (40), 859 (86), 845 (61), 803 (7), 770 (10), 691 (8), 656 (10), 604 (17) cm^{-1} ; **MS** (FAB⁻): m/z = 306.4 [M-H⁻]; **drophammer**: 2 J; **friction tester**: 36 N; **ESD**: 0.1 J; **grain size**: 100–500 μm .

3.9 References

- [1] K. O. Christe, R. Haiges, *Inorg. Chem.* **2013**, 52, 7249–7260.
- [2] J. Feierfeil, M. A. Kettner, T. M. Klapötke, M. Sućeska, S. Wunder, *New Trends in Research of Energetic Materials* (NTREM), Proceedings of the Seminar, 17th, Pardubice, Czech Republic, Apr. 9–11, **2014**, 2, 738–743.
- [3] M. A. Kettner, T. M. Klapötke, *Chem. Eur. J.* **2015**, 21(9), 3755–3765.
- [4] a) T. M. Klapötke, *Chemie der hochenergetischen Materialien*, de Gruyter, Berlin, New York, **2009**; b) T. M. Klapötke, *Chemistry of High-Energy Materials*, 2nd Eng. ed., de Gruyter, Berlin, New York, **2011**.
- [5] a) T. M. Klapötke, D. G. Piercey, *Inorg. Chem.* **2011**, 50, 2732–2734; b) T. M. Klapötke, N. Fischer, D. Fischer, D. Piercey, J. Stierstorfer, M. Reymann, *WO 2013026768 A1*, **2013**.
- [6] a) A. Dippold, T. M. Klapötke, F. A. Martin, *Z. Anorg. Allg. Chem.* **2011**, 637, 1181–1193; b) T. M. Klapötke, Thomas, C. Pflüger, M. Sućeska, *New Trends in Research of Energetic Materials*, NTREM, Proceedings of the 17th Seminar, Pardubice, Czech Republic, April 9–11, **2014**, Part 2, 754–768.
- [7] a) R. Wang, Y. Guo, Z. Zheng, B. Twamley, J. M. Shreeve, *Chem. Eur. J.* **2009**, 15, 2625–2634; b) M. A. Hiskey, D. E. Chavez, R. L. Bishop, J. F. Kramer, S. A. Kinkead, *U.S. Patent 6358339*, Assignee: The Regents of the University of California, Los Alamos, NM, USA, **2002**.
- [8] M. Göbel, K. Karaghiosoff, T. M. Klapötke, D. G. Piercey, J. Stierstorfer, *J. Am. Chem. Soc.* **2010**, 132, 17216–17226.
- [9] T. M. Klapötke, D. G. Piercey, J. Stierstorfer, *Propellants Explos. Pyrotech.* **2011**, 36, 160–167.
- [10] a) H. Gao, R. Wang, B. Twamley, M. A. Hiskey, J. M. Shreeve, *Chem. Commun.* **2006**, 38, 4007–4009; b) T. M. Klapötke, A. Preimesser, J. Stierstorfer, *Z. Naturforsch. B* **2013**, 68(12), 1310–1320; c) T. M. Klapötke, A. Preimesser, S. Schedlbauer, J. Stierstorfer, *Cent. Eur. J. Energ. Mater.* **2013**, 10(2), 151–170.
- [11] B. Das, C. R. Reddy, D. N. Kumar, M. Krishnaiah, R. Narender, *Synlett* **2010**, 3, 391–394.
- [12] T. M. Klapötke, C. M. Sabaté, J. Stierstorfer, *New J. Chem.* **2009**, 33, 136–147.
- [13] T. M. Klapötke, J. Stierstorfer, *Helv. Chim. Acta* **2007**, 90, 2132–2150.
- [14] a) T. M. Klapötke, S. M. Sproll, *J. Polym. Sci., Part A: Polym. Chem.* **2010**, 48, 122–127; b) T. M. Klapötke, S. M. Sproll, *Eur. J. Org. Chem.* **2010**, 1169–1175; c) F. M. Betzler, R. Boller, A. Grossmann, T. M. Klapötke, *Z. Naturforsch.* **2013**, 68b, 714–718; d) F. M. Betzler, T. M. Klapötke, S. M. Sproll, *Eur. J. Org. Chem.* **2013**, 509–514.
- [15] M.-J. Crawford, T. M. Klapötke, H. Radies, *J. Fluorine Chem.* **2008**, 129(12), 1199–1205; b) E.-C. Koch, A. Hahma, T. M. Klapötke, H. Radies, *Propellants Explos. Pyrotech.* **2010**, 35(3), 248–253; c) E.-C. Koch, T. M. Klapötke, H. Radies, K. Lux, A. Hahma, *Z. Naturforschung* **2011**, 66(4), 378–386.
- [16] a) Q. J. Axthammer, M. A. Kettner, T. M. Klapötke, R. Moll, S. F. Rest, *New Trends in Research of Energetic Materials*, NTREM, Proceedings of the 16th Seminar, Pardubice, Czech Republic, April 10–12, **2013**, Part 1, 29–39; b) Q. J. Axthammer, M. A. Kettner, T. M. Klapötke, R. Moll, S. F. Rest, *Development of High Energy Dense Oxidisers based on CHNO(F)-materials*, EUCASS Conference, Munich, Germany, July 3rd, **2013**; c) M. A. Kettner, T. M. Klapötke, *Synthesis of New Oxidisers for Potential Use in Solid Rocket Propellants*, New Energetic Materials and Propulsion Techniques for Space Exploration, Milano, Italy, June 9–10, **2014**.
- [17] M. Göbel, T. M. Klapötke, *Adv. Funct. Mater.* **2009**, 19, 347–365.

- [18] V. Grakauskas, A. H. Albert, *J. Heterocyclic Chem.* **1981**, 18, 1477–1479.
- [19] A. V. Fokin, Y. N. Studnev, A. I. Rapkin, V. A. Komarov, O. V. Verenikin, T. M. Potarina, *Izv. Akad. Nauk SSSR, Ser. Khim.* **1981**, 7, 1592–1595.
- [20] R. A. Wiesboeck, J. R. Ruff, *J. Org. Chem.* **1968**, 33(3), 1257–1258.
- [21] a) E. D. McLanahan, J. L. Campbell, D. C. Ferguson, B. Harmon, J. M. Hedge, K. M. Crofton, D. R. Mattie, L. Braverman, D. A. Keys, M. Mumtaz, J. W. Fisher, *Toxicol. Sci.* **2007**, 97, 308–317; b) R. E. Tarone, L. Lipworth, J. K. McLaughlin, *Occup. Environ. Med.* **2010**, 52, 653; c) A. K. Mandal, G. M. Kunjir, J. Singh, S. S. Adhav, S. K. Singh, R. K. Pandey, B. Bhattacharya, M. L. Kantam, *Cent. Eur. J. Energetic Mater.* **2014**, 11, 83–97.
- [22] J. Dumont, *SERDP Project ER-1236*, **2008**.
- [23] B. Sellers, K. Weeks, W. R. Alsop, *Perchlorate Environmental Problems and Solutions*, CRC/Taylor & Francis, Boca Raton, FL (USA), **2007**.
- [24] G. D. Silva, S. C. Rufino, K. Iha, *J. Aerosp. Technol. Manag.* **2013**, 5, 139–144.
- [25] N. Fischer, K. Karaghiosoff, T. M. Klapötke, J. Stierstorfer, *Z. Anorg. Allg. Chem.* **2010**, 636, 735–749.
- [26] L. I. Vereshchagin, O. N. Verkhovina, F. A. Pokatilov, S. K. Strunevich, A. G. Proidakov, V. N. Kizhnyayev, *Russ. J. Org. Chem.* **2007**, 43, 1710–1714.
- [27] D. W. Hutchinson, M. Naylor, *Nucleic Acids Res.* **1985**, 13, 8519–8530.
- [28] C. H. Lim, S. Hong, K.-H. Chung, J. S. Kim, J. R. Cho, *Bull. Korean Chem. Soc.* **2008**, 29, 1415–1417.
- [29] a) J. Majer, J. Denkstein, *Collect. Czech. Chem. Commun.* **1966**, 31, 2547–2557; b) B. Aas, M. A. Kettner, T. M. Klapötke, M. Sućeska, C. Zoller, *Eur. J. Inorg. Chem.* **2013**, 6028–6036.
- [30] M. Conrad, A. Schulze, *Ber. Dtsch. Chem. Ges.* **1909**, 42, 735–742.
- [31] C. O. Parker, *Tetrahedron* **1962**, 17, 109–116.
- [32] C. O. Parker, *US 3415867*, **1968**.
- [33] K. P. C. Vollhardt, N. E. Schore, *Organische Chemie*, 3. Aufl., Wiley-VCH Verlag GmbH, Weinheim, **2000**; b) R. Brückner, *Reaktionsmechanismen*, 3. Aufl., Elsevier GmbH, München, **2004**.
- [34] H.-O. Kalinowski, S. Berger, S. Braun, *¹³C NMR-Spektroskopie*, Thieme, Stuttgart, **1984**.
- [35] M. Witanowski, L. Stefaniak, G. A. Webb, *Annual Reports on NMR Spectroscopy*, Vol. 25, Academic Press Inc., London, **1993**.
- [36] a) M. Hesse, H. Meier, B. Zeeh, *Spektroskopische Methoden in der organischen Chemie*, Georg Thieme Verlag KG, Stuttgart, **2005**; b) G. Socrates, *Infrared and Raman Characteristic Group Frequencies: Tables and Charts*, 3rd ed., Wiley, New York, **2004**.
- [37] A. F. Holleman, E. Wiberg, *Lehrbuch der Anorganischen Chemie*, 101st ed., de Gruyter, Berlin, **1995**, 1842.
- [38] Y. Oyumi, T. B. Brill, A. L. Rheingold, *J. Phys. Chem.* **1985**, 89, 4824–4828.
- [39] A. Bondi, *J. Phys. Chem.* **1964**, 68, 441–451.
- [40] T. M. Klapötke, F. X. Steemann, *Propellants Explos. Pyrotech.* **2010**, 35, 114–129.
- [41] N. Fischer, K. Karaghiosoff, T. M. Klapötke, J. Stierstorfer, *Z. Anorg. Allg. Chem.* **2010**, 636, 735–749.
- [42] *NATO Standardization Agreement (STANAG) on Explosives*, Impact Tests, No. 4489, 1st ed., Sept. 17, **1999**.
- [43] *WIWEB-Standardarbeitsanweisung 4-5.1.02, Ermittlung der Explosionsgefährlichkeit, hier der Schlagempfindlichkeit mit dem Fallhammer*, Nov. 08, **2002**.
- [44] a) Bundesanstalt für Materialforschung (BAM), <http://www.bam.de>, which lays down test methods pursuant to Regulation (EC) No. 1907/2006 of the European Parliament and of

- the Council on the Evaluation, Authorisation and Restriction of Chemicals (REACH), ABl. L142, **2008**; b) T. M. Klapötke, B. Krumm, N. Mayr, F. X. Steemann, G. Steinhauser, *Safety Science* **2010**, 48, 28–34.
- [45] *NATO Standardization Agreement (STANAG) on Explosives*, Friction Tests, No. 4487, 1st ed., Aug. 22, **2002**.
- [46] *WIWEB-Standardarbeitsanweisung 4-5.1.03, Ermittlung der Explosionsgefährlichkeit, hier der Reibempfindlichkeit mit dem Reibeapparat*, Nov. 08, **2002**.
- [47] *NATO Standardization Agreement (STANAG) on Explosives, Electrostatic Discharge Sensitivity Tests*, no. 4490, 1st ed., Feb. 19, **2001**.
- [48] <http://www.ozm.cz/en/sensitivity-tests/esd-2008a-small-scale-electrostatic-spark-sensitivity-test/>.
- [49] a) *Test methods according to the UN Manual of Tests and Criteria, Recommendations on the Transport of Dangerous Goods*, United Nations Publication, New York, Geneva, 4th revised ed., **2003**: Impact: insensitive >40 J, less sensitive ≥35 J, sensitive ≥4 J, very sensitive ≤3 J; friction: insensitive >360 N, less sensitive: 360 N, sensitive <360 N and >80 N, very sensitive ≤80 N, extremely sensitive ≤10 N; b) www.reichel-partner.de.
- [50] F. P. Bowden, A. D. Yoffe, *Initiation and Growth of Explosion in Liquids and Solids*, Cambridge University Press, **1952**.
- [51] a) M. J. Kamlet, NAVORD Rep. 6206, US Naval Ordnance Lab, Whiteoak, Maryland, **1959**; b) J. P. Agrawal, R. D. Hodgson, *Organic Chemistry of Explosives*, 1st ed., Wiley, **2006**, p. 33.
- [52] a) GAUSSIAN09W, Version 7.0, M. J. Frisch, G. W. Trucks, H. B. Schlegel, G. E. Scuseria, M. A. Robb, J. R. Cheeseman, G. Scalmani, V. Barone, B. Mennucci, G. A. Petersson, H. Nakatsuji, M. Caricato, X. Li, H. P. Hratchian, A. F. Izmaylov, J. Bloino, G. Zheng, J. L. Sonnenberg, M. Hada, M. Ehara, K. Toyota, R. Fukuda, J. Hasegawa, M. Ishida, T. Nakajima, Y. Honda, O. Kitao, H. Nakai, T. Vreven, J. A. Montgomery Jr., J. E. Peralta, F. Ogliaro, M. Bearpark, J. J. Heyd, E. Brothers, K. N. Kudin, V. N. Staroverov, R. Kobayashi, J. Normand, K. Raghavachari, A. Rendell, J. C. Burant, S. S. Iyengar, J. Tomasi, M. Cossi, N. Rega, J. M. Millam, M. Klene, J. E. Knox, J. B. Cross, V. Bakken, C. Adamo, J. Jaramillo, R. Gomperts, R. E. Stratmann, O. Yazyev, A. J. Austin, R. Cammi, C. Pomelli, J. W. Ochterski, R. L. Martin, K. Morokuma, V. G. Zakrzewski, G. A. Voth, P. Salvador, J. J. Dannenberg, S. Dapprich, A. D. Daniels, Ö. Farkas, J. B. Foresman, J. V. Ortiz, J. Cioslowski, D. J. Fox, Gaussian, Inc., Wallingford CT, **2009**; b) GAUSS-VIEW 5, Version 5.0.8, T. K. R. Dennington, J. Millam, Semichem Inc., Shawnee Mission, **2009**.
- [53] a) EXPLO5, Version 6.02, M. Sućeska, Zagreb, Croatia, **2014**; b) M. Sućeska, *Propellants Explos. Pyrotech.* **1991**, 16, 197–202; c) M. Sućeska, *Propellants Explos. Pyrotech.* **1999**, 24, 280–285; d) M. Suceška, H. G. Ang, H. Y. Chan, *Mater. Sci. Forum* **2011**, 673, 47–52.
- [54] a) J. F. Köhler, R. Meyer, A. Homburg, *Explosivstoffe*, 10. Aufl., Wiley-VCH Verlag GmbH & Co. KGaA, Weinheim, **2008**; b) P. W. Cooper, *Explosives Engineering*, 1st ed., Wiley-VCH, Weinheim, **1996**.
- [55] a) NASA, Space Shuttle News Reference, 2-20-22-21, <http://de.scribd.com/doc/-17005716/NASA-Space-Shuttle-News-Reference-1981>; b) NASA, press release: STS-122 The Voyage of Columbus, **2008**, 82–84.
- [56] G. P. Sutton, *Rocket Propulsion Elements*, 7th ed., John Wiley & Sons, **2001**.

CHAPTER 4

ENERGETIC BI-OXADIAZOLES

This chapter deals with the synthesis and characterisation of polynitromethyl bi-1,2,4-oxadiazole derivatives as potential high energy dense oxidisers. As mentioned in the last chapter the acidities associated with polynitroazoles can be problematic. By using bi-cyclic systems this issue is avoided. Moreover the oxygen content can be increased by the introduction of oxadiazoles. While furazanes have been explored intensively in energetic materials research and are favoured owing to their high positive heats of formation, the three other possible oxadiazole derivatives have barely attracted the attention. The transfer of the concept from bi-1,2,4-oxadiazoles to bi-1,3,4-oxadiazoles will be emblazed within this chapter by the synthesis of a model material, and theoretical calculations will be presented. The main part of this chapter is reproduced with permissions from:

M. A. Kettner, T. M. Klapötke*

“5,5'-Bis-(trinitromethyl)-3,3'-bi-(1,2,4-oxadiazole): A Stable Ternary CNO-compound with High Density”^[1]

DOI: 10.1039/c3cc49879d

Copyright 2014 Royal Chemical Society

M. A. Kettner, K. Karaghiosoff, T. M. Klapötke,* M. Sućeska, S. Wunder

“3,3'-Bi-(1,2,4-oxadiazoles) Featuring the Fluorodinitromethyl and Trinitromethyl Groups”^[2]

DOI: 10.1002/chem.201402291

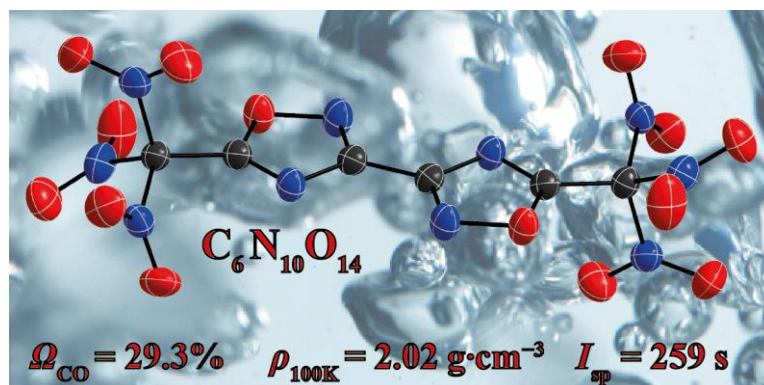
Copyright 2014 Wiley Chemistry - A European Journal

M. A. Kettner, T. M. Klapötke,* T. G. Witkowski, F. von Hundling

“Synthesis, Characterisation and Crystal Structures of two Bi-Oxadiazole Derivatives Featuring the Trifluoromethyl Group”^[3]

DOI: 10.1002/chem.201406436

Copyright 2015 Wiley Chemistry - A European Journal



4.1 Introduction

The challenges in the field of the development of energetic materials include the search for materials with higher performance, better safety and improved environmental compatibility.^[4] In general, compounds with high densities are preferable, because these result in higher performance values.^[5] In recent years compounds with high nitrogen content such as tetrazine,^[6] tetrazole^[7] or triazole^[8] derivatives have successfully fulfilled many of these requirements, especially in the field of secondary explosives and gun propellants. In particular nonfused bi-ring systems were shown to be very promising, for example the dihydroxylammonium salts of 5,5'-bi-(tetrazole-*N*-oxide) (TKX-50)^[9] and 5,5'-bi-(3-nitro-1,2,4-triazole-*N*-oxide) (MAD-X1, Figure 1).^[10]

However, in the field of propellants and energetic oxidisers compounds with high oxygen content are desired. They are necessary to provide oxygen to the actual fuel (Al) for its appropriate combustion in an oxygen-poor or oxygen-deficient environment.^[5] As such oxygen carriers are the main ingredient in solid rocket composite propellants (up to 70%),^[11] elevated densities result in space-saving effects. It is also desired that the compounds do not detonate, but burn fast (deflagrate) in an open flame test.^[4]

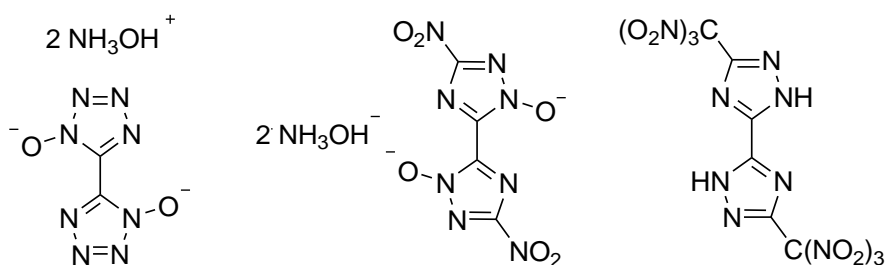


Figure 1: From left to right: molecular structures of TKX-50,^[9] MAD-X1,^[10] and 5,5'-bi-(3-trinitromethyl-1,2,4-1*H*-triazole).^[20]

A new approach to the development of energetic oxidisers is the heterocyclic class of oxadiazoles – formally derived just by replacing the NH-group of any triazole derivative by an oxygen atom in order to increase the oxygen balance of these five-membered ring systems. This class includes four different isomers. They find application as ingredients for drugs,^[12] dyestuffs,^[13] ionic liquids,^[14] and scintillators.^[15] The non-fused bi-oxadiazoles form two further isomers, owing to the asymmetry of the 1,2,3- and 1,2,4-oxadiazoles, which can be linked at two different carbon atoms (Figure 17). Unsymmetrically mixed bi-oxadiazole isomers are omitted from this study. In the area of energetic materials, largely only 1,2,5-oxadiazole (furoxane) derivatives have been exhaustively investigated.^[16] A series of bi-furoxane (1,2,5-oxadiazole) derivatives with trinitroethylamine and fluorodinitroethylamine substituents has been synthesised recently.^[17] Furoxanes or furoxanes are not necessarily the thermally and chemically most stable derivatives of this class, but are favoured due to their positive heats of formation and high densities.^[16d] In contrast 1,2,3-, 1,2,4-, and 1,3,4-oxadiazoles have only been explored sparsely with respect to derivatives in which energetic moieties such as polynitro groups or azides are attached.^[18, 19] Despite their lower heats of formation (see Figure 17), they seem to be excellent candidates for pyrotechnics and propellants with similar properties to tetrazole- or furoxane based compounds, but showing up

enhanced oxygen content. A good example is the previously synthesised dianion 3,3'-bi(5-dinitromethylide-1,2,4-oxadiazolate), which shows remarkable high densities of its salts.^[19]

In this work the ammonium salt of 3,3'-bi(5-dinitromethylide-1,2,4-oxadiazole)^[19] represents the starting material for both the nitration and the fluorination furnishing two hydrogen atom free 3,3'-bi-(5-polynitromethyl-1,2,4-oxadiazoles) with two trinitromethyl or fluorodinitromethyl groups each. Also a second method with an improved yield for the trinitromethyl derivative will be presented. The compounds are analogous to 5,5'-bi-(3-trinitromethyl-1,2,4-triazole) synthesised by PETRIE *et al.* in 2012 (Figure 1).^[20] In comparison to trinitromethyl and fluorodinitromethyl substituted tetrazoles or triazoles, the heterocyclic system 3,3'-bi-(1,2,4-oxadiazole) avoids the problematic acidities associated with these polynitroazoles (see Chapter 3).

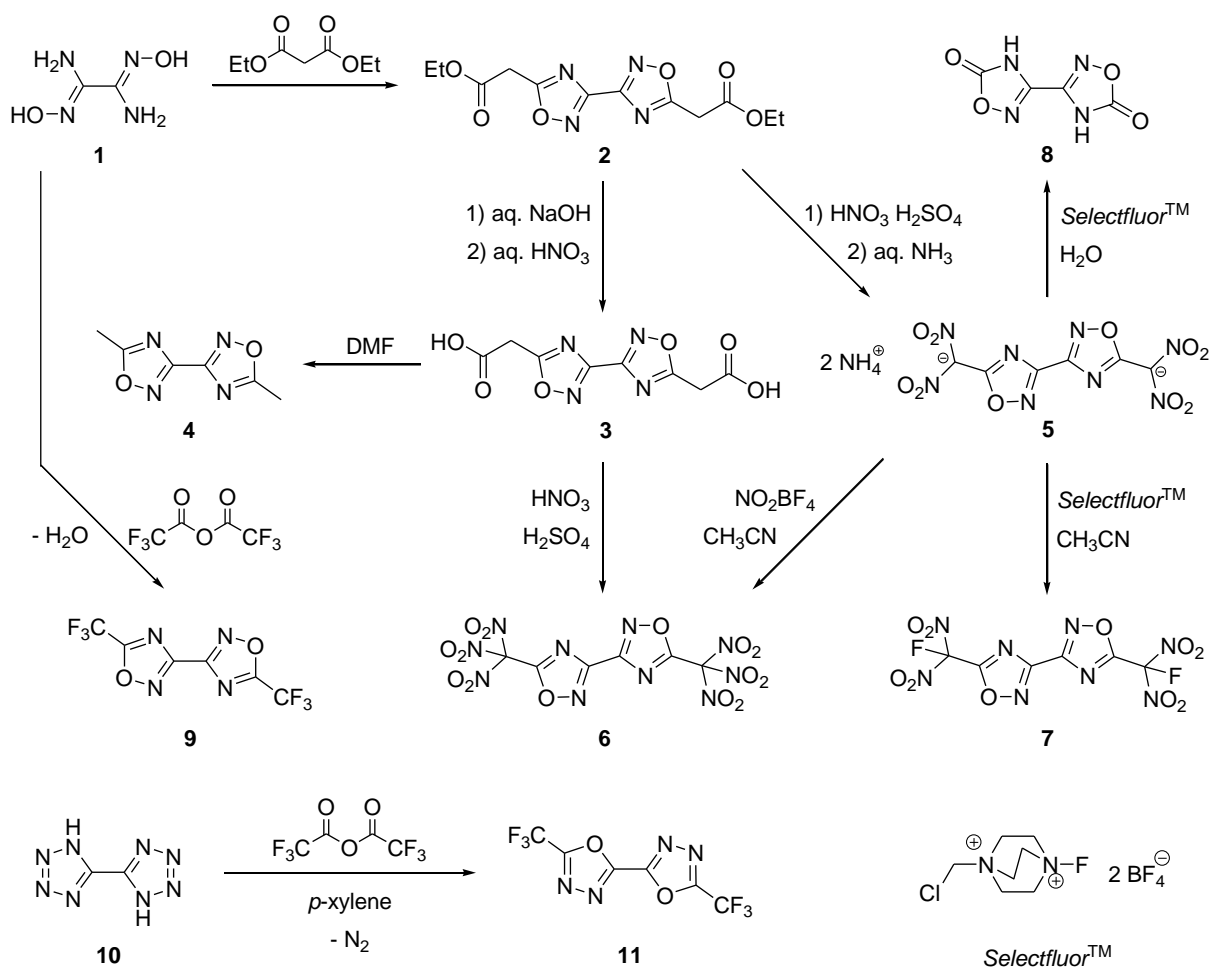
The strategy in the design of new oxygen carriers of using the trinitromethyl (TNM) and fluorodinitromethyl (FDNM) moieties for increased oxygen contents and densities has been discussed in detail in the General Introduction of this work. In addition, this chapter describes molecules containing the trifluoromethyl group. They serve as non-energetic model groups with electron withdrawing character, in which the fluorine atoms can be substituted stepwise by nitro groups. At the end of this chapter the experimental and theoretical investigations on the transfer of the concept from the bi-(1,2,4-oxadiazole) to the bi-(1,3,4-oxadiazole) ring system as linker for two polyfluoro- and polynitromethyl groups will be presented.

The hydrogen atom free and neutral CNO molecules presented in this chapter exhibit densities in the range of that observed for various furazane derivatives, which are close to $2.00 \text{ g}\cdot\text{cm}^{-3}$.^[21] In the case of pure CNOF compounds, there is only one known oxadiazole derivative featuring the fluorodinitromethyl moiety with a similar X-ray density as that observed for 3,3'-bi-(5-fluorodinitromethyl-1,2,4-oxadiazole). It is the mono-cyclic compound 2,5-bis-(fluorodinitromethyl)-1,3,4-oxadiazole with a density of $2.024 \text{ g}\cdot\text{cm}^{-3}$ (153 K) presented by FAENZIL'BERG *et al.* in 1994.^[22]

4.2 Syntheses

An overview about all syntheses described in this chapter is depicted in Scheme 1. 3,3'-Bi-(1,2,4-oxadiazolyl)-5,5'-diacetic acid diethylester (**2**)^[23] and diammonium 3,3'-bi-(5-dinitromethylide-1,2,4-oxadiazole) (**5**)^[19] were prepared according to literature known procedures starting from *N,N'*-dihydroxyoxal-amidine (**1**). Compound **5** represents the precursor for both the nitration and the fluorination yielding compounds **6** and **7**. 3,3'-Bi-(5-trinitromethyl-1,2,4-oxadiazole) (TNM₂-BOD, **6**) can be prepared via two different methods. First route is the nitration of the dinitromethanide salt **4** using nitronium tetrafluoroborate in anhydrous acetonitrile at 0 °C for one hour. Since the reaction yield using this method was rather low with 27%, a more convenient route as used in Chapter 3 was established. The decarboxylative nitration of the bi-carbonic acid **2** using fuming nitric acid in concentrated sulfuric acid furnished TNM₂-BOD (**5**) in much higher yield of 89%. Therefore the saponification of the diethylester **2** was performed by the standard method in aqueous sodium hydroxide and subsequent treatment with aqueous nitric acid (60%) yielding the hitherto unknown bi-carbonic acid **3**. Attempted re-crystallisation of compound **3** from DMF furnished crystals

suitable for X-ray diffraction of the decarboxylated product 3,3'-bi-(5-methyl-1,2,4-oxadiazole) (**4**) in quantitative yield, thus showing the readiness of the carboxy groups for the following decarboxylative nitration yielding compound **6**.



Scheme 1: The syntheses of all compounds discussed in this chapter. Compounds **2** (30%),^[23] **5** (2-steps: 94%)^[19] and **9** (75%)^[26] were synthesised according the literature known procedures. Compound **3** (76%) was synthesised by a standard saponification from compound **2**. Compound **4** (99%) was formed by decarboxylation of compound **3** in DMF. Decarboxylative nitration of compound **3** (89%) or nitration of compound **5** using NO₂BF₄ under anhydrous conditions furnished compound **6** (27%). Fluorination of compound **4** using SelectfluorTM under anhydrous conditions yielded compound **7** (66%), while the same reaction in water gave crystals of the literature known compound **8**.^[24] Compound **11** (93%)^[27] was synthesised by a convenient method from compound **10** with evolution of N₂.^[28]

The synthesis of 3,3'-bi-(5-fluorodinitromethyl-1,2,4-oxadiazole) (FDNM₂-BOD, **6**) was performed by fluorination of compound **4** using SelectfluorTM in anhydrous acetonitrile with moderate yield (66%). When using water as solvent for the reaction the well known 3,3'-bi-(1,2,4-oxadiazol-5-one) (**8**) crystallised from the solution after 20 hours and was identified by its X-ray crystal structure.^[24] This might be due to alkaline hydrolysis, induced by slightly alkaline 1-(chloromethyl)-1,4-diaza-bicyclo[2.2.2]octane tetrafluoroborate, which remains in

the aqueous solution after the fluorination with *Selectfluor*TM.^[25] During the two synthetic routes for TNM₂-BOD (**6**) in acidic media the formation of compound **8** was not observed. Also the analogue 3,3'-bi-(5-trifluoromethyl-1,2,4-oxadiazole) (TFM₂-¹²⁴BOD, **9**) was synthesised from *N,N'*-dihydroxyoxal-amidine (**1**) according to a slightly modified procedure in which trifluoromethyl acetic acid anhydride acts as both the solvent and the reactant, resulting in an increase of the yield by 11% in comparison with the previously reported yield.^[26] Literature known 5,5'-bi-(2-trifluoromethyl-1,3,4-oxadiazole (TFM₂-¹³⁴BOD, **11**)^[27] was synthesised using another more convenient literature method for the formation of bi-1,3,4-oxadiazoles. The conversion of bi-5,5'-tetrazoles (**10**) into the 1,3,4-oxadiazole **11** with formation of N₂ results in very high yields (93%) and a high purity of the target compound.^[28] For purification compounds **9** and **11** could either be re-crystallised from ethanol or be sublimed under reduced pressure.

4.3 Multinuclear NMR Spectroscopy

Compounds **3**, **4**, **6**, **7**, **9** and **11** were characterised by ¹H, ¹³C{¹H} and ¹⁴N{¹H} NMR spectroscopy. Additionally, the ¹⁹F NMR spectra of compounds **7**, **9** and **11** were recorded, as well as the ¹⁵N NMR spectra of compounds **9** and **11** for comparison of the two oxadiazole isomers (Table 1). For the measurements compounds **3**, **9** and **11** were dissolved in *d*6-DMSO, compound **4** in CD₃CN, and compounds **6** and **7** in CD₂Cl₂.

In the ¹H NMR spectra of compounds **3** and **4** the chemical shifts of the CH₂ and CH₃ groups are observed at δ = 4.31 and 2.67 ppm, respectively. The protons of the carboxylic acid OH groups in compound **3** are shifted to δ = 13.33 ppm.^[29]

Table 1: Multinuclear NMR chemical shifts δ of compounds **3**, **9** and **11** in *d*6-DMSO, compound **4** in CD₃CN, and compounds **6** and **7** in CD₂Cl₂ [ppm].

Nucleus	Assignment	3	4	6	7	9	11
¹ H	CH ₂ / CH ₃	4.31	2.67	–	–	–	–
	OH	13.33 (br)	–	–	–	–	–
¹³ C{ ¹ H}	CH ₂ / CH ₃	33.4	11.7	–	–	–	–
	COOH	168.0	–	–	–	–	–
	OCN	176.6	179.0	163.6	164.8 (d)	166.5 (q)	155.3 (q)
	CC	160.1	160.1	159.9	159.9	159.3	153.8
¹⁴ N	C(NO ₂) _x F _y	–	–	117.5 (sept)	111.9 (d _{quint})	115.4 (q)	115.7 (q)
	C(NO ₂) _x F _y	–	–	–43	–34 (d)	–	–
¹⁵ N	2- <i>N</i> / 3- <i>N</i>	–	–	–	–	–9.3	–64.2 (q)
	4- <i>N</i>	–	–	–	–	–134.8 (q)	–64.6
¹⁹ F	CF _y	–	–	–	–98.9 (quint)	–65.1 (br)	–64.7 (br)

(br) broad; x = 0, 2, 3; y = 0, 1, 3; (d) doublet; (q) quartet; (quint) quintet; (sept) septet.

In the ¹³C{¹H} NMR spectra of compounds **3** and **4** the signals of the CH₂ and CH₃ groups are observed at δ = 33.4 and 11.7 ppm, respectively. The signal of the carboxy carbon atoms in compound **3** is shifted to δ = 168.0 ppm. The chemical shifts of the ring connecting 3,3'-carbon atoms of the 3,3'-bi-(1,2,4-oxadiazoles) **3**, **4**, **6**, **7** and **9** are observed in the very narrow range of δ = 160.1–159.3 ppm, while the signal of the 5,5'-carbon atoms in compound **11** is shifted slightly to higher field (δ = 153.8 ppm). The signals of the 5,5'-carbon

atoms of the 3,3'-bi-(1,2,4-oxadiazoles) **3**, **4**, **6**, **7** and **9** are observed in the range of $\delta = 176.6$ – 163.6 ppm depending on the electron withdrawing or pushing character of the groups attached. For compound **7** the signal splits into a doublet due to $^2J_{C-F}$ coupling with one fluorine atom and with a coupling constant of 28.8 Hz, while for compound **9** it splits into a quartet due to $^2J_{C-F}$ coupling with three fluorine atoms and with a coupling constant of 44.8 Hz. In compound **11** the signal for the 2,2'-carbon atoms is shifted to $\delta = 155.3$ ppm and also splits into a quartet due to $^2J_{C-F}$ coupling with three fluorine atom and with a coupling constant of 44.7 Hz. The trinitromethyl groups in compound **6** show a septet at $\delta = 117.5$ ppm due to J_{C-14N} coupling with a coupling constant of 9.4 Hz (Figure 2), while the fluorodinitromethyl groups in compound **7** show a doublet of quintets at $\delta = 111.9$ ppm with coupling constants of $J_{C-F} = 297.1$ Hz and $J_{C-14N} = 9.6$ Hz (Figure 3). The carbon signals of the trifluoromethyl groups in compounds **9** and **11** are shifted to $\delta = 115.4$ and 115.7 ppm, respectively, and are splitted into quartets due to J_{C-F} coupling with coupling constants of 273.4 and 271.9 Hz.^[29]

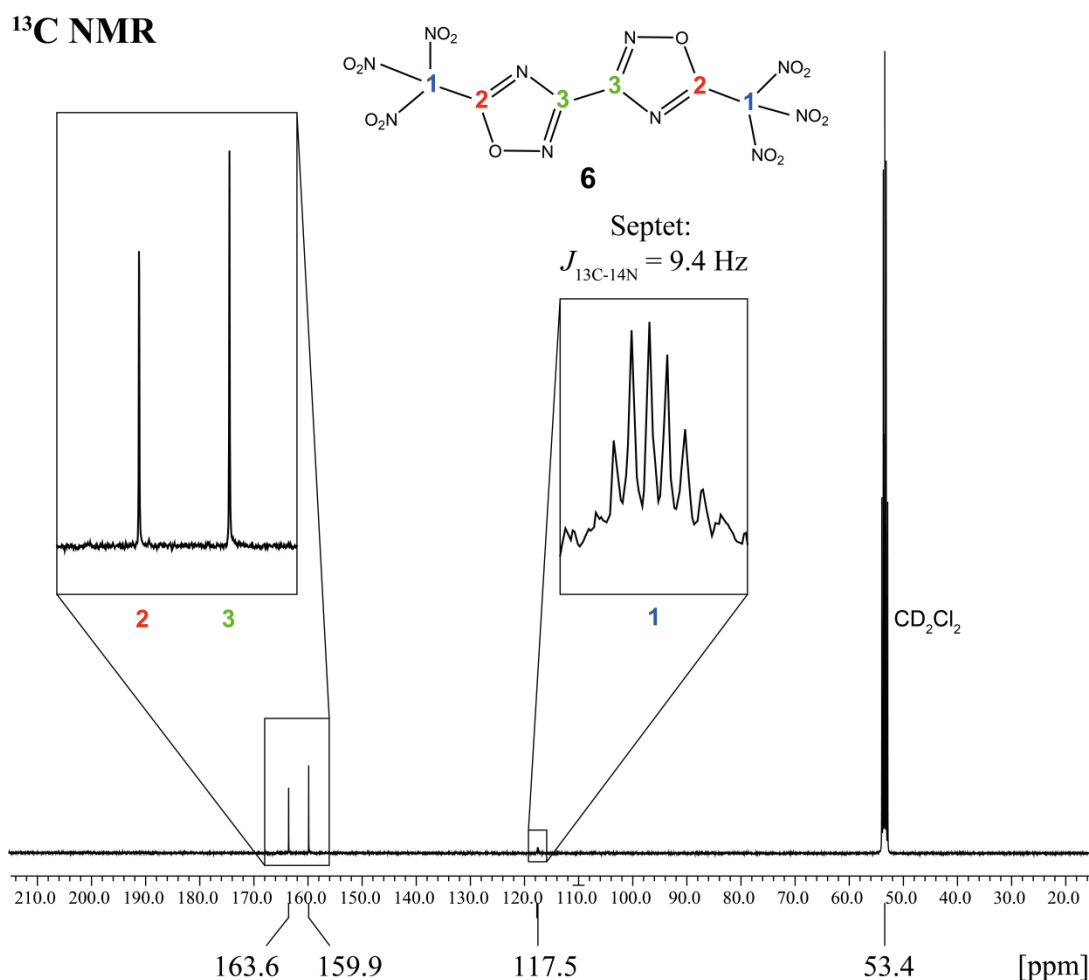


Figure 2: $^{13}C\{^1H\}$ NMR spectrum of compound **6** showing the chemical shifts and the septet for the carbon atom of the trinitromethyl group due to J_{C-14N} coupling. The spectrum was recorded applying a 30° pulse and a pulse delay of 2 s (32700 scans).

In the $^{14}\text{N}\{^1\text{H}\}$ NMR spectra the signal of the nitro groups in compound **6** is shifted to $\delta = -43$ ppm, and in the spectrum of compound **7** it is observed at $\delta = -34$ ppm as a doublet with a coupling constant of 9.9 Hz due to $^2J_{\text{N-F}}$ coupling. The nitrogen atoms in the ring systems cannot be observed in the $^{14}\text{N}\{^1\text{H}\}$ NMR spectra. For comparison of the two oxadiazole isomers the ^{15}N NMR spectra of compounds **9** and **11** were recorded. The 1,2,4-oxadiazole derivative **9** shows the chemical shift of the 2-N atom at $\delta = -9.3$ ppm, and the one of the 4-N atom shifted to $\delta = -134.8$ ppm splitted into a quartet due to $^3J_{^{15}\text{N-F}}$ with a coupling constant of 1.9 Hz. As expected the ^{15}N NMR spectrum of the 1,3,4-oxadiazole derivative **11** shows the signals of the 3-N and 4-N atoms nearby to each other at $\delta = -64.2$ and -64.6 ppm, whereat the signal of the 3-N atoms are again splitted into a quartet due to $^3J_{^{15}\text{N-F}}$ with a coupling constant of 1.5 Hz.^[30]

The ^{19}F NMR spectrum of compound **7** shows the fluorine shift of the fluorodinitromethyl groups at $\delta = -98.9$ ppm as a quintet due to $^2J_{\text{F-}^{14}\text{N}}$ coupling with a coupling constant of 9.8 Hz. The ^{19}F NMR spectra of compounds **9** and **11** show the chemical shifts of the fluorine atoms at $\delta = -65.1$ and -64.7 ppm, respectively, as broad singlets indicating multiplets.

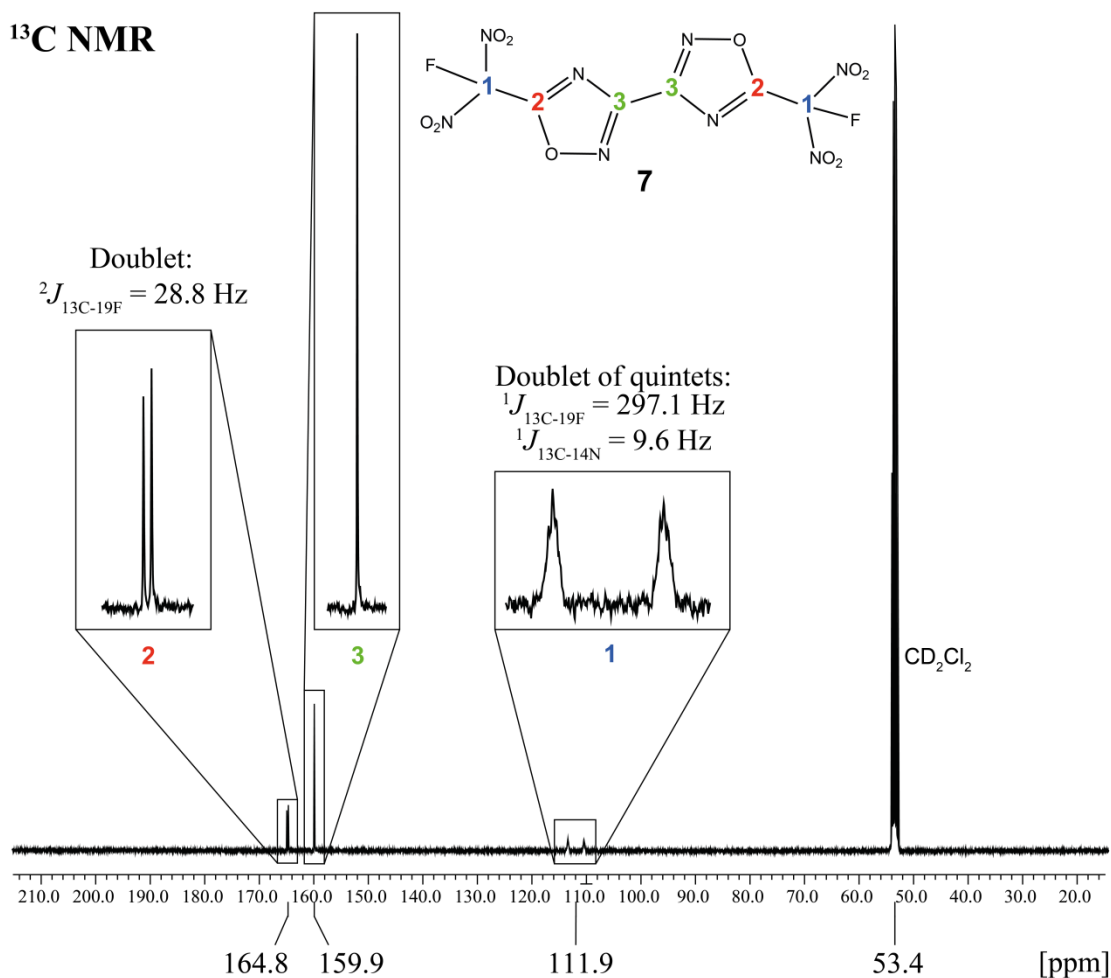


Figure 3: $^{13}\text{C}\{^1\text{H}\}$ NMR spectrum of compound **7** showing its chemical shifts with various multiplets and their assignments. The spectrum was recorded applying a 30° pulse and a pulse delay of 2 s (14500 scans).

4.4 Vibrational Spectroscopy

IR and Raman spectra of compounds **3**, **4**, **6**, **7**, **9** and **11** were recorded and the frequencies were assigned according to literature known data (Table 2 and 3).^[31, 32]

For all these derivatives the NO stretching vibrations of the ring system are observed in the narrow range of $\tilde{\nu} = 1233\text{--}1211\text{ cm}^{-1}$ (IR), but are overlapped in the spectra of the fluorine containing compounds **7**, **9** and **11** by the characteristic symmetric stretching bands $\nu_s(\text{C--F})$ of the carbon fluorine bonds. The C=N stretching vibrations $\nu(\text{C=N})$ of all compounds are observed in the range of $\tilde{\nu} = 1605\text{--}1561\text{ cm}^{-1}$ in both the IR and Raman spectra. The stretching modes of the methyl and methylene groups [$\nu(\text{C--H})$, $\nu_s(\text{CH}_3)$ and $\nu_{as}(\text{CH}_3)$] in the spectra of compounds **3** and **4** were found in the expected range. The carboxyl group vibrations of compound **3** are observed at $\tilde{\nu} = 2617$ and 1707 cm^{-1} (IR) and disappear after decarboxylation in the spectrum of compound **4**.

Table 2: Characteristic IR and Raman vibrations of compounds **3**, **4** and **6** [cm^{-1}].

Assignment	3		4		6	
	IR	Raman	IR	Raman	IR	Raman
$\nu_{as}(\text{NO}_2)$	—	—	—	—	1608	1621
$\nu(\text{C=N})$	1585	1595	1576	1596	1561	1595
$\nu_s(\text{NO}_2)$	—	—	—	—	1271	1275
$\nu(\text{C=O})$	1233	—	1227	—	1227	—

The vibrational analysis of compounds **6** and **7** showed the characteristic asymmetric nitro group stretching vibrations $\nu_{as}(\text{NO}_2)$ in the range of $\tilde{\nu} = 1628\text{--}1608\text{ cm}^{-1}$, and the symmetric stretching vibrations $\nu_s(\text{NO}_2)$ between $1275\text{--}1259\text{ cm}^{-1}$. All vibrations of the nitro groups are in a close range, explained by the similarity of the functional groups. Compound **7** shows additionally the C–F stretching mode at $\tilde{\nu} = 1241\text{ cm}^{-1}$ (IR) and 1244 cm^{-1} (Raman). The characteristic stretching modes ν_s and ν_{as} of the CF_3 groups in compounds **9** and **11** are observed in the IR spectra at $\tilde{\nu} = 1212$ and 1171 cm^{-1} (**9**), and at $\tilde{\nu} = 1227$ and 1169 cm^{-1} (**11**), respectively.

Table 3: Characteristic IR and Raman vibrations of compounds **7**, **9** and **11** [cm^{-1}].

Assignment	7		9		11	
	IR	Raman	IR	Raman	IR	Raman
$\nu_{as}(\text{NO}_2)$	1620	1628	—	—	—	—
$\nu(\text{C=N})$	1572	1597	1605	1601	1579	1580
$\nu_s(\text{NO}_2)$	1259	—	—	—	—	—
$\nu_s(\text{C--F})$	1241	1244	1212	—	1227	—
$\nu_{as}(\text{C--F})$	—	—	1171	1185	1169	—

4.5 X-ray Crystal Structures

Single crystals suitable for X-ray diffraction measurements were obtained at 8 °C by slow evaporation of dimethyl formamide (**4**), diethyl ether (**6**), dichloromethane (**7**), ethanol (**9**), or by sublimation (**11**). All relevant crystallographic and structural refinement data are listed in Tables 4 and 5. The refined atom positions and anisotropic thermal displacement parameters are listed in the Appendix 4.11. All crystal structures in the following will be shown with perpendicular and lateral view on the rings demonstrating the planarity of these non-fused bi-cyclic systems. The structure of the parent heterocycle 3,3'-bi-(1,2,4-oxadiazole) has been described previously in the literature.^[33] The structures of compounds **4**, **7**, **9** and **11** are centrosymmetric with the centre of inversion bisecting the C–C bond between the two rings, as found also for other 3,3'-bi-(1,2,4-oxadiazole) derivatives, for example 3,3'-bi-(5-azidomethyl-1,2,4-oxadiazole).^[34]

Table 4: Crystal structure parameters of Me₂-BOD (**4**) and TNM₂-BOD (**6**) at 100(2)K and 293(2) K. Standard deviations are given in parentheses.

	4	6	
Refined formula	C ₆ H ₆ N ₄ O ₂	C ₆ N ₁₀ O ₁₄	
Formula weight	166.14	436.12	
Crystal dimensions	0.40×0.20×0.05	0.50×0.33×0.03	
Crystal description	colourless block	colourless plate	
Crystal system	triclinic	monoclinic	
Space group	<i>P</i> −1	<i>P</i> 2 ₁ / <i>c</i>	
<i>a</i> [Å]	4.722(1)	10.684(1)	10.905(1)
<i>b</i> [Å]	5.890(1)	5.861(1)	5.870(1)
<i>c</i> [Å]	6.999(1)	23.539(1)	23.568(2)
α [°]	73.77(1)	90	
β [°]	85.57(2)	102.94(1)	102.76(1)
γ [°]	73.99(1)	90	
<i>V</i> [Å³]	179.6(1)	1436.5(1)	1496.4(2)
<i>Z</i>	1	4	
ρ_{calcd} [g cm^{−3}]	1.536	2.017	1.936
μ [mm^{−1}]	0.120	0.200	0.192
temperature [K]	100(2)	100(2)	293(2)
θ range [°]	4.13–26.00	4.18–26.37	4.33–27.00
<i>F</i>(000)	86	872	
dataset <i>h</i>	−5 ≤ <i>h</i> ≤ 5	−13 ≤ <i>h</i> ≤ 13	−13 ≤ <i>h</i> ≤ 13
dataset <i>k</i>	−7 ≤ <i>k</i> ≤ 7	−7 ≤ <i>k</i> ≤ 7	−7 ≤ <i>k</i> ≤ 7
dataset <i>l</i>	−8 ≤ <i>l</i> ≤ 8	−29 ≤ <i>l</i> ≤ 29	−30 ≤ <i>l</i> ≤ 27
reflections measured	1758	20654	10663
reflections independent	690	2909	3204
reflections unique	567	2515	2246
<i>R</i>_{int}	0.0294	0.0391	0.0396
<i>R</i>1, <i>wR</i>2 (2σ data)	0.0351, 0.0741	0.0423, 0.0929	0.0632, 0.1646
<i>R</i>1, <i>wR</i>2 (all data)	0.0467, 0.0810	0.0505, 0.0966	0.0900, 0.1833
Data/restraints/parameters	690/0/67	2909/0/271	2314/0/271
GOOF on <i>F</i>²	1.069	1.145	1.067
Residual electron density	−0.175/0.198	−0.240/0.328	−0.249/0.365
CCDC number	963151	963150	982817

Table 5: Crystal structure parameters of FDNM₂-BOD (**7**) at 100(2) K and 293(2) K, TFM₂-¹²⁴BOD (**9**) and TFM₂-¹³⁴BOD (**11**). Standard deviations are given in parentheses.

	7		9	11
Refined formula	C ₆ N ₈ O ₁₀ F ₂		C ₆ N ₄ O ₂ F ₆	
Formula weight	382.14		274.10	
Crystal dimensions	0.30×0.23×0.03		0.40×0.29×0.07	0.55×0.34×0.19
Crystal description	colourless plate		colourless plate	colourless block
Crystal system	monoclinic		monoclinic	
Space group	<i>P</i> 2 ₁ / <i>c</i>		<i>P</i> 2 ₁ / <i>c</i>	
<i>a</i> [Å]	5.587(1)	5.669(1)	11.158(1)	10.997(1)
<i>b</i> [Å]	12.055(2)	12.126(1)	4.762(1)	5.157(1)
<i>c</i> [Å]	9.408(1)	9.578(1)	8.746(1)	8.219(1)
α [°]	90		90	90
β [°]	100.99(2)	100.46(1)	103.14(1)	99.43(2)
γ [°]	90		90	90
<i>V</i> [Å ³]	622.1(1)	647.4(1)	452.5(1)	459.8(1)
<i>Z</i>	2		2	
ρ_{calcd} [g cm ⁻³]	2.040	1.960	2.012	1.980
μ [mm ⁻¹]	0.210	0.202	0.230	0.227
temperature [K]	100(2)	293(2)	173(2)	
θ range [°]	4.29–25.98	4.24–26.37	4.67–28.27	4.38–28.27
F(000)	380		268	
dataset <i>h</i>	$-6 \leq h \leq 6$	$-6 \leq h \leq 7$	$-14 \leq h \leq 14$	$-14 \leq h \leq 14$
dataset <i>k</i>	$-9 \leq k \leq 14$	$-9 \leq k \leq 15$	$-3 \leq k \leq 6$	$-6 \leq k \leq 6$
dataset <i>l</i>	$-11 \leq l \leq 11$	$-11 \leq l \leq 11$	$-11 \leq l \leq 10$	$-10 \leq l \leq 10$
reflections measured	3132	3314	3724	4399
reflections independent	1212	1292	1104	1133
reflections unique	946	926	876	922
<i>R</i> _{int}	0.0308	0.0281	0.0245	0.0206
<i>R</i>1, <i>wR</i>2 (2σ data)	0.0335, 0.0708	0.0364, 0.0753	0.0390, 0.0977	0.0437, 0.1107
<i>R</i>1, <i>wR</i>2 (all data)	0.0495, 0.0795	0.0583, 0.0867	0.0530, 0.1097	0.0544, 0.1201
Data/restraints/parameters	1212/0/113	1292/0/118	1104/0/82	1133/0/82
GOOF on <i>F</i>²	1.039	0.998	1.026	1.074
Residual electron density	−0.280/0.326	−0.168/0.185	−0.298/0.261	−0.421/0.377
CCDC number	963149	982802	1030581	1030580

Crystal Structure of 3,3'-Bi-(5-Methyl-1,2,4-Oxadiazole) (**4**)

Me₂-BOD (**4**) crystallises as colourless blocks in the triclinic space group *P*−1 with two molecules in the unit cell and a calculated maximum density of 1.536 g·cm^{−3} at 100(2) K. The bi-(1,2,4-oxadiazole) ring system as well as the methyl groups attached show a planar arrangement, which is reflected in the dihedral angles (Figure 4). All bond length and angles are in the expected ranges.^[35]

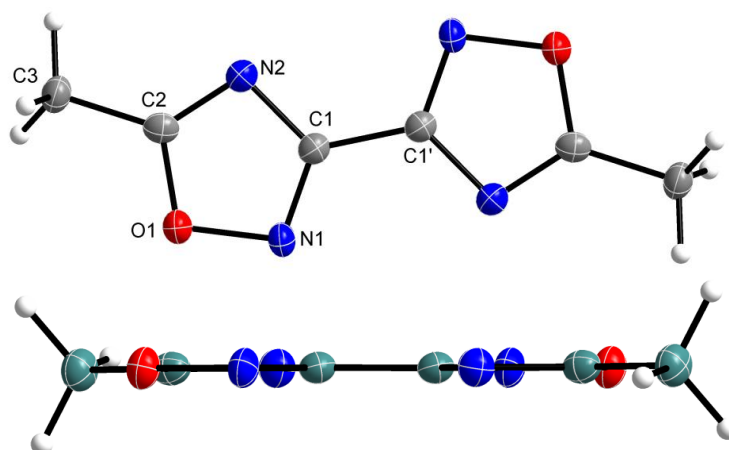


Figure 4: Crystal structure of compound **4** with perpendicular and lateral view showing the planarity of the ring system. Selected bond lengths [Å] and angles [°]: C1–C1' 1.469(3), O1–C2 1.352(2), O1–N1 1.417(2), N1–C1 1.304(2), N2–C2 1.298(2), N2–C1 1.381(2), C2–C3 1.489(2), average C3–H 1.010(2); C2–O1–N1 106.6(1), N2–C2–O1 113.3(1), N2–C2–C3 129.31(14), O1–N1–C1–C1' –179.8(2), C1–N2–C2–C3 –179.6(2). Symmetry operator: ') $-x, 1-y, 1-z$.

Figure 5 shows how the single molecules span layers parallel to the c axis supported by very weak electrostatic interactions (yellow dashed lines, C3–H1...N1). These layers are once more connected through such weak interactions (blue dashed lines, C3–H2...N2).

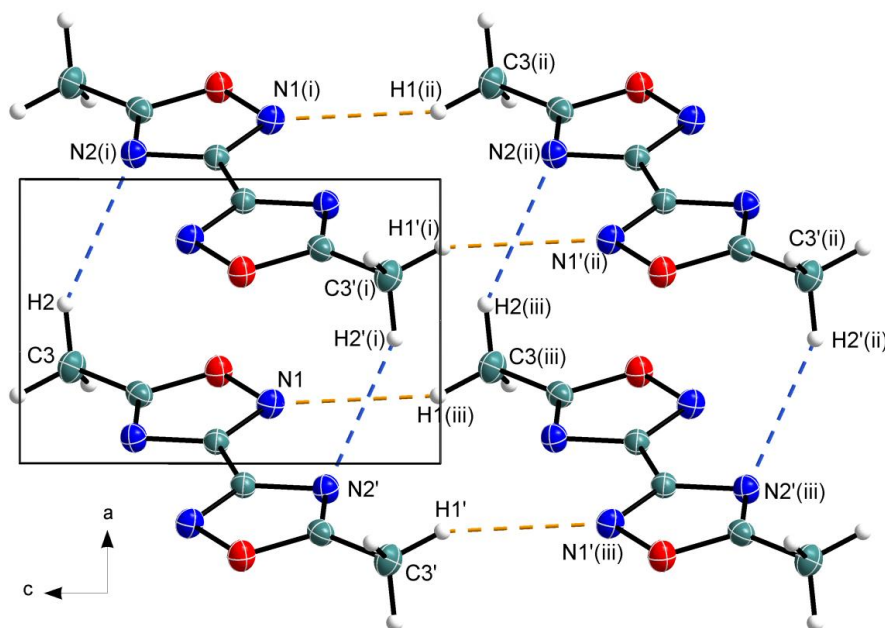


Figure 5: The weak intermolecular interactions within the crystal structure of compound **4** forming layers for the structural parameters listed in Table 6. Symmetry operators: ') $-x, 1-y, 1-z$; (i) $1+x, y, z$; (ii) $1+x, y, -1+z$; (iii) $x, y, -1+z$.

Table 6: Structural parameters of the very weak intermolecular interactions in the crystal structure of compound **4** presented in Figure 5 as blue and yellow dashed lines.

D–H...A	d (D–H) [Å]	d (H...A) [Å]	d (D–H...A) [Å]	∠ (D–H...A) [°]
C3–H2...N2(i)	1.01(2)	2.72(2)	3.616(2)	148.5(4)
C3(ii)–H1(ii)...N1(i)	1.01(2)	2.74(1)	3.609(2)	144.2(1)
Symmetry operators: ') $-x, 1-y, 1-z$; (i) $1+x, y, z$; (ii) $1+x, y, -1+z$; (iii) $x, y, -1+z$.				

Crystal Structure of 3,3'-Bi-(5-Trinitromethyl-1,2,4-Oxadiazole) (6)

TNM₂-BOD (**6**) crystallises as colourless plates in the monoclinic space group $P2_1/c$ with four molecules in the unit cell. The calculated maximum density at 100(2) K is 2.017 g cm⁻³ and at ambient temperature [293(2) K] 1.936 g·cm⁻³ (Figure 6). All bond length and angles are in the expected ranges.^[35] Even the C1–C2 and C5–C6 bond lengths are rather similar to the C2–C3 bond length of compound **4**.

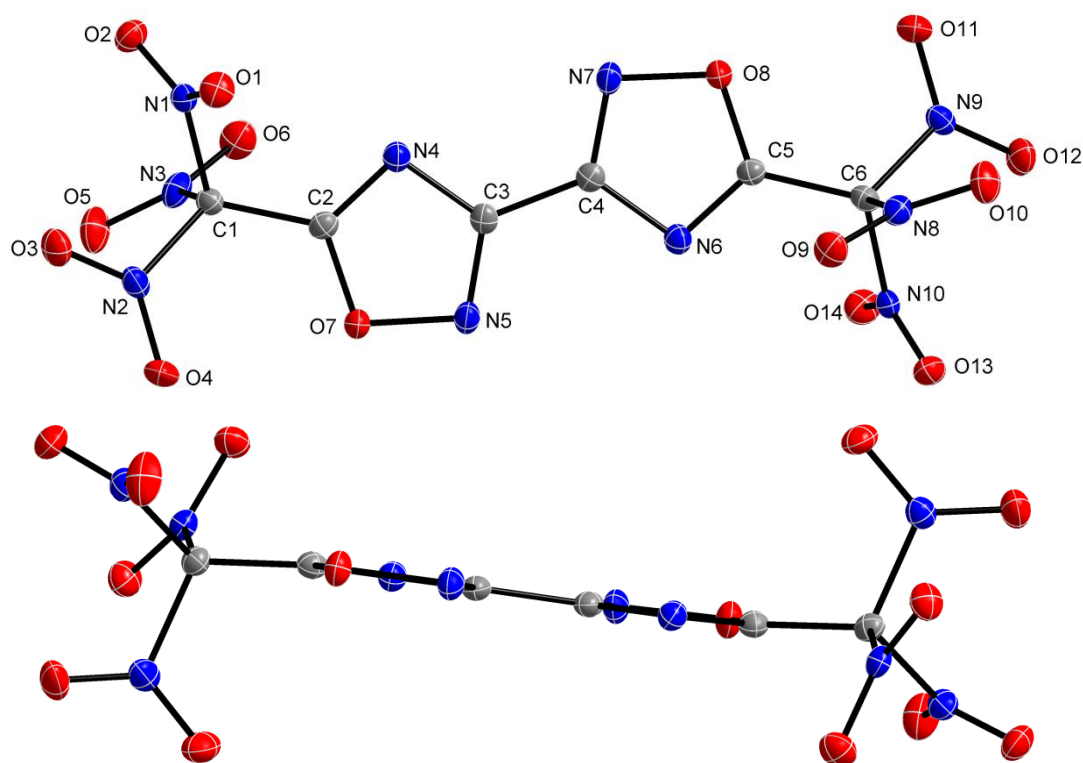


Figure 6: Crystal structure of compound **6** with perpendicular and lateral view showing the planarity of the ring system. Selected bond lengths [Å] and angles [°]: N1–O2 1.208(2), C1–C2 1.492(3), N1–O1 1.218(2), N1–C1 1.525(3), N2–O3 1.209(2), N2–O4 1.214(3), N2–C1 1.529(3), O5–N3 1.209(2), O7–C2 1.347(3), O7–N5 1.407(2), N3–O6 1.211(2), N3–C1 1.549(3), N5–C3 1.307(3), N4–C2 1.290(3), C3–C4 1.466(3), N4–C3 1.374(3), O13–N10 1.207(2), N8–O10 1.212(2), C6–C5 1.495(3); O2–N1–O1 128.4(2), O2–N1–C1 117.1(2), C2–O7–N5 105.2(2), C3–N5–O7 102.9(2), C2–N4–C3 100.8(2), N5–C3–N4 116.0(2), N5–C3–C4 121.2(2), C2–C1–N1 111.1(2), C2–C1–N2 116.2(2), C2–C1–N3 110.3(2), N1–C1–N3 106.8(2); C2–O7–N5–C3 –0.4(2), O7–N5–C3–N4 0.4(2), C5–N6–C4–C3 –178.0(2), N5–C3–C4–N7 –178.6(2), N4–C3–C4–N7 1.5(3), N5–C3–C4–N6 –0.1(3), N4–C3–C4–N6 180.0(2), C4–N6–C5–C6 173.5(2), N7–O8–C5–N6 –0.1(2).

Compared to other solid trinitromethyl containing materials, which tend to have X-ray densities between 1.47 g·cm⁻³ (2,4,6-trimethyl-1-(2,2,2-trinitroethyl)benzene)^[36] and 2.05 g·cm⁻³ (hexanitroethane)^[37], TNM₂-BOD (**6**) belongs to the compounds showing the highest densities.^[38] Among the hydrogen atom free and neutral CNO-compounds TNM₂-BOD (**6**) displays a remarkably high density, which is in the range of that observed for various furazane derivatives,^[21] although not reaching the values of the pernitroated alkanes such as hexanitroethane (2.05 g·cm⁻³)^[37] and octanitrocubane (1.98 g·cm⁻³),^[39] or

pernitroarenes as hexanitrobenzene ($1.99 \text{ g}\cdot\text{cm}^{-3}$).^[40] In contrast to the volatile hexanitroethane,^[37] TNM₂-BOD shows practically no tendency to sublime at ambient temperature, however.

The high density might be explained by the presence of weak attractive electrostatic interactions (short contacts) between the nitro groups within the trinitromethyl moieties. In the crystal, intramolecular as well as intermolecular short N \cdots O contacts are observed. Such interactions have been widely observed for the solid state in polynitro compounds.^[41] Within the molecules of compound **6** various N \cdots O distances are found, which are clearly shorter than the sum of van der Waals radii (N,O = 3.07 \AA)^[42] as shown in Figure 7. The distances N1 \cdots O3, N2 \cdots O5 and N3 \cdots O2 are about 2.55 \AA (blue dashed lines in Figure 7), while for N2 \cdots O1, N3 \cdots O4 and N1 \cdots O6 distances between 2.94 and 3.07 \AA are observed (grey dashed lines in Figure 7). Overall the trinitromethyl group arranges to the typical propeller-like orientation of the nitro groups with torsion angles C2–C1–N–O between $-36.6(3)^\circ$ and $-50.9(2)^\circ$ as described by BRILL *et al.* ($23\text{--}67^\circ$).^[43] There are also weak interactions of N2 and O1 from the trinitromethyl group to O7 and N4 of the oxadiazole ring (black dashed lines in Figure 7). Very similar sterical and electrostatic interactions are observed in the second trinitromethyl group at the opposite side of the molecule.

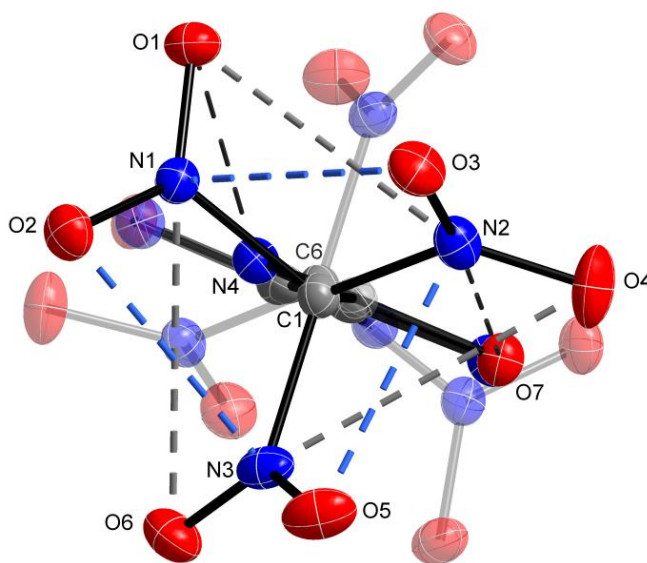
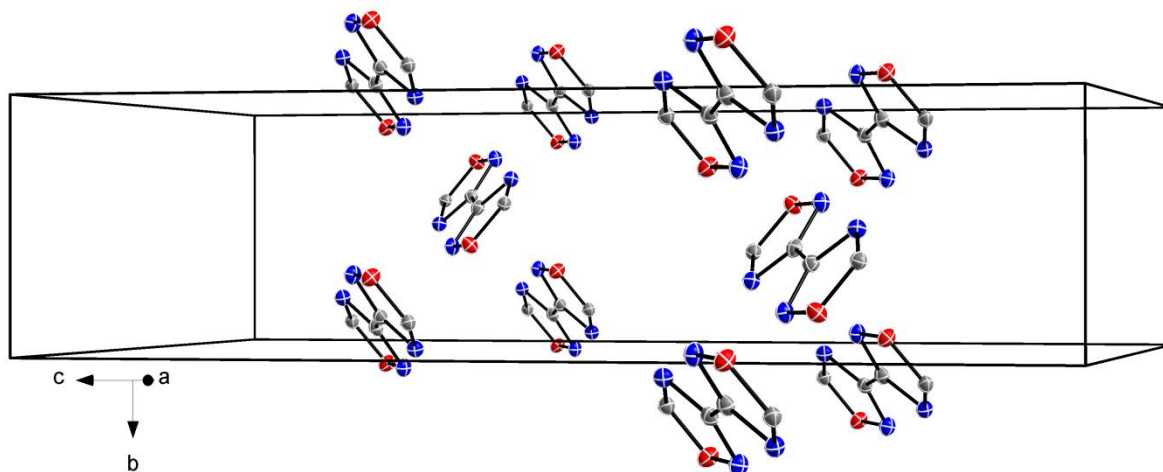


Figure 7: View along C1 \cdots C6 bond displaying the intramolecular interactions within the trinitromethyl moiety with atom distances as dashed lines: N1 \cdots O3 $2.543(2)$, N2 \cdots O5 $2.568(3)$, N3 \cdots O2 $2.566(2) \text{ \AA}$ (blue), N1 \cdots O6 $2.967(2)$, N2 \cdots O1 $2.924(3)$, N3 \cdots O4 $3.071(3) \text{ \AA}$ (grey), N2 \cdots O7 $2.981(2)$, N4 \cdots O1 $2.896(2) \text{ \AA}$ (black); and torsion angles [$^\circ$]: C2–C1–N1–O1 $-50.9(2)$, C2–C1–N2–O4 $-36.6(3)$, C2–C1–N3–O6 $-42.9(2)$; ΣvdW : (N,O) = 3.07 \AA .^[42]

There is also a series of short intermolecular N \cdots O contacts observed in the crystal structure, indicating the presence of weak interactions between the single molecules in the solid state. The respective atom distances are listed in Table 7. The interactions occur mostly between the oxygen atoms of the nitro groups and all four nitrogen atoms within the oxadiazole rings (N4, N5, N6 and N7). Between the bi-(1,2,4-oxadiazole) rings no intermolecular contacts shorter than the sum of van der Waals radii are observed (Figure 8).

Table 7: Intermolecular atom distances shorter than the sum of van der Waals radii [\AA] in the crystal structure of compound **6**.

X...Y	atom distance [\AA]
N1...O12	2.927(3)
N3...O1	2.945(3)
N6...O3	2.946(2)
N10...O3	3.010(3)
N4...O12	3.011(2)
N5...O11	3.040(3)
N7...O4	3.055(3)
$\Sigma \text{vdWals radii: N}\cdots\text{O } 3.07^{[42]}$	

**Figure 8:** Unit cell content with omitted trinitromethyl groups for demonstrating the orientation of the bi-(1,2,4-oxadiazole) units in one direction and their wave-like arrangement without showing any intermolecular contacts with each other.

Crystal Structure of 3,3'-Bi-(5-Fluorodinitromethyl-1,2,4-Oxadiazole) (**7**)

FDNM₂-BOD (**7**) crystallises as colourless plates in the monoclinic space group $P2_1/c$ with four molecules per unit cell and a remarkable high density of $2.040 \text{ g}\cdot\text{cm}^{-3}$ at $100(2) \text{ K}$. The density at ambient temperature [$293(2) \text{ K}$] is $1.960 \text{ g}\cdot\text{cm}^{-3}$ (Figure 9). The bi-(1,2,4-oxadiazole) ring system shows a planar arrangement, which is reflected in the dihedral angles of almost 0° and 180° , respectively [$\text{N4-O5-C2-N3 } -0.1(2)^\circ$, $\text{N4-O5-C2-C1 } -178.4(2)^\circ$]. The C1–N bonds are in the range of 1.54 \AA and are significantly elongated as compared to a standard C–N single bond (1.47 \AA), while the C1–F1 bond length is slightly shortened compared to a standard C–F single bond (1.36 \AA).^[35] The C1–C2 bond length is again slightly elongated compared to the corresponding bond lengths in compounds **4** and **6**.

As observed for the trinitromethyl derivative **6** also the nitro groups of the fluorodinitromethyl moieties are twisted into the propeller-like conformation.^[23, 43, 44] This results in intramolecular sterical interactions within this moiety, which are clearly observed in the structure and showing $\text{N}\cdots\text{O}$, $\text{F}\cdots\text{O}$ and $\text{F}\cdots\text{N}$ distances well below the sum of van der Waals radii^[42] as seen by view along the C1...C1' axis (Figure 10).

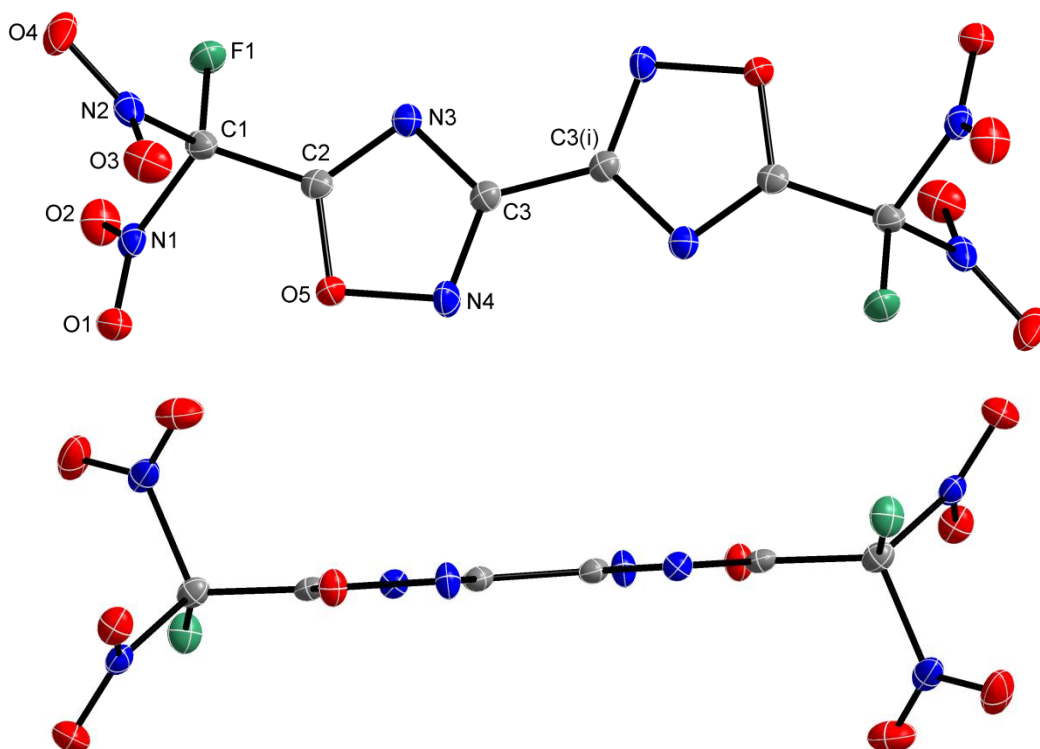


Figure 9: Crystal structure of compound **7** with perpendicular and lateral view showing the planarity of the ring system. Selected bond lengths [Å] and angles [°]: F1–C1 1.314(2), O5–C2 1.336(2), O5–N4 1.408(2), average N1–O 1.215(2), N1–C1 1.545(2), N3–C2 1.291(2), N3–C3 1.383(2), average N2–O 1.218(2), N2–C1 1.547(2), C2–C1 1.500(3), C3–N4 1.308(2), C3–C3' 1.463(4); O2–N1–O1 128.4(2), O2–N1–C1 116.7(2), O1–N1–C1 114.9(2), C2–N3–C3 100.4 (2), F1–C1–N2 108.3(1), C2–C1–N2 110.2(2), N1–C1–N2 104.9(1), N4–C3–N3 115.6(2), N3 C3–C3' 123.2(2), C3–N4–O5 103.0(2); C3–N3–C2–O5 0.0(2), C2 N3 C3 N4 0.0(2), N4–O5–C2–C1 –178.4(2), O2–N1–C1–F1 2.5(2), O1–N1–C1–C2 59.6(2), O3–N2–C1–C2 –31.6(2), C2–N3–C3–C3' –179.4(2).

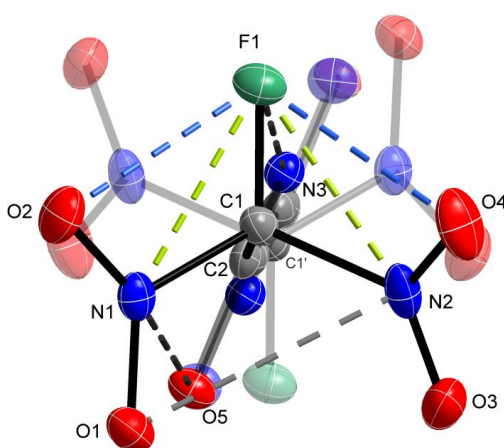


Figure 10: View along the C1...C1' axis displaying the intramolecular interactions within the fluorodinitromethyl moiety as dashed lines: F1...O2 2.517(1), F1...O4 2.553(2) Å (blue), F1...N1 2.329(2), F1...N2 2.332(2) Å (yellow), N2...O1 2.803(1) Å (grey), N1...O5 2.869(2), F1...N3 2.768(1) Å (black); Σ vdW: (F,O) = 2.99, (F,N) = 3.02, (N,O) = 3.07 Å.^[42]

The high density might be explained by the interlocking of the FDNM moieties building a three dimensional network of two intercalated wave-like layers, mainly supported by two short attractive intermolecular contacts [O1(i)⋯N2 and F1⋯O5(i)] as depicted in Figure 11. Figure 12 displays another perspective of the crystal structure of compound **7**. The view along the *c* axis shows the wave-like arrangement of the layers. There are no direct contacts between the ring systems, similar to the structure of compound **7**.

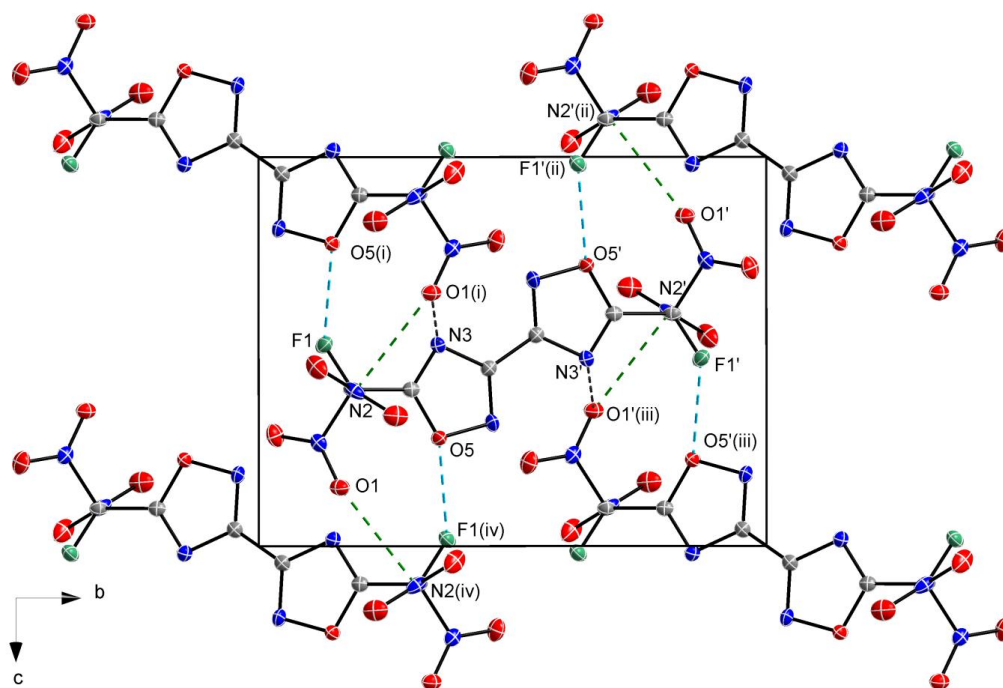


Figure 11: View along the *a* axis in the crystal structure of compound **7**. Intermolecular short contacts below the Σ vdW radii [Å]: F1⋯O5(i) 2.868(1), O1(i)⋯N2 2.965(2); Σ vdW: (N,O) = 3.07 Å, (F,O) = 2.99 Å;^[42] symmetry operators: (') $2-x, 1-y, 1-z$; (i) $-\frac{1}{2}+x, \frac{1}{2}-y, -\frac{1}{2}+z$; (ii) $\frac{1}{2}-x, \frac{1}{2}+y, \frac{1}{2}-z$; (iii) $2\frac{1}{2}-x, \frac{1}{2}+y, 1\frac{1}{2}-z$; (iv) $\frac{1}{2}+x, \frac{1}{2}-y, \frac{1}{2}+z$.

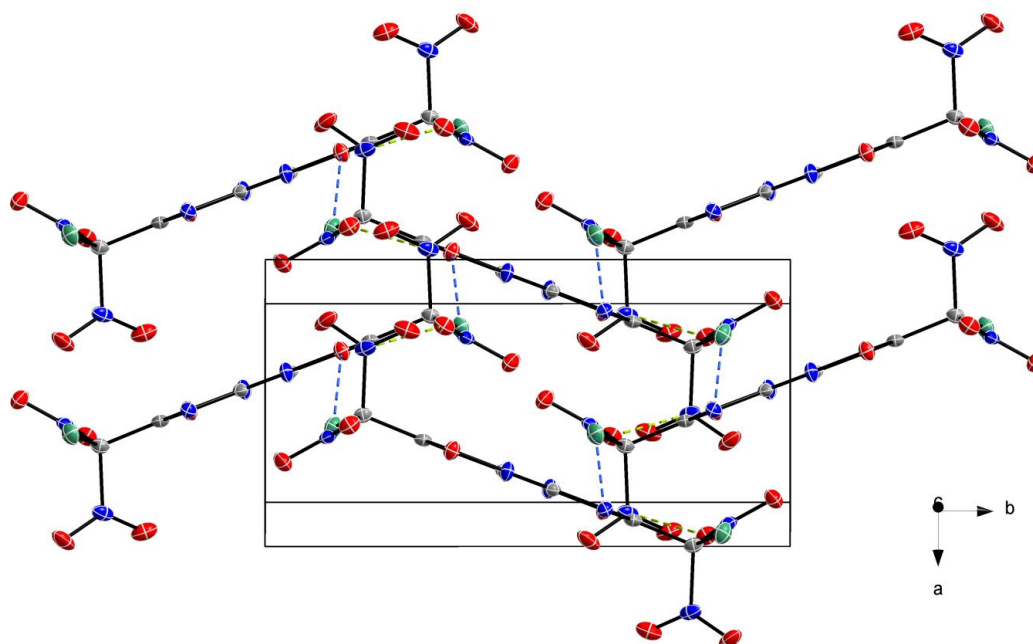


Figure 12: View along the *c* axis showing the wave-like arrangement of the layers supported by the intermolecular electrostatic interactions (blue and yellow dashed lines) shown in Figure 11.

Comparison of the Crystal Structures of 3,3'-Bi-(5-Trifluoromethyl-1,2,4-Oxadiazole) (9) and 5,5'-Bi-(2-Trifluoromethyl-1,3,4-Oxadiazole) (11)

Compounds **9** and **11** are analogous regarding the exchange of an oxygen with a nitrogen atom within the five-membered rings. They crystallise from ethanol as very thin colourless plates or by sublimation as thin needles (**9**) or blocks (**11**). Both compounds crystallise in the monoclinic space group $P2_1/c$ with two molecules per unit cell and show remarkable high densities of $2.012 \text{ g}\cdot\text{cm}^{-3}$ (**9**) and $1.980 \text{ g}\cdot\text{cm}^{-3}$ (**11**) at 173(2) K, hence a higher density for the bi-1,2,4-oxadiazole derivative **9** is obtained. Figures 13 and 14 depict the molecular structures of both TFM₂-BODs viewed perpendicular and lateral to the ring systems, which are planar in both molecules.

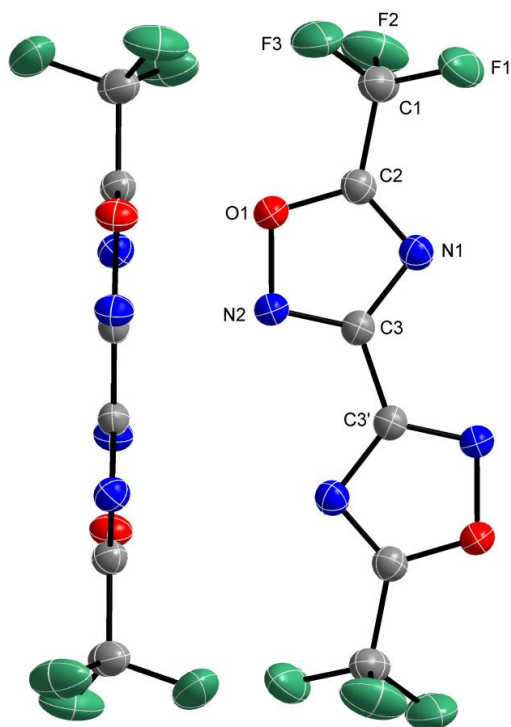


Figure 13: Crystal structure of compound **9** with perpendicular and lateral view showing the planarity of the ring system. Selected bond lengths [Å] and angles [°]: O1–C2 1.332(2), O1–N2 1.405(2), N1–C2 1.285(2), N1–C3 1.380(2), N2–C3 1.301(2), average F–C1 1.315(2), C3–C3' 1.458(3), C2–C1 1.510(2); average F–C1–F 108.2(2), C2–C1–F 110.8(3), N2–C3–N1 115.7(1), O1–N2–C3–C3' 178.6(2), N2–O1–C2–C1 178.7(1). Symmetry operator: ') $-x, -y, -z$.

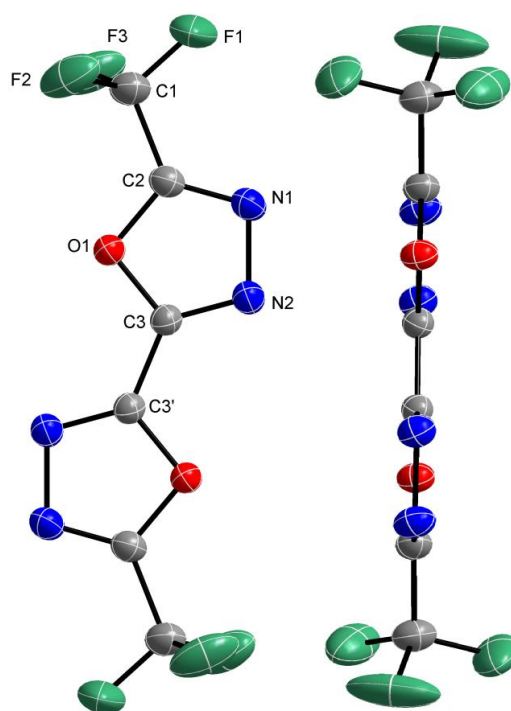


Figure 14: Crystal structure of compound **11** with perpendicular and lateral view showing the planarity of the ring system. Selected bond lengths [Å] and angles [°]: O1–C2 1.350(2), O1–C3 1.353(2), N2–C3 1.288(2), N2–N1 1.405(2), N1–C2 1.278(2), average F–C1 1.306(2), C3–C3' 1.446(3), C2–C1 1.504(2); average F–C1–F 107.9(2), C2–C1–F 111.0(2), N2–C3–O1 114.1(1), C2–O1–C3 100.8(1), N1–N2–C3–C3' $-179.1(2)$, N2–N1–C2–C1 $-178.3(2)$. Symmetry operator: ') $1-x, -y, 2-z$.

The structures exhibit some short intermolecular contacts that are well below the sum of van der Waals radii. For example, in the structure of compound **9**, N2...C3(i) 3.105(2) and O1...C3(i) 3.122(2) Å [symmetry operator: (i) $-x, \frac{1}{2}+y, \frac{1}{2}-z$], and in the structure of

compound **11**, N1...C3(i) 3.062(2) and N2...C3(i)' 2.984(2) Å [symmetry operator: (i) 1-x, -1/2+y, 1/2-z; ΣvdW: (N,C) = 3.25, (O,C) = 3.22 Å].^[42] These short contacts may be responsible for the high densities observed for compounds **9** and **11**.

When comparing the crystal structures of the bi-1,2,3-oxadiazoles **4**, **6**, **7** and **9** no remarkable differences in the bond lengths and angles can be observed. Thus, the moieties attached to the rings at the 5-positions 5-C-CX [CX = CH₃ (**4**), C(NO₂)₃ (**6**), C(NO₂)₂F (**7**), CF₃ (**9**)] seem to have minor influence on the 3,3'-bi-(1,2,4-oxadiazole) system. The 5-C-CX bond length range from 1.489(2) Å in compound **4** to 1.510(2) Å in compound **9**.

4.6 Physical, Chemical and Energetic Properties

Owing to the high combined nitrogen and oxygen content, the multiple nitro groups and the high densities of compounds **6** and **7** their energetic behaviour has been determined. Their investigated physical and thermodynamic properties are summarised in Table 8, and the calculated detonation and combustion parameters are listed in Table 9. For convenience, the molecular structures are shown in Figure 15.

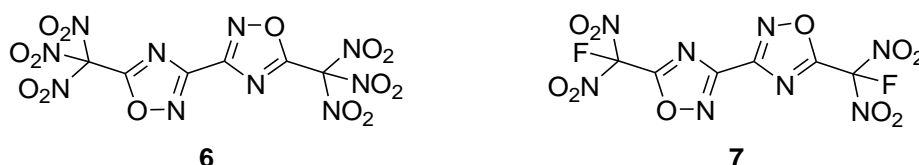


Figure 15: Molecular structures of the compounds discussed in this section with physical and thermodynamic properties and calculated performances listed in Tables 8 and 9.

Table 8: Physical and thermodynamic data for compounds **6** and **7**.

	6	7
Formula	$C_6N_{10}O_{14}$	$C_6N_8O_6F_2$
FW [g·mol⁻¹]	436.12	382.14
IS [J]^a	10	10
FS [N]^b	80	192
ESD [J]^c	0.8	1.0
grain size [μm]	<100	<100
N [%]^d	32.12	29.33
N+O [%]^e	83.48	71.20
Ω_{CO} [%]^f	29.3	16.8
Ω_{CO2} [%]^f	7.3	-8.4
T_{melt} [°C]^g	119	67
T_{dec} [°C]^h	124	151
ρ_{RT} [g·cm⁻³]ⁱ	1.94	1.96
Δ_fH° [kJ·mol⁻¹]^j	61.9	-362.4
ΔU° [kJ·kg⁻¹]^k	210.2	-883.6

a) Impact sensitivity (BAM drophammer, method 1 out of 6);^[45–47] b) friction sensitivity (BAM friction tester, method 1 out of 6);^[47–49] c) electrostatic discharge sensitivity (OZM);^[50, 51] d) nitrogen content; e) combined nitrogen and oxygen content; f) absolute oxygen balance assuming the formation of CO or CO₂ and HF; g) melting temperature from DSC at a heating rate of 5 °C min⁻¹; h) decomposition temperature from DSC at a heating rate of 5 °C min⁻¹; i) density measured by X-ray diffraction at ambient temperature [298(2) K]; j) calculated heat of formation at the CBS-4M level of theory;^[55] k) internal energy of formation.

The sensitivities towards impact and friction were determined experimentally according to the standards of the German Federal Institute for Materials Research and Testing (BAM).^[45–49] Compounds **6** and **7** show equal impact sensitivities of 10 J. This result stands in contrast to KAMLETS theory, that TNM containing materials are more sensitive towards impact than their FDNM containing analogues due to restricted rotation of the C–NO₂ bonds.^[52] The friction sensitivity is 80 N for the trinitromethyl derivative **6** and drops to 192 N for the fluorodinitromethyl derivative **7**. Thus, according to the UN recommendations on the transport of dangerous goods compounds **6** and **7** shall be classified as sensitive towards both impact and friction.^[53] The electrostatic discharge test (ESD) was carried out in order to determine whether the compounds are ignitable by the human body, which can generate up to

0.025 J of static energy.^[50, 51] Compounds **6** and **7** are insensitive towards this energy. For a practical use as energetic oxidisers the benchmark sensitivities are defined to be not higher than that of PETN (pentaerythrityl tetranitrate: IS = 4 J, FS = 80 N, ESD = 0.1 J). Thus, the sensitivities of compounds **6** and **7** are in a good range for new oxygen-carriers. The oxygen balance Ω_{CO} of compounds **6** (29.3%) is found to be in between the values of AP (34.0%) and ADN (25.8%). According to DSC measurements TNM₂-BOD (**6**) melts at 119 °C with subsequent decomposition at 124 °C. The analogue FDNM₂-BOD (**7**) melts at 67 °C and has a higher decomposition point at 151 °C (Figure 16). The heats of formation were computed by *ab initio* calculations using the GAUSSIAN 09 program package at the CBS-4M level of theory.^[54] The heat of formation of compound **6** is positive, while for compound **7** a negative value is obtained due to the contribution of the two C–F bonds.

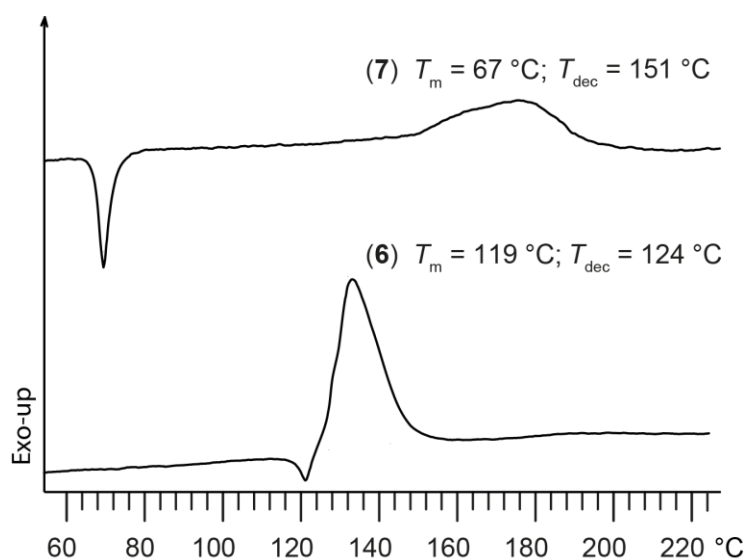


Figure 16: DSC plots of the polynitro compounds **6** and **7** recorded with a heating rate of 5 °C·min⁻¹.

Based on the heats of formation, and attributed to the corresponding densities at ambient temperature, the calculation of the detonation and combustion parameters was performed using the EXPLO5 computer code (Table 9).^[55]

The calculated detonation velocities D_V and pressures p_{CJ} of compounds **6** (8830 m·s⁻¹, 337 kbar) and **7** (8567 m·s⁻¹, 309 kbar) are comparable with those calculated for RDX (1,3,5-trinitroperhydro-1,3,5-triazine: 8838 m·s⁻¹, 343 kbar) and PETN (8404 m·s⁻¹, 309 kbar), respectively.^[55] These calculated values for known explosives stand in agreement with the literature known values.^[56] Therefore both compounds might also be useful as high performing and oxygen rich energetic materials with sensitivities that allow good handling and operation. In an open flame test compounds **6** and **7** burn fast without audible detonation.

The calculation of the isobaric combustion in a chamber with 70 bar inner pressure against atmosphere with equilibrium expansion conditions at the nozzle was also performed using the EXPLO5 (Version 6.02) computer code (Table 9).^[55] The specific impulses I_{sp} for the neat compounds **6** and **7** were calculated to 246 s and 238 s, respectively. In addition, the I_{sp} for propellant compositions with different ratios (20–30%) of aluminium were computed and are about 10–15 s higher than the values of the neat compounds.

Table 9: Detonation and combustion parameters of compounds **6** and **7** calculated with the EXPLO5 computer code (Version 6.02).^[55]

	6	7
$-\Delta_{\text{Ex}}U^\circ$ [kJ·kg ⁻¹] ^a	5551	3949
T_{det} [K] ^b	4356	3355
p_{CJ} [kbar] ^c	337	309
D_V [m·s ⁻¹] ^d	8830	8567
V_0 [L·kg ⁻¹] ^e	675	676
I_{sp} (neat) [s] ^f	246 (3466)	238 (3474)
I_{sp} (+20% Al) [s] ^g	257 (4619)	254 (4468)
I_{sp} (+25% Al) [s] ^g	254 (4690)	243 (4322)
I_{sp} (+30% Al) [s] ^g	247 (4630)	228 (3980)
I_{sp} (+16% Al, 14% PBAN) [s] ^h	249 (2945)	235 (2890)
I_{sp} (+10% Al, 14% PBAN) [s] ⁱ	256 (3338)	237 (2732)
I_{sp} (+18% Al, 12% HTPB) [s] ^j	249 (2990)	236 (3008)
I_{sp} (+12% Al, 12% HTPB) [s] ^k	259 (3507)	239 (2891)

a–e) Detonation parameters calculated with EXPLO5 (V6.02) using the 'BKW EOS' equation of state with the default 'BKWG-S' set of constants;^[55] a) heat of detonation; b) detonation temperature; c) detonation pressure; d) detonation velocity; e) volume of gaseous detonation products (assuming only gaseous products).

f–h) Isobaric combustion parameters calculated with EXPLO5 (V6.02) using isobaric combustion conditions, chamber pressure of 70.0 bar versus ambient pressure with equilibrium expansion conditions at the nozzle throat;^[55] isobaric combustion temperature in the combustion chamber in parentheses [K]; f) specific impulse of the neat compound; g) specific impulse of mixtures with 20–30% aluminium; h) specific impulse of mixtures with 70% oxidiser, 16% aluminium, 12% polybutadiene acrylonitrile (PBAN) and 2% epoxyresin as curing agent; the analogue mixture with AP used in the Space Shuttle Programm of NASA^[57] reveals $I_{\text{sp}} = 262$ s and $T_c = 3380$ K; i) higher specific impulse values achieve mixtures in PBAN with 76% oxidiser, 10% aluminium and 2% epoxyresin; j) specific impulse of mixtures with 18% aluminium, 10% hydroxyterminated polybutadiene (HTPB) and 2% hexamethylene diisocyanate as curing agent; the analogue mixture with AP reveals $I_{\text{sp}} = 264$ s and $T_c = 3564$ K; k) higher specific impulse values achieve mixtures in HTPB with 76% oxidiser, 12% aluminium and 2% hexamethylene diisocyanate.

Finally, the I_{sp} for propellant compositions with aluminium and two common binder systems (PBAN and HTPB) were calculated for comparison with the rocket motor composition for solid rocket boosters used by the NASA Space Shuttle program. It consists of 70% ammonium perchlorate as oxidiser, 16% aluminium as high performing fuel which additionally increases the combustion temperature, 12% PBAN binder (polybutadiene acrylonitrile), and 2% bisphenol-A ether as curing agent,^[57] and achieves a specific impulse I_{sp} of 262 s.^[55] In the corresponding mixtures of compounds **6** and **7** only the ratio of oxidiser/aluminium was varied while the portion of PBAN binder was kept at 14 % (maximum solid loading of PBAN is 86%).^[58] For TNM₂-BOD (**6**) the 76/10 mixture achieves the highest specific impulse of 256 s, which is 6 s below the value of the AP composition. The analogous mixture of compound FDNM₂-BOD (**7**) achieves a considerably lower I_{sp} of 235 s. Reasons for that might be the lower oxygen balance and the lower heat of formation of the fluorodinitromethyl derivative **7**.

Recent compositions for solid rocket boosters use HTPB (hydroxyterminated polybutadiene) instead of PBAN. A realistic mixture is composed of 70% ammonium perchlorate, 18% aluminium, 10% HTPB, and 2% hexamethylene diisocyanate as curing agent,^[59] which reaches a I_{sp} of 264 s. Also in this case the optimum oxidiser/aluminium ratio to accomplish the maximum I_{sp} is the 76/12 mixture. The formulations of compounds **6** and **7** achieve

impulse values of 259 s and 239 s, respectively. Thus, the trinitromethyl derivative **6** gets into the range of the AP compositions and also the temperature in the combustion chamber of about 3500 K is similar to the AP mixture. TNM₂-BOD (**6**) seems to be a promising oxidiser candidate with acceptable sensitivities, an oxygen balance Ω_{CO} of 29.3%, which is just between AP and ADN, and a thermal stability in the range of ADN ($T_{\text{dec}} = 127\text{ }^{\circ}\text{C}$).

4.7 Computational Evaluation of the Energetic Performance of 5,5'-Bi-(2-Polynitromethyl-1,3,4-Oxadiazoles)

The heterocyclic class of oxadiazoles includes four different isomers that find various applications.^[12–15] The bi-oxadiazoles form two further constitutional isomers, owing to the asymmetry of the 1,2,3- and 1,2,4-oxadiazoles, which can be linked at two different carbon atoms (Figure 17). Only the bi-1,2,3- and bi-1,2,5-oxadiazoles contain C₄-chains. As mentioned in the introduction, the area of energetic materials largely only 1,2,5-oxadiazole (furazane) derivatives have been investigated, which are preferred owing to their positive heats of formation.^[16–17] Figure 17 does not only show all the oxadiazole isomers, but also their heats of formation in the gas phase [kJ·mol^{−1}] displaying the trend that is given when considering these ring systems as linker for polynitro groups. In the series of oxadiazoles, after the furazanes follow the 1,2,3-, 1,2,4-, and 1,3,4-oxadiazoles in this row of decreasing heats of formation. In the same order the heats of formation of the bi-oxadiazoles fall, whereby only marginal differences of 3–7 kJ·mol^{−1} are observed when connecting bi-1,2,3- or bi-1,2,4-oxadiazoles at different positions. The (bi-)1,3,4-oxadiazoles show the lowest heats

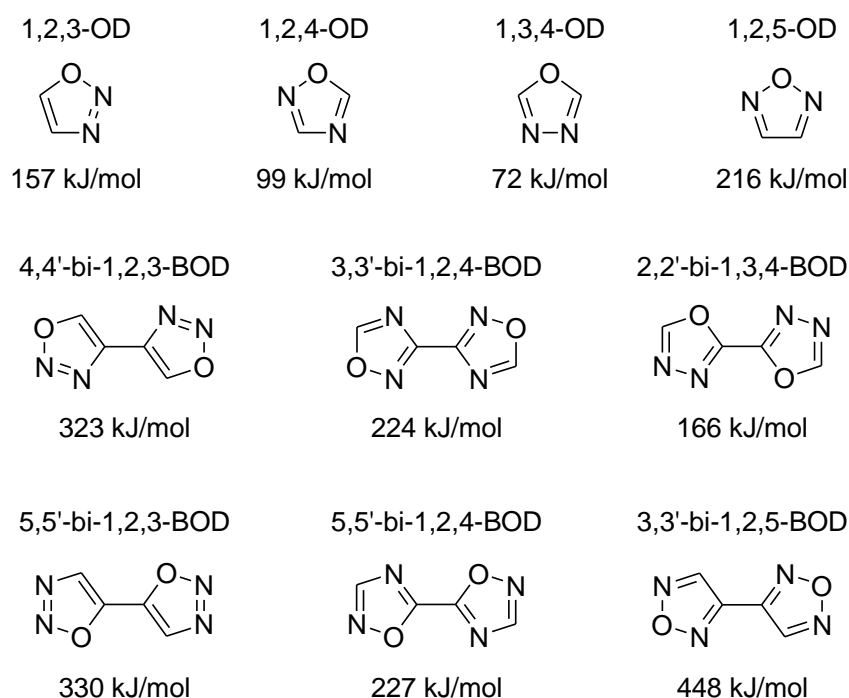


Figure 17: All oxadiazole (OD) and symmetric bi-oxadiazole (BOD) isomers and their calculated gas phase heats of formation using the atomisation method, based on the electronic enthalpies calculated at the CBS-4M level of theory.

of formation in that series. However, the ring system might show up other properties that could be advantageously, for instance compounds that are more chemically inert or have higher decomposition temperatures.

In attempting to transfer the successful concept of the bi-1,2,4-oxadiazole **6** as linker for two polynitromethyl groups to the bi-1,3,4-oxadiazole system, the two constitutional isomers **9** and **11** with non-energetic trifluoromethyl groups have been synthesised. When comparing these two model compounds, it turns out that the density of the bi-1,2,4-oxadiazole **9** is slightly higher than for the bi-1,3,4-oxadiazole **11**. However, according to DSC measurements compound **9** melts at 98 °C and boils at 142 °C, whereas compound **11** melts at 169 °C and boils at 199 °C (Table 10). Both compounds showed no decomposition until a temperature of 400 °C in a closed aluminium vessel in the DSC measurements. Hence, a higher thermal stability for the bi-1,3,4-oxadiazoles can be assumed. As expected, the heat of formation $\Delta_f H^\circ$ of compound **11** was calculated to be slightly more negative than that of compound **9**.

Table 10: Thermal and thermodynamic data for compounds **9** and **11**.

	9	11
Formula	$C_6N_4O_2F_6$	
FW [g·mol⁻¹]	274.10	
T_{melt} [°C]^a	98	169
T_{boil} [°C]^b	142	199
ρ_{cryst} [g·cm⁻³]^c	2.01	1.98
ρ_{RT} [g·cm⁻³]^c	1.97	1.95
$\Delta_f H^\circ$ [kJ·mol⁻¹]^d	-1135.1	-1191.0
ΔU° [kJ·kg⁻¹]^e	-4087.4	-4133.9

a) Melting temperature from DSC at a heating rate of 5 °C·min⁻¹; b) boiling temperature from DSC at a heating rate of 5 °C·min⁻¹; c) density measured by X-ray diffraction at 173(2) K and from pycnometer measurements at ambient temperature; d) calculated heat of formation, and e) internal energy of formation at the CBS-4M level of theory.^[55]

For the evaluation of the energetic performances of the 2,2'-bi-(5-polynitro/polyfluoromethyl-1,3,4-oxadiazoles) **12**, **13** and **14**, the heats of formation $\Delta_f H^\circ$ were computed by quantum chemical calculations at the CBS-4M level of theory (Figure 2).^[54] The contribution of C–F bonds on the $\Delta_f H^\circ$ can clearly be observed in this series of polyfluoro/polynitro compounds: the more C–F bonds in the molecule the more negative the heat of formation $\Delta_f H^\circ$. The trinitromethyl derivative **14** shows a positive value for $\Delta_f H^\circ$, while all other compounds have negative values for $\Delta_f H^\circ$.

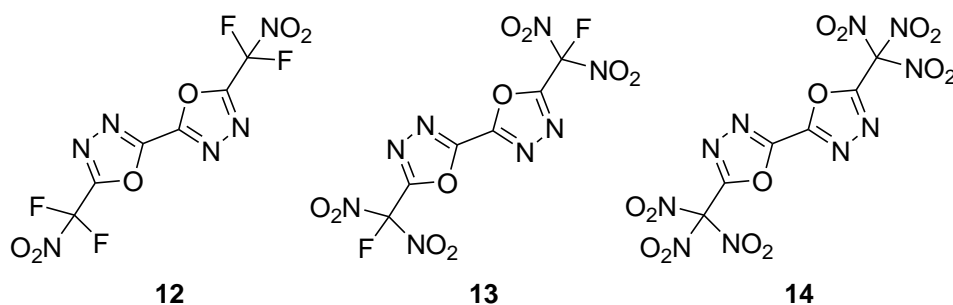


Figure 18: Molecular structures of 2,2'-bi-(5-difluoronitromethyl-1,3,4-oxadiazole) (**12**), 2,2'-bi-(5-fluorodinitromethyl-1,3,4-oxadiazole) (**13**) and 2,2'-bi-(5-trinitromethyl-1,3,4-oxadiazole) (**14**) with successive substitution of the fluorine atoms by nitro groups.

Using these values and an estimated density of $1.90 \text{ g}\cdot\text{cm}^{-3}$ (minimum estimation supported by previous work) the detonation and combustion parameters were calculated by means of the EXPLO5 (V6.02) computer code (Table 11).^[55] Comparing the specific impulse I_{sp} values of compounds **13** and **14** with compounds **6** and **7**, in all mixtures and formulations the I_{sp} are about 2–4 s higher for the bi-1,3,4-oxadiazoles **13** and **14**. Compound **14** exhibits a I_{sp} of 264 s in the composition with 12% aluminium embedded in 12% cured HTPB, just the same value as the AP composition achieves. Providing the thermal stability of the non-fused heterocyclic system is not decreased too much by the trinitromethyl moiety, the bi-1,3,4-oxadiazole derivative **14** might represent a suitable candidate as oxidiser in solid rocket propellants with improved performance compared to its analogous bi-1,2,4-oxadiazole **6**.

Table 11: Calculated detonation and combustion performance of compounds **12**, **13** and **14** using the EXPLO5 (V6.02) computer code.^[55]

	12	13	14
Formula	$\text{C}_6\text{N}_6\text{O}_6\text{F}_4$	$\text{C}_6\text{N}_8\text{O}_{10}\text{F}_2$	$\text{C}_6\text{N}_{10}\text{O}_{14}$
FW [$\text{g}\cdot\text{mol}^{-1}$]	328.09	382.11	436.12
N+O [%] ^a	54.87	71.20	83.48
Ω_{CO} [%] ^b	−29.3	16.8	29.3
Ω_{CO_2} [%] ^b	0.0	−8.4	7.3
ρ_{est} [$\text{g}\cdot\text{cm}^{-3}$] ^c	1.90	1.90	1.90
$\Delta_f H^\circ$ [$\text{kJ}\cdot\text{mol}^{-1}$] ^d	−685.2	−212.3	231.4
ΔU° [$\text{kJ}\cdot\text{kg}^{-1}$] ^e	−2028.0	−490.7	598.8
$-\Delta_{\text{Ex}} U^\circ$ [$\text{kJ}\cdot\text{kg}^{-1}$] ^f	1606	4316	5893
T_{det} [K] ^g	2220	3647	4633
p_{CJ} [kbar] ^h	248	297	332
D_V [$\text{m}\cdot\text{s}^{-1}$] ⁱ	6898	8440	8764
V_0 [$\text{L}\cdot\text{kg}^{-1}$] ^j	597	677	677
I_{sp} (neat) [s] ^k	203 (2894)	244 (3581)	252 (3562)
I_{sp} (+20% Al) [s] ^l	230 (3583)	258 (4522)	260 (4660)
I_{sp} (+25% Al) [s] ^l	223 (3453)	248 (4405)	257 (4720)
I_{sp} (+30% Al) [s] ^l	216 (3391)	232 (4119)	250 (4669)
I_{sp} (+16% Al, 14% PBAN) [s] ^m	221 (2908)	238 (2952)	253 (2957)
I_{sp} (+10% Al, 14% PBAN) [s] ⁿ	220 (2734)	241 (2833)	262 (3450)
I_{sp} (+18% Al, 12% HTPB) [s] ^o	222 (3040)	239 (3022)	252 (3092)
I_{sp} (+12% Al, 12% HTPB) [s] ^p	225 (2930)	243 (2963)	264 (3613)

a) Combined nitrogen and oxygen content; b) absolute oxygen balance assuming the formation of CO and CO₂ and HF; c) worst case estimation on density; d) heat of formation, and e) internal energy of formation calculated at the CBS-4M level of theory; f–j) Detonation parameters calculated with EXPLO5 (V6.02) using the 'BKW EOS' equation of state with the default 'BKWG-S' set of constants;^[55] f) heat of detonation; g) detonation temperature; h) detonation pressure; i) detonation velocity; j) volume of gaseous detonation products (assuming only gaseous products); k–p) Isobaric combustion parameters calculated with EXPLO5 (V6.02) using isobaric combustion conditions, chamber pressure of 70.0 bar versus ambient pressure with equilibrium expansion conditions at the nozzle throat;^[55] isobaric combustion temperature in the combustion chamber in parentheses [K]; k) specific impulse of the neat compound; l) specific impulse of mixtures with 20–30% aluminium; m) specific impulse of mixtures with 70% oxidiser, 16% aluminium, 12% polybutadiene acrylonitrile (PBAN) and 2% epoxyresin as curing agent; the analogue mixture with AP used in the Space Shuttle Programm of NASA^[57] reveals $I_{\text{sp}} = 262 \text{ s}$ and $T_c = 3380 \text{ K}$; n) higher specific impulse values achieve mixtures in PBAN with 76% oxidiser, 10% aluminium and 2% epoxyresin; o) specific impulse of mixtures with 18% aluminium, 10% hydroxyterminated polybutadiene (HTPB) and 2% hexamethylene diisocyanate as curing agent; the analogue mixture with AP reveals $I_{\text{sp}} = 264 \text{ s}$ and $T_c = 3564 \text{ K}$; p) higher specific impulse is achieved by a mixture of 76% oxidiser, 12% aluminium in 12% HTPB.

4.8 Summary, Conclusions and Outlook

In this study two synthetic routes for so far unknown 3,3'-bi-(5-trinitromethyl-1,2,4-oxadiazole) (**6**) have been developed. The new compound **6** represents a rare example of a ternary CNO-species. As compared to the volatile hexanitroethane, it combines its properties with those of the bi-(1,2,4-oxadiazole) ring system and represents an interesting non volatile and high energetic alternative. Furthermore, 3,3'-bi-(5-fluorodinitromethyl-1,2,4-oxadiazole) (**7**) was synthesised for the first time by fluorination of diammonium 5,5'-bis(dinitromethanide)-3,3'-bi-(1,2,4-oxadiazole) (**5**) using *Selectfluor*TM. In the course of these studies also unknown 3,3'-bi-(1,2,4-oxadiazolyl)-5,5'-diacetic acid (**3**) and 3,3'-bi-(5-dimethyl-1,2,4-oxadiazole) (**4**) were isolated. All compounds were fully characterised including their X-ray crystal structures except for the dicarboxylic acid **3**. The two new hydrogen atom free bi-(1,2,4-oxadiazoles) **6** and **7** with trinitromethyl or fluorodinitromethyl moieties attached overcome the problematic acidity associated with related polynitroazoles. Their remarkable high densities can be rationalised by various intra- and intermolecular electrostatic N \cdots O interactions involving the nitro groups observed within the crystal structure. For these two compounds the energetic behaviour was determined. Their sensitivities are in an acceptable range. The calculated detonation parameters are in the range of RDX and PETN, respectively. The specific impulse of a composition of compound **6** with aluminium in two inert binders reveals a slightly lower value than comparable ammonium perchlorate formulations used for solid rocket boosters (Table 12). Advantageously, the burning of compound **6** produces no toxic substances such as hydrogen chloride.

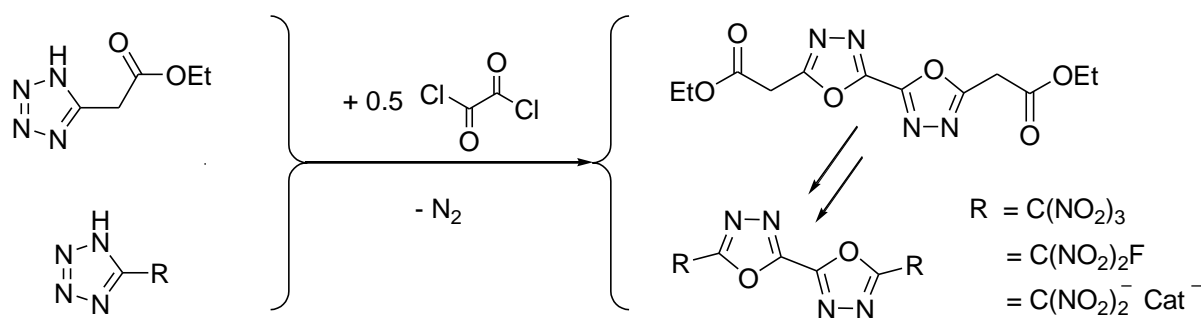
Table 12: Molecular structures of the promising compound **6** and the assumed compound **14** with their characteristic properties, calculated performances and possible applications.

	6	14
Molecular structure		
<i>IS</i> [J]	10	–
<i>FS</i> [N]	80	–
<i>T</i> _{dec} [°C]	119	–
Ω_{CO} [%]	29.3	29.3
ρ_{RT} [g·cm ⁻³]	1.94	1.90 (est.)
<i>D</i> _V [m·s ⁻¹]	8830	8764
<i>p</i> _{CJ} [kbar]	337	332
<i>I</i> _{sp} (Al+HTPB) [s]	259	264
Possible applications	oxidiser/propellant	oxidiser/propellant

Moreover, the literature known 3,3'-bi-(5-trifluoromethyl-1,2,4-oxadiazole) (**9**) and its analogous 5,5'-bi-(2-trifluoromethyl-1,3,4-oxadiazole) (**11**) have been synthesised and additional analytical information is presented. The compounds were considered as model compounds for the transfer of the concept from bi-1,2,4-oxadiazoles to their constitutional isomer bi-1,3,4-oxadiazoles. Compounds **9** and **11** were compared to each other regarding thermal stability and density, thereby showing slightly lower density, but considerably higher thermal stability for the bi-1,3,4-oxadiazole derivative **11**. Consequently, a theoretical study

has been conducted, in which the fluorine atoms in compound **11** were substituted successively by nitro groups, thus representing the analogue bi-1,3,4-oxadiazole derivatives of the synthesised compounds **6** and **7**. The calculated material 2,2'-bi-(5-trinitromethyl-1,3,4-oxadiazole) (**14**) is analogue to TNM₂-BOD (**6**), but exhibits an even higher specific impulse, which achieves the values of comparable ammonium perchlorate formulations in two different polymeric matrices. It is absolutely recommended to synthesise this material and investigate it in terms of thermal stability, density and sensitivity for a direct comparison.

Possible synthetic routes to compounds **13** and **14** are presented in Scheme 2 for future work. Therefore a convenient literature known route by VERESHCHAGIN *et al.* from 2006 is suggested.^[28] Similar to the synthesis of compound **11** from 5,5'-bi-1*H*-tetrazole, also 5-substituted tetrazoles can be converted into the corresponding bi-1,3,4-oxadiazoles using oxalyl chloride under N₂ evolution. The compounds from Chapter 3 are suitable for these reactions: either ethyl 2-(1*H*-tetrazol-5-yl)acetate might be converted and then it can proceed likewise compounds **6** and **7** from this chapter, or the 5-(polynitromethyl)-2*H*-tetrazoles might be converted directly to compounds **13** and **14**. Also salts of 5,5'-bi-(dinitromethylidene-1,3,4-oxadiazole) might be accessible through this method.



Scheme 2: Possible synthetic routes towards bi-1,3,4-oxadiazoles **13** and **14** following a literature known procedure for the conversion of 5-substituted tetrazoles.^[28]

4.9 Experimental Section

The starting materials **2** (30%)^[23] and **5** (95%)^[19] were prepared according to the literature known procedures.

3,3'-Bi-(1,2,4-oxadiazolyl)-5,5'-diacetic acid (3): 500 mg sodium hydroxide (12.05 mmol) was added to a suspension of 500 mg of compound **2** (1.61 mmol) in water (25 mL) and the reaction mixture was stirred for 1 h at 30 °C. The mixture was acidified to pH = 3 with aqueous HNO₃ (60 %) and concentrated under reduced pressure. It was cooled by means of an ice bath and the precipitate was filtered yielding 310 mg of compound **3** (1.22 mmol, 76%) as colourless solid.

DSC (T_{onset}): $T_{\text{melt}} = 160$ °C, $T_{\text{dec}} = 236$ °C; **¹H NMR** (d_6 -DMSO): $\delta = 13.33$ (s, 2H, OH), 4.31 (s, 4H, CH₂); **¹³C{¹H} NMR** (d_6 -DMSO): $\delta = 176.6$ (OCN), 168.0 (COO), 160.1 (CC), 33.4 (CH₂) ppm; **EA**: C₈H₆N₄O₆ (254.16 g·mol⁻¹) calcd: C 37.81, N 22.04, H 2.38; found: C 37.83, N 22.34, H 2.41 %; **IR**: $\tilde{\nu}$ (rel. int.) = 2986 (w), 2617 (w), 1707 (s), 1585 (m), 1432 (m), 1404 (m), 1330 (m), 1300 (m), 1272 (w), 1233 (s), 1202 (m), 1161 (m), 1022 (m), 956 (w), 933 (m), 904 (m), 825 (m), 713 (m), 676 cm⁻¹ (s); **Raman** (300 mW): $\tilde{\nu}$ (rel. int.) = 2988 (22), 2943 (60), 1595 (100), 1434 (17), 1406 (12), 1339 (5), 1299 (5), 1235 (3), 1163 (4), 1046 (22), 1005 (11), 911 (5), 769 (14), 707 (3), 643 (3), 579 (5) cm⁻¹; **MS** (FAB⁺): $m/z = 255.2$ [M+H⁺]; (FAB⁻): $m/z = 253.2$ [M-H⁻].

3,3'-Bi-(5-methyl-1,2,4-oxadiazole) (4): Compound **3** was dissolved in DMF and heated to 60 °C for 1 h. The evolution of CO₂ was confirmed by testing with an aqueous Ba(OH)₂ solution. Compound **4** crystallised quantitatively overnight at 8 °C from DMF.

DSC (T_{onset}): $T_{\text{melt}} = 166$ °C, $T_{\text{dec}} = 266$ °C; **¹H NMR** (CD₃CN): $\delta = 2.67$ ppm (s, 6 H, CH₃); **¹³C{¹H} NMR** (CD₃CN): $\delta = 179.0$ (OCN), 160.1 (CC), 11.7 ppm (CH₃); **EA**: C₆H₆N₄O₂ (166.14 g·mol⁻¹) calcd: C 43.38, N 33.72, H 3.64; found: C 43.27, N 33.44, H 3.54 %; **IR**: $\tilde{\nu}$ (rel. int.) = 3020 (w), 2932 (w), 2621 (w), 1931 (w), 1576 (s), 1544 (w), 1438 (m), 1413 (m), 1395 (w), 1374 (m), 1265 (s), 1218 (s), 1113 (w), 1047 (m), 1036 (m), 976 (m), 949 (m), 908 (s), 701 (s), 680 (m) cm⁻¹; **Raman** (300 mW): $\tilde{\nu}$ (rel. int.) = 3193 (4), 3020 (21), 2982 (28), 2932 (85), 2738 (4), 1961 (3), 1596 (100), 1585 (28), 1446 (15), 1403 (8), 1384 (4), 1264 (3), 1056 (6), 1019 (9), 983 (5), 925 (6), 774 (3), 171 (11), 661 (4), 509 (3), 422 (4), 369 (7) cm⁻¹; **MS** (DEI⁺): $m/z = 166.2$ [M⁺].

3,3'-Bi-(5-trinitromethyl-1,2,4-oxadiazole) (6):

Method 1: 250 mg of compound **3** (0.66 mmol) was added in small portions over a period of 10 min to a solution of 200 mg NO₂BF₄ (1.50 mmol) in anhydrous acetonitrile (100 mL) at -10 °C. The reaction mixture was stirred for one hour at 0 °C and the solvent removed under reduced pressure. To the remaining yellowish solid was added diethyl ether (50 mL) and the mixture was heated under stirring to 40 °C in a closed vessel for 30 min. The solid was filtrated and the solvent concentrated under reduced pressure to about 3 mL yielding a crystalline solid at 8 °C overnight. The remaining diethyl ether was removed furnishing 80 mg of compound **6** (0.18 mmol, 27%) as colourless crystals.

Method 2: Concentrated sulfuric acid (6.6 mL, 96%) was cooled to $-10\text{ }^{\circ}\text{C}$ and HNO_3 (2.0 mL, 100%) was added dropwise. 250 mg of compound **3** (0.98 mmol) was added in small portions over a period of 30 min. The flask was equipped with a drying tube and the reaction mixture was stirred for 16 h while allowed to warm up to room temperature. The mixture was poured onto ice (40 g), the precipitated solid was filtered off and washed with ice water. Drying under reduced pressure yielded 380 mg of compound **6** (0.87 mmol, 89%) as a colourless solid. Re-crystallisation from diethyl ether of dichloromethane gave single crystals. **DSC** (T_{onset}): $T_{\text{melt}} = 119\text{ }^{\circ}\text{C}$, $T_{\text{dec}} = 124\text{ }^{\circ}\text{C}$; $^{13}\text{C}\{^1\text{H}\}$ NMR (CD_2Cl_2): $\delta = 163.6$ (OCN), 159.9 (CC), 117.5 (sept, $J_{\text{C-N}} = 9.4\text{ Hz}$, $\text{C}(\text{NO}_2)_3$); $^{14}\text{N}\{^1\text{H}\}$ NMR (CD_2Cl_2): $\delta = -43\text{ ppm}$ (NO_2); **EA**: $\text{C}_6\text{N}_{10}\text{O}_{14}$ ($436.12\text{ g}\cdot\text{mol}^{-1}$) calcd: C 16.52, N 32.12; found: C 16.52, N 31.02 %; **IR**: $\tilde{\nu}$ (rel. int.) = 1710 (w), 1608 (s), 1561 (m), 1405 (w), 1347 (w), 1291 (m), 1271 (s), 1227 (s), 1139 (s), 1072 (s), 1038 (s), 975 (m), 962 (m), 933 (m), 904 (s), 839 (s), 792 (s), 725 (m), 668 (m), 656 (m) cm^{-1} ; **Raman** (300 mW): $\tilde{\nu}$ (rel. int.) = 1621 (23), 1595 (100), 1573 (45), 1415 (32), 1349 (8), 1294 (10), 1275 (11), 1097 (4), 1023 (11), 960 (29), 933 (16), 844 (45), 799 (4), 769 (5), 627 (7), 518 (12) cm^{-1} ; **MS** (DCI^+): $m/z = 437.3$ [$\text{M}+\text{H}^+$]; **drophammer**: 10 J; **friction tester**: 80 N; **grain size**: $<100\text{ }\mu\text{m}$.

3,3'-Bi-(5-fluorodinitromethyl-1,2,4-oxadiazole) (7): 400 mg of compound **5** (0.95 mmol) was diluted in anhydrous acetonitrile (100 mL) and 1.34 g *Selectfluor*TM (3.79 mmol) was added at ambient temperature. The yellow mixture was stirred until decolourised (about 2 h) and the solvent was then evaporated under reduced pressure. Anhydrous diethyl ether (150 mL) was added to the yellowish residue and this mixture was heated while stirring to $40\text{ }^{\circ}\text{C}$ in a closed vessel for 30 min. The solid was filtrated and the solvent concentrated under reduced pressure to about 5 mL yielding a crystalline solid at $8\text{ }^{\circ}\text{C}$ overnight. The solvent was removed furnishing 240 mg of compound **7** (0.63 mmol, 66%) as colourless crystals.

DSC (T_{onset}): $T_{\text{melt}} = 67\text{ }^{\circ}\text{C}$, $T_{\text{dec}} = 151\text{ }^{\circ}\text{C}$; $^{13}\text{C}\{^1\text{H}\}$ NMR (CD_2Cl_2): $\delta = 164.8$ (d, $^2J_{\text{C-F}} = 28.8\text{ Hz}$, OCN), 159.9 (CC), 111.9 (d_{quint}, $J_{\text{C-F}} = 297.1\text{ Hz}$, $J_{\text{C-N}} = 9.6\text{ Hz}$, $\text{C}(\text{NO}_2)_2\text{F}$); $^{14}\text{N}\{^1\text{H}\}$ NMR (CD_2Cl_2): $\delta = -34$ (d, $^2J_{\text{N-F}} = 9.9\text{ Hz}$, NO_2); ^{19}F NMR (CD_2Cl_2): $\delta = -98.9\text{ ppm}$ (quint, $^2J_{\text{F-N}} = 9.8\text{ Hz}$, CF) ppm; **EA**: $\text{C}_6\text{N}_8\text{O}_{10}\text{F}_2$ ($382.11\text{ g}\cdot\text{mol}^{-1}$) calcd: C 18.86, N 29.33; found: C 19.25, N 28.18 %; **IR**: $\tilde{\nu}$ (rel. int.) = 1620 (s), 1572 (m), 1445 (w), 1363 (w), 1334 (w), 1297 (m), 1259 (m), 1241 (m), 1212 (m), 1065 (m), 1016 (s), 954 (m), 917 (w), 831 (m), 793 (s), 744 (w), 716 (m), 700 (m), 661 (w) cm^{-1} ; **Raman** (300 mW): $\tilde{\nu}$ (rel. int.) = 1628 (15), 1597 (100), 1586 (44), 1424 (31), 1335 (10), 1244 (5), 1016 (9), 951 (24), 922 (20), 833 (24), 627 (5), 493 (15), 404 (16), 368 (13), 340 (9), 318(9) cm^{-1} ; **MS** (DCI^+): $m/z = 383.2$ [$\text{M}+\text{H}^+$]; **drophammer**: 10 J; **friction tester**: 192 N; **grain size**: $<100\text{ }\mu\text{m}$.

3,3'-Bi-(5-trifluoromethyl-1,2,4-oxadiazole) (9):^[26] 1.00 g *N,N'*-dihydroxyoxal-amidine (**1**, 8.47 mmol) was added to 10 mL trifluoroacetic anhydride and stirred at $35\text{ }^{\circ}\text{C}$ for 3 h. The solution was kept under reduced pressure, and the acid was collected into an external cooling trap ($-78\text{ }^{\circ}\text{C}$). On cooling, the crude product precipitated and was filtered using a glass frit (porosity 4). The white precipitate was re-crystallised from hot ethanol yielding 1.72 g of compound **9** (6.27 mmol, 75%) as colourless crystals. Alternatively, the crude compound can be sublimed under reduced pressure.

DSC (T_{onset}): $T_{\text{melt}} = 98\text{ }^{\circ}\text{C}$; $T_{\text{boil}} = 142\text{ }^{\circ}\text{C}$; $^{13}\text{C}\{^1\text{H}\}$ NMR (d_6 -DMSO): $\delta = 166.5$ (q, $^2J_{\text{C-F}} = 44.8\text{ Hz}$, OCN), 159.3 (CC), 115.4 (q, $J_{\text{C-F}} = 273.4\text{ Hz}$, CF_3); $^{15}\text{N}\{^1\text{H}\}$ NMR (d_6 -DMSO): $\delta =$

−9.3 (ONC), −134.8 (q, $^3J_{15\text{N-F}} = 1.9$ Hz, CNC); **^{19}F NMR** (d_6 -DMSO): $\delta = -65.1$ (br, CF_3) ppm; **EA**: $\text{C}_6\text{N}_8\text{O}_{10}\text{F}_2$ (274.10 $\text{g}\cdot\text{mol}^{-1}$) calcd: C 26.29, N 20.44; found: C 26.29, N 20.60 %; **IR**: $\tilde{\nu}$ (rel. int.) = 1605 (w, $\nu_{\text{C=N}}$), 1453 (vw), 1431 (w), 1334 (m), 1276 (vw), 1212 (s, $\nu_{\text{sym,C-F}}$), 1171 (vs, $\nu_{\text{asym,C-F}}$), 1138 (vs), 996 (m), 951 (w), 911 (m), 758 (s), 668 (m) cm^{-1} ; **Raman** (200 mW): $\tilde{\nu}$ (rel. int.) = 1615 (17), 1601 (100), 1432 (12), 1329 (4), 1185 (5, $\nu_{\text{asym,C-F}}$), 1150 (4), 1022 (9), 994 (38), 923 (8), 766 (22), 737 (10) cm^{-1} ; **MS** (DCI^+): $m/z = 275.2$ [$\text{M}+\text{H}^+$], (DEI^+): $m/z = 274.2$ [M^+].

5,5'-Bi-(2-trifluoromethyl-1,3,4-oxadiazole) (11): To a stirred suspension of 2.15 g 5,5'-bi-2*H*-tetrazole (**10**, 15.56 mmol) in *p*-xylene (30 mL), a solution of 8.40 g trifluoroacetic acid anhydride (5.56 mL, 40.0 mmol) in *p*-xylene (12 mL) was added dropwise. The reaction mixture was stirred at 100 °C until N_2 no longer evolved. The mixture was allowed to cool to room temperature and was then adjusted to pH = 9 using a saturated sodium bicarbonate solution. The white precipitate was filtered off, washed with water, and dried under reduced pressure yielding 3.97 g of pure compound **11** (14.48 mmol, 93%). The compound can be sublimed under reduced pressure for further purification.

DSC (T_{onset}): $T_{\text{melt}} = 169$ °C; $T_{\text{boil}} = 199$ °C; **$^{13}\text{C}\{^1\text{H}\}$ NMR** (d_6 -DMSO): $\delta = 155.3$ (q, $^2J_{\text{C-F}} = 44.7$ Hz, OCN), 153.8 (CC), 115.7 (q, $J_{\text{C-F}} = 271.9$ Hz, CF_3); **$^{15}\text{N}\{^1\text{H}\}$ NMR** (d_6 -DMSO): $\delta = -64.2$ (q, $^3J_{15\text{N-F}} = 1.5$ Hz, 3-*N*), −64.6 (4-*N*); **^{19}F NMR** (d_6 -DMSO): $\delta = -64.7$ (br, CF_3) ppm; **EA**: $\text{C}_6\text{N}_8\text{O}_{10}\text{F}_2$ (274.10 $\text{g}\cdot\text{mol}^{-1}$) calcd: C 26.29, N 20.44; found: C 26.21, N 20.33 %; **IR**: $\tilde{\nu}$ (rel. int.) = 1579 (w, $\nu_{\text{C=N}}$), 1476 (s, $\nu_{\text{C=N}}$), 1378 (s), 1227 (w, $\nu_{\text{sym,C-F}}$), 1169 (vs, $\nu_{\text{asym,C-F}}$), 1118 (vs, $\nu_{\text{C-O}}$), 1005 (vs), 974 (s), 950 (s), 755 (s), 735 (s), 674 (s) cm^{-1} ; **Raman** (200 mW): $\tilde{\nu}$ (rel. int.) = 1651 (64), 1580 (4, $\nu_{\text{C=N}}$), 1037 (11), 973 (7), 764 (5), 721 (4) cm^{-1} ; **MS**: (DEI^+): $m/z = 274.1$ [M^+].

4.10 References

- [1] M. A. Kettner, T. M. Klapötke, *Chem. Commun.* **2014**, 50(18), 2268–2270.
- [2] M. A. Kettner, K. Karaghiosoff, T. M. Klapötke, M. Sućeska, S. Wunder, *Chem. Eur. J.* **2014**, 20, 7622–7631.
- [3] M. A. Kettner, T. M. Klapötke, T. W. Witkowski, F. von Hundling, *Chem. Eur. J.* **2015**, 21(11), 4238–4241.
- [4] J. Akhavan, *Chemistry of Explosives*, 2nd ed., RSC Paperbacks, Cambridge (UK), **2005**.
- [5] a) T. M. Klapötke, *Chemie der hochenergetischen Materialien*, de Gruyter, Berlin, New York, **2009**; b) T. M. Klapötke, *Chemistry of High-Energy Materials*, 2nd Eng. ed., de Gruyter, Berlin, New York, **2011**.
- [6] H. V. Huynh, M. A. Hiskey, J. G. Archuleta, E. L. Roemer, R. Gilardi, *Angew. Chem.* **2004**, 116, 5776–5779; *Angew. Chem. Int. Ed.* **2004**, 43, 5658–5661.
- [7] a) R. P. Singh, R. D. Verma, D. T. Meshri, J. M. Shreeve, *Angew. Chem.* **2006**, 118, 3664–3682; *Angew. Chem. Int. Ed.* **2006**, 45, 3584–3601; b) M. Göbel, K. Karaghiosoff, T. M. Klapötke, D. G. Piercey, J. Stierstorfer, *J. Am. Chem. Soc.* **2010**, 132, 17216–17226.
- [8] a) V. Thottampudi, F. Forohor, D. A. Parrish, J. M. Shreeve, *Angew. Chem.* **2012**, 124, 10019–10023; *Angew. Chem. Int. Ed.* **2012**, 51, 9881–9885; b) V. Thottampudi, H. Gao, J. M. Shreeve, *J. Am. Chem. Soc.* **2011**, 133, 6464–6471; c) K. Wang, D. A. Parrish, J. M. Shreeve, *Chem. Eur. J.* **2011**, 17, 14485–14492.
- [9] a) D. Fischer, N. Fischer, T. M. Klapötke, D. G. Piercey, J. Stierstorfer, *J. Mater. Chem.* **2012**, 22, 20418–20422; b) T. M. Klapötke, N. Fischer, D. Fischer, D. Piercey, J. Stierstorfer, M. Reymann, *WO 2013026768 A1*, **2013**.
- [10] A. Dippold, T. M. Klapötke, F. A. Martin, *Z. Anorg. Allg. Chem.* **2011**, 637, 1181–1193.
- [11] a) M. Göbel, T. M. Klapötke, *Z. Anorg. Allg. Chem.* **2007**, 633, 1006–1017; b) Q. J. Axthammer, M. A. Kettner, T. M. Klapötke, R. Moll, S. F. Rest, *New Trends in Research of Energetic Materials* (NTREM), Proceedings of the Seminar, Pardubice, Czech Republic, April 10–12, **2013**, Part 1, 29–39; c) Q. J. Axthammer, M. A. Kettner, T. M. Klapötke, R. Moll, S. F. Rest, *Development of High Energy Dense Oxidisers based on CHNO(F)-materials*, EUCASS Conference, Munich, Germany, July 3rd, **2013**.
- [12] a) M. Heitzmann, Sandoz AG, *CH 661270*, **1987**; b) T. Kim, J. W. Suh, J. C. Ryu, B. C. Chung, J. Park, *J. Chromatogr. B* **1996**, 687, 79–83.
- [13] a) D. V. Nightingale, R. M. Brooker, *J. Am. Chem. Soc.* **1950**, 72, 5539–5543; b) K.-H. Kim, H.-J. Lee, *US 20140231757 A1*, **2014**.
- [14] a) A. Pace, P. Pierro, *Org. Biomol. Chem.* **2009**, 7, 4337–4348; b) J. A. Pedro, J. R. Mora, E. Westphal, H. Gallardo, H. D. Fiedler, F. Nome, *J. Mol. Struct.* **2012**, 1016, 76–81; c) E. Westphal, D. Henrique da Silva, F. Molin, H. Gallardo, *RSC Adv.* **2013**, 3, 6442–6454.
- [15] a) J. B. Birks, *GB 1286622*, **1972**; b) M. Hyman, Jr., *US 4017738 A*, **1977**; c) V. Rimbau Barreras, *ES 551136 A1*, **1987**; d) F. Dubois, R. Knochenmuss, R. Zenobi, *Int. J. Mass Spectrom. Ion Processes* **1997**, 169/170, 89–98.
- [16] a) D. Chavez, L. Hill, M. Hiskey, S. Kinkead, *J. Energ. Mater.* **2000**, 18, 219–236; b) D. Fischer, T. M. Klapötke, M. Reymann, J. Stierstorfer, *Chem. Eur. J.* **2014**, 20, 6401–6411; c) A. B. Sheremetev, *J. Heterocycl. Chem.* **1995**, 32, 371–385; d) P. W. Leonard, D. E. Chavez, P. F. Pagoria, D. L. Parrish, *Propellants Explos. Pyrotech.* **2011**, 36, 233–239; e) R. Wang, Y. Guo, Z. Zeng, B. Twamley, J. M. Shreeve, *Chem. Eur. J.* **2009**, 15, 2625–2634; f) V. Zelenov, A. Lobanova, S. Sysolyatin, N. Sevodina, *Russ. J. Org. Chem.* **2013**, 49, 455–465; g) A. M. Churakov, S. L. Ioffe, V. A. Tartakovsky, *Mendeleev Commun.* **1995**, 5, 227–228; h) N. N.

- Makhova, *New Trends in Research of Energetic Materials* (NTREM), Proceedings of the Seminar, Pardubice, Czech Republic, April 9–11th, **2014**, Part 2, 647–652.
- [17] A. DeHope, P. F. Pagoria, D. Parrish, *New Trends in Research of Energetic Materials* (NTREM), Proceedings of the Seminar, Pardubice, Czech Republic, April 10–12th, **2013**, Part 1, 130–136.
- [18] a) L. Zhanxiong, O. Yuxiang, C. Boren, <http://www.mdpi.org/cji/cji/2001/033013ne.htm> (accessed: 06.11.2014), *Chem. J. Internet* **2001**, 3, 13; b) V. Thottempudi, J. Zhang, C. He, J. M. Shreeve, *RSC Adv.* **2014**, 4, 50361–50364.
- [19] a) M. Weyrauther, T. M. Klapötke, J. Stierstorfer, *New Trends in Research of Energetic Materials* (NTREM), Proceedings of the Seminar, Pardubice, Czech Republic, April 10–12th, **2013**, Part 1, 982–995; b) T. M. Klapötke, N. Mayr, J. Stierstorfer, M. Weyrauther, *Chem. Eur. J.* **2014**, 20, 1410–1417.
- [20] M. A. Petrie, G. Koolpe, R. Malhotra, P. Penwell, *ONR Final Report*, SRI international, SRI Project No. PI8608, March, **2012**.
- [21] a) N. I. Golovina, A. N. Titkov, A. V. Raevskii, L. O. Atovmyan, *J. Solid State Chem.* **1994**, 113, 229–238; b) A. B. Sheremetev, E. A. Ivanova, N. P. Spiridonova, S. F. Melnikova, I. V. Tselinsky, K. Y. Suponitsky, M. Y. Antipin, *J. Heterocycl. Chem.* **2005**, 42, 1237–1242; c) P. W. Leonard, C. J. Pollard, D. E. Chavez, B. M. Rice, D. A. Parrish, *Synlett* **2011**, 14, 2097–2099.
- [22] A. S. Batsanov, Y. T. Struchkov, A. A. Gakh, A. A. Fainzil'berg, *Russ. Chem. Bull.* **1994**, 43, 588–590.
- [23] V. V. Kiseleva, A. A. Gakh, A. A. Fainzil'berg, *Bull. Acad. Sci. USSR Div. Chem. Sci.* **1991**, 100, 1888–1895.
- [24] a) T. M. Klapötke, A. J. Maier, N. T. Mayr, *New Trends in Research of Energetic Materials* (NTREM), Proceedings of the Seminar, Pardubice, Czech Republic, April 9–12, **2008**, Part 2, 653–660; b) T. M. Klapötke, M. H. Kunzmann, N. T. Mayr, S. Seel, *New Trends in Research of Energetic Materials* (NTREM), Proceedings of the Seminar, Pardubice, Czech Republic, April 1–13rd, **2009**, Part 2, 581–595; c) T. M. Klapötke, N. T. Mayr, S. Seel, *New Trends in Research of Energetic Materials* (NTREM), Proceedings of the Seminar, Pardubice, Czech Republic, April 1–13rd, **2009**, Part 2, 596–607; d) I. V. Ovchinnikov, K. A. Lyssenko, N. N. Makhova, *Mendeleev Commun.* **2009**, 19, 144–146.
- [25] S. Stavber, M. Zupan, *Acta Chim. Slov.* **2005**, 52, 13–26.
- [26] V. G. Andrianov, V. G. Semenikhina, A. V. Ereemeev, *Chem. Heterocycl. Compd.* **1994**, 30, 475–477.
- [27] G. Seitz, C. H. Gerninghaus, *Pharmazie* **1994**, 49, 102–106.
- [28] L. I. Vereshchagin, A. V. Petrov, V. N. Kizhnyaev, F. A. Pokatilov, A. I. Smirnov, *Russ. J. Org. Chem.* **2006**, 42, 1049–1055.
- [29] H.-O. Kalinowski, S. Berger, S. Braun, *¹³C NMR Spektroskopie*, Thieme, Stuttgart, New York, **1984**.
- [30] M. Witkowski, L. Stefaniak, G. A. Webb, *Annual Reports on NMR Spectroscopy*, Vol. 25, Academic Press, London, **1993**.
- [31] a) G. Socrates, *Infrared and Raman Characteristic Group Frequencies: Tables and Charts*, 3rd ed., Wiley, Chichester (UK), **2004**; b) M. Hesse, H. Meier, B. Zeeh, *Spektroskopische Methoden in der organischen Chemie*, Georg Thieme Verlag KG, Stuttgart, **2005**; c) F. Billes, H. Endredi, G. Keresztury, *J. Mol. Struct. THEOCHEM* **2000**, 530, 183–200.
- [32] a) K. Hemming, *Comp. Heterocycl. Chem. III* **2008**, 5(4), 243–314; b) J. Suwiński, W. Szczepankiewicz, *Comp. Heterocycl. Chem. III* **2008**, 5(6), 397–466.
- [33] C. Richardson, P. J. Steel, *Inorg. Chem. Commun.* **2007**, 10, 884–887.
- [34] L. Zhanxiong, O. Yuxiang, C. Boren, *Chem. J. Internet* **2001**, 3, 13; <http://www.mdpi.org/cji/>

- cji/2001/033013ne.htm (accessed: 03.03.2015).
- [35] A. F. Holleman, *Lehrbuch der Anorganischen Chemie*, 101st ed., de Gruyter, Berlin, New York, **1995**, p. 1842.
 - [36] C. P. Butts, L. Ebersson, K. L. Fulton, M. P. Hartshorn, W. T. Robinson, D. J. Timmerman-Vaughan, *Acta Chem. Scand.* **1996**, 50, 991–1008.
 - [37] D. Bougeard, R. Boese, M. Polk, B. Woost, B. Schrader, *J. Phys. Chem. Solids* **1986**, 47, 1129–1137.
 - [38] M. Göbel, T. M. Klapötke, *Adv. Funct. Mater.* **2009**, 19, 347–365.
 - [39] M.-X. Zhang, P. E. Eaton, R. Gilardi, *Angew. Chem. Int. Ed.* **2000**, 39(2), 401–404.
 - [40] Z. A. Akopyan, Y. T. Struchkov, V. G. Dashevii, *Zh. Strukt. Khim.* **1966**, 7(3), 408–416.
 - [41] A. Sikorski, D. Trzybinski, *J. Mol. Struct.* **2013**, 1049, 90–98.
 - [42] A. Bondi, *J. Phys. Chem.* **1964**, 68, 441–451.
 - [43] Y. Oyumi, T. B. Brill, A. L. Rheingold, *J. Phys. Chem.* **1985**, 89, 4824–4828.
 - [44] T. M. Klapötke, B. Krumm, S. F. Rest, M. Reynders, R. Scharf, *Eur. J. Inorg. Chem.* **2013**, 5871–5878.
 - [45] *NATO Standardization Agreement (STANAG) on Explosives*, Impact Tests, No. 4489, 1st ed., Sept. 17, **1999**.
 - [46] *WIWEB-Standardarbeitsanweisung 4-5.1.02, Ermittlung der Explosionsgefährlichkeit, hier der Schlagempfindlichkeit mit dem Fallhammer*, Nov. 08, **2002**.
 - [47] a) Bundesanstalt für Materialforschung (BAM), <http://www.bam.de>, which lays down test methods pursuant to Regulation (EC) No. 1907/2006 of the European Parliament and of the Council on the Evaluation, Authorisation and Restriction of Chemicals (REACH), ABl. L142, **2008**; b) T. M. Klapötke, B. Krumm, N. Mayr, F. X. Steemann, G. Steinhauser, *Safety Science* **2010**, 48, 28–34.
 - [48] *NATO Standardization Agreement (STANAG) on Explosives*, Friction Tests, No. 4487, 1st ed., Aug. 22, **2002**.
 - [49] *WIWEB-Standardarbeitsanweisung 4-5.1.03, Ermittlung der Explosionsgefährlichkeit, hier der Reibempfindlichkeit mit dem Reibeapparat*, Nov. 08, **2002**.
 - [50] *NATO Standardization Agreement (STANAG) on Explosives, Electrostatic Discharge Sensitivity Tests*, no. 4490, 1st ed., Feb. 19, **2001**.
 - [51] <http://www.ozm.cz/en/sensitivity-tests/esd-2008a-small-scale-electrostatic-spark-sensitivity-test/>.
 - [52] a) M. J. Kamlet, NAVORD Rep. 6206, US Naval Ordnance Lab, Whiteoak, Maryland, **1959**; b) J. P. Agrawal, R. D. Hodgson, *Organic Chemistry of Explosives*, 1st ed., Wiley, **2006**, p. 33.
 - [53] a) *Test methods according to the UN Manual of Tests and Criteria, Recommendations on the Transport of Dangerous Goods*, United Nations Publication, New York, Geneva, 4th revised ed., **2003**: Impact: insensitive >40 J, less sensitive ≥ 35 J, sensitive ≥ 4 J, very sensitive ≤ 3 J; friction: insensitive >360 N, less sensitive: 360 N, sensitive <360 N and >80 N, very sensitive ≤ 80 N, extremely sensitive ≤ 10 N; b) www.reichel-partner.de.
 - [54] a) GAUSSIAN09, Version 7.0, M. J. Frisch, G. W. Trucks, H. B. Schlegel, G. E. Scuseria, M. A. Robb, J. R. Cheeseman, G. Scalmani, V. Barone, B. Mennucci, G. A. Petersson, H. Nakatsuji, M. Caricato, X. Li, H. P. Hratchian, A. F. Izmaylov, J. Bloino, G. Zheng, J. L. Sonnenberg, M. Hada, M. Ehara, K. Toyota, R. Fukuda, J. Hasegawa, M. Ishida, T. Nakajima, Y. Honda, O. Kitao, H. Nakai, T. Vreven, J. A. Montgomery Jr., J. E. Peralta, F. Ogliaro, M. Bearpark, J. J. Heyd, E. Brothers, K. N. Kudin, V. N. Staroverov, R. Kobayashi, J. Normand, K. Raghavachari, A. Rendell, J. C. Burant, S. S. Iyengar, J. Tomasi, M. Cossi, N. Rega, J. M. Millam, M. Klene, J. E. Knox, J. B. Cross, V. Bakken, C. Adamo, J. Jaramillo, R. Gomperts, R. E. Stratmann, O. Yazyev, A. J. Austin, R. Cammi, C. Pomelli, J. W. Ochterski, R. L. Martin, K. Morokuma, V. G. Zakrzewski, G. A. Voth, P. Salvador, J. J. Dannenberg, S.

- Dapprich, A. D. Daniels, Ö. Farkas, J. B. Foresman, J. V. Ortiz, J. Cioslowski, D. J. Fox, Gaussian, Inc., Wallingford CT, **2009**; b) GAUSS-VIEW 5, Version 5.0.8, T. K. R. Dennington, J. Millam, Semichem Inc., Shawnee Mission, **2009**.
- [55] a) EXPLO5, Version 6.02, M. Sućeska, Zagreb, Croatia, **2014**; b) M. Sućeska, *Propellants Explos. Pyrotech.* **1991**, *16*, 197–202; c) M. Sućeska, *Propellants Explos. Pyrotech.* **1999**, *24*, 280–285; d) M. Sućeska, H. G. Ang, H. Y. Chan, *Mater. Sci. Forum* **2011**, *673*, 47–52.
- [56] a) J. F. Köhler, R. Meyer, A. Homburg, *Explosivstoffe*, 10. Aufl., Wiley-VCH Verlag GmbH & Co. KGaA, Weinheim, **2008**; b) P. W. Cooper, *Explosives Engineering*, 1st ed., Wiley-VCH, Weinheim, **1996**.
- [57] a) NASA, Space Shuttle News Reference, 2-20-22-21, <http://de.scribd.com/doc/-17005716/NASA-Space-Shuttle-News-Reference-1981>; b) NASA, press release: STS-122 The Voyage of Columbus, **2008**, 82–84.
- [58] T. L. Moore, American Institute of Aeronautics and Astronautics, Inc., **1997**.
- [59] G. P. Sutton, *Rocket Propulsion Elements*, 7th ed., John Wiley & Sons, **2001**.

IV GENERAL PROCEDURES

1 General Synthetical Methods



Unless otherwise noted all reactions were carried out at ambient temperature, pressure and at air. When undertaking work by means of SCHLENK techniques,^[1] Argon of purity 4.8 from *Air Liquide* was used as inert gas.^[2] Most compounds described in this thesis are sensitive towards impact, friction and electrostatic discharge and therefore have to be handled carefully, stored in plastic tubes and in appropriate explosion proofed boards. Although no incidents occurred during preparation and manipulation, additional proper protective precautions like face shield, leather coat or bulletproof vest, earthed equipment and shoes, KEVLARTM gloves, and ear plugs should be used when undertaking work with these compounds. Corresponding sensitivities are given in the experimental parts as well as are listed and discussed in accordant chapters.

2 Chemicals

Solvents and deuterated solvent for NMR experiments were used as received from the suppliers. If SCHLENK techniques were used for reactions, the solvents were distilled freshly over according drying agents and checked by NMR spectroscopy for remaining traces of water. The drying agents were sodium for toluene and diethyl ether, calcium hydride for dichloromethane, and phosphorus pentoxide for acetonitrile.^[1] Special fluorinating and nitration agents used frequently in the present work are listed in Table 1.

Table 1: Fluorinating and nitration agents with purity grade and supplier.

	Purity	Supplier
<i>Selectfluor</i> TM	≥95%	Sigma-Aldrich
NO ₂ BF ₄	95%	abcr
HNO ₃ (100%)	≥99.5%	Sigma-Aldrich

3 Analytical Methods and Facilities

Thermal Analysis

Melting points T_{melt} and decomposition points T_{dec} were measured with a PERKIN–ELMER PYRIS 6 DSC (T_{onset}),^[3] using a heating rate of 5 °C min⁻¹. These T_{onset} points were additionally checked by a BÜCHI MELTING POINT B-540 apparatus.^[4] For the long-term stability tests a RADEX V5 oven was used.^[5] It was previously shown that tempering a substance for 48 h at 40 °C below its decomposition temperature results in storage periods over approximately 50 years at room temperature.^[6]

Nuclear Magnetic Resonance Spectroscopy (NMR)

All NMR spectra were recorded at ambient temperature with a JEOL ECLIPSE 270, 400 or ECX 400e instrument (Table 2).^[7] The chemical shifts are reported with respect to external Me₄Si (¹H, ¹³C), MeNO₂ (¹⁴N, ¹⁵N), and CCl₃F (¹⁹F). Unless otherwise noted ¹³C, ¹⁴N and ¹⁹F NMR spectra were recorded ¹H decoupled, and all spectra were recorded at ambient temperature.

Table 2: External standards and frequencies [MHz] of according NMR spectrometers.

Isotope	External standard $\delta = 0.00$ ppm	Frequency Eclipse 270	Frequency Eclipse 400	Frequency ECX 400e
¹ H	TMS	270.17	399.78	400.18
¹³ C	TMS	67.94	100.53	100.63
¹⁴ N	CH ₃ NO ₂	-	28.89	28.99
¹⁵ N	CH ₃ NO ₂	-	-	40.55
¹⁹ F	CCl ₃ F	109.37	376.5	161.99

Elemental Analysis

Analyses of C/H/N/O contents were performed with an ELEMENTAR VARIO EL or VARIO MICRO ANALYSER.^[8]

Infrared (IR) and Raman Spectroscopy

Infrared spectra were measured with a PERKIN-ELMER SPECTRUM BX-FTIR spectrometer equipped with a SMITHS DURASAMPLIR II ATR device.^[9] Gas phase infrared spectra were recorded in a glass vessel with NaCl windows in a PERKIN-ELMER SPECTRUM ONE FTIR spectrometer.^[10] Raman spectra were recorded with a BRUKER RAM II MULTIRAM spectrometer fitted with a Nd:YAG laser ($\lambda = 1064$ nm).^[11]

Mass Spectrometry

Mass spectrometric data were obtained with a JEOL MStation JMS 700 spectrometer (DCI \pm , DEI \pm and FAB \pm).^[12]

Sensitivities

The sensitivities towards impact and friction were determined with a BAM drophammer and a BAM friction tester, respectively (method 1 out of 6).^[13] The compounds were then classified according the UN recommendations on the transport of dangerous goods.^[14] The electrostatic discharge sensitivity was determined with an electric spark tester from OZM.^[15]

Room Temperature Densities

Ambient temperature densities of energetic materials are necessary when their energetic performance is calculated, because the detonation parameters depend directly on the density (energy per space).^[16] These densities were determined either by room temperature X-ray diffraction, or if no crystals were obtained by means of a QUANTACHROME ULTRAPYC 1200e pycnometer.^[17] If crystals were obtained, but measured at low temperature and not enough

material was available for the pycnometer, the room temperature density was re-calculated from the X-ray densities according an equation for the volume expansion of crystals:^[18]

$$d_{298K} = \frac{d_T}{1 + \alpha_V(298 - T_0)}$$

with α_V being the coefficient of volume expansion and set to $1.6 \cdot 10^{-4} \text{ K}^{-1}$.^[18]

4 X-ray Diffraction Measurements

For all compounds in the present work an OXFORD XCALIBUR3 diffractometer with a CCD area detector was employed for data collection using Mo- K_α radiation ($\lambda = 0.71073 \text{ \AA}$).^[19] The data collection was realized by using CRYSTALISPRO software.^[20] The structures were solved by direct methods using SIR92,^[21] SIR97,^[22] or SIR2004,^[23] refined by full-matrix least-squares on F^2 (SHELXL-97)^[24] and finally checked using the PLATON software^[25] integrated in the WinGX software suite.^[24b] The absorptions were corrected by a SCALE3 ABSPACK multiscan method.^[26] All non-hydrogen atoms were refined anisotropically. In most cases the hydrogen atom positions were located in a difference Fourier map and then refined freely. Otherwise their positions were calculated according to the electron density found. This is pointed out by a ‘*’ in according tables in every chapters appendix. DIAMOND plots are shown with thermal ellipsoids at the 50% probability level unless otherwise noted.^[27] Crystallographic data (excluding structure factors) for the structures reported in this thesis have been deposited with the Cambridge Crystallographic Data Centre (CCDC).^[28] Supplementary publication numbers can be found in the corresponding crystallographic data tables. Copies of the data can be obtained free of charge on application to CCDC, 12 Union Road, Cambridge CB2 1EZ, UK [e-mail: deposit@ccdc.cam.ac.uk].

5 Computational Details and Thermodynamic Background

All quantum chemical calculations were carried out using the program package GAUSSIAN 09,^[29] and visualised by GAUSSVIEW 5,^[30] The thermodynamic data of a molecule can be calculated by applying *ab initio* quantum chemical methods. This requires the solution of the time-independent electronic SCHRÖDINGER equation:

$$\hat{H}_{el}\Psi_{el}(r_i; R_A) = E_{el}(R_A)\Psi_{el}(r_i; R_A)$$

with R_A representing the coordinates of the nuclei and r_i the electrons. The electronic Hamiltonian \hat{H}_{el} includes the kinetic energy of the electrons and their interaction with the cores as well as the interactions among each other. The HARTREE-FOCK Method (HF) sets the basic algorithm for an approximate solution of the time-independent electronic SCHRÖDINGER equation.^[31] The trouble causing interactions between the electrons is described as an interaction of an electron with the potential fields of the other respective electrons. Although this method is rather successful in many cases, this description still comprises a major

approximation. Therefore so-called POST-HARTREE-FOCK methods for even more accurate treatment of the electrons correlations were developed, for instance the MØLLER-PLESSET Perturbation Theory (MP n) that describes different perturbation orders n .^[32] A further factor for accuracy and computation time is the description of the wave function Ψ_{el} in the equation above. It is usually composed of different atomic centred GAUSSIAN functions, which are called the basis set. The complete basis set CBS-4M is a method that provides a practical compromise between accuracy and computation time, and has been used in the present work for all calculations of the enthalpies of formation ($H_{\text{CBS-4M}}$) and free energies ($G_{\text{CBS-4M}}$) in the gas phase.^[33] The CBS models use the known asymptotic convergence of PAIR NATURAL ORBITAL (PNO) expressions to extrapolate from calculations using a finite basis set to the estimated complete basis set limit. CBS-4 starts with a HF/3-21G(d) geometry optimisation,^[34] which is the initial guess for the following SCF calculation as a base energy and a final MP2/6-31+G** calculation with a CBS extrapolation to correct the energy in second order.^[35] The used re-parameterised CBS-4M method additionally implements a MP4(SDQ)/6-31G calculation to approximate higher order contributions and also includes some additional empirical corrections.^[36]

The solid state enthalpies and energies of formation of all neutral compounds in the present work were calculated from the corresponding enthalpy derived from these quantum chemical CBS-4M calculations ($H_{\text{CBS-4M}}$). Therefore, the enthalpies of formation of the gas phase species were computed according to the atomisation energy method.^[37] The solid state enthalpies of formation (ΔH_f°) were estimated by subtracting the gas phase enthalpies with the corresponding enthalpy of sublimation obtained by the TROUTON'S Rule.^[38]

If the compound consisted of an ionic species the enthalpies of formation ($H_{\text{CBS-4M}}$) of the ions were calculated separately. The solid state enthalpies of formation were then derived from the calculation of the corresponding lattice energies (U_L) and lattice enthalpies (H_L). These were calculated from the corresponding molecular volumes, by the equations provided by JENKINS *et al.*^[39]

The derived molar standard enthalpies of formation for the solid state (ΔH_m) were used to calculate the solid state energies of formation (ΔU_m) according to the following equation with Δn being the change in the number of mol of gaseous components and R the gas constant:

$$\Delta U_m = \Delta H_m - \Delta nRT$$

All calculations affecting the detonation parameters were carried out using the latest version 6.02 of the program package EXPLO5,^[40] with CBS-4M calculated enthalpies of formation, and are attributed to the densities at ambient temperature obtained as described in the analytical methods section. The detonation parameters were calculated at the C-J point (CHAPMAN-JOUGUET Point) with the aid of the steady-state detonation model using a modified BECKER-KISTIAKOWSKI-WILSON (BKW) Equation of state for modelling the system. The C-J point is found from the HUGONIOT Curve of the system by its first derivative.^[41]

Also the specific impulses I_{sp} were calculated with the EXPLO5, V6.02 program,^[40] assuming an isobaric combustion, and a chamber pressure of 70.0 bar against an ambient pressure of 1.0 bar with equilibrium expansion conditions at the nozzle throat. In most cases the values for the specific impulses I_{sp} calculated with EXPLO5 were recalculated and checked with the ICT THERMODYNAMIC CODE.^[42] The deviations in the specific impulses I_{sp} as well as in the temperatures in the combustion chamber T_C are negligible.

6 References

- [1] K. Schwetlick, *Organikum*, 22. Aufl., Wiley-VCH, Weinheim, **2004**.
- [2] <http://www.airliquide.de/> (accessed: 15.03. 2015)
- [3] <http://www.perkinelmer.com/catalog/category/id/pyris%206%20dsc> (accessed: 15.03. 2015)
- [4] <http://www.sigmaaldrich.com/catalog/product/aldrich/z319279?lang=de®ion=DE> (accessed: 15.03. 2015)
- [5] <http://www.systag.ch> (accessed: 15.03. 2015)
- [6] T. M. Klapötke, N. K. Minar, J. Stierstörfer, *Polyhedron* **2009**, 28, 13–26.
- [7] <http://www.jeolusa.com/PRODUCTS/NuclearMagneticResonance/tabid/234/Default.aspx> (accessed: 15.03. 2015)
- [8] <http://www.elementar.de/en/products/vario-serie/vario-el-cube.html> (accessed: 15.03. 2015)
- [9] <http://www.perkinelmer.com/catalog/product/id/11185255> (accessed: 15.03. 2015)
- [10] <http://www.perkinelmer.com/catalog/category/id/spectrum%20one%20nts> (accessed: 15.03. 2015)
- [11] <http://www.bruker.com/products/infrared-near-infrared-and-raman-spectroscopy.html> (accessed: 15.03. 2015)
- [12] <http://www.jeol.de/electronoptics/produktuebersicht/molekularanalytische-systeme/massenspektrometer/jms-700-m-station.php> (accessed: 15.03. 2015)
- [13] a) Bundesanstalt für Materialforschung (BAM), <http://www.bam.de> (accessed: 15.03. 2015); laying down the test methods pursuant to Regulation (EC) No. 1907/2006 of the European Parliament and of the Council on the Evaluation, Authorisation and Restriction of Chemicals (REACH), ABl. L 142, **2008**; b) NATO Standardisation Agreement (STANAG) on Explosives, Impact Tests, No. 4489, 1st ed., Sept. 17th, **1999**; c) WIWEB-Standardarbeitsanweisung 4–5.1.02, Ermittlung der Explosionsgefährlichkeit, hier: der Schlagempfindlichkeit mit dem Fallhammer, Nov. 8th, **2002**; d) NATO Standardisation Agreement (STANAG) on Explosives, Friction Tests, No. 4487, 1st ed., Aug. 22nd, **2002**; e) WIWEB-Standardarbeitsanweisung 4–5.1.03, Ermittlung der Explosionsgefährlichkeit, hier: der Reibempfindlichkeit mit dem Reibeapparat, November 8th, **2002**; f) T. M. Klapötke, B. Krumm, N. Mayr, F. X. Steemann, G. Steinhauser, *Safety Science* **2010**, 48, 28–34.
- [14] a) Test methods according to the UN Manual of Tests and Criteria, Recommendations on the Transport of Dangerous Goods, United Nations Publication, New York, Geneva, 4th revised ed., **2003**: Impact: insensitive >40 J, less sensitive ≥ 35 J, sensitive ≥ 4 J, very sensitive ≤ 3 J; friction: insensitive >360 N, less sensitive 360 N, sensitive <360 N and >80 N, very sensitive ≤ 80 N and extremely sensitive ≤ 10 N; b) <http://www.reichel-partner.de> (accessed: 15.03. 2015).
- [15] a) NATO Standardisation Agreement (STANAG) on Explosives, Electrostatic Discharge Sensitivity Tests, No. 4490, 1st ed., Feb. 19th, **2001**; b) D. Skinner, D. Olson, A. Block-Bolten, *Propellants Explos. Pyrotech.* **1998**, 23, 34–42; c) S. Zeman, V. Pelikán, J. Majzlík, *Cent. Eur. J. Energ. Mater.* **2006**, 3, 45–51; d) <http://www.ozm.cz/en/sensitivity-tests/esd-2008a-small-scale-electrostatic-spark-sensitivity-test/> (accessed: 15.03. 2015).
- [16] a) T. M. Klapötke, *Chemie der hochenergetischen Materialien*, de Gruyter, Berlin, New York, **2009**; b) T. M. Klapötke, *Chemistry of High-Energy Materials*, 2nd Eng. ed., de Gruyter, Berlin, New York, **2011**.
- [17] http://www.quantachrome.com/density/auto_pycnometer.html (accessed: 15.03. 2015)
- [18] C. Xue, J. Sun, B. Kang, Y. Liu, X. Liu, G. Song, Q. Xue, *Propellants, Explos. Pyrotech.* **2010**, 35(4), 333–338.

- [19] <http://www.hedm.cup.uni-muenchen.de/about/equipment/index.html#x-ray> (accessed: 15.03. 2015)
- [20] a) CRYALISPRO, Version 1.171.35.11 (release 16.05.2011 CrysAlis171.net), Agilent Technologies, **2011**; b) L. J. Farrugia, *J. Appl. Crystallogr.* **1999**, 32, 837–838.
- [21] A. Altomare, G. Cascarano, C. Giacovazzo, A. Guagliardi, *J. Appl. Crystallogr.* **1993**, 26, 343–350.
- [22] a) A. Altomare, G. Cascarano, C. Giacovazzo, A. Guagliardi, A. G. G. Moliterni, M. C. Burla, G. Polidori, M. Camalli, R. Spagna, *SIR97*, **1997**; b) A. Altomare, M. C. Burla, M. Camalli, G. L. Cascarano, C. Giacovazzo, A. Guagliardi, A. G. G. Moliterni, G. Polidori, R. Spagna, *J. Appl. Crystallogr.* **1999**, 32, 115–119.
- [23] M. C. Burla, R. Caliandro, M. Camalli, B. Carrozzini, G. L. Cascarano, L. De Caro, C. Giacovazzo, G. Polidori, R. Spagna, *J. Appl. Crystallogr.* **2005**, 38, 381–388.
- [24] a) SHELXL-97, G. M. Sheldrick, University of Göttingen, Göttingen (Germany), **1997**; b) L. J. Farrugia, *J. Appl. Crystallogr.* **1999**, 32, 837–838; c) G. M. Sheldrick, *Acta Crystallogr. Sect. A* **2008**, 64, 112–122; d) A. L. Spek, *Acta Crystallogr. Sect. D* **2009**, 65, 148–155.
- [25] A. L. Spek, PLATON, A Multipurpose Crystallographic Tool, Utrecht University, The Netherlands, **1999**.
- [26] SCALE3 ABSPACK – An Oxford Diffraction program (1.0.4, gui: 1.0.3), Oxford Diffraction Ltd., **2005**.
- [27] K. Brandenburg, Diamond – *Informationssystem für Kristallstrukturen*, University of Bonn, Germany, **1996**.
- [28] <http://www.ccdc.cam.ac.uk/Community/Depositastructure/pages/DepositaStructure.aspx> (accessed: 15.03. 2015)
- [29] GAUSSIAN 09, Revision C.01, M. J. Frisch, G. W. Trucks, H. B. Schlegel, G. E. Scuseria, M. A. Robb, J. R. Cheeseman, G. Scalmani, V. Barone, B. Mennucci, G. A. Petersson, H. Nakatsuji, M. Caricato, X. Li, H. P. Hratchian, A. F. Izmaylov, J. Bloino, G. Zheng, J. L. Sonnenberg, M. Hada, M. Ehara, K. Toyota, R. Fukuda, J. Hasegawa, M. Ishida, T. Nakajima, Y. Honda, O. Kitao, H. Nakai, T. Vreven, J. A. Montgomery, Jr., J. E. Peralta, F. Ogliaro, M. Bearpark, J. J. Heyd, E. Brothers, K. N. Kudin, V. N. Staroverov, R. Kobayashi, J. Normand, K. Raghavachari, A. Rendell, J. C. Burant, S. S. Iyengar, J. Tomasi, M. Cossi, N. Rega, J. M. Millam, M. Klene, J. E. Knox, J. B. Cross, V. Bakken, C. Adamo, J. Jaramillo, R. Gomperts, R. E. Stratmann, O. Yazyev, A. J. Austin, R. Cammi, C. Pomelli, J. W. Ochterski, R. L. Martin, K. Morokuma, V. G. Zakrzewski, G. A. Voth, P. Salvador, J. J. Dannenberg, S. Dapprich, A. D. Daniels, . Farkas, J. B. Foresman, J. V. Ortiz, J. Cioslowski, D. J. Fox, Gaussian, Inc., Wallingford, CT, **2009**.
- [30] GAUSSVIEW 5, Version 5.0.8, T. K. R. Dennington, J. Millam, Semichem Inc., Shawnee Mission, **2009**.
- [31] A. Szabo, N. S. Ostlund, *Modern Quantum Chemistry: Introduction to Advanced Electronic Structure Theory*, Dover Publications, Inc., New York, **1996**.
- [32] a) M. Head-Gordon, J. A. Pople, M. J. Frisch, *Chem. Phys. Lett.* **1988**, 153, 503–506; b) R. V. Parish, *Chem. Phys. Lett.* **1972**, 14, 91.
- [33] a) J. J. A. Montgomery, M. J. Frisch, J. W. Ochterski, G. A. Petersson, *J. Chem. Phys.* **2000**, 112, 6532–6542; b) J. W. Ochterski, G. A. Petersson, J. J. A. Montgomery, *J. Chem. Phys.* **1996**, 104, 2598–2619; c) T. M. Klapötke, J. Stierstorfer, *Phys. Chem. Chem. Phys.* **2008**, 10, 4340–4346.
- [34] J. S. Binkley, J. A. Pople, W. J. Hehre, *J. Am. Chem. Soc.* **1980**, 102, 939–947.
- [35] G. A. Petersson, M. R. Nyden, *J. Chem. Phys.* **1981**, 75, 3423–3425.

- [36] J. J. A. Montgomery, M. J. Frisch, J. W. Ochterski, G. A. Petersson, *J. Chem. Phys.* **2000**, *112*, 6532–6542.
- [37] a) E. F. C. Byrd, B. M. Rice, *J. Chem. Phys. A* **2006**, *110*, 1005–1013; b) L. A. Curtiss, K. Raghavachari, P. C. Redfern, J. A. Pople, *J. Chem. Phys.* **1997**, *106*, 1063–1079.
- [38] a) F. Trouton, *Philos. Mag.* **1884**, *18*, 54–57; b) P. Atkins, *Physical Chemistry*, Oxford University Press, Oxford, **1978**.
- [39] a) H. D. B. Jenkins, H. K. Roobottom, J. Passmore, L. Glasser, *Inorg. Chem.* **1999**, *38*, 3609–3620; b) H. D. B. Jenkins, D. Tudela, L. Glasser, *Inorg. Chem.* **2002**, *41*, 2364–2367.
- [40] a) EXPLO5, Version 6.02, M. Sućeska, Zagreb (Croatia), **2014**; b) M. Sućeska, *Propellants Explos. Pyrotech.* **1991**, *16*, 197–202; c) M. Sućeska, *Propellants Explos. Pyrotech.* **1999**, *24*, 280–285; d) M. Sućeska, H. G. Ang, H. Y. Chan, *Mater. Sci. Forum* **2011**, *673*, 47–52.
- [41] a) T. M. Klapötke, B. Krumm, F. X. Steemann, K. D. Umland, *Z. Anorg. Allg. Chem.* **2010**, *636*, 2343–2346; b) M. Sućeska, *Propellants Explos. Pyrotech.* **1991**, *16*, 197–202.
- [42] F. Volk, H. Balthet, ICT-THERMODYNAMIC CODE (ICT-Code), 27th International Annual Conference of ICT, Karlsruhe, Germany, 92/1–16, **1996**.

V APPENDIX

1 Abbreviations

Table 1: Abbreviations used in the present thesis

Å	Angström	h	hour
BAM	Bundesanstalt für Materialforschung und -prüfung	Hal	halogen
°C	degree celsius	IR	infra red
ca	circa	m	medium (IR), multiplet (NMR)
calcd	calculated	MeOH	methanol
d	doublet (NMR)	min	minutes
DCI	direct chemical ionisation	NBO	natural bond orbital
DCM	dichloromethane	NMR	nuclear magnetic resonanz
DEI	direct electron impact ionisation	ppm	parts per million
DMF	dimethylformamide	q	quartet (NMR)
DSC	differential scanning calorimetry	quint	quintet (NMR)
e.g.	for example	RT	room temperature
ESD	electrostatic discharge	s	singlet (NMR), strong (IR)
Et₂O	diethylether	sec	second
EtOAc	ethylacetate	sept	septet
EtOH	ethanol	TNE/TNM	trinitroethyl/trinitromethyl
FAB	fast atom bombardement	TMS	tetramethylsilan
FDNE/FDNM	fluorodinitroethyl/fluorodinitromethyl	vs	very strong (IR)
GooF	Goodness of Fit	vw	very weak (IR)

2 List of Compounds Prepared in the Present Thesis

Table 2: Compounds in Chapter 1

#	Compound name	#	Compound name
1	<i>N</i> -Methylnitramide	4c	Hydrazinium <i>N</i> -methylnitramide
1a	Lithium <i>N</i> -methylnitramide	4d	3,5-Diamino-1,2,4-triazolium <i>N</i> -methylnitramide
1b	Sodium <i>N</i> -methylnitramide	4e	Guanidinium <i>N</i> -methylnitramide
1c	Potassium <i>N</i> -methylnitramide	4f	Aminoguanidinium <i>N</i> -methylnitramide
1d	Caesium <i>N</i> -methylnitramide	4g	Diaminoguanidinium <i>N</i> -methylnitramide
1e	Strontium <i>N</i> -methylnitramide	4h	Triaminoguanidinium <i>N</i> -methylnitramide
1f	Barium <i>N</i> -methylnitramide	4i	<i>N,N</i> -Dimethylguanidinium <i>N</i> -methylnitramide
1g	Calcium <i>N</i> -methylnitramide	4j	<i>N</i> -Guanylurea <i>N</i> -methylnitramide
1h	Silver <i>N</i> -methylnitramide	5	2-Nitro-2-azapropanol
1i	Zink <i>N</i> -methylnitramide	6	2-Nitro-2-azapropyl chloride
1j	Copper <i>N</i> -methylnitramide	7	2-Nitro-2-azapropyl acetate
2	<i>N,N'</i> -Dinitro- <i>N,N'</i> -dimethyloxamide	9	2-Nitro-2-azapropyl isocyanate
3	<i>N,N'</i> -Dimethyloxamide	10	2-Nitro-2-azapropyl phthalimide
4a	Ammonium <i>N</i> -methylnitramide	12	2-Nitro-2-azapropyl amine hydrochloride
4b	Hydoxylammonium <i>N</i> -methylnitramide		

Table 3: Compounds in Chapter 2

#	Compound name	#	Compound name
2	<i>N,N</i> -Bis-(2-nitro-2-azapropyl)-urea	10	2-Fluoro-2,2-dinitroethyl-(2-nitro-2-azapropyl)-carbamate
3	<i>N,N</i> -Bis-(2-nitro-2-azapropyl)-carbamate	11	2,2,2-Trinitroethyl-(2-nitro-2-azapropyl)- <i>N</i> -nitrocarbamate
8	1,3-Bis-(2-nitro-2-azapropyl-carbamate)-2,2-dinitropropane	12	2-Fluoro-2,2-dinitroethyl-(2-nitro-2-azapropyl)- <i>N</i> -nitrocarbamate
9	2,2,2-Trinitroethyl-(2-nitro-2-azapropyl)-carbamate	13	1,3-dinitro-1,3-diazabutane

Table 4: Compounds in Chapter 3

#	Compound name	#	Compound name
2	Ethyl 2-(1 <i>H</i> -tetrazol-5-yl)-acetate	6	Dipotassium 5-(dinitromethylide)-tetrazolate
3	5-(Tetrazol-1 <i>H</i> -yl)-acetic acid	8	2-(2-nitro-2-azapropyl)-5-(trinitromethyl)-2 <i>H</i> -tetrazole
4	Ammonium 5-(trinitromethyl)-2 <i>H</i> -tetrazolate	14	Ammonium 5-(fluorodinitromethyl)-2 <i>H</i> -tetrazolate
5	Dihydroxylammonium 5-(dinitromethylide)-tetrazolate	15	2-(2-nitro-2-azapropyl)-5-(fluorodinitromethyl)-2 <i>H</i> -tetrazole

Table 5: Compounds in Chapter 4

#	Compound name	#	Compound name
3	3,3'-Bi-(1,2,4-oxadiazolyl)-5,5'-diacetic acid	7	3,3'-Bi-(5-fluorodinitromethyl-1,2,4-oxadiazole)
4	3,3'-Bi-(5-methyl-1,2,4-oxadiazole)	9	3,3'-Bi-(5-trifluoromethyl-1,2,4-oxadiazole)
6	3,3'-Bi-(5-trinitromethyl-1,2,4-oxadiazole)	11	5,5'-Bi-(2-trifluoromethyl-1,3,4-oxadiazole)

3 List of Publications

JOURNAL PAPERS

Asymmetric Carbamate Derivatives Containing Secondary Nitramine, 2,2,2-Trinitroethyl, and 2-Fluoro-2,2-dinitroethyl Moieties

B. Aas, M. A. Kettner, T. M. Klapötke, M. Sućeska, and C. Zoller
Eur. J. Inorg. Chem. **2013**, 2013(35), 6028–6036.

5,5'-Bis(trinitromethyl)-3,3'-bi-(1,2,4-oxadiazole): A Ternary CNO-Compound With Remarkable High Density

M. A. Kettner and T. M. Klapötke
Chem. Commun. **2014**, 50(18), 2268–2270.

3,3'-Bi-(1,2,4-oxadiazoles) featuring the Fluorodinitromethyl and Trinitromethyl Groups

M. A. Kettner, K. Karaghiosoff, T. M. Klapötke, M. Sućeska, and S. Wunder
Chem. Eur. J. **2014**, 20, 7622–7631.

Contributions to the Chemistry of *N*-Methylnitramine: Crystal Structure, Synthesis of Nitrogen-Rich Salts, and Reactions towards 2-Nitro-2-azapropyl Derivatives

M. A. Kettner, T. M. Klapötke, T. G. Müller, and M. Sućeska
Eur. J. Inorg. Chem. **2014**, 4756–4771.

New Polynitrotetrazoles

M. A. Kettner and T. M. Klapötke
Chem. Eur. J. **2015**, 21(9), 3755–3765.

Synthesis, Characterisation and Crystal Structures of two Bi-Oxadiazole Derivatives featuring the Trifluoromethyl Group

M. A. Kettner, T. M. Klapötke, T. G. Witkowski, and F. von Hundling
Chem. Eur. J. **2015**, 21, 4238–4241.

CONFERENCE TALKS

Progress in the Development of High Energy Dense Oxidisers based on CHNO(F)-Compounds

16th Seminar on New Trends in Research of Energetic Materials (NTREM)
 Pardubice/Czech Republic, 10–12 April, **2013**
 Q. J. Axthammer, M. A. Kettner, T. M. Klapötke, R. Moll and S. F. Rest

Development of High Energy Dense Oxidisers based on CHNO(F)-Materials

5th European Conference for Aeronautics and Space Sciences (EUCASS)
 Munich/Germany, 1–5 July, **2013**
 Q. J. Axthammer, M. A. Kettner, T. M. Klapötke, R. Moll and S. F. Rest

Development of Novel High Energy Dense Oxidisers for Rocket Propulsion

Symposium of the European Academy of Sciences (EURASC)

Toulouse/France, 7–8 November, **2013**

Q. J. Axthammer, M. A. Kettner, T. M. Klapötke, B. Krumm and S. F. Rest

Synthesis of New Oxidisers for Potential Use in Solid Rocket Propellants

New Energetic Materials and Propulsion Techniques for Space Exploration

Milano/Italy, 9–10 June, **2014**

M. A. Kettner and T. M. Klapötke

CONFERENCE POSTERS

Energetic Phosphine Oxides

7th European Workshop on Phosphorus Chemistry (EWPC)

Budapest/Hungary, 25–26 April, **2010**

M. A. Kettner, A. Nieder, K. Karaghiosoff, and T. M. Klapötke

Reactivity of Tris(chloromethyl)phosphine Oxide

8th European Workshop on Phosphorus Chemistry (EWPC)

Münster/Germany, 25–26 March, **2011**

M. A. Kettner, K. Karaghiosoff, T. M. Klapötke, and A. Nieder

NMR Evidence for Oxalic Acid Dinitrate Ester

14th Seminar on New Trends in Research of Energetic Materials (NTREM)

Pardubice/Czech Republic, 13–15 April, **2011**

M. A. Kettner, K. Karaghiosoff, and T. M. Klapötke

Influence of Intramolecular Interactions on the Reactivity of Tris-(chloromethyl)-phosphine Oxide and 1,3-Dichloro-2,2-dinitropropane

2nd IUCr Satellite Workshop on “Categorizing Halogen Bonding and Other Noncovalent Interactions Involving Halogen Atoms”

Sigüenza/Spain, 20–21 August, **2011**

C. Evangelisti, M. A. Kettner, T. M. Klapötke, A. Nieder, and A. Penger

Synthesis and Characterization of Alkylated Trinitromethyl- and Fluorodinitromethyl-tetrazoles

17th Seminar on New Trends in Research of Energetic Materials (NTREM)

Pardubice/Czech Republic, 9–11 April, **2014**

J. Feierfeil, M. A. Kettner, T. M. Klapötke, M. Sućeska, and S. Wunder

BOOK CHAPTER

M. A. Kettner, T. M. Klapötke, **Synthesis of New Oxidisers for Potential Use in Chemical Rocket Propulsion**, in *Chemical Rocket Propulsion: A Comprehensive Survey of Energetic Materials*, Editor: Luigi De Luca, Milano, Italy, Springer Verlag, **2015**, *in press*.